1987

The thermal behavior of film cooled turbulent boundary layers as affected by longitudinal vortices.

Ortiz, Alfredo.

NAVAL POSTGRADUATE SCHOOL

Monterey, California

THESIS

THE THERMAL BEHAVIOR OF FILM COOLED
TURBULENT BOUNDARY LAYERS AS
AFFECTED BY LONGITUDINAL VORTICES

by

Alfredo Ortiz

September 1987

Thesis Advisor: P. M. Ligrani

UNCLASSIFIED

REPORT DOCUMENTATION PAGE

Report Security Classification: UNCLASSIFIED	Restrictive Markings
Security Classification Authority	Distribution/Availability of Report: Approved for public release; distribution is unlimited
Declassification/Downgrading Schedule	
Performing Organization Report Number(s)	Monitoring Organization Report Number(s)
Name of Performing Organization: aval Postgraduate School; Office Symbol (if applicable): Code 69	Name of Monitoring Organization: Wright Aeronautical Laboratories
Address (City, State and ZIP Code): onterey, California, 93943-5000	Address (City, State and ZIP Code): Wright-Patterson Air Force Base Ohio 45433
Name of Funding/Sponsoring Organization: right Aeronautical Lab.; Office Symbol (if applicable)	Procurement Instrument Identification Number: Mipr No. FY 1455-86-N0616
Address (City, State and ZIP Code): right-Patterson Air Force Base hio 45433	Source of Funding Numbers: Program Element No; Project No; Task No; Work Unit Accession No

Title (Include Security Classification): THE THERMAL BEHAVIOR OF FILM COOLED TURBULENT OUNDARY LAYERS AS AFFECTED BY LONGITUDINAL VORTICES

Personal Author(s): Alfredo Ortiz

Type of Report	Time Covered	Date of Report (Year, Month, Day)	Page Count
ster's Thesis	From ______ To ______	1987 September	208

Supplementary Notation

COSATI Codes: Field | Group | Sub-Group

Subject Terms (Continue on reverse if necessary and identify by block number): Embedded vortex, film cooling, heat transfer endwall secondary flows

Abstract (Continue on reverse if necessary and identify by block number)

Heat transfer effects of longitudinal vortices embedded within film cooled turbulent boundary layers on a flat plate were examined for freestream velocities of 10 m/s and 15 m/s, and for blowing ratios ranging from 0.47 to 1.26. Moderate stregth vortices were employed having circulation to freestream velocity ratios of about 1.6 cm. Spatially resolved heat transfer measurements from a constant heat flux surface and mean

Distribution/Availability of Abstract: Unclassified/Unlimited ☐ Same as RPT ☐ DTIC Users	Abstract Security Classification: UNCLASSIFIED
Name of Responsible Individual: hillip M. Ligrani	Telephone (Include Area Code): (408) 646-3382; Office Symbol: Code 69Li

ORM 1473, 84 MAR — 83 APR edition may be used until exhausted. All other editions are obsolete.

Security Classification of This Page: UNCLASSIFIED

19 ABSTRACT (CONT.)

temperature distributions in spanwise planes show that local heat local heat transfer is significantly affected by spanwise vortex position, and blowing ratio. Of particular significance are boundary layer and vortex structural changes which occur at high blowing ratios.

The Thermal Behavior of Film Cooled Turbulent Boundary Layers as Affected by Longitudinal Vortices

by

Alfredo Ortiz
Lieutenant, Colombian Navy
B.S., Escuela Naval "ALMIRANTE PADILLA", 1983

Submitted in partial fulfillment of the
requirements for the degree of

MASTER OF SCIENCE IN MECHANICAL ENGINEERING
and
MECHANICAL ENGINEER

form the

NAVAL POSTGRADUATE SCHOOL
September 1987

ABSTRACT

Heat transfer effects of longitudinal vortices embedded within film cooled turbulent boundary layers on a flat plate were examined for freestream velocities of 10 m/s and 15 m/s, and for blowing ratios ranging from 0.47 to 1.26. Moderate strength vortices were employed having circulation to freestream velocity ratios of about 1.6 cm. Spatially resolved heat transfer measurements from a constant heat flux surface and mean temperature distributions in spanwise planes show that local heat transfer is significantly affected by spanwise vortex position, and blowing ratio. Of particular significance are boundary layer and vortex structural changes which occur at high blowing ratios.

TABLE OF CONTENTS

LIST OF FIGURES

B. BOUNDARY LAYER WITH SINGLE VORTEX

C. FILM COOLING MEASUREMENTS

ACKNOWLEDGEMENT

This study was supported by Wright Aeronautical Laboratories, Wright-Patterson Air Force Base, MIPR number FY 1455-86-N0616. Dr. Charles MacArthur was program monitor. Technical contributions were made by Dr Russ V. Westphal of NASA- AMES, Professor John K. Eaton of Stanford University, LTCDR David L. Evans USN, LT Stephen L. Joseph USN and Michelle O'Neill.

I wish to express my gratitude to Professor Phillip Ligrani for his guidance, patience and understanding, I also like to thank the staff of the NPS Department of Mechanical Engineering, especially James T. Scholfield, Charles E. Crow, William Dames Jr. and Thomas Christian, who were always available to help and correct problems with the experimental apparatus. Last but by no means least, I like to thank my wife, Erika who gave me her complete support and understanding during the entire project.

TABLE OF SYMBOLS

A	-	area, m^2
C_d	-	discharge coefficient
C_p	-	specific heat at constant pressure, J/Kg ºK
d	-	injection hole diameter, m
E_{bi}	-	emissive power, W/m^2
F_{ij}	-	radiation view factor
h	-	heat transfer coefficient (spanwise averaged) as define by, $q''/(T_{r\infty} - T_w)$, W/m^2 ºK
h_f	-	heat transfer coefficient with film cooling (spanwise averaged) as define by, $q''/(T_{aw} - T_w)$
J_i	-	radiosity, W/m^2
K	-	thermal conductivity, W/m ºC
M	-	blowing rate
P	-	static pressure, Pa
R	-	gas constant
Re_d	-	Reynolds number based on the diameter of injection holes
Re_x	-	Reynolds number based on the downstream distance from the boundary layer trip.
St	-	Stanton number
St_0	-	baseline Stanton number, no film cooling, no vortex
St_f	-	Stanton number with film cooling only
T	-	static temperature, ºK, ºC

U - mean velocity, m/s

X - downstream distance as measured from the boundary layer trip, m

Y - vertical distance from the test surface upward, cm

Z - spanwise distance from the test section center line, cm

ξ - unheated starting length (1.10 m)

ε - radiation emissitivity

η - effectiveness of film cooling

ρ - density, Kg/m^3

θ - non-dimensional coolant temperature, $(T_{rc} - T_{r\infty})/(T_w - T_{r\infty})$

δ - boundary layer displacement thickness, m

σ - Stefan-Bolzman constant

SUBSCRIPTS

aw - adiabatic wall

c - coolant at exit of injection holes

i - isentropic

o - stagnation condition

p - in plenum chamber

r - recovery condition

w - wall

∞ - free stream

I. INTRODUCTION

The increasing need for greater efficiency in gas turbine engines has resulted in higher turbine inlet temperatures. Consequently, combustors and turbine blading are subject to greater amounts of thermal stress, thermal fatigue, and creep. At present, gas turbines such as those associated with military applications, have inlet temperatures as high as 1800-2000 ºC, [Ref. 1]. While the development of improved alloys with higher melting points is part of the solution, the development of efficient cooling systems is just as important [Ref. 2]. In order to design an efficient cooling configuration, the heat transfer distributions for the gas turbine components are needed. Because of the complex geometries and flows involved near blades and endwalls, accurate convective heat transfer rates are difficult to obtain. [Ref. 3]

Ongoren, [Ref. 4], described the flow in a turbine cascade. As the inlet boundary layer approaches the blade, just in front of the blade, a horseshoe vortex forms. At the saddle point, it splits into a vortex on the suction side, and a vortex on the pressure side. The pressure side vortex becomes the passage vortex, moving from the leading edge of the blade towards the low pressure side of the adjacent blade. As the suction side vortex convects along the blade, it is eventually pushed away by the passage vortex from the adjacent blade. A smaller, corner vortex rotates in opposite direction to the passage vortex as was verified by Sieverding, [Ref. 5].

The passage vortex is an example of a longitudinal vortex embedded in a film cooled turbulent boundary layer. In most cases, an embedded vortex has a cross-stream length scale approximately equal to the boundary layer thickness. Therefore, the vortex is capable of strongly perturbing the boundary layer structure and modifying the heat transfer characteristics. In addition, longitudinal vortices usually maintain their coherence over a long streamwise distance, meaning that the heat transfer effects behind an effective vortex generator are likely to be very persistent. [Ref. 6]

Film cooling is used to provide a layer of cool fluid between a surface and high temperature free stream gases to which it is exposed. The film cooling not only acts as a thermal insulator but also as heat sink for the hot freestream gases. The overall effect of the film cooling is to reduce the temperature of the developing boundary layer, which in turn reduces the heat transfer to the surface. In the present study, the heat flux is calculated from :

$$q'' = h(T_W - T_{r\infty}) \qquad \text{(eqn. 1.1)}$$

where h, includes the effect of the film cooling for constant wall heat flux, q'', and constant free stream temperature, $T_{r\infty}$. In the present experiment variations of h correspond to variations of the wall temperature, T_W. When $T_W = T_{r\infty}$, equation 1.1 indicates that q'' = 0, which may not be the case when film cooling is present.

Goldstein and Chen, [Ref. 2], defined an adiabatic wall effectiveness for film cooling using:

$$\eta = \frac{T_{aw} - T_r}{T_{oc} - T_r} \qquad \text{(eqn. 1.2)}$$

The heat transfer is then calculated from :

$$q'' = h_f(T_w - T_{aw}) \qquad \text{(eqn. 1.3)}$$

Here, $q''= 0$ when $T_w = T_{aw}$ with film cooling. Without film cooling $T_{r\infty} = T_{aw}$, and equations 1.1 and 1.3 are the same.

Numerous studies have been conducted on the effects of film cooling on heat transfer, effects of secondary flows on heat transfer, and more recently, on effects of film cooling and secondary flows on heat transfer in a turbulent boundary layer. Summarizing the results of experimental research on the effects of secondary flows in turbine blades passages over the past decade, Sieverding (1984) concluded that it is absolutely essential to establish the significance of secondary flows at off design conditions, in particular in regard to leading edge vortices.

Studying the effects of film cooling and secondary flows on heat transfer, Golstein and Chen (1985) performed an experimental study on the influence of the end wall on film cooling of gas turbine blades using a single row of injection holes. Two years later, the same authors performed a similar study but this time employed two rows of injection holes for the film cooling, [Ref 7]. From these two studies, the authors concluded that, in the convex side of the blade there is a triangular region where coolant is swept away from the surface by the passage vortex, while the concave side was not significantly affected by secondary flows originating near the endwall. Other study on film cooling effects is given in [Ref. 8].

Eibeck and Eaton (1987), conducted a study of a longitudinal vortex embedded in a turbulent boundary layer over a constant heat flux plate. The authors found significant increases and decreases in local Stanton numbers, due to the thinning of the boundary layer on the downwash side of the vortex and thickening on the upwash side of the vortex. Spanwise heat transfer variations became larger as the circulation of embedded vortices increased. [Ref. 6]

Investigating the interaction between a single weak streamwise vortex and a two-dimensional turbulent boundary layer, Russel, Pauley and Eaton (1987), observed a rapid growth of the vortex core, and a flattening of the core shape when the dimension of the core radius became comparable to the distance of the vortex center to the surface. Adverse pressure gradient caused an increase in the rate of core growth, and a stronger distortion of the core shape. These authors also provide an extensive review of work on vortices in boundary layers. [Ref 9]

In [Ref. 10], a study was conducted on heat transfer distributions and film cooling effectiveness on the endwall of an airfoil, using a full annular low aspect ratio vane cascade. The authors demonstrated the importance of the horseshoe vortices and secondary flows on the heat transfer and film cooling distributions.

Recently, Joseph (1986), conducted a study of the effects of embedded vortices on heat transfer in film cooled turbulent boundary layers. The author showed that the effects of the vortex on heat transfer are significant and important : on the downwash side of the vortex, heat transfer is augmented, effects of the film cooling are negated and local hot spots will exist.

Near the upwash side of the vortex, coolant is pushed to the side, appearing to augment the protection provided by the film cooling, [Ref. 3]. Evans (1987), studied the fluid mechanics of vortices in boundary layers with film cooling, and showed that the vortices completely dominate the flow field, especially near the downwash side [Ref. 1].

The objective of this thesis is to increase the understanding of the effects on heat transfer, of a longitudinal vortex embedded in a film cooled turbulent boundary layer as affected by : 1) spanwise vortex position relative to the location of film cooling injection holes and, 2) blowing ratio. These effects are important regarding turbine blade and endwall heat transfer. The study was carried out under a series of steps. The first, was the design and construction of the heat transfer test surface, followed by qualification test to verify uniform wall heat flux, and an energy balance to identify and quantify the heat losses. After completion of the experimental apparatus, four types of heat transfer test were conducted : (1) heat transfer data with developing boundary layer only, (2) boundary layer and embedded vortex, (3) boundary layer with film cooling only, and (4) boundary layer with film cooling and embedded vortex.

II. EXPERIMENTAL APPARATUS

A. WIND TUNNEL

The wind tunnel pictured in Figure 3., built by Aerolab, was designed to provide a flow field from the nozzle with uniform velocity and low turbulence intensity. It is designated the NPS Shear Layer Research Facility (SLRF).

1. Description.

The SLRF is a wind tunnel of the open circuit blower type with fan upstream and air entering the blower inlet from the surrounding room. The air speed through the test section can be adjusted from 5 to 40 m/s. The tunnel frame has leveling screws to adjust the center line of the tunnel to a horizontal position. The discharge of the fan slips into the inlet of the diffuser with a 1.6 mm clearance to isolate vibrations from the fan to the wind tunnel body. The diffuser section contains a filter pack and a nozzle leading to test section. The test section is a rectangular duct, 3.048 m long and 0.6090 m wide. It is designed with numerous pressure tabs and four 38 x 20.3 cm access ports along each of the side walls to provide easy access. The top wall is a continuous panel fabricated from 4.76 mm thick Lexan sheet, continuously sealed with neoprene along the edges. The ceiling height is adjustable to permit changes in the pressure gradient along the length of the test section. Additionally, the top wall contains numerous instrument ports for the measurements of various flow characteristics. The floor of the test section consists of three 0.6096 m and one 1.2192 m long sections which are removable and replaceable. These sections are all 0.6090 m wide and are sealed with "O" rings around the sides. Further discussions of the wind tunnel are contained in [Ref. 11] and [Ref. 3: pp. 38].

A schematic of the test section components with the coordinate system employed in the present study are shown in Figure 1. An unheated starting length of 1.10 m exists upstream of the heated test surface. The injection nozzles are located 1.08 m downstream of the boundary layer trip and 0.02 m upstream of the test surface. The leading edges of the vortex generators are placed 0.479 m downstream of the boundary layer trip as shown in Figure 2.

2. Qualification and Performance.

Prior to its relocation, extensive qualification tests of the Shear Layer Research Facility were conducted by Ligrani, [Ref. 12]. Results show that the variation of total pressure at the exit plane of the nozzle is less than 0.4% at 26 m/s and 34 m/s. Mean velocity varies less than 0.7% for the same mean freestream speeds. From five-hole pressure probe measurements, the velocity angle deviation is nowhere greater than 0.6 degrees at the nozzle exit plane.

Profile measurements of the mean velocity and longitudinal turbulence intensity in the turbulent boundary layer developing at 20 m/s indicate normal, spanwise uniform behavior. For this qualification test, and all results which follow, the boundary layer was tripped near the exit of the nozzle with a 1.5 mm high strip of tape. For the present study, total pressure measurements along the test section were made after relocation of the SLRF, in order to adjust the top wall for zero pressure gradient. The maximum pressure difference along the test section was 0.007 in of H_2O. Free stream turbulence intensity was measured to be 0.00085 (8.5 one hundredths of one percent or 0.085%) at 20 m/s, increasing to 0.00095 at 30 m/s.

B. INJECTION SYSTEM.

The injection system provides film coolant at temperatures above ambient. The coolant is ejected from a single row of injection holes into the boundary layer developing along the bottom wall of the test section. The diameters of the injection holes were scaled relative to boundary layer thickness to be similar to a turbine blade, with δ/d ratio ranging from 0.37 to 0.40. The free stream air is at ambient temperature, thus the direction of heat transfer is opposite that of a gas turbine. The temperature difference $T_w - T_{r\infty}$ range for this study has been kept less than 20 ºC. to minimize the effects of variable fluid properties.

The injection parameters M and θ were scaled to resemble parameters near gas turbine blades where M ranges from 0.47 to 1.26 and θ varied from 1.39 to 1.69. Since the average temperatures of the coolant, plate and freestream were approximately the same for different runs, T_{rc} = 51 ºC, and T_w = 40 ºC and $T_{r\infty} \approx$ 20 ºC, variation of θ was not a parameter considered in this study. Due to the reverse direction of heat transfer for the present experimental apparatus $T_{rc} : T_{r\infty} : T_w$ ratio is 1.27 : 0.5- 0.55 :1.0 as compared to 0.67- 0.83 : 1.5 : 1.0 for actual gas turbines.

1. Description

Air for the injection system originates in a two stage, 150 psig Ingersol-Rand air compressor, 10 HP, model # 71TD. From the compressor air flows through an adjustable pressure regulator, a cut-off valve, a reinforce flexible tubing (2.54 cm inside diameter), a moisture separator, a flow regulator, a Fisher and Portor rotometer (full scale 9.345E-3 m^3/s, 19.8 SCFM, model # 10A3565A), a diffuser, and finally into the injection heat exchanger and plenum chamber. The rotometer monitors the flow rate for film cooling.

A photograph of the chamber, the row of film cooling holes and vortex generator is shown in Figure 3.b. The chamber is constructed of 1.27 cm plexiglass, with outside dimensions of 0.305 x 0.508 x 0.457 m. The internal structure consists of three thin metal plates 0.381 x 0.508 m, starting 5.08 cm from the bottom and proceeding up at 5.08 cm intervals. Two silicon rubber heaters, 0.381 x 0.483 m, 120 volts, are separately placed over the bottom two plates. The heaters are controlled through a Powerstat variable autotransformer, type 136. The top surface contains 13 plexiglass injection tubes 8 cm long each, with an inside diameter of 0.952 cm (3/8 in), with a l/d ratio of 8.42. The 13 injection nozzles are incline at angle of 30º, with a three diameter spanwise spacing between center lines. The middle tube is located on the center line of the test surface.

Three pressure taps, positioned at the center of the front and two side faces of the injection plenum chamber, are used to measure P_{oc} - P_{∞}. Three 0.254 mm diameter copper-constantan wire thermocouples with welded joints are placed at different locations inside the plenum chamber to measure T_{op}.

2. **Qualification and Performance**.

Extensive qualification of the injection system was conducted by Joseph, [Ref. 3: pp. 23-26]. Results show that the uniformity of the plenum chamber pressure, P_{oc}, was satisfactory over the range of the injection conditions with differences of about 1% in the spanwise direction and a maximum of 4% occurring for only one case at low flow rate of 0.327E-4 m^3/s. This is equivalent of a blowing ratio M of 0.004 at U_∞ = 10 m/s

The plenum produces a reservoir of air at an elevated temperature and pressure, which is near stagnation conditions. The temperature at the exits of the injection tubes, T_{rc}, is different from the temperature of the plenum of the injection chamber, T_{op}, due to conduction through the tubes surface to the surrounding air. It is more convenient to measure T_{op}, whereas T_{rc} is needed to calculate the injection parameters. Thus a relation between T_{rc} and T_{op} was needed and found from experiment to be $T_{oc} = 1.455\ T_{op}^{0.868}$. Because of the low velocities employed, (and negligible viscous dissipation), $T_{oc} \approx T_{rc}$ within a fraction of a degree.

In order to determine injection parameters, the following quantities must be measured, P_∞, T_∞ V_c, P_{oc}, T_{oc}, and A, the area normal to the flow of the injection holes, designed to be 9.2633E-4 m^2. The coolant velocity is then given by:

$$U_c = \frac{V_c}{A} \qquad \text{(eqn. 2.1)}$$

The static density is estimated using :

$$\rho_c = \frac{P_\infty}{RT_c} \qquad \text{(eqn. 2.2)}$$

The mass flux, m_c, is the product of U_c and ρ_c. To calculate the isentropic mass flow, ρ_{ci} and U_{ci} are found using

$$\rho_{ci} = \frac{P_\infty}{RT_{op}} \qquad \text{(eqn. 2.3)}$$

and

$$U_{ci} = \sqrt{\frac{2(P_{oc} - P_\infty)}{\rho_{ci}}} \qquad \text{(eqn. 2.4)}$$

The product of ρ_{ci} and U_{ci} for compressible flows may be given as :

$$(r_c U_c)_i = P_\infty \left[\frac{P_\infty}{P_{\cdot\cdot}} \right]^{\frac{2}{7}} \left\{ \frac{7}{RT_\infty} \left[1 - \left[\frac{P_\infty}{P_{\cdot\cdot}} \right]^{\frac{2}{7}} \right] \right\}^{0.5} \qquad \text{(eqn. 2.5)}$$

Discharge coefficients, C_d, are then estimated using :

$$C_d = \frac{\rho_c U_c}{(\rho_c U_c)_i} \qquad \text{(eqn. 2.6)}$$

In order to check the injection system, discharge coefficients were measured as volumetric flow rate was changed. Results are given in Figure 4 as a function of Reynolds number for 13 injection hole locations and 7 injection hole locations. Discharge coefficients range between 0.5 and 0.730, and increase with Reynolds number. For Re > 3×10^3, discharge coefficients collapse closely around a value of approximately 0.72 . Because these results are consistent with those of [Ref. 8], satisfactory injection system performance is indicated.

C. HEAT TRANSFER SURFACE.

The heat transfer surface was designed and developed to provide a constant heat flux over its area. The average surface temperature may be adjusted and maintained from ambient up to about 60 ºC. The plate was constructed so that its upward facing part is adjacent to the wind tunnel air stream, with minimal heat loss by conduction from the sides and beneath the test surface. The plate itself has been instrumented to measure temperatures with thermocouples placed just beneath the foil surface. A film of liquid crystals is sprayed over a layer of black paint painted on the foil.

1. Description.

A photograph of the heat transfer surface is shown in Figure 5.a. The design is based on ones used at the University of Minnesota [Ref. 13] and [Ref. 14], and provides more uniform heat flux and better spatial resolution of temperature than the surface used by Joseph, [Ref. 3: pp. 27-36]. It consists of a thin stainless steel foil, AISI 302 full hard, 0.2032 mm x 1.3 m x 0.467 m, painted flat black with 7 layers of liquid crystals. Attached to the under side of the surface are 126 copper-constantan thermocouples. 120 of these have flattened tips and were manufactured by Marchi associates (type MA 396T-30-96-FEP-FJ), the remaining six have round junctions and were manufactured by Omega Engineering, Inc. Thermocouple lead wires are located in grooves cut into a triple sheet of 0.254 mm (10 mil) thick double sided tape, manufactured by the 3M Company), as shown in Figure 5.b. The grooves are then filled with RTV. A thin foil constant heat flux heater, 1.0 mm x 1.143 m x 0.457 m, 120 V/1500 W, manufactured by Marchi Associates, is attached to the tape with Electrobond epoxy. Beneath the heater is a 12.7 mm (1/2 in) thick lexan sheet, followed by a 25.4 mm of foam insulation, 82.55 mm thick styrofoam, three sheets of .254 mm each lexan and one sheet of 9.53 mm thick balsa wood, as shown in Figure 7.

Around the edges of the foil, grease was inserted between it and the plexiglass frame to fill any small gaps resulting from thermal expansion. In addition, both the upstream edge and the trailing edge were taped to the bottom wall of the test section. Since additional vertical movement of the foil above the bottom wall of the test section occurs due to thermal expansion during heating, the level of the surface is adjustable and maintained level with the test surface by adjusting screws in the plexiglass frame supporting the heat transfer surface from below. During heat transfer tests, the top surface of the foil remained remarkably flat and smooth with minimal surface irregularities. The surface temperature is controlled by adjusting input voltage to the heater using a Standard Electrical Product Co. variac, type 3000B. With this type of heat transfer surface, good resolution of temperature was achieved without hot spots.

Thermocouples are placed on the surface as shown in Figure 6. In each of the six rows, 21 thermocouples are located 1.27 cm apart from each other. The first row of thermocouples is located at 5 cm from the leading edge of the test surface, the second is 10 cm further downstream with respect to the first, the third is 15 cm apart downstream from the second row, and the rest of the thermocouple rows are 20 cm apart from each other

2. **Qualification and Performance**

The present test surface was the second one constructed for this experiment. The first one could not be used since it had hot spots located under the thermocouple lead wires where the surrounding liner was not properly attach to the heater. In the second surface, this problem was remedied by increasing the thickness of the liner.

To test the second heat transfer surface, a Huges Probeye Thermal Series 4000 Video System , consisting of a infrared and video camera with display screen, was used. Surface temperatures were measured as the test surface was heated outside the wind tunnel, since the system could not see through wind tunnel walls. With this system temperature variations as small as 1 ºC, can be measured. The surface was observed under three operating conditions : natural convection with a surface temperature of approximately 35 ºC, forced convection from the leading edge with a surface temperature of about 40 ºC, and force convection from the trailing edge, with a surface temperature of about 40 ºC. Results showed that most of the heat transfer surface temperatures were spanwise uniform within a fraction of a degree for all three tests. The only exceptions were several small cool spots with temperatures about 1 ºC lower than the rest of the plate, located between rows of thermocouple lead wires near the edges of the plate.

A second test using the liquid crystals was performed to further qualify the test surface. The liquid crystals, manufactured by Davis Liquid Crystals, Inc., are rated from 30 to 35 ºC. Temperature variations as small as

1.2 ºC can be measured with an uncertainty of ± .2 ºC. The test was conducted with natural convection with a surface temperature of approximately 32 ºC. Results were consistent with the infrared test with temperatures variations not greater than 1.2 ºC across most of the surface. As for the early test, small hot spots were evident near some thermocouple lead wire locations.

3. Energy Balance.

An energy balance was performed to determine the heat loss by conduction from the heat transfer test surface used to obtain final results. During the energy balance, heat loss by radiation and convection were prevented since the metal foil surface, ordinarily exposed to convection in the wind tunnel, was covered with three layers of 25.4 mm thick foam insulation. For the energy balance, and for all wind tunnel testing, foam insulation was also placed around the sides of the test surface located below the wind tunnel convection surface. To estimate heat loss through the insulation placed on top of the foil surface, program ENERGB was employed with an algorithm involving the one dimensional, linear form of Fourier's conduction equation:

$$q_w = KA\frac{\Delta X}{\Delta T} \qquad \text{(eqn. 2.7)}$$

For the insulation, K is 0.4 W/m ºC, A is 0.4897 m^2, ΔX is 0.0254 m, and ΔT is the temperature drop in the X direction in ºC. Heat conduction through the bottom and sides of the heat transfer device is then given by:

$$q_c = VI - q_w \qquad \text{(eqn. 2.8)}$$

Here, VI is the power into the test plate, and q_w is the conduction loss through the top insulation. Tests were made at five power levels 11.02, 13.0, 15.25, 16.52 and 18.2 Watts, chosen to give conduction losses at the same levels as experienced under normal operating conditions. Figure 8 shows q_c vs. $T_w - T_{amb}$ results, where T_w is the average plate surface temperature. A second order polynomial was fitted to this data in order to predict conduction losses during heat transfer measurements:

$$q_c = 0.683 + 0.954Tdiff - 0.016Tdiff^2 \qquad \text{(eqn. 2.9)}$$

where $Tdiff = T_w - T_{amb}$. This equation is valid over a range of $T_w - T_{amb}$ from 10 to 30 ºC. When exposed to convection in the wind tunnel, conduction losses are only 1.5 to 2.5% of the total power, and thus, a 25% error in the estimate of conduction losses will cause less than a 0.5% error in the estimate of the heat transfer by convection.

Radiation losses were estimated using two different approaches. For the first:

$$q_{ij} = \frac{\sigma(T_w^4 - T_{amb}^4)}{\frac{1-e_i}{e_i A_i} + \frac{1}{A_i F_{ij}} + \frac{1-e_j}{e_j A_j}} \qquad \text{(eqn. 2.10)}$$

and

$$q_{rad} = \sum_{j=1}^{n} q_{ij} \qquad \text{(eqn. 2.11)}$$

[Ref. 15]. For the second approach,

$$q_{rad} = \frac{E_{bi} - J_i}{(1-\varepsilon_i)/\varepsilon_i A_i} = \sum_{j=1}^{n} \frac{J_i - J_j}{(A_i F_{ij})^{-1}} \qquad \text{(eqn. 2.12)}$$

[Ref. 16]. The view factors, F_{ij}, for the top and each of the side walls were estimated to be 0.54 and 0.23, respectively [Ref. 16], where

$$\sum_{j=1}^{n} F_{ij} = 1 \qquad \text{(eqn. 2.13)}$$

From these two methods, the radiation losses for an average plate temperature of 40 ºC were estimated to be 55 Watts, approximately 8.5% of the total power into the heat transfer surface.

4. <u>Contact Resistance Temperature Drop</u>

Local surface temperatures were measured using thermocouples placed in contact with the underside of the metal foil surface. The junctions of these thermocouples were held in place next to the foil with three layers of 0.254 mm thick double–sided lining tape and RTV silicon rubber epoxy. During the heat transfer tests, temperatures measured by the thermocouples were greater than those of the surface of the plate, due to thermal contact resistance between the thermocouples and the foil and conduction through the foil. The resulting temperature difference ΔT is given by:

$$\Delta T = q\left(\frac{1}{h_c A} + \frac{\Delta X}{KA}\right) \qquad \text{(eqn. 2.14)}$$

where $\Delta X/KA$ accounts for conduction across the foil thickness and $1/h_cA$ accounts for the thermal contact resistance. q is the heat flux through the foil. The contact resistance is highly dependent on the contact pressure as well as the area of the surfaces in contact.

The value of contact resistance used in the present study was the same as used by Joseph [Ref. 3]. In his study liquid crystals were applied to the surface to measure its temperature distribution during convection tests, so that ΔT in eqn. 2.13 could be determined. Stanton numbers from baseline tests matched expected correlations after accounting for contact resistance. The empirical relationship for turbulent boundary layers at constant free stream velocity, along a flat plate with constant wall heat flux and unheated starting length of ξ = 1.10 m. [Ref. 14] is given by

$$St_x Pr^{0.4} = 0.030 Re_x^{-0.2} \left(1 - \left(\frac{\xi}{X}\right)^{0.9}\right)^{-.111} \qquad \text{(eqn. 2.15)}$$

Data in Figures 10 and 13 show that this equation matches the data well for $5 \times 10^5 < Re_x < 2.0 \times 10^6$. From these measurements, the two terms in brackets in equation 2. 13 were estimated to be 0.014 °K/Watt. The same value was used for all thermocouples. However, on the present test plate, contact pressure and the area of the thermocouples in contact with the surface varied slightly from one thermocouple to another. Because contact resistance for each individual thermocouple may vary from this value, small deviations in the spanwise heat transfer coefficients and Stanton numbers result, which were independent of flow conditions. In the present study, the effects of these small variations were minimized by presenting results for local conditions in terms of Stanton number ratios .

D. TEMPERATURE MEASUREMENT.

All thermocouples employed in the present study are type–T, copper-constantan thermocouples. 120 of these were manufactured by Marchi Associates, Inc and attached beneath of the heat transfer surface. These thermocouples, have a flattened junctions, so that they may be placed in good contact with the surface. One of these thermocouples was calibrated using a temperature regulated bath consisting of liquid nitrogen and electric heaters and a platinum resistance temperature reference (± 0.01 ºC). The calibration was performed over the temperature range of 0 - 45.32 ºC. A second order was used to convert microvolts to temperature :

$$T = 0.018205 + 0.025846E - 0.000000581E^2 \qquad \text{(eqn. 2.16)}$$

where:

$$E = \text{microvolts} \times 10^6 \ \text{Volts} \qquad \text{(eqn. 2.17)}$$

This calibration was used for all Marchi Associates thermocouples attached to the plate, since all thermocouples indicated very similar behavior as temperatures were changed.

Thermocouples manufactured by Omega Engineering Co. were used to measure six plate temperatures, as well as temperatures of the plenum air, freestream air, and the boundary layer as traverses were made. The calibration of Joseph, [Ref. 3.: pp. 37], was first verified, and then used for all of these measurements except the traverses:

$$T = 26.573E - 1.937E^2 + 0.998E^3 - 0.261E^4 \qquad \text{(eqn. 2.18)}$$

Here,

$$E = \text{millivolts x } 1000 \qquad \text{(eqn. 2.19)}$$

Temperatures surveys of $T - T_\infty$, were performed using the automated traversing device. For this, two thermocouples manufactured by Omega Engineering were used, after calibration using the technique mentioned above. Simultaneous measurement of free stream temperature was made for every boundary layer location to minimize scatter due to wind tunnel temperature drift. For the thermocouple mounted in the probe that travels the flow field, the following equation was used to convert voltage to temperature:

$$T = 0.1836 + 0.025667E - 0.0000004882E^2 \qquad \text{(eqn. 2.20)}$$

For the thermocouple used to measure the free stream, the equation employed was :

$$T_\infty = 0.07832 + 0.0231054E - 0.0000006786E^2 \qquad \text{(eqn. 2.21)}$$

As before, E = microvolts x 10^6. The automated traversing mechanism has two degrees of freedom which allowed measurement of a plane the flow field. Each survey consisted of 800 probe locations, covering an area of 12 cm x 22 cm. Both, spanwise and vertical traversing blocks are mounted on a 20-thread per inch drive screw and two ground steel case hardened steel guide/support shafts. Each drive shaft is directly coupled to a SLO-SYN type

M092-FD310 steeping motor. Motors are controlled by a MITAS two-axis Motion Controller. Both the motors and the controller are manufactured by The Superior Electric Co. The MITAS controller comes equipped with 2K bytes of memory and a MC68000, 16-bit microprocessor which allows the user to program the start, stop, duration, speed,acceleration and deceleration of the steeping motors.

E. DATA ACQUISITION SYSTEM

The data acquisition system was designed to rapidly measure thermocouple voltages and convert them to temperature in degrees C. Using these temperatures along with user supplied information on ambient conditions, freestream conditions, power input, and flow rates into the injection chamber, the system calculates free stream velocity, density, local heat transfer coefficients, Stanton numbers, spanwise averaged Stanton numbers, and injection parameters such as blowing ratio and discharge coefficient.

1. Hardware

A Hewlett-Packard Series 300, Model 9836S computer, equipped with a MC68000, 8 MHz 16/32–bit processor, dual 5-1/4 inch floppy disk drives, and 1M bytes of memory RAM, was used in the study. The computer was used to process signals from the data acquisition system as well as the information supplied by the user in order to process, store, display and print results. An HP Think Jet printer was used to print data, and an HP 7470 two pen plotter was employed for graphics. Voltages from the thermocouples are read by an HP-3497A Data Acquisition/Control Unit with an HP-3498A

Extender. The unit communicates with the computer through a HP-829737A Interface.

2. **Software.**

Programs STANFC1, STANFC2 and ACQTPRO were developed to process temperature and Stanton number data, program ENERGB was developed to estimate the conduction losses, and programs PTSLC, PTSTAV, PLSTRVOR, PLSTRTIO, PLSTRFC, PLSTVV, SURFCONT and PLOTRUN were developed for plotting data. All these programs are listed in Appendix C. The data files created by the heat transfer programs are listed in Appendix D.

Programs STANFC1 and STANFC2 are modified versions of STDAT1, which was developed by Ligrani, Ortiz and Joseph, [Ref. 3.: pp. 41]. Program STANFC1 prompts the user if film cooling is being used. If the answer is affirmative, the program prompts the user to enter the percentage of flow to the injection chamber from the rotometer and the pressure difference between the injection chamber and the static pressure in the wind tunnel. These inputs are transformed to SI units and stored in a data file named "FILDT". The program continues by prompting the user for the stagnation pressure of the free stream (in inches of H_2O), the ambient pressure (in Hg), the current (Amps) and voltage supplied to the heater. The program then reads the thermocouple voltages and converts them into temperatures. These are then stored in a data file named "TDAFC". After all temperatures have been calculated, the free stream density and velocity are calculated. Parameters previously calculated such as the free stream density, free stream velocity, ambient pressure, and the power in are stored in a data file named "IDAFC".

Program STANFC2, processes the data files TDAFC, IDAFC and FILDT. The program begins by prompting the user whether a vortex generator is being used or not, then it accounts for conduction, radiation losses and contact resistance. It continues by calculating local heat transfer coefficients and Stanton numbers, average spanwise Stanton numbers and Reynolds number based on downstream distance. These data are printed out and two data files, "STRFCV" and "STAV", are created. In "STRFC" the local heat transfer coefficients and Stanton numbers are stored, along with their spanwise position and downstream positions along the test plate. Spanwise averaged Stanton numbers with their corresponding down stream Reynolds numbers, are located in "STAV". The last section of the program includes a subroutine to calculate film cooling parameters, such as discharge coefficients, density ratios, mass flux ratios, momentum flux ratios and blowing rate.

Program ACQTPRO, developed by Ortiz, acquires temperatures from a thermocouple probe mounted on the automatic traversing device and from another thermocouple that senses the freestream temperature. This program was used to create the data to plot the temperature surveys of $T - T_\infty$. The program begins by prompting the user for the downstream distance from the boundary layer trip, the number of points in the spanwise direction where temperatures are going to be measured, the number of points in the vertical direction, the spanwise resolution in inches, the vertical resolution in inches and the initial position of the probe with respect to the plate, in both Z and Y coordinates, in inches. A matrix of data points is then computed. Freestream temperature is calculated and ambient conditions are input. The program then enters a loop which samples each temperature 25 times per probe position and 5 times the free stream temperature. Upon acquiring these temperatures and obtaining their respective average, $T - T_\infty$ is calculated for each probe location. The temperature difference along with their respective coordinates are stored in a matrix. At the end of the data collection run, these values are read into a data file named "TPRO", on a floppy disk. These data are plotted using program "TPROPUN".

III. EXPERIMENTAL RESULTS

A. BASE LINE MEASUREMENTS

Heat transfer measurements were made at free stream velocities of 10 m/s and 15 m/s, without vortex and without film cooling. These were done in order to determine how heat transfer from the plate compares with existing correlations. These measurements validated and qualified the performance of the heat transfer plate and measurements procedures used. Results are given in Figures 9-11 for 10 m/s, and in Figures 12-13 for 15 m/s.

Figure 9 shows the spanwise uniformity of the local heat transfer coefficient of the test surface at 10 m/s. Except for row 1, the spanwise uniformity is very good with maximum variation of 10% (based on the average for a given row). These small variations are probably due to slight differences in the spatial uniformity of the heat transfer test surface, especially differences in the conduction contact resistance between different thermocouples and the metal foil, which comprises the top of the heat transfer plate. Larger spanwise variations for row 1 are believed to be due to multi-dimensional heat transfer by conduction through the leading edge and through the front corners of the test plate in addition to the contact resistance. These variations are not as large as those observed by Joseph [Ref. 3: pp. 45, 77-78].

The spanwise-averaged Stanton Numbers for 10 m/s are shown in Figure 10. Six data points are shown, where each corresponds to a different thermocouple row. The data shows excellent agreement with the empirical equation for turbulent boundary layers on a flat plate at constant free stream velocity, with constant heat flux and unheated starting length of x = 1.10 m [Ref. 15].

$$St.Pr^{0.4} = 0.030Re_x^{-0.2}\left(1 - \left(\frac{\xi}{X}\right)^{0.9}\right)^{-0.111} \qquad \text{(eqn. 3.1)}$$

A survey of $T - T_\infty$ in degrees Centigrade was obtained at X = 1.48 m, using a calibrated copper-constantan thermocouple, positioned using the automated traversing device. Results are shown in Figure 11, for U_∞=10 m/s with no vortex and no film cooling. In this figure, results for an area normal to the flow of 11 cm x 20 cm. are given, as measured using 800 probe positions. The survey evidences good spanwise uniformity of the temperature boundary layer.

Figure 12 and 13 show the spanwise variations of the heat transfer coefficient and averaged Stanton numbers as function of Reynolds number for 15 m/s free stream velocity. Results are consistent with those obtained for 10 m/s. In Figure 12, the data show good spanwise uniformity, except for the first row, where variations are slightly larger than for the 10 m/s case. In Figure 13, the data again show excellent agreement with equation (3.1).

B. BOUNDARY LAYER WITH SINGLE VORTEX

Heat transfer measurements were made at free stream velocities of 10 m/s and 15 m/s with an embedded longitudinal vortex and no film cooling. These were done to further qualify the heat transfer surface for spatially resolved heat transfer measurements. To produce the vortex, vortex generator #2,(see Joseph [Ref. 3: pp 76]), was positioned 0.479 m downstream from the boundary layer trip, and 4.79 cm in the positive Z-direction, as shown in Figure 2.

The spanwise variation of local St/Sto for 10 m/s and 15 m/s are presented in Figures 14 and 15, respectively. Here, Sto is the local Stanton number without an embedded vortex. In both of these, the effect of the vortex on wall heat transfer is evident. The Stanton number ratios approach 1 away from the vortex. As Z decreases from +15cm, the ratios increase until maximum values of 1.2 and 1.25 are reached for 10 and 15 m/s, respectively. These maxima correspond to locations on downwash sides of vortices, where secondary flows result in boundary layers which are locally thinner than at other locations. For $-5.0<Z<0.0$ cm a large gradient of heat transfer exists at each downstream location. The location of this gradient moves to smaller Z as the vortex develops downstream. For smaller Z, Stanton number ratios for 10 and 15 m/s, reach minima of 0.92 and 0.90 at locations which correspond to the upwash sides of vortices. Here, the boundary layer is locally thicker than at other locations.

The results in Figures 14 and 15 are in excellent quantitative agreement with those of Joseph [Ref. 3: pp. 87-88], for the same experimental conditions, (The sign of the Z coordinate in this experiment is opposite to the one employed by Joseph). The results in 14 and 15 also show qualitative agreement with the measurements of Eibeck and Eaton [Ref. 6], where small quantitative differences are a result of different vortex generator geometries.

C. BOUNDARY LAYER WITH FILM COOLING

In order to further qualify the heat transfer surface and the film cooling injection system, measurements were made with film cooling without embedded vortex. Results were obtained at 10 m/s, at θ = 1.614, 1.699 and 1.50 with blowing ratios of 0.68, 0.98 and 1.26 respectively, and at 15 m/s, at θ = 1.393 and 1.586 with blowing ratios of 0.47 and 0.86 respectively. Results are presented in Figures 16-30.

Figures 16-18 show the spanwise variations of St/Sto at 10 m/s, for blowing ratios of 0.68, 0.98 and 1.26, respectively. The first data set was obtained using 13 injection holes, which produce a film wide enough (25.4 cm) to cover the entire span of the measuring heat transfer surface. Because of the limitations on the secondary air supply, 9 and 7 injection holes were required to produce blowing ratios of 0.98 and 1.26, respectively. In these cases the coolant was injected such that it covered a portion of the center span of the heat transfer test surface. Consequently, Stanton number ratios are higher near the edges of the plate, as shown in Figures 17 and 18. The latter Figure for only 7 injection holes, shows this effect to be particularly significant, however, in spite of this a large spanwise uniform area exists in the center portion of the plate where adequate spanwise averages may be obtained. Apart from this, the spanwise uniformity of Stanton number ratios in Figures 16-18 is excellent with a maximum deviation of about 10 percent.

Figures 19 and 20 show the spanwise variations of the Stanton number ratios at 15 m/s. Results for blowing ratios of 0.47 and 0.86 were obtained using 13 and 7 injection holes respectively. Spanwise variations in Figures

19 and 20 are larger than in Figures 16-18, though qualitative trends are very similar.

A summary of spanwise averaged St/Sto as dependent upon Reynolds number is given in Figure 21. Graphs showing individual curves are presented in Figures 22- 26, where averaged St/Sto are given for blowing ratios of 0.68, 0.98 and 1.26 at 10 m/s, and 0.47 and 0.86 at 15 m/s, respectively. Referring to Figure 21, the lowest St/Sto are observed for M = 0.68 at 10 m/s and for M = 0.47 at 15 m/s. For each individual data set, the lowest ratio is present for the two rows of thermocouples nearest the film cooling holes, where X/d is 7.35 and 17.48. Here, X is distance from the down stream edge of the injection holes, and d the injection hole diameter. The data in figures 21-26 are plotted as function of the blowing ratio in figures 27 and 28. Results in 21-28 are qualitatively consistent with the fully turbulent measurements of Goldstein and Yoshida, [Ref. 15], also for a single row of injection holes.

Two surveys of $T - T_\infty$ in degrees C were obtained in the film cooled turbulent boundary layer at X = 1.48 m, X/d = 41.94. Both surveys were made at a free stream velocity of 10 m/s, with M = 0.98 and a coolant injection temperature of 51 ºC. In one case, the plate was heated to 40 ºC (Figure 30.), and in the other, the plate was maintained at the free stream temperature (Figure 29.). The latter experimental arrangement with unheated plate allowed the determination of the presence and distribution of heated film coolant as indicated by higher temperatures. In Figure 30 with a heated plate, the locations of coolant jets are evident as local hot spots near the wall.

Comparing these results to ones in Figure 11. without film cooling shows that the thermal boundary layer is about twice as thick.

D. BOUNDARY LAYER WITH SINGLE VORTEX AND FILM COOLING

In this part of the study the effect of an embedded vortex on a film cooled turbulent boundary layer was studied. This section of the experiment was conducted in four different parts. For all the parts of the experiment the same vortex generator was employed. The first consisted in repeating Joseph data, [Ref. 3. : pp. 97-104]: U_∞= 10 m/s, vortex generator #2 at Z = 4.79 cm and blowing ratio, M = 0.68, in order to provide additional check on measurements, equipment and procedures. In the second step, a blowing ratio of M = 0.98 was employed, at U_∞ = 10 m/s. The position of the vortex was changed to three different locations with respect to test section center line. Vortex position A corresponds to vortex generator at Z = 3.52 cm, vortex position B to Z = 4.79 cm, and vortex position C to Z = 6.06 cm. In the third step, a freestream velocity of 15 m/s, with M = 0.47 were employed, in order to study the effect of blowing ratio. In the fourth part, a blowing ratio of M = 1.26, at U_∞ = 10 m/s was employed, in order to study the effect of high blowing ratio. Here, information was also obtained on changes in boundary layer structure which occurred for higher blowing ratios.

1. Freestream 10 m/s. Blowing ratio. M = 0.68. Repeat of Joseph data.

These heat transfer measurements were obtained to compare with those of Joseph, [Ref. 3]. He first showed that embedded vortices cause significant changes in heat transfer in film cooled turbulent boundary layers. This finding is also evident from the present study. To obtain the present data set, vortex generator #2 was placed at position B, and all 13 injection holes were used for film cooling. Results are presented in Figures 31a.-31.f, and in Figure 32. Overall effects are now discussed. The embedded vortex produces a thicker boundary layer in the upwash side thus augmenting the film cooling protection. Near the downwash side, the boundary layer is locally thinner, and the protection provided by the film cooling is minimized. The undercooled region produced on the upwash side vortex is very persistent not only in the down stream direction, but also in the spanwise direction. Here, Stanton numbers are .5 to 5.5 percent lower than those in boundary layers with film cooling only.

Figures 31.a-f., show the spanwise variation of the Stanton number ratios, St/Sto with film cooling and embedded vortex. Here, St is the local Stanton number and Sto is the Stanton number for the same location and free stream velocity but without film cooling and without embedded vortex. A St/Sto = 1 thus indicates an undisturbed thermal boundary layer. As shown in the set of Figures 31.a - 31f, the lowest St/Sto is 0.55 at X = 1.15 m, X/d = 7.35, and the maximum is 1.025 at X = 2.00 m, X/d = 96.59. If these results are compared with those of Joseph [Ref. 3. : pp. 97-103], a general qualitative agreement can be observed. Differences are due to improvements in the present heat transfer test plate, especially better spanwise temperature resolution and more uniform heat flux.

Figure 32. shows surface contours of St/Stf. Here, St is the local Stanton number, and Stf is the local Stanton number at the same location with film cooling but without embedded vortex. A very steep heat transfer gradient is present which is near the same location as the axis of the vortex.

At the upstream end of the plate this gradient is located near Z = - 2 cm. A hot spot is present at larger Z, and a region of high heat transfer is present at smaller Z on the upwash side of the vortex. These results are in qualitative agreement with those of Joseph [Ref. 3.: pp. 104], except the most significant hot spots are located further downstream in the present study.

2. <u>Free stream 10 m/s, Blowing ratio, M = 0.98</u>

In order to achieve the blowing ratio used for this data, 9 injection holes were employed for film cooling. Here, injection covers the midspan of the test plate from -12 cm < Z < 12 cm. Vortex generator #2, was placed 60 cm upstream of the row of injection holes, at vortex position A, B and C, to investigate the effect of the vortex position with respect to film cooling injection holes. Results are presented in Figures 33 - 42.

a. Data overview.

Spanwise variations of St/Sto for the vortex position B are shown in Figures 33a-33f. These data show the same overall qualitative trends as measurements at 10 m/s and M = 0.68 (Figure 31). With embedded vortex, the normalized Stanton numbers in 33a-33f are increased on the downwash side and decreased on the upwash side relative to the boundary layer with film cooling only. The only significant quantitative difference between these results and those in 31 are higher St/Sto at X/d = 17.48 and at X/d = 33.59 resulting from a less effective film cooling at M = 0.98.

b. Effect of downstream development.

In Figures 33a - 33f, a double peak of St/Sto is present at X/d = 17.48, and at X/d = 33.59. As the boundary layer develops further downstream, one peak becomes smaller (Z ≈ -2.0 cm), and one increases in magnitude (Z ≈ 3.0 cm), until at X/d = 54.59 the St/Sto distribution shows one large peak. This St/Sto peak increases in magnitude to become equal to 1.05, or about 34 percent greater than the St/Sto with film cooling only. St/Stf data in Figure 34, indicate that this hot spot covers an area along the center and spanwise downstream half of the plate. Such behavior evidences highly three-dimensional interactions within the boundary layer.

Figure 34 shows the St/Stf distribution for vortex position B and M = 0.98. A steep heat transfer gradient is evident along the the length of the test surface, which corresponds to the path of the vortex center. This path is at an angle to the streamwise direction, moving to smaller Z as the vortex convects downstream. Compared to results for M = 0.68 in Figure 32, the heat transfer gradient is steeper, and a larger region where St/Stf is less than 1 is present over the top third of the test plate. This follows since a larger amount of coolant is swept by the vortex at higher blowing ratio.

For Z values smaller than those along the location of the vortex center, Figure 33 shows values of Stanton ratios which are about 5 per cent lower than those with film cooling only. The same trend is evident in Figure 34, where almost 1/3 of the plate shows 0.90 < St/Stf < 0.98. These locations are on the upwash side of the vortex, where film coolant seems to be pushed and spread over a very large portion of the plate. Similar phenomena were observed by Goldstein and Chen, [Refs. 2 and 7], in a study of film cooling of a turbine blade with injection through one and two rows of holes in the near-endwall region.

Figures 35a- 35d show the T - T_∞ temperature field as it develops downstream at X/d = 41.9, 82.9, 109.2 and 147.0. For these tests, film cooling jets were heated to 51 ºC without providing any heat to the test plate. Thus, the temperature field shows how fluid from the film cooling holes is convected and distorted by the vortex, where higher temperatures indicate greater amounts of coolant. The most dramatic effect evident from Figures 35a-d occurs on the upwash side of the vortex, where coolant is lifted away from the thermal boundary layer which is ordinarily about 4 cm thick with film cooling. At X/d = 41.9 fluid affected by the film cooling is 6.5 cm from the surface, and at X/d = 147.0, the temperature field is more than 10 cm from the surface. Also, evident are cooler temperatures with downstream development resulting as coolant is convected and diffused. The areas indicated by low St/Sto and St/Stf values correspond to $0. < Z < -5.$ cm, where coolant seems lifted from the surface to accumulate in one small area. Figures 35a-d clearly show how the coolant is pushed and spread over an area by the vortex, and how this area increases in size, as the flow convects downstream.

On the downwash side of the vortex, secondary flows cause freestream fluid to be located very near the wall. Here, the thermal boundary layer is greatly thinned and very little effect of the film cooling remains. From Figure 35c for X/d = 82.94, the local hot spot is located at to $0 < Z < -5$ cm, which seems to indicate that film coolant is moved to other locations in the boundary layer by the vortex.

In Figure 36, the temperature field is presented for an experiment in which the heat transfer plate is heated to 40 ºC and film coolant to 51 ºC. The temperature difference contours show the same qualitative trends as in Figure 35. In particular, the positions of many temperature gradients and the dimensions of the area affected by the vortex are about the same. Results in Figure 36 are different from those in 35 since : (1) it is not as easy to discern which part of the temperature field is due to film cooling only, (2) overall temperature differences are larger, and (3) local hot spots corresponding to film cooling locations are more easily discernable every 3 cm starting at $Z = -12$ cm.

The temperature gradient at $Z = -14$ cm, corresponds to the spanwise edge of the film cooling for blowing rate of $M = 0.98$.

c. Effect of spanwise vortex position.

To study the effect of the vortex position relative to the film cooling injection, the vortex position was changed from A to B to C locations. Distributions of St/Sto are shown in Figures 33, 37 and 40, distributions of St/Stf in Figures 34, 38, 41 and distributions of $T - T_\infty$ are given in Figures 35, 39 and 42. Regardless of the vortex position, the following phenomena were observed :(1) on the upwash side of the vortex a low heat transfer region exists, where St/Sto is less than for a film cooled turbulent boundary layer only, (2) on the downwash side of the vortex a wide region of high St/Sto exists, because of thinning of the boundary layer by the vortex, and (3) at $X/d = 7.4$, the film cooling dominates the flow and the vortex seems to have very little effect on the heat transfer.

Comparisons of Figures 33, 37 and 40, show that for low X/d values up to 17.5, a double peak in the St/Sto distributions is present for vortex positions A and B. At X/d = 33.6 and further downstream for vortex positions A and C, the double peak in St/Sto distributions starts to grow spanwise enlarging the portion of the plate covered by the hot spot. In these cases, St/Sto peaks are not as high as for the vortex position B case (Figure 33). A maximum St/Sto of 1.05 was observed for the vortex position B at X/d = 96.6, or about 30 percent greater than the St/Sto with film cooling only. Low St/Sto and St/Stf regions on the upwash side of the vortex were observed for all three vortex positions. These were less significant for position C, while varying between 2– 6 percent for the other two vortex positions.

St/Stf distributions from Figures 34, 38 and 40 show that the location, shape and size of the hot spot vary depending on the vortex spanwise position. In Figure 34, for vortex position B, this hot spot is located from the middle length of the plate, growing in size as the vortex develops downstream. For vortex position A, the hot spot is shifted upstream and is not as wide, nor as long as for position B. For vortex position C, the hot spot begins early upstream but persists further downstream, but it does not reach the end of the test section, and it is very narrow. A region of high heat transfer is observed in all three cases, but this area is larger for vortex position A, covering about 2/3 of the test plate. A heat transfer gradient is aligned along the vortex center for all three vortex positions, but it is steeper and more persistent for vortex position B. The region of low heat transfer, where St/Stf is less than 1, is largest for position B and smallest for position C.

Figures 35, 39 and 42 show the T - T_∞ temperature field in degrees C for X/d = 41.9. For these results the heat transfer plate was maintained at the freestream temperature and the coolant was heated to 51 ºC, (unheated plate). Overall qualitative trends for all three vortex positions are similar: coolant is lifted away the wall by the upwash side of the vortex, on the downwash side of the vortex, secondary flows cause the freestream fluid to be located very near the wall, making the boundary layer very thin and minimizing the effect of the film cooling. A significant spanwise gradient in temperature exists which is located near the vortex core, and extends about 5 cm from the wall. As expected, the spanwise location of this gradient changes with vortex position. The effect of the downwash side of the vortex is most significant for vortex position B. For this case Figure 35a shows that the boundary layer is thinned such that it only extends 2 cm from the wall. Significant changes also occur near the upwash side of the vortex where secondary flows from the vortex convect film coolant away from the wall. The most significant changes in this part of the flow occur for vortex position C.

3. Free stream 15 m/s, blowing ratio, M = 0.47. Effect of low blowing ratio.

Measurements were made at U_∞ =15 m/s, with a blowing ratio M of 0.47, in order to determine the effect of low blowing ratio on heat transfer. These tests were also conducted to obtain additional verification of general conclusions from results obtained at 10 m/s and M = 0.98 blowing ratio. For these tests, vortex generator #2, was used at positions A, B and C.

Results are shown in Figures 43 – 48. Distributions of St/Sto are shown in Figures 43, 45, and 47, and distributions of St/Stf are given in Figures 44, 46 and 48.

From a general qualitative point of view, the results at 15 m/s and M = 0.47 are similar to those of 10 m/s and M = 0.98. The most significant quantitative difference is that St/Sto maxima are higher, and St/Sto minima are lower for M = 0.47. In addition, the peaks of local heat transfer seem to increase more rapidly with downstream distance. At the downstream end of the plate where X/d = 96.6, local St/Sto for M = 0.47 may be as high as 1.12 compared to about 1.05 for M = 0.98. The rapid downstream growth of these maxima becomes more apparent when one considers the film cooled boundary layer alone, since St/Sto ratios at M = 0.47 are lower than those at M = 0.98.

At M = 0.47, the effect of changes in the spanwise position of the vortex are much less significant than at M = 0.98. At higher blowing ratio, many quantitative changes in the local heat transfer result as the vortex position is changed. In particular, primary and secondary peaks of St/Sto were observed at X/d = 17.5 and 33.6 for vortex position B, and X/d = 54.6 and 75.6 for vortex position C. At the M = 0.47 blowing ratio, the shapes of St/Sto distributions for different vortex positions are very similar, especially for X/d = 54.6, 75.6 and 96.6. Generally, quantitative changes for M = 0.47 occur only in the spanwise locations of the St/Sto maxima and minima. At X/d = 7.4, the effect of the vortex position changes is minimal and the spanwise heat transfer rates are mostly affected by the film cooling. At X/d = 17.5 both primary and secondary St/Sto peaks are present for all three vortex positions. The only significant St/Sto changes with vortex position occur at X/d = 33.6 where a small secondary St/Sto peak is observed when the vortex is located at position A only. Such behavior indicates that the effects of film cooling at M = 0.47 do not persist as far downstream as at higher blowing ratios. In addition, the vortex seems to more completely dominate the flow field as the blowing ratio decreases.

4. **Free stream 10 m/s, blowing ratio, M = 1.26. Effect of high blowing ratio.**

In order to study the effect of high blowing ratio on the film cooled turbulent boundary layer with embedded vortex, measurements were made at U_∞ = 10 m/s. with M = 1.26 and the vortex at position B. Results are shown in Figures 49- 52.

The St/Sto and St/Stf data in 49 and 50 show the same overall qualitative trends shown by measurements at M = 0.98, 0.47, and 0.68 : augmented heat transfer near the downwash side of the vortex and reduced heat transfer near the upwash side. Also, at X/d = 7.4, film cooling rather than the vortex dominates the spanwise variation of heat transfer. The most important quantitative differences between these results and those at other blowing ratios are the magnitudes of St/Sto with film cooling only. Figure 26 shows M = 1.26 St/Sto data at 10 m/s which is, on the whole, greater than data at M = 0.68, but just lower than results for M = 0.98. Results presented in Figure 49 reflect the same overall trends.

Details of the spatial variations of normalized Stanton numbers in Figures 49 and 50 are now discussed. At X/d = 17.5, 33.6 and 54.6 double peaks in St/Sto distributions are present. These seem to result from interaction between cooling jets and the vortex, occurring at Z = -2– -3 cm and at Z = 2 – 3 cm.

Contours of $T - T_\infty$ (ºC), at X/d = 41.9 in Figure 51, show that the peak near +2–3 cm results from the downwash of free stream fluid to near wall regions by the vortex. The corresponding St/Sto peak increases in magnitude as the the boundary layer convects downstream reaching magnitudes as high as 1.05 at X/d 75.6 and 96.6. At these downstream locations, augmented St/Sto cover a large spanwise portion of the film cooled test surface extending from -5 cm to +5 cm (Figures 49 and 50). Magnitudes of St/Sto maxima in these hot spots at M = 1.26 are about the same as those at M = 0.98.

Figure 50 shows the heat transfer rate over the test plate in terms of St/Stf. Here, the hot spot is located from X/d = 54.6 to X/d = 96.6. This region is very large, confined to the downwash side of the vortex. The temperature gradient on the upwash side of the vortex is not very steep in some streamwise locations. A comparison between Figure 50 and Figure 32 where M = 0.68, show that, the hot spot is present at the same spanwise and streamwise location in both cases, but in 50 the hot spot is thinner, and the area of low St/Sto on the upwash side of the vortex is larger.

Temperature contours at X/d = 41.9 in Figure 51, show that the St/Sto peak at Z = -2–-3 cm. lies beneath a region of large temperature gradients very near the vortex center. Figure 52d. shows strong secondary flows at this location which apparently sweep coolant further from the vortex center (to smaller Z), such that it collects near $-5 < Z < -8$ cm. Contours of vorticity magnitude, calculated from these secondary flow vectors for M =

1.26 vortex position B, are shown in Figure 52e. These show that (1) the core of the primary vortex is located at Z = -2 cm., Y = 3.5 cm., and (2) that the secondary peak in heat transfer is not a result of any form of secondary vortex. Augmented mixing is initially created by the secondary flows beneath the vortex center, resulting in locally higher heat transfer. This secondary peak shown in Figure 49 at X/d = 17.5, 33.6 and 54.6 eventually becomes indistinguishable at larger X/d equal to 75.6 and 96.6. The secondary peak is bigger and more persistent than at M = 0.98, indicating that the shear layer interaction causing higher heat transfer is dependent upon the mass flux of film cooling.

Another important feature of the results in Figure 51 is the gradient of heat transfer present at Z = -10— -12 cm. for 0 < Y < 5.0 cm. This gradient is present at the edge of the film cooled region : coolant was injected from only 7 holes extending across a span from -9 cm. to +9 cm.

Additional flow field information at X = 1.48 m, X/d = 41.9 is given in Figures 52a.–c for 10 m/s, M = 1.26 and vortex position B. Data was taken using a five-hole pressure probe, [Ref. 1.: pp. 14-15], to measure pressure at 800 points in a spanwise plane in order to further investigate the effect of the high blowing ratio in the turbulent boundary layer with embedded vortex. These results are consistent with those of Evans, [Ref.1]. They show : (1) that high velocity, high total pressure fluid is swept near the wall on the downwash side of the vortex, (2) a velocity and total pressure deficits exist at the center of the vortex, and (3) low velocity fluid is swept away from the wall near the upwash side of the vortex. Vorticity contours in 52e. show a large region of negative vorticity in the upwash region,($-8 < Z < -4$ cm). In addition, two other regions of negative vorticity result from the secondary flows present.

IV. SUMMARY AND CONCLUSIONS.

Heat transfer measurements were made of turbulent boundary layers with film cooling and embedded vortices for freestream velocities of 10 and 15 m/s . To obtain the data, a heat transfer test surface was designed and developed to provide constant heat flux over its area, with 126 embedded thermocouples for detailed spanwise resolution of temperature. Extensive qualification tests show that the surface gives excellent spatially resolved heat transfer coefficients over an area of 43.815 cm x 1111.76 cm.

Baseline measurements show excellent agreement with Stanton number correlations for a flat plate with constant wall heat flux and unheated starting length. Results of turbulent boundary layer with embedded vortex show excellent agreement with Joseph, [Ref. 3.], and with the literature. Results of turbulent boundary layer with film cooling at different blowing ratios show expected trends, consistent with the data of Goldstein and Yoshida, [Ref. 18].

Longitudinal vortices cause significant changes in heat transfer and structural characteristics of film cooled turbulent boundary layers. Heat transfer augmentations as large as 30 percent, and reductions as high as 10 percent were observed to persist as many as 23 boundary layer thicknesses or 96 film cooling hole diameters downstream of film cooling injection locations. The effects of the embedded vortex on heat transfer in film cooled boundary layers are significant and important :

1.) Near the downwash side of the vortex the heat transfer is augmented, vortex effects totally dominate the flow behavior, and the effects of the film cooling are negated. " Hot spots " will exist for blowing ratios ranging from 0.47 to 1.26, and vortex circulation to freestream velocity ratios of about 1.6 cm.

2.) Near the upwash side of the vortex, the coolant is lifted off the wall and pushed to the side of the vortex, increasing the surface area protected by the film cooling.

3.) Changing the position of the vortex with respect to the film cooling jets results in significant local quantitative changes in heat transfer occur, even though the overall qualitative trends remain unchanged.

4.) Near film cooling injections locations for X/d up to 7.4, the film cooling dominates the flow behavior and the vortex seems to have very little effect on spanwise variations of heat transfer.

Results (1) and (2) are mostly a consequence of the intense secondary flows produced in the plane perpendicular to the axis of mean vorticity. These results are consistent with those obtained by Joseph, [Ref. 3.: pp. 54], and Evans, [Ref. 1.: pp. 28].

At high blowing ratios:

1.) A double peak in the St/Sto distributions was observed to occur between X/d = 7.4 and 54.6.

2.) The change in spanwise position of the vortex in relation with the film cooling jets affects the magnitude, shape and spanwise position of St/Sto peaks, and

3.) Secondary St/Sto peaks become higher in magnitude and more persistent with respect to downstream development as the blowing ratio increases. The double peaks observed at M = 1.26 were not due to a secondary vortex, but to an interaction between the vortex and film cooling which depends on blowing ratio.

At low blowing ratios:

1.) The change in spanwise position of the vortex has very little effect on local heat transfer distributions except to change the locations of Stanton number minima and maxima, and

2.) St/Sto distributions exhibit only one peak which increases in magnitude with downstream development.

It is recommended that flow visualization study of the interaction of the vortex and film cooling be conducted in order to enhance the understanding of some of the complex phenomena observed during the course of this study.

APPENDIX A

FIGURES

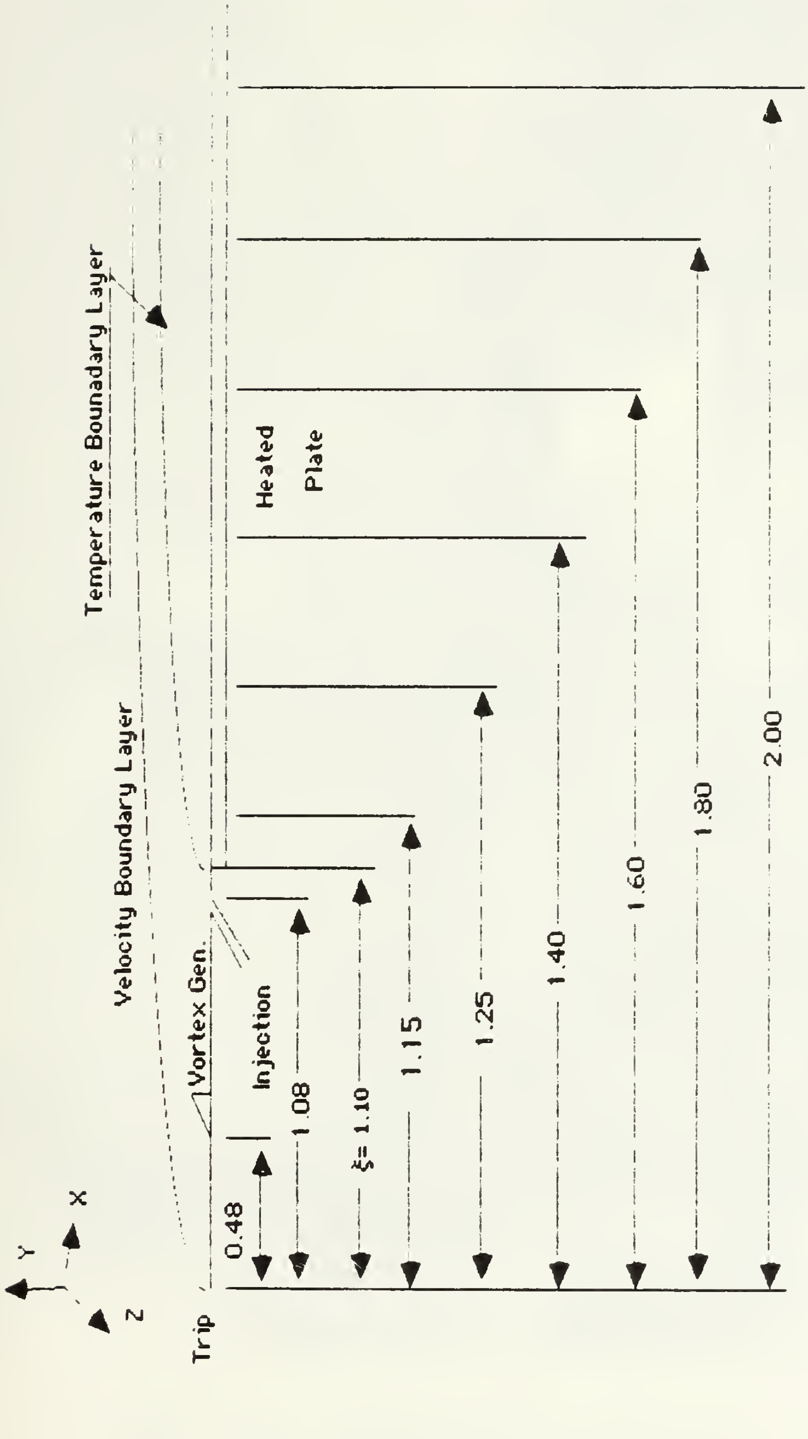

ALL DIMENSIONS IN METERS

Fig. 1. Coordinate System of the Test Section

VORTEX GENERATOR #2 POSITION

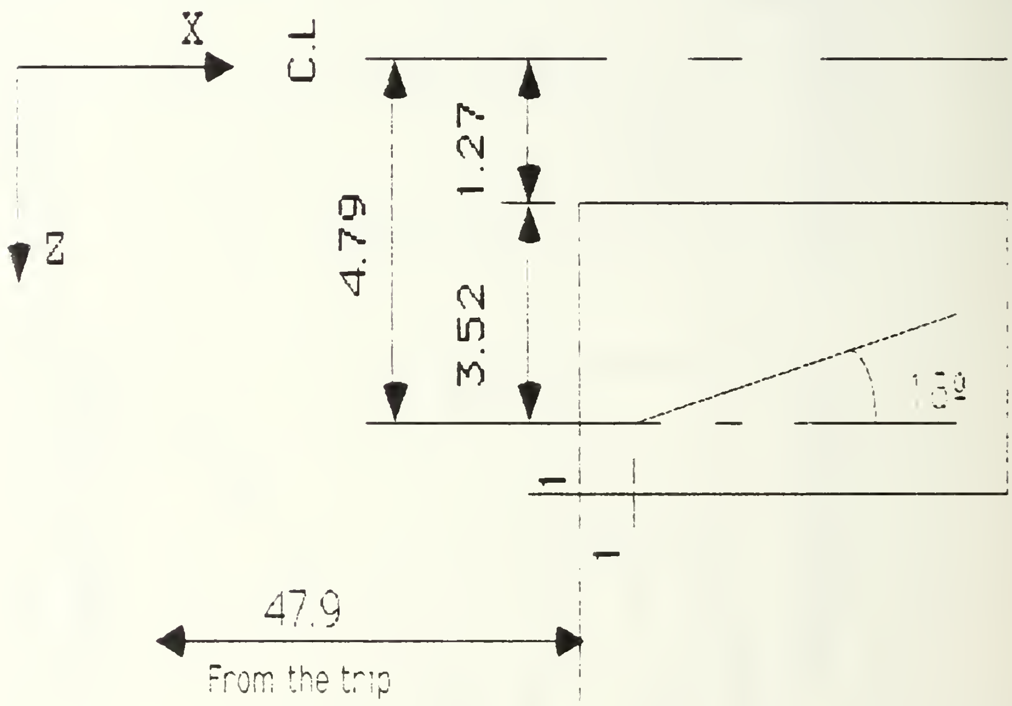

All Dimensions in cm.

Fig. 2. Vortex Generator Position.

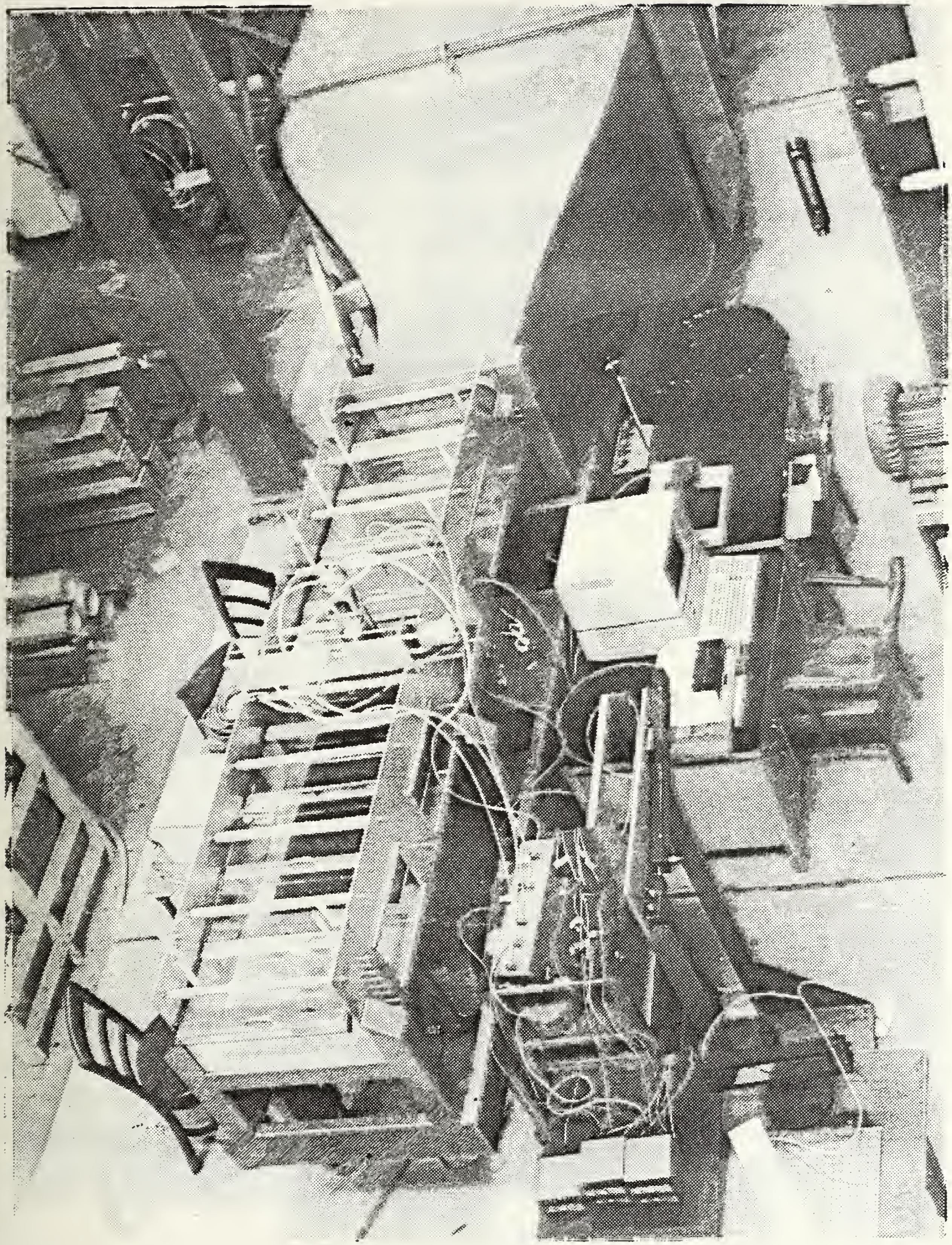

Fig. 3a. Experimental Set-up

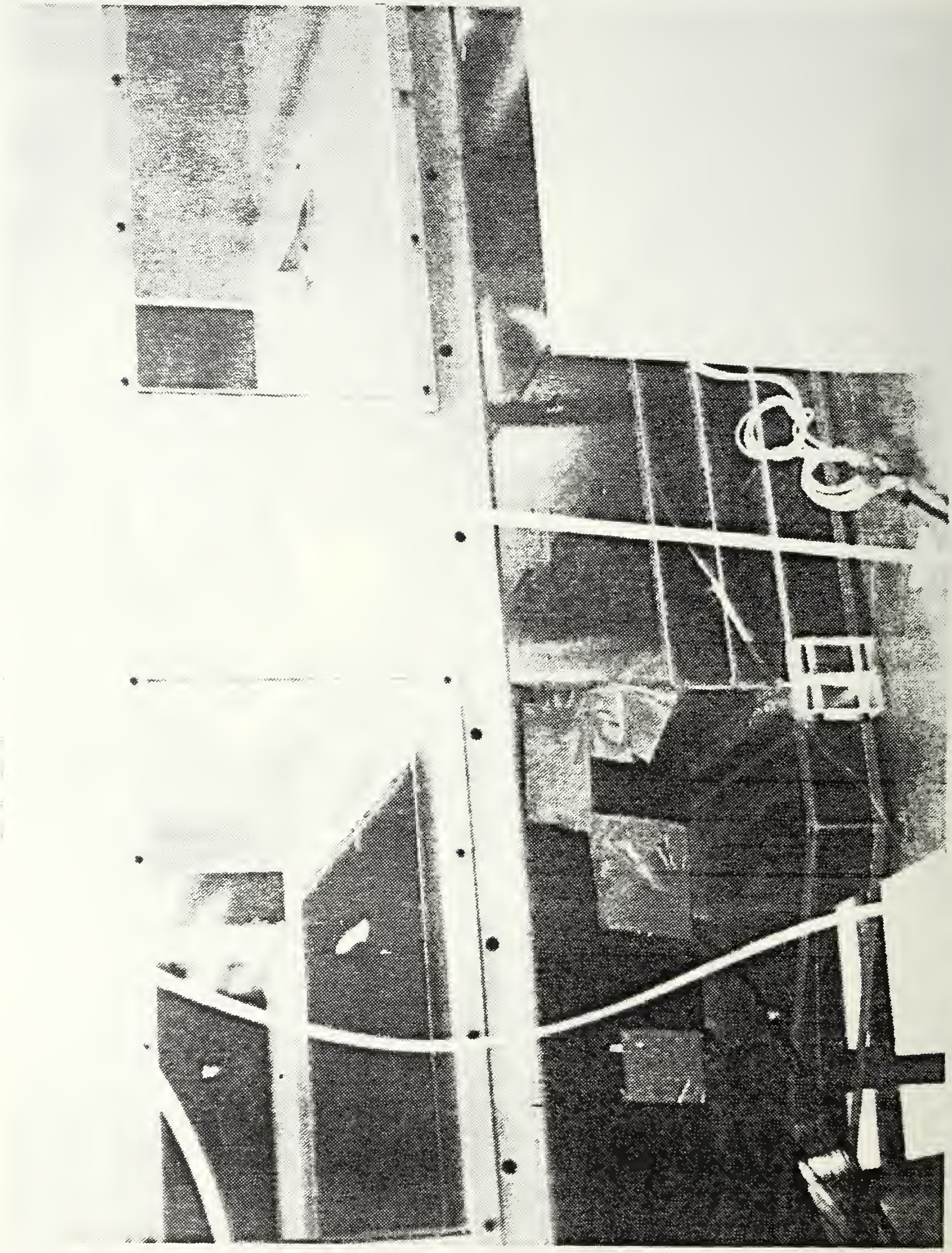

Fig. 3b. Detail of the Injection Plenum and Vortex Generator

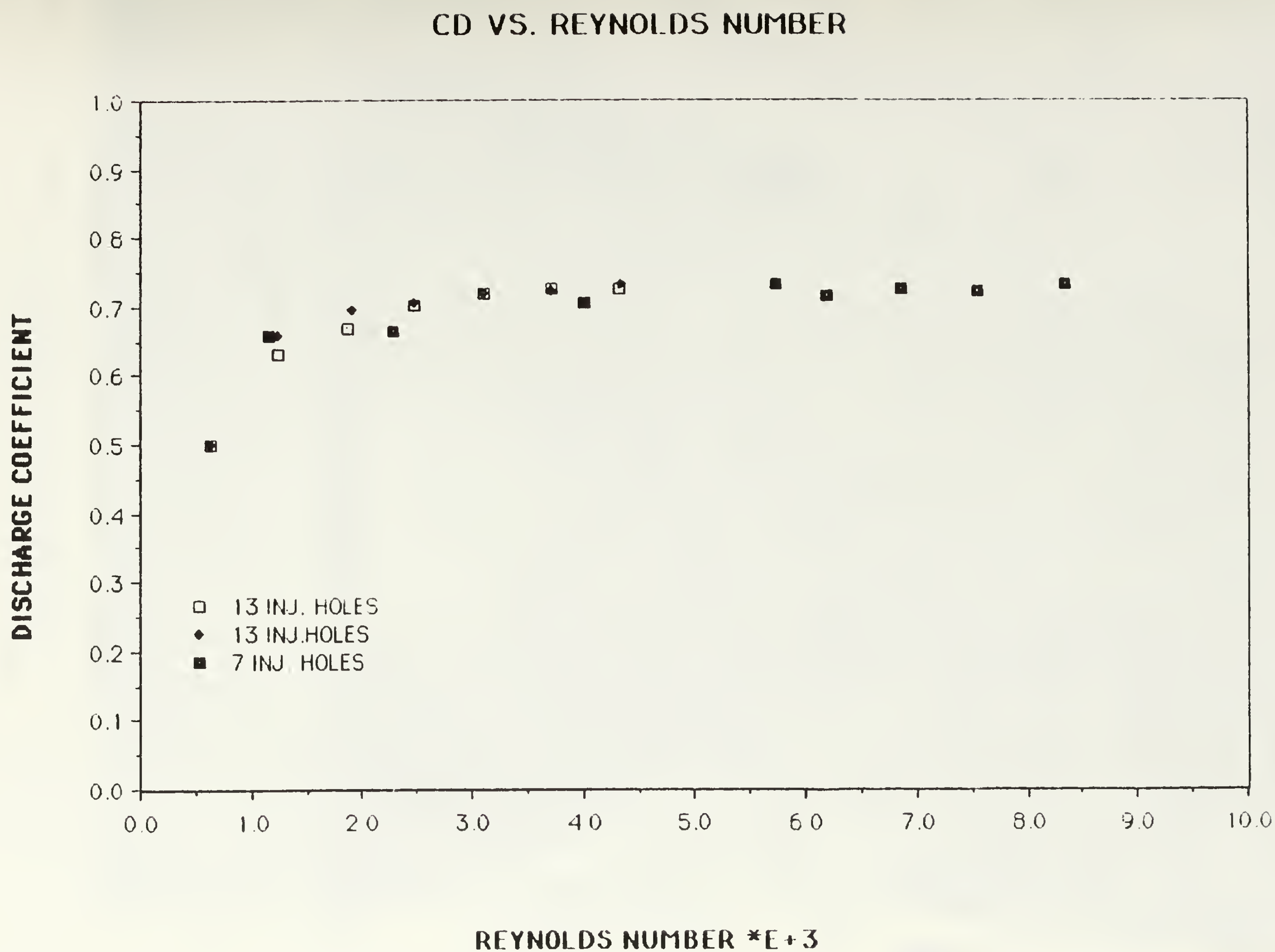

Fig. 4. Discharge Coefficient vs. Reynolds Number

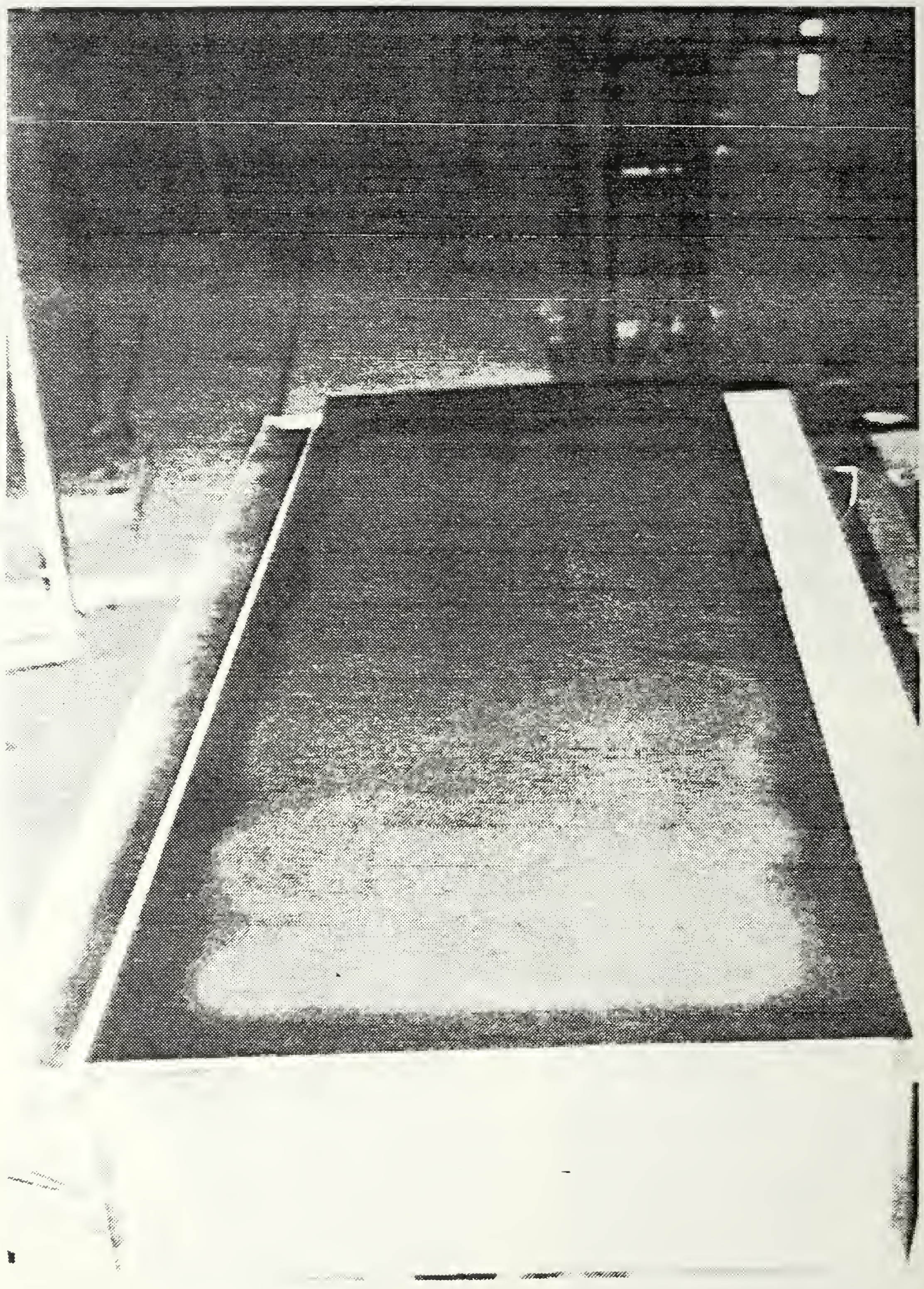

Fig. 5a. Heat Transfer Test Plate

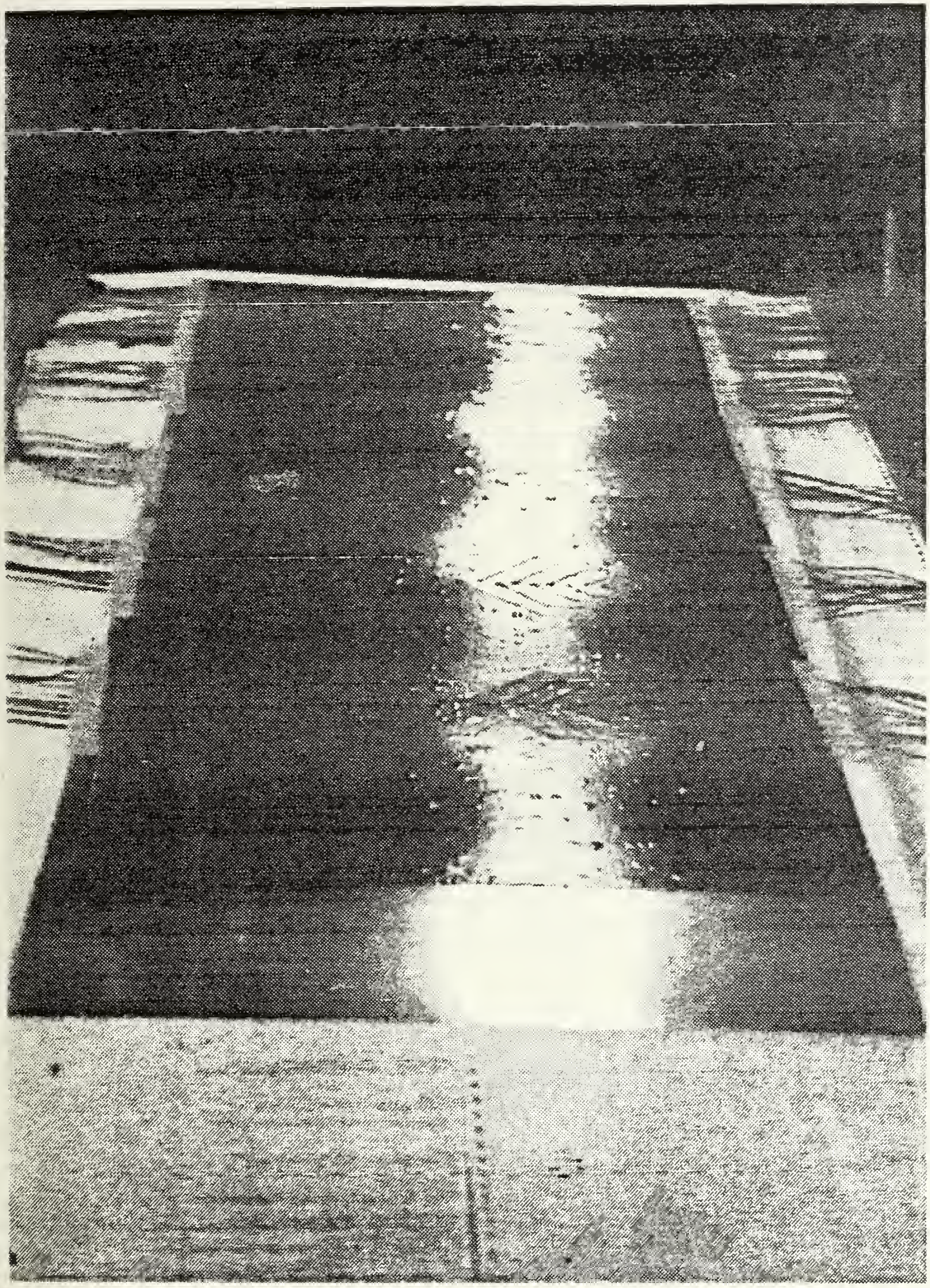

Fig. 5b. Detail Of Heat Transfer Plate

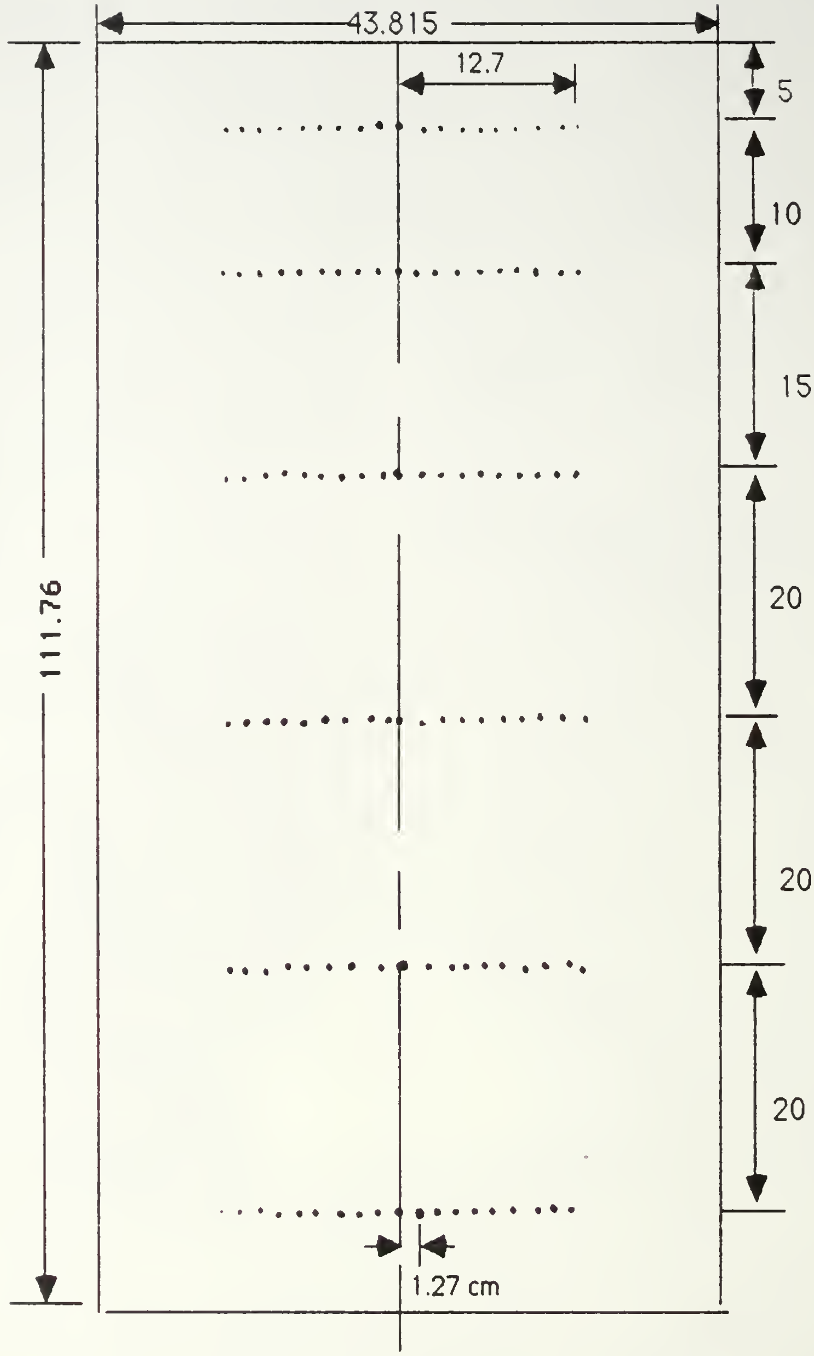

All dimensions in cm.

Fig. 6. Thermocouple Placement on Plate

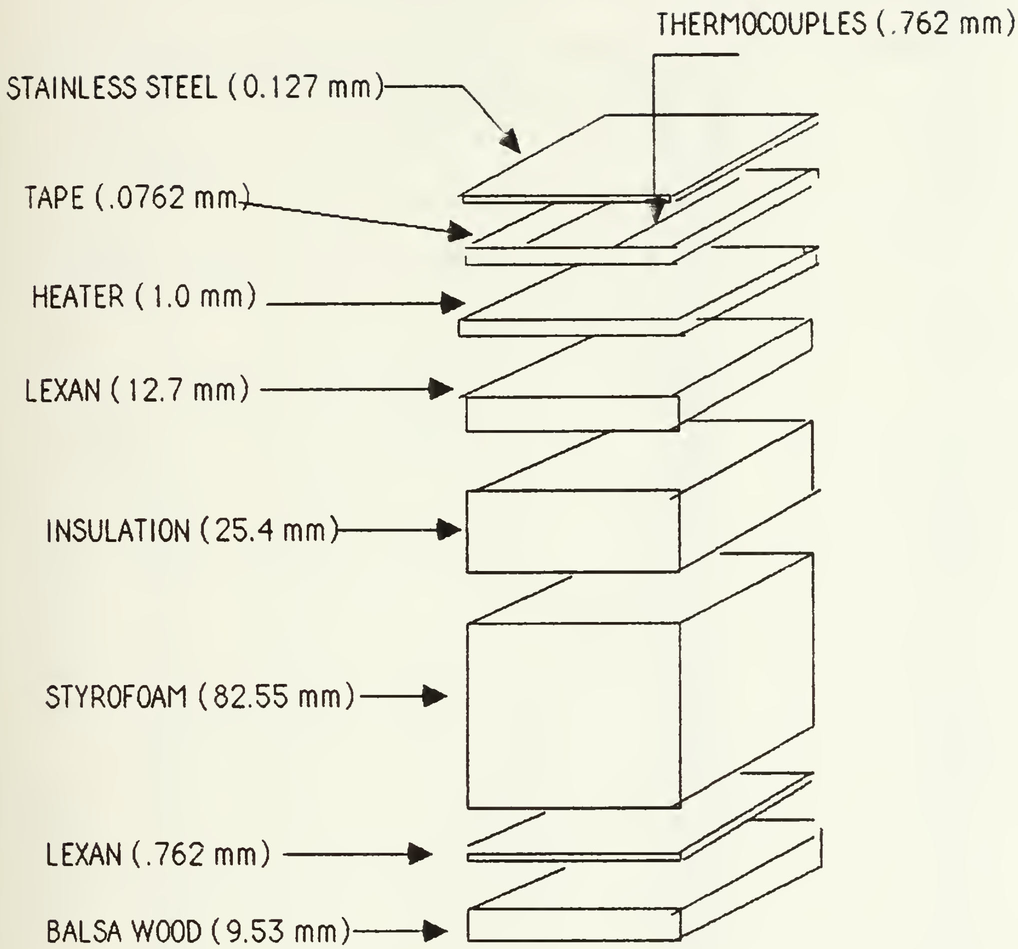

Fig. 7. Cross Section of Test Surface

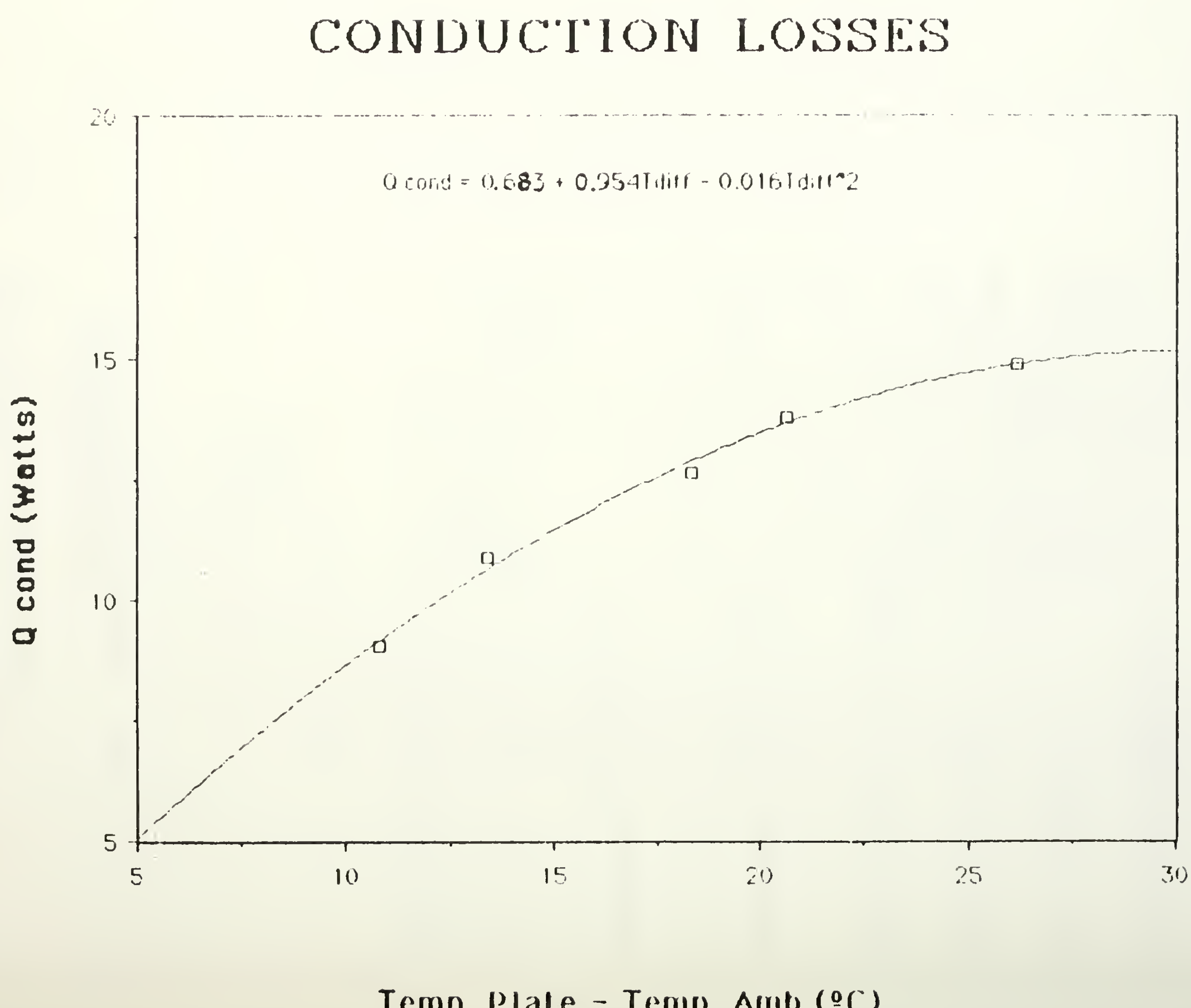

Fig. 8. Conduction Losses

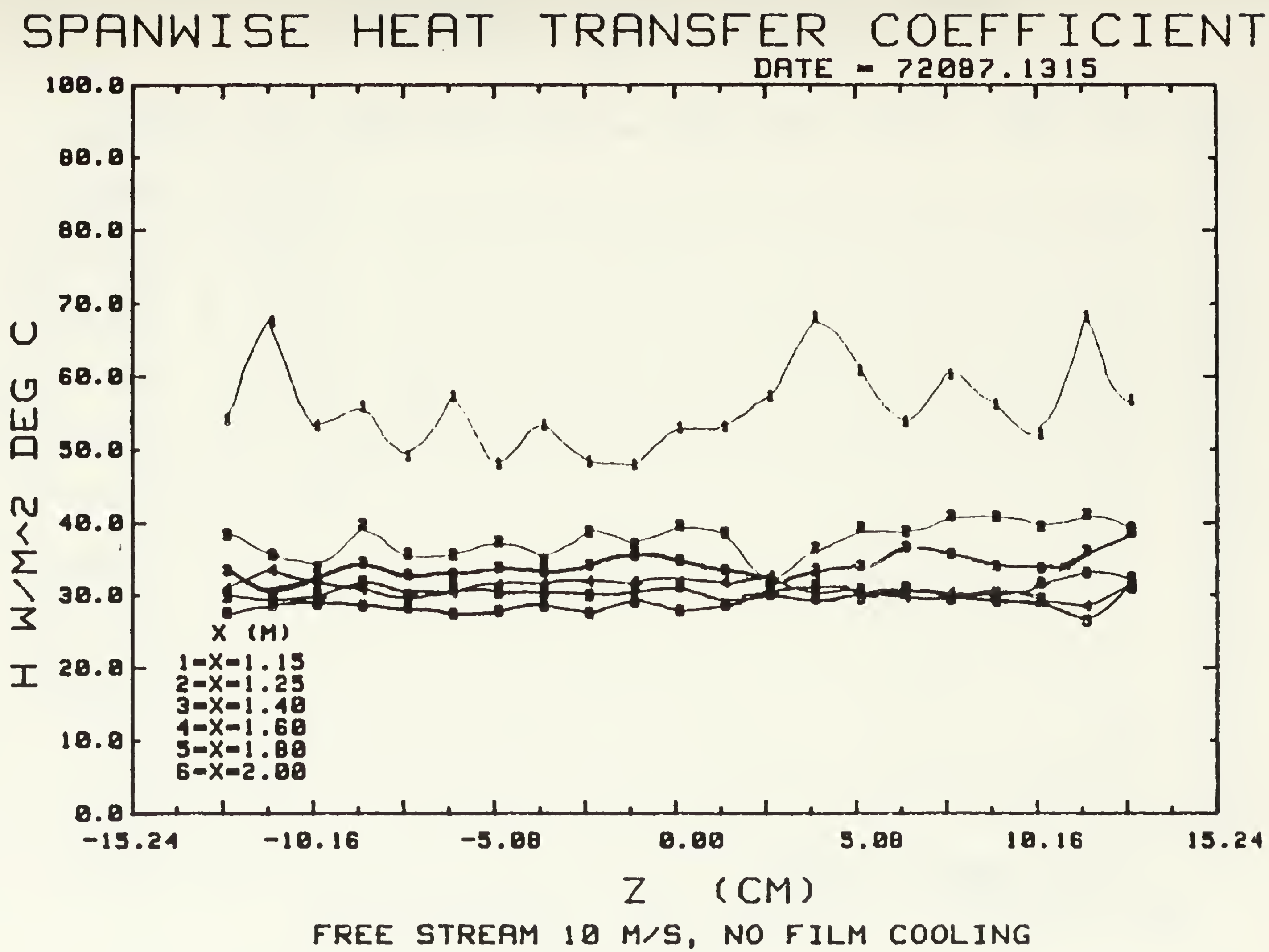

Fig. 9. Spanwise Variation of Heat Transfer Coefficients.

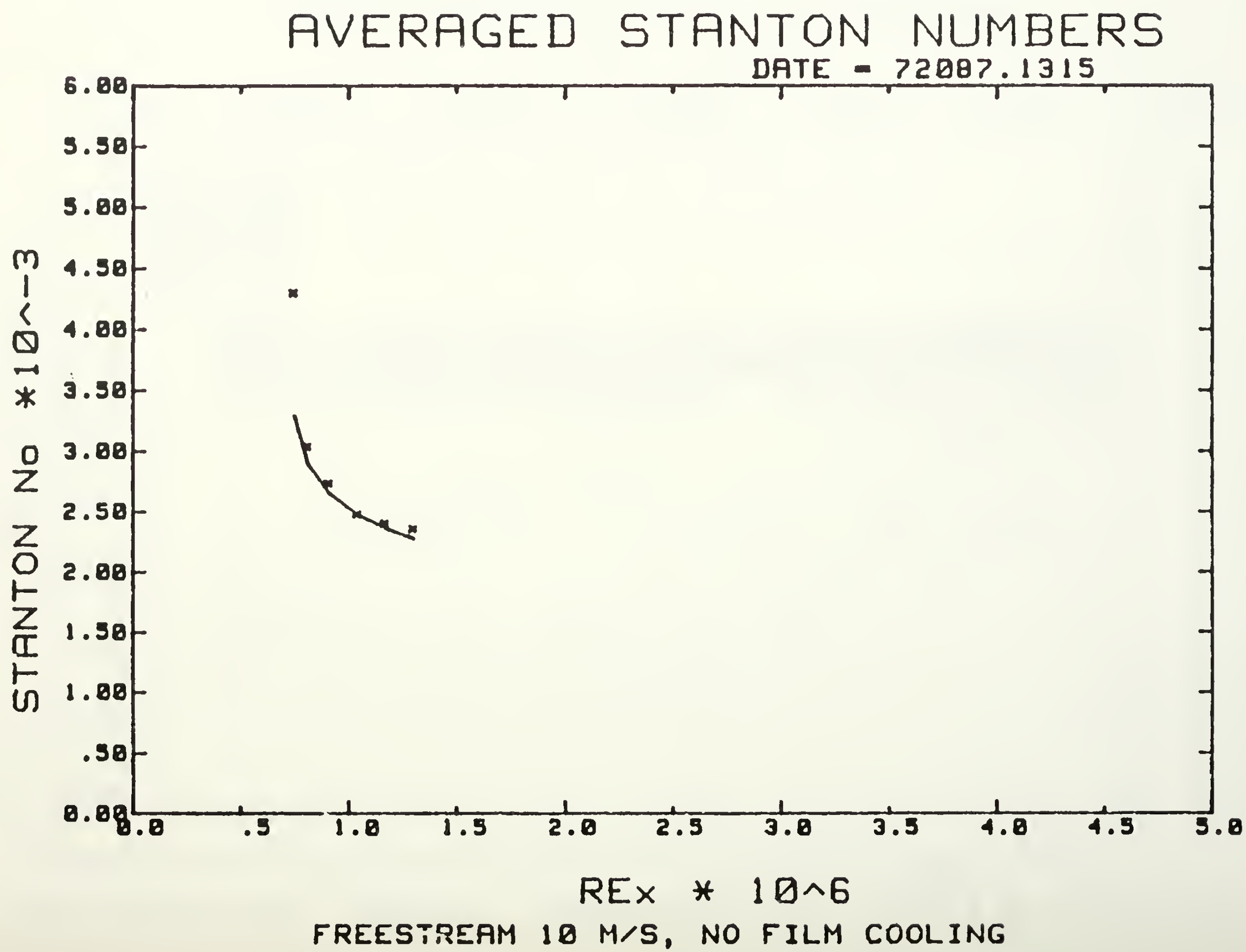

Fig. 10. Spanwise Averaged Stanton Numbers.

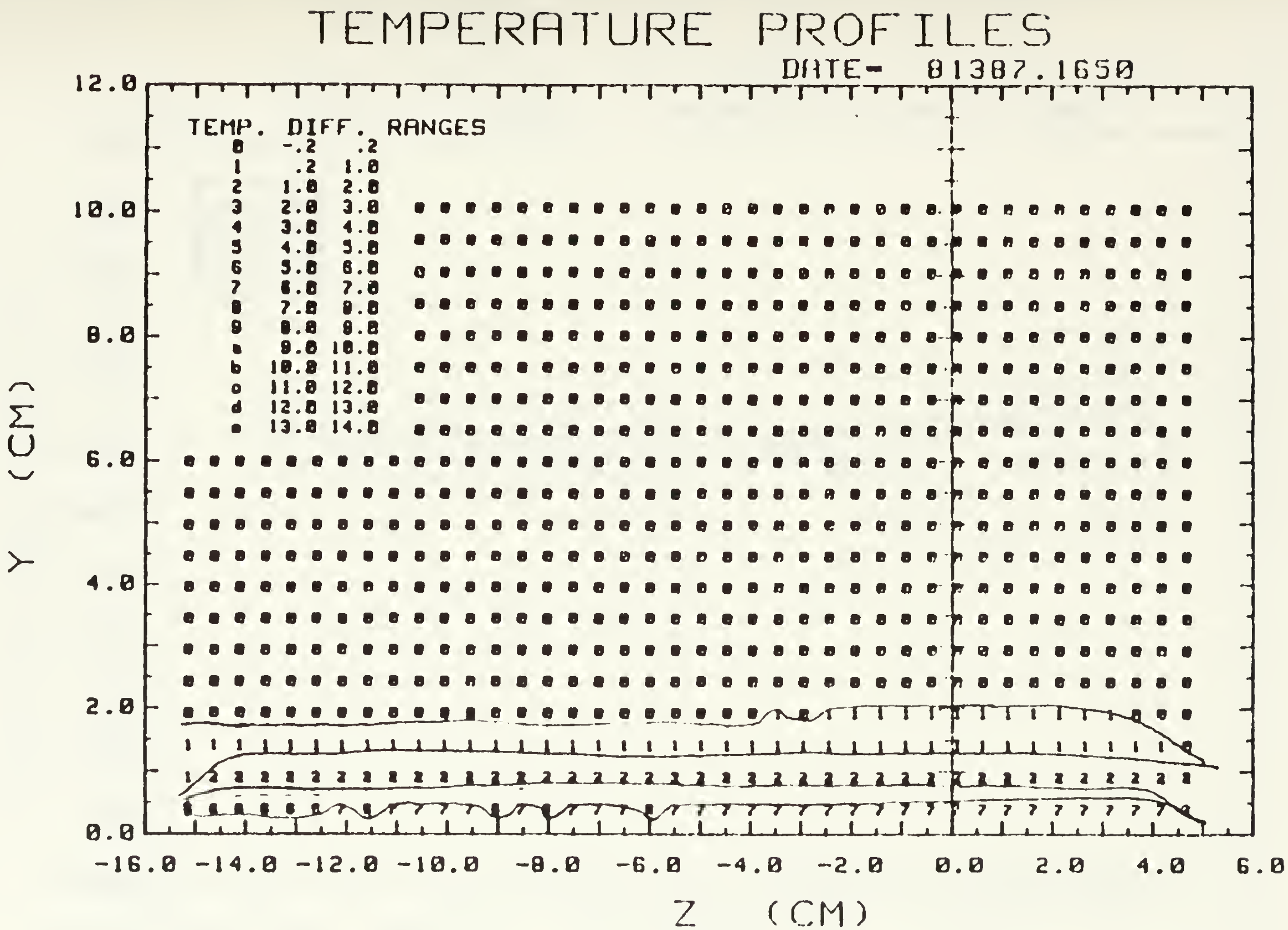

Fig. 11. BOUNDARY LAYER, 10 M/S NO FILM COOLING
X=1.480 M, HEATED PLATE, NO VORTEX

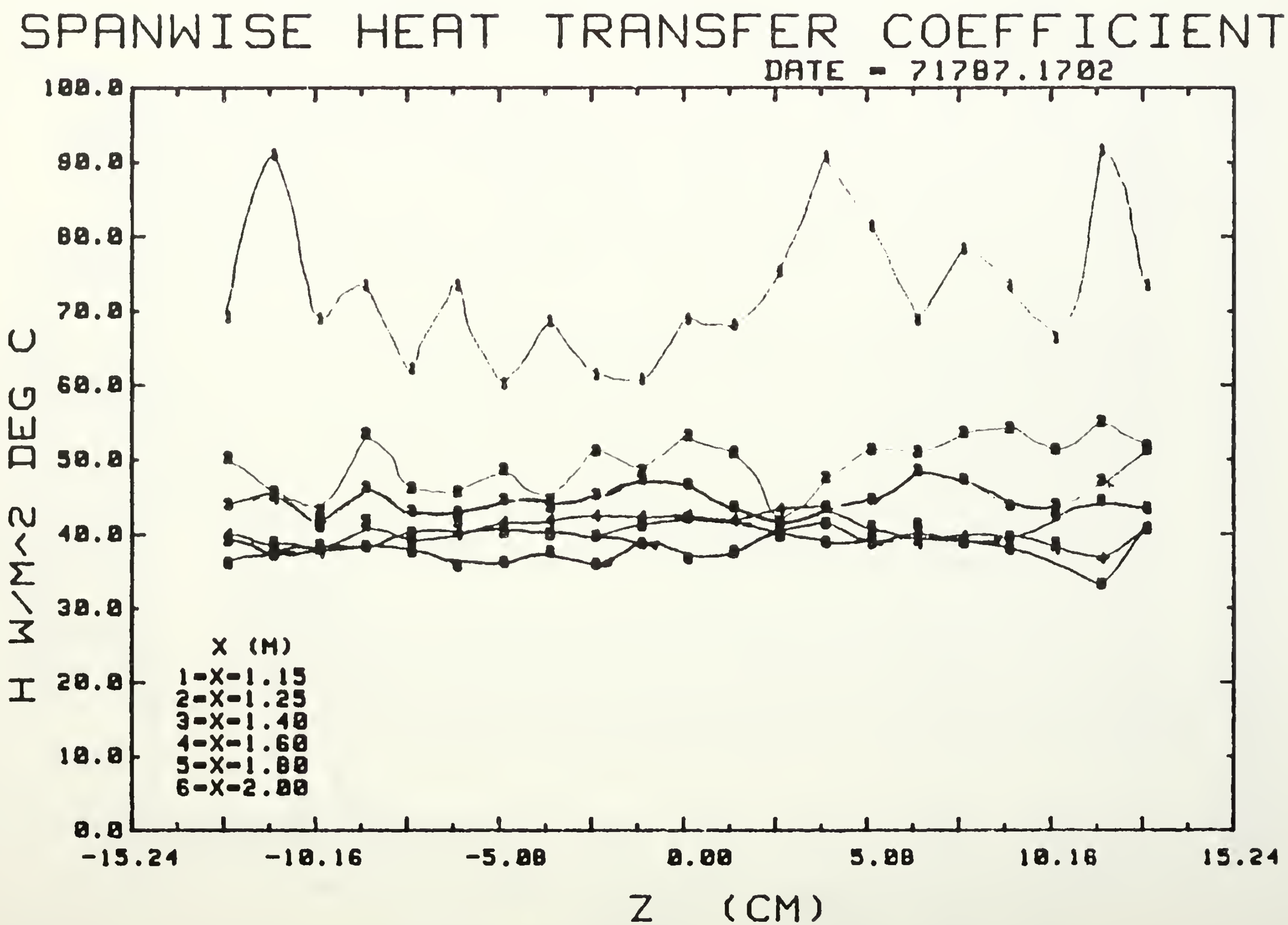

FREE STREAM 15 M/S, NO FILM COOLING

Fig. 12. Spanwise Variation of Heat Transfer Coefficients.

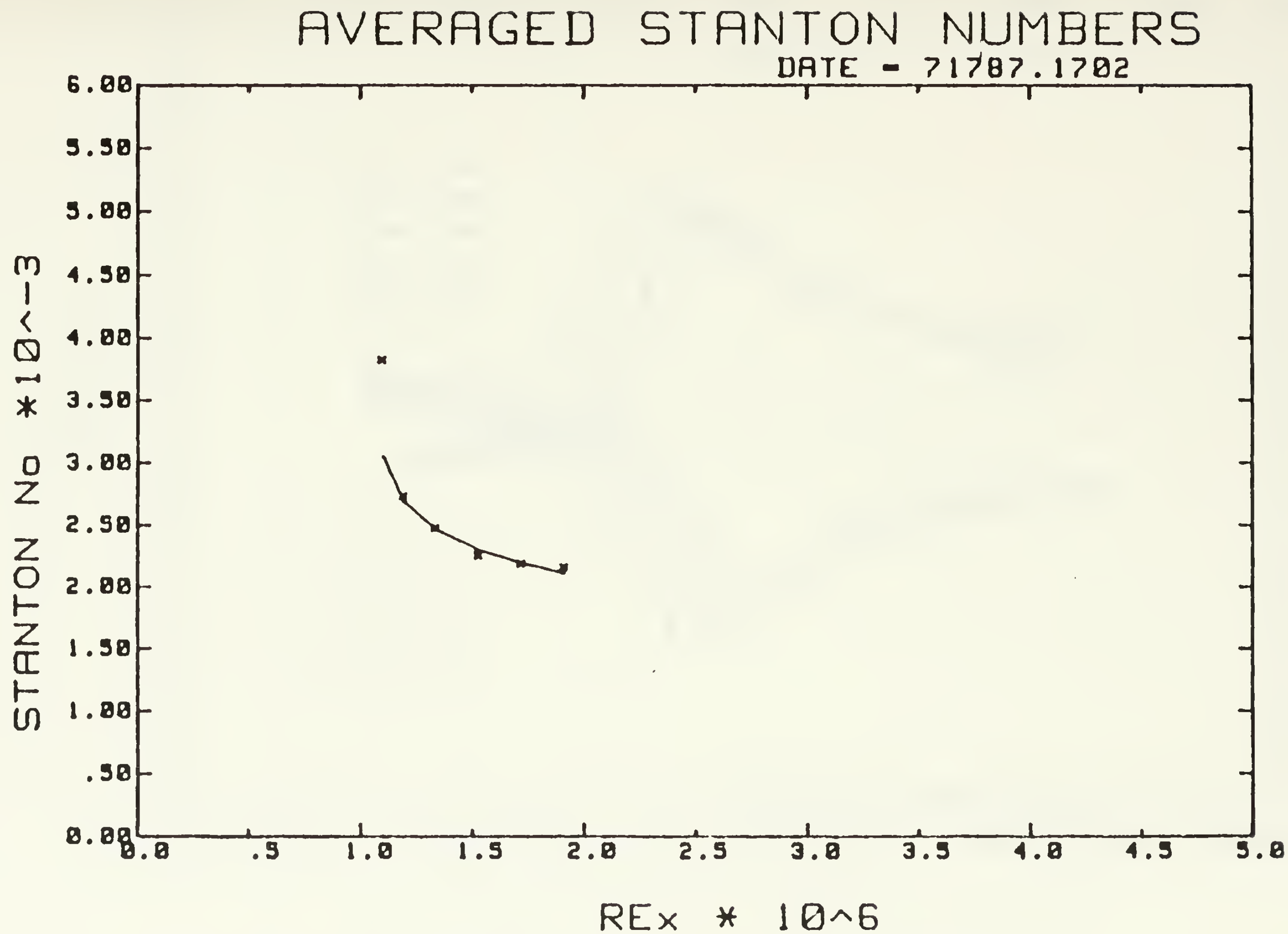

Fig. 13. FREESTREAM 15 M/S, NO FILM COOLING

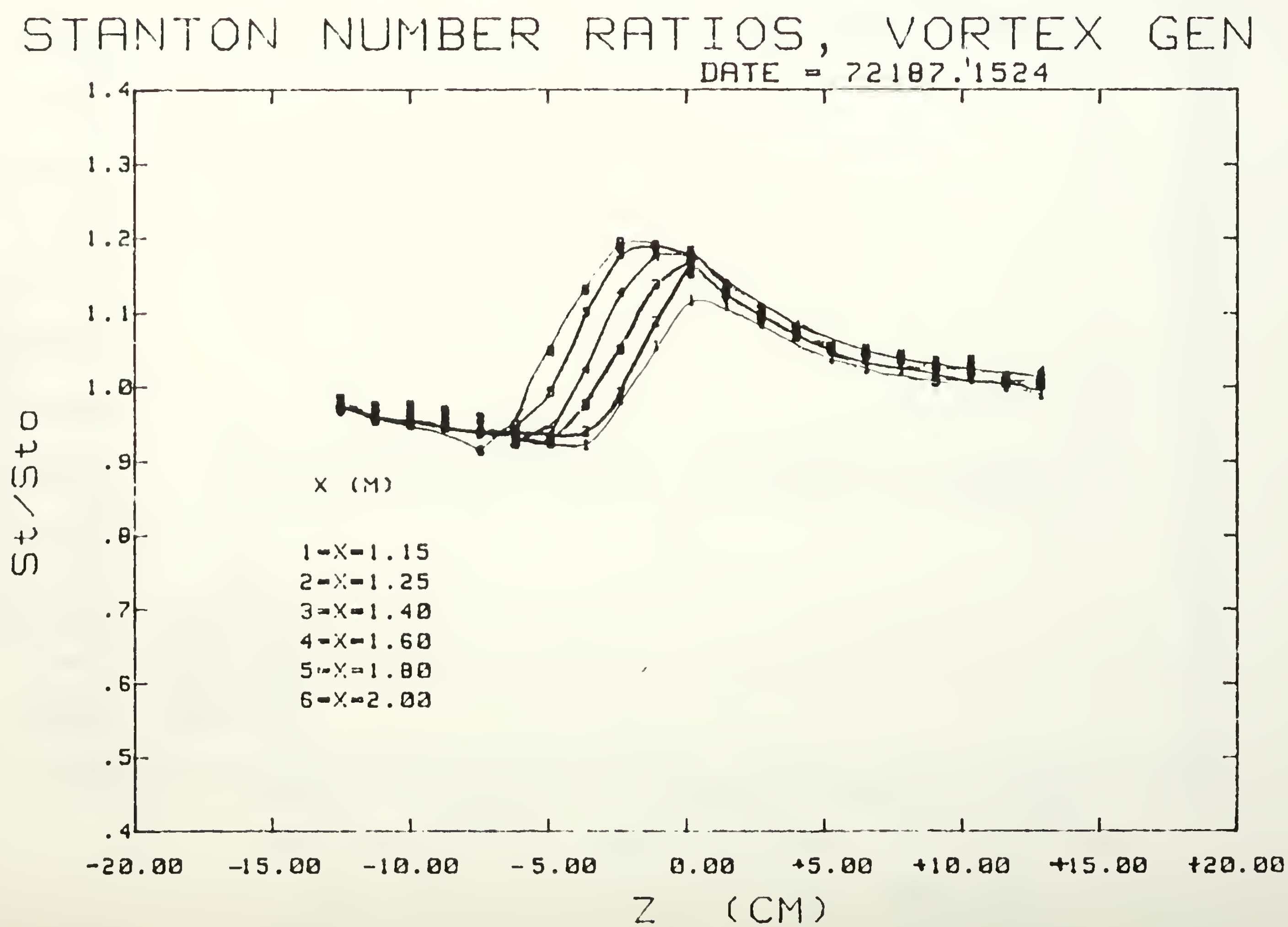

Fig. 14. FREE STREAM 10 M/S, NO FILM COOLING

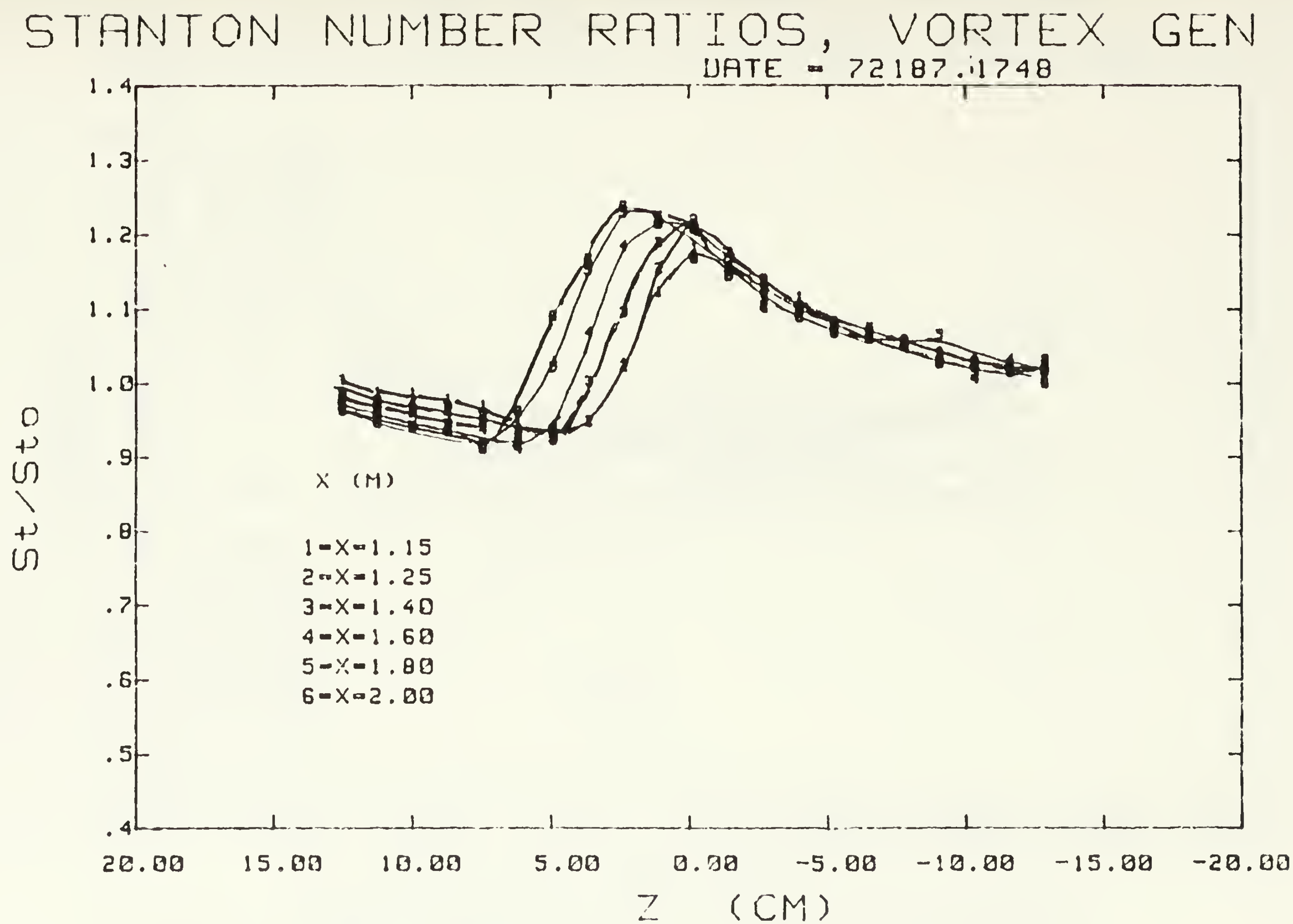

Fig. 15. FREE STREAM 15 M/S, NO FILM COOLING

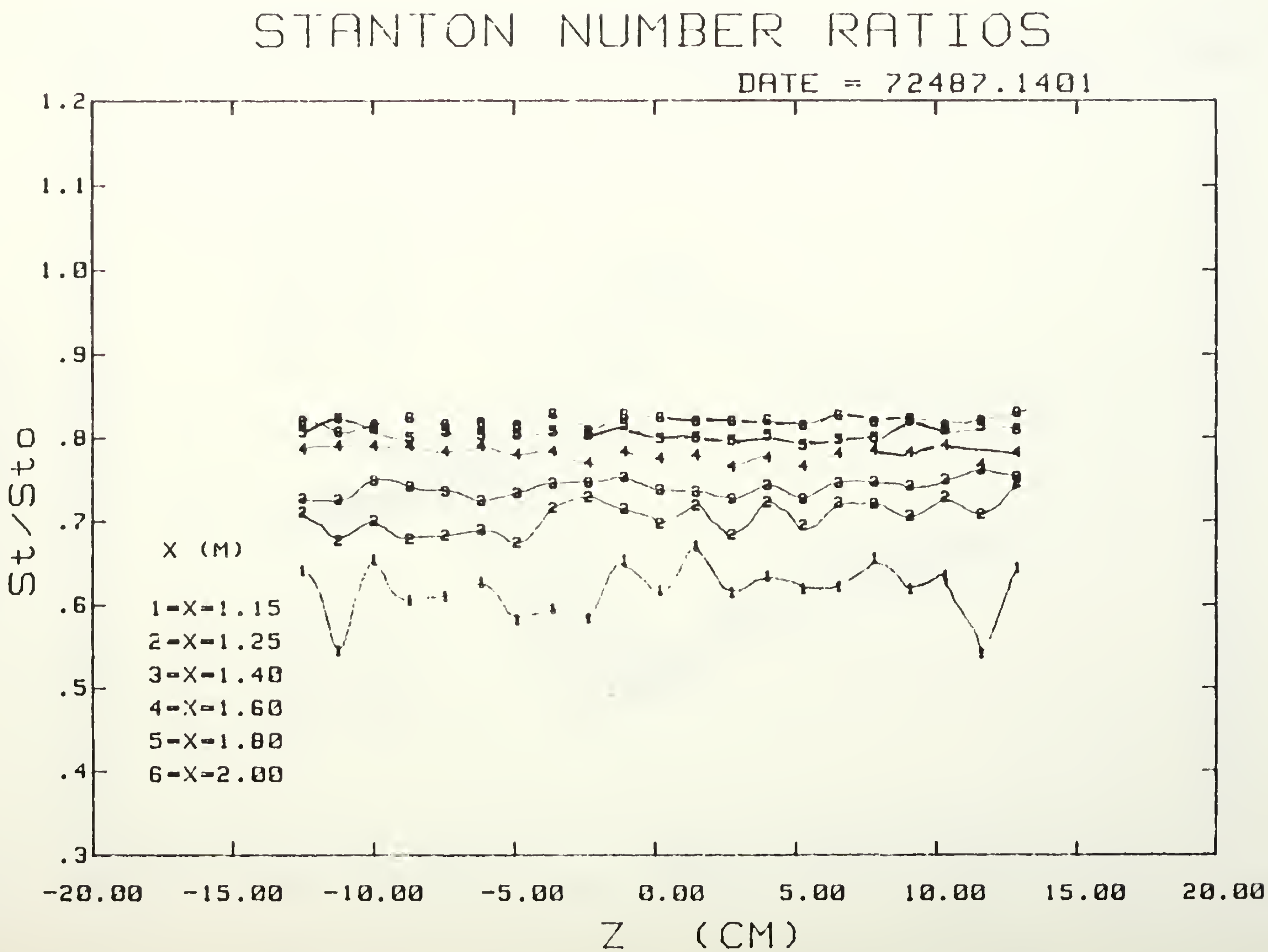

Fig. 16. FREE STREAM 10 M/S, WITH FILM COOLING

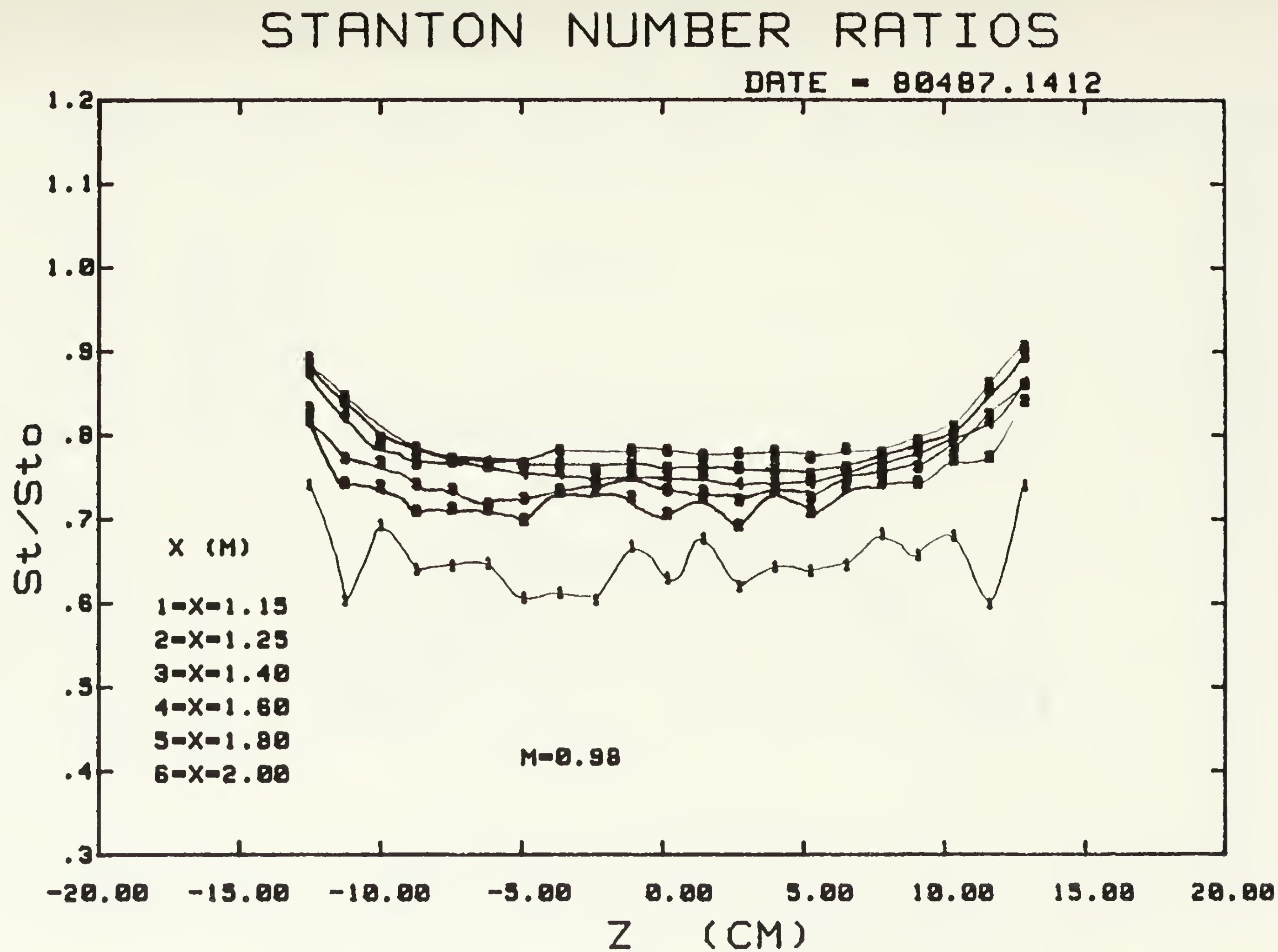

Fig. 17. FREE STREAM 10 M/S, WITH FILM COOLING

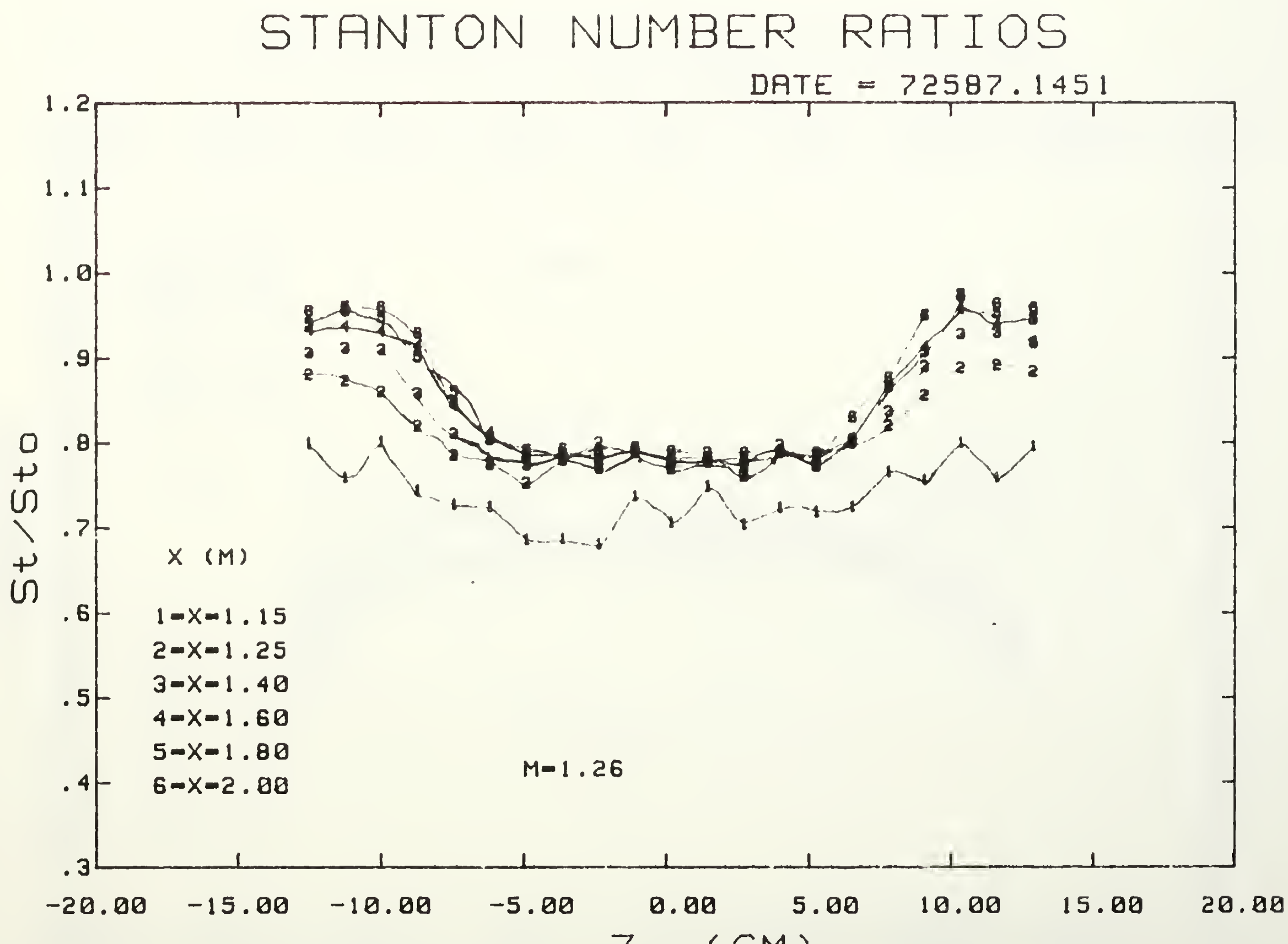

Fig. 18. FREE STREAM 10 M/S, WITH FILM COOLING

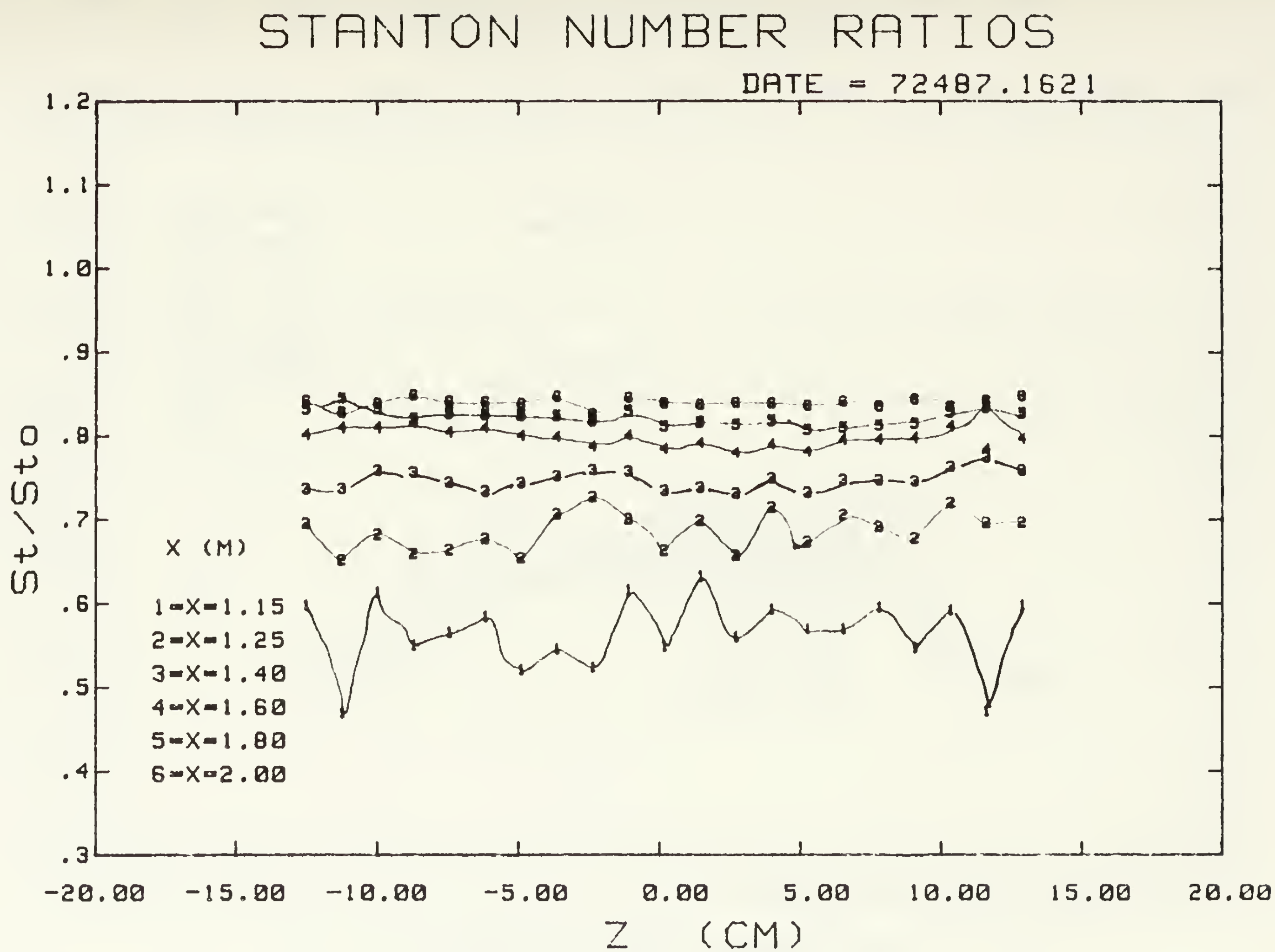

Fig. 19. FREE STREAM 15 M/S, WITH FILM COOLING

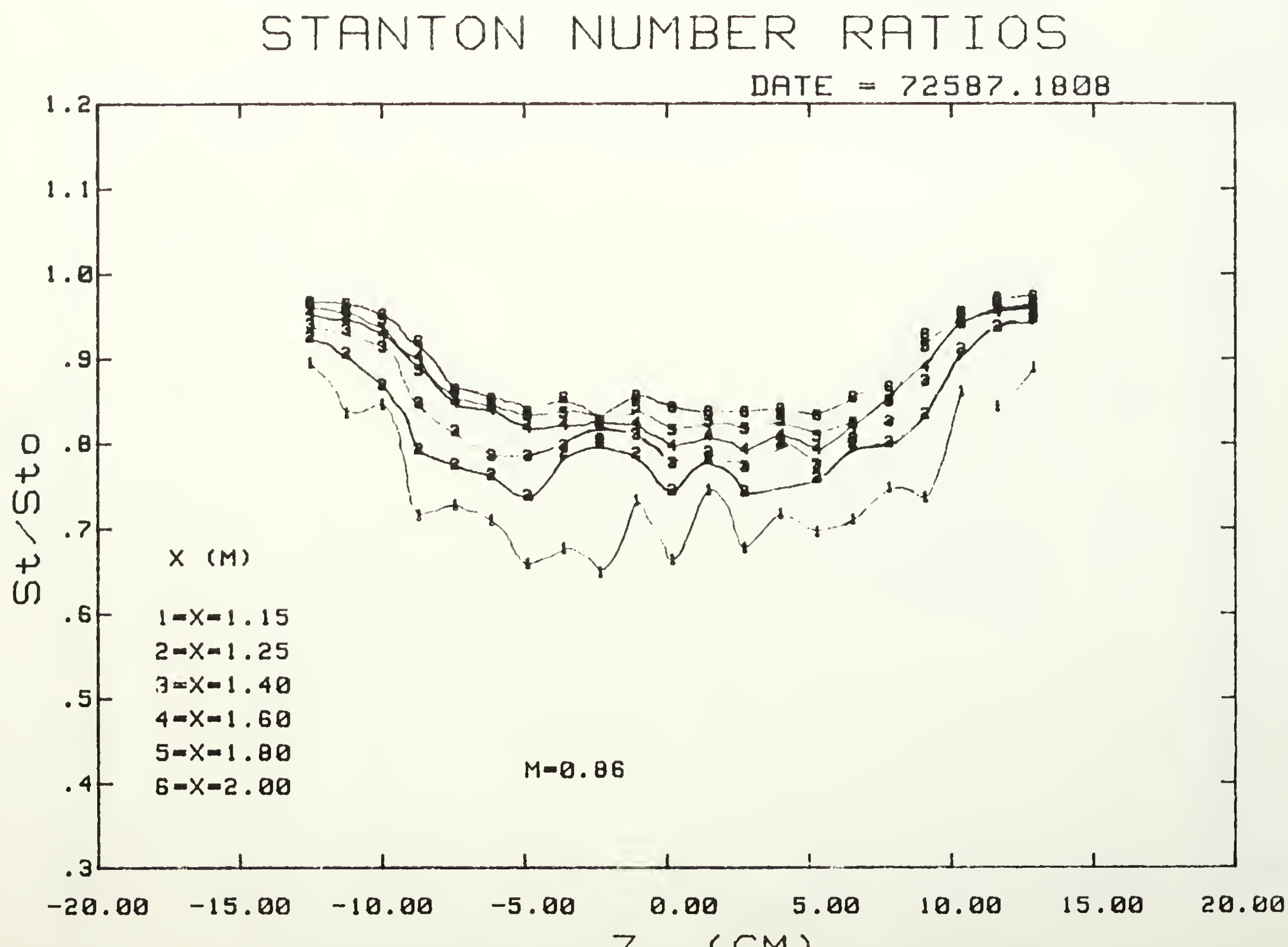

Fig. 20. FREE STREAM 15 M/S, WITH FILM COOLING

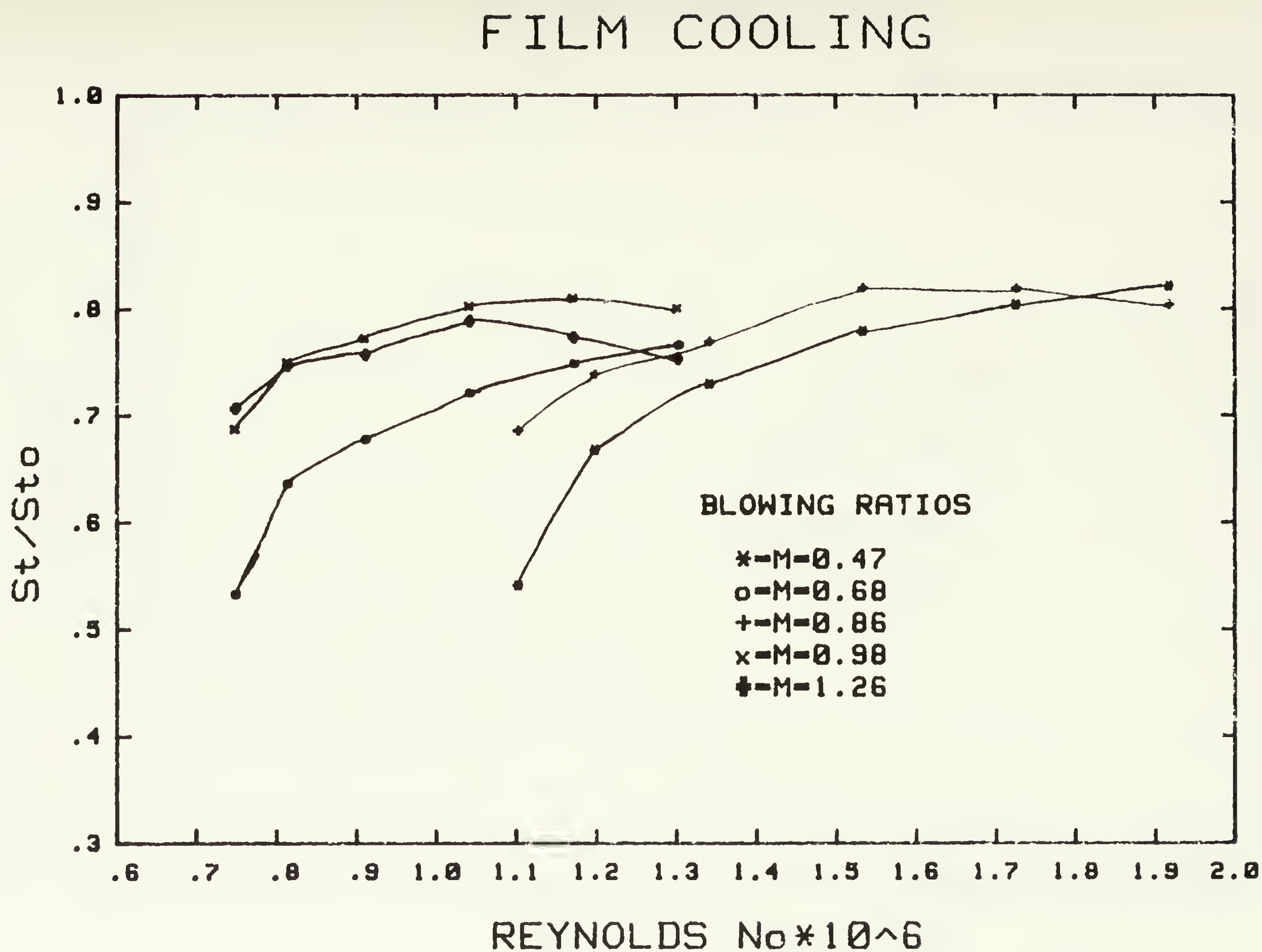

Fig. 21. Averaged Stanton No. Ratios For Different Blowing Ratios.

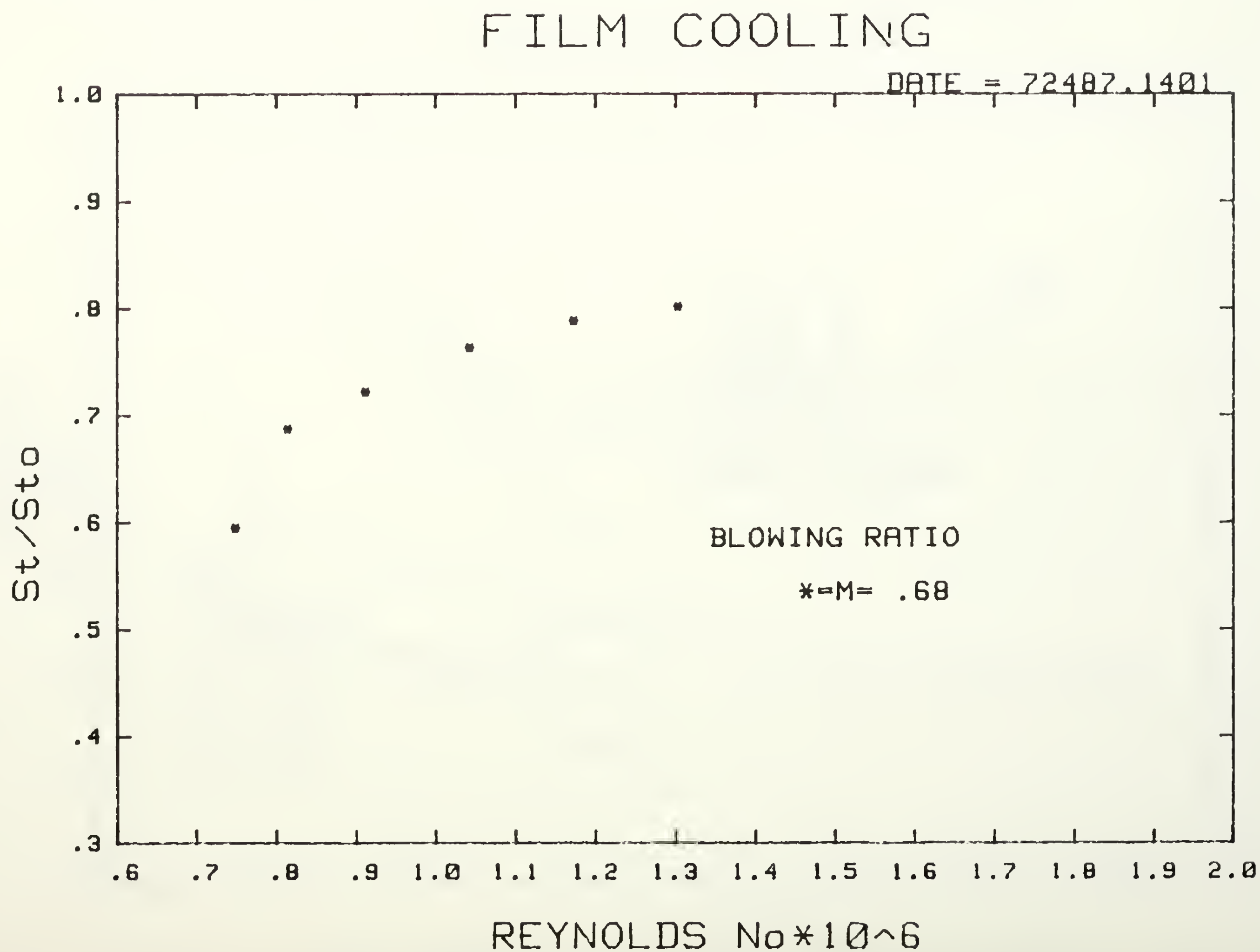

Fig. 22. FREE STREAM 10 M/S

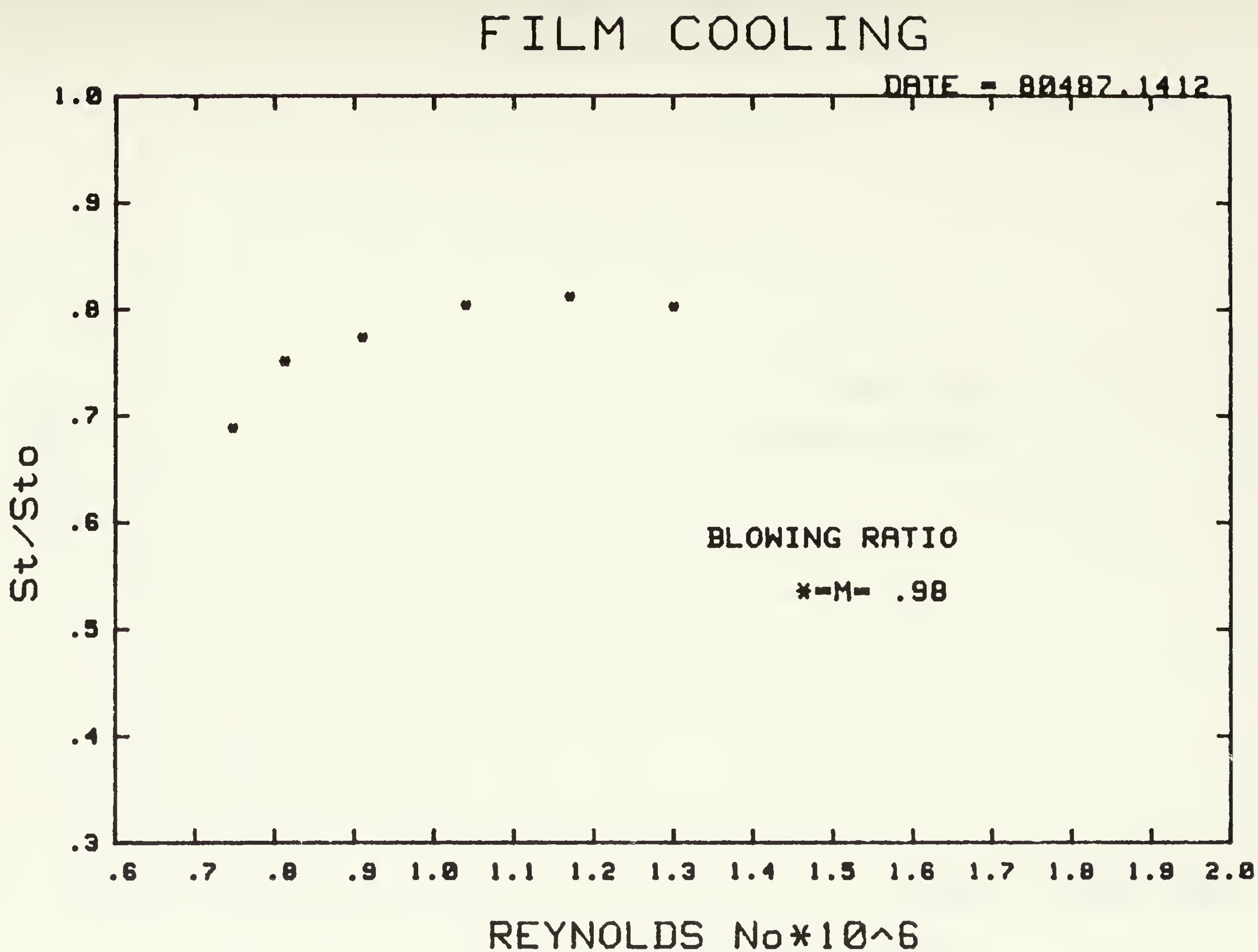

Fig. 23. FREE STREAM 10 M/S

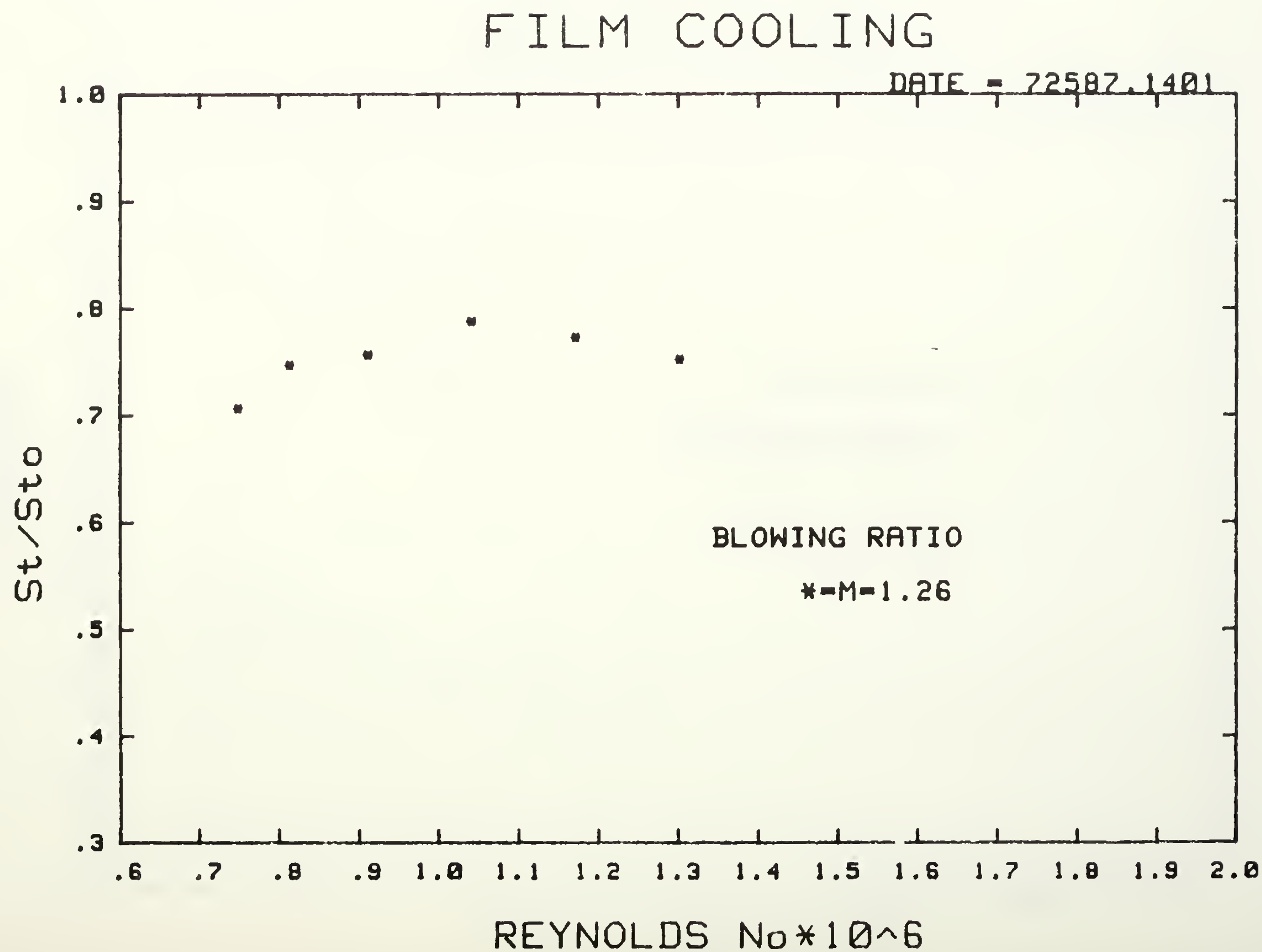

Fig. 24. FREE STREAM 10 M/S

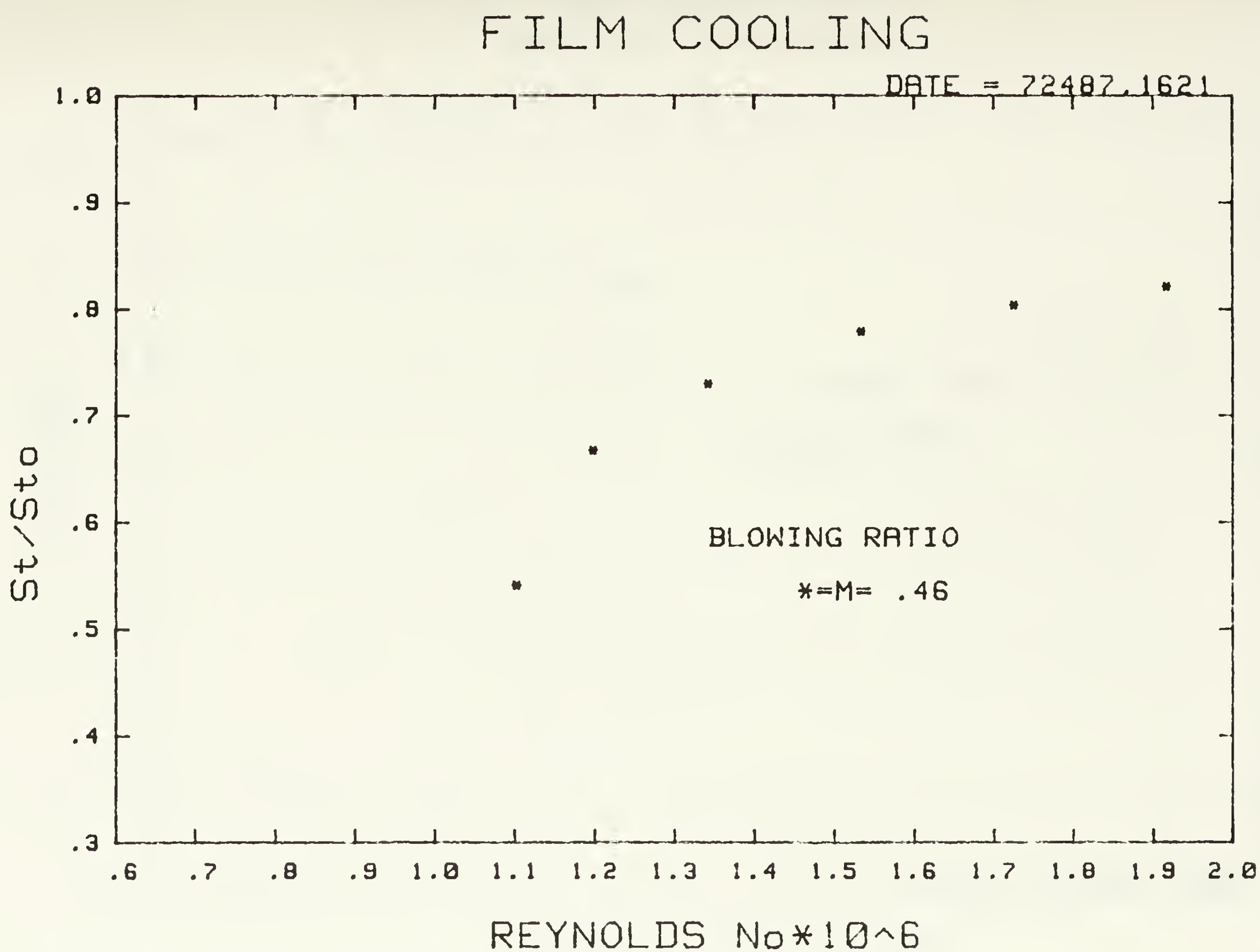

Fig. 25. FREE STREAM 15 M/S

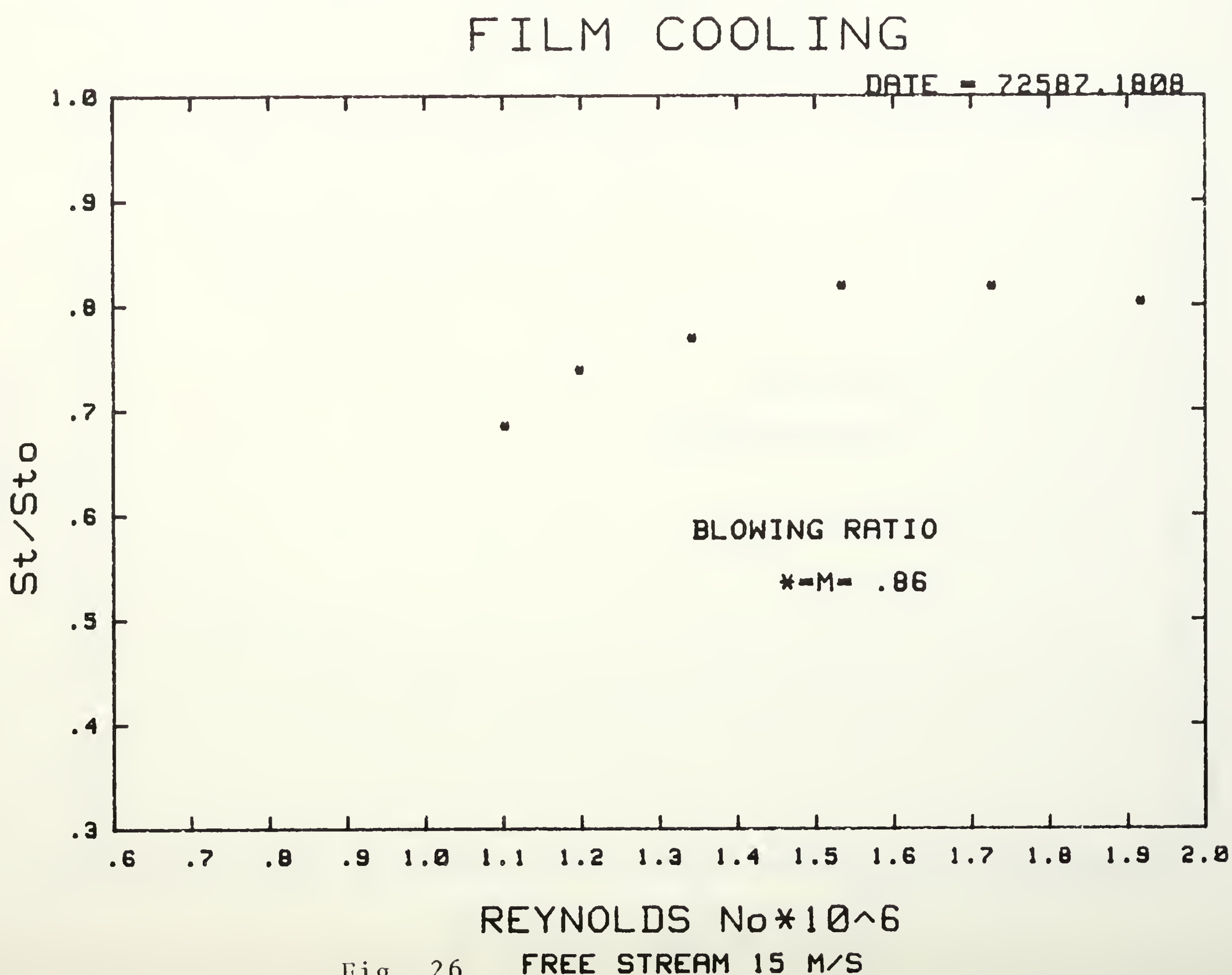
FILM COOLING
DATE = 72587.1808
1.0
.9
.8
.7
.6
.5
.4
.3
St/Sto
BLOWING RATIO
*=M= .86
.6
.7
.8
.9
1.0
1.1
1.2
1.3
1.4
1.5
1.6
1.7
1.8
1.9
2.0
REYNOLDS No*10^6
FREE STREAM 15 M/S

Fig. 26

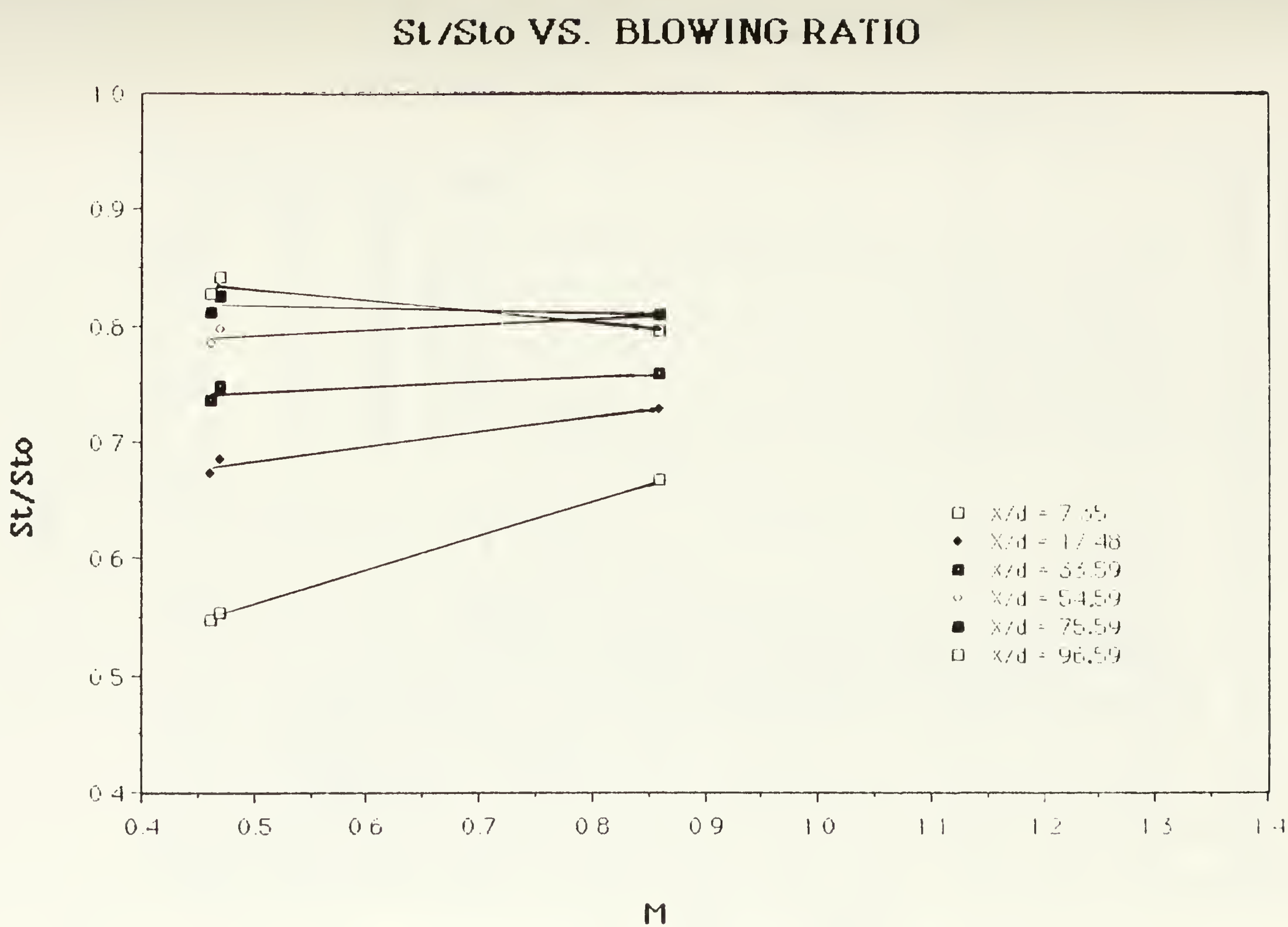

Fig. 27. Free Stream Velocity 15 m/s

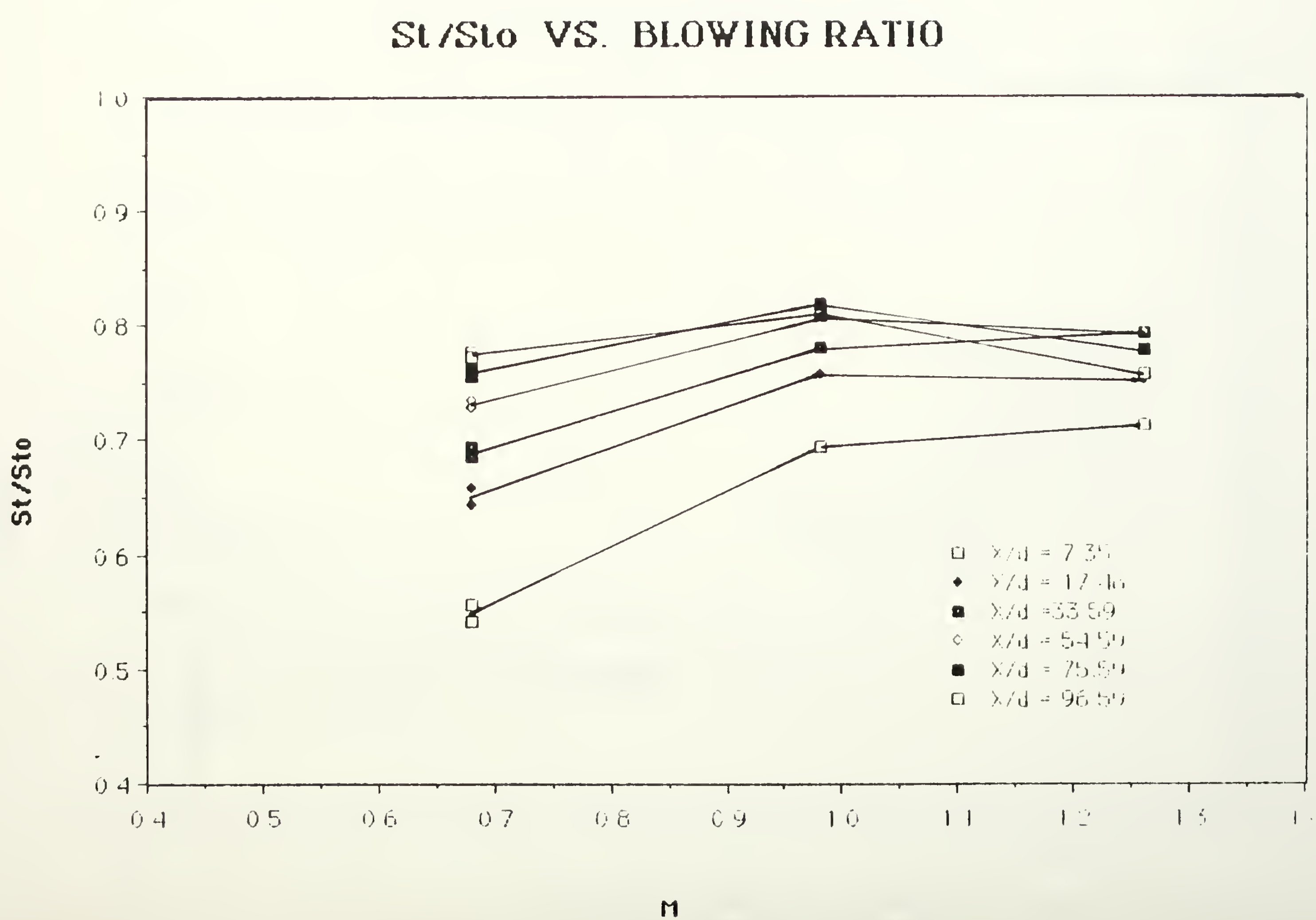

Fig. 28. Free Stream Velocity 10 m/s

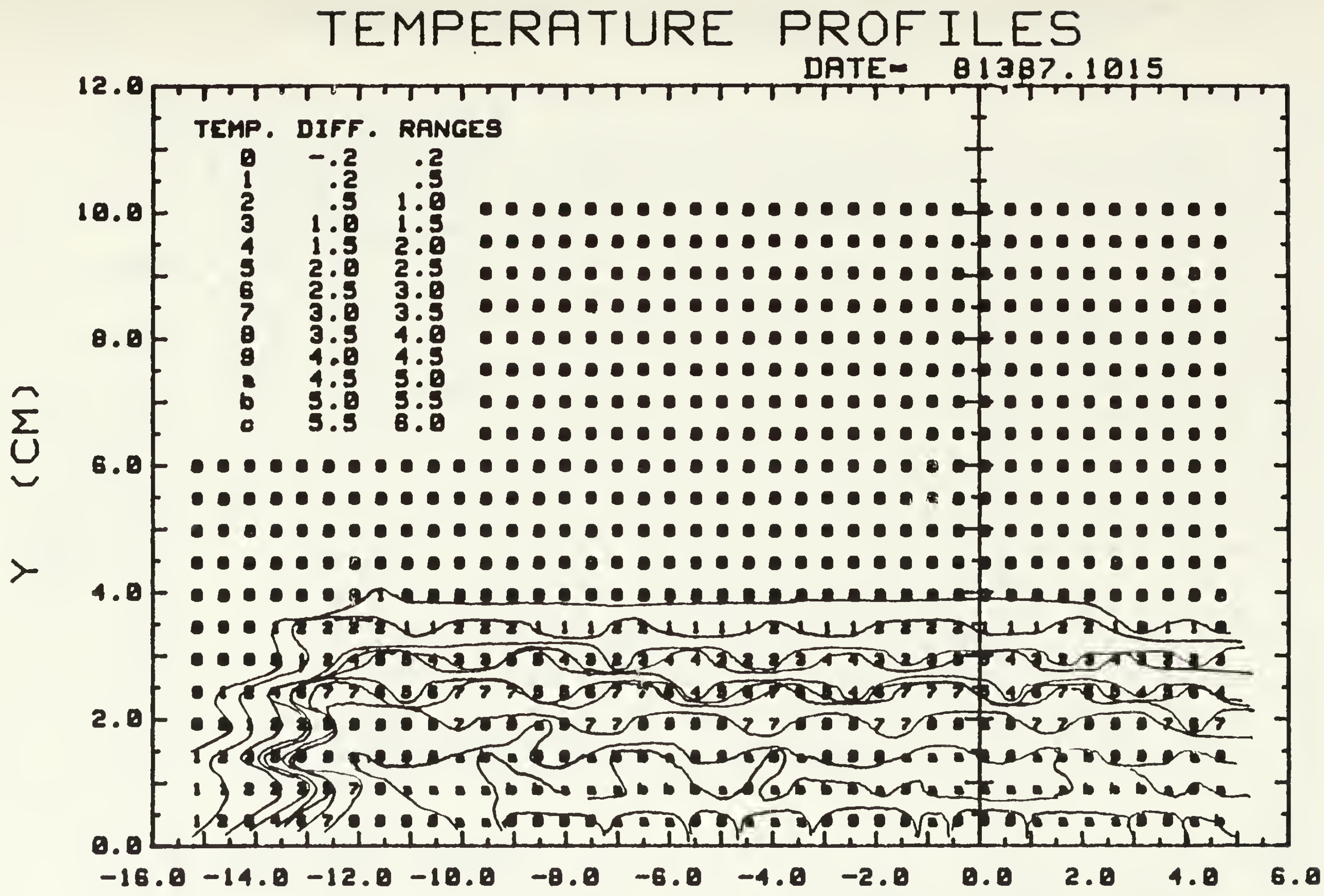

BOUNDARY LAYER, 10 M/S WITH FILM COOLING,M=.98
Fig. 29. X=1.480 M, UNHEATED PLATE,NO VORTEX

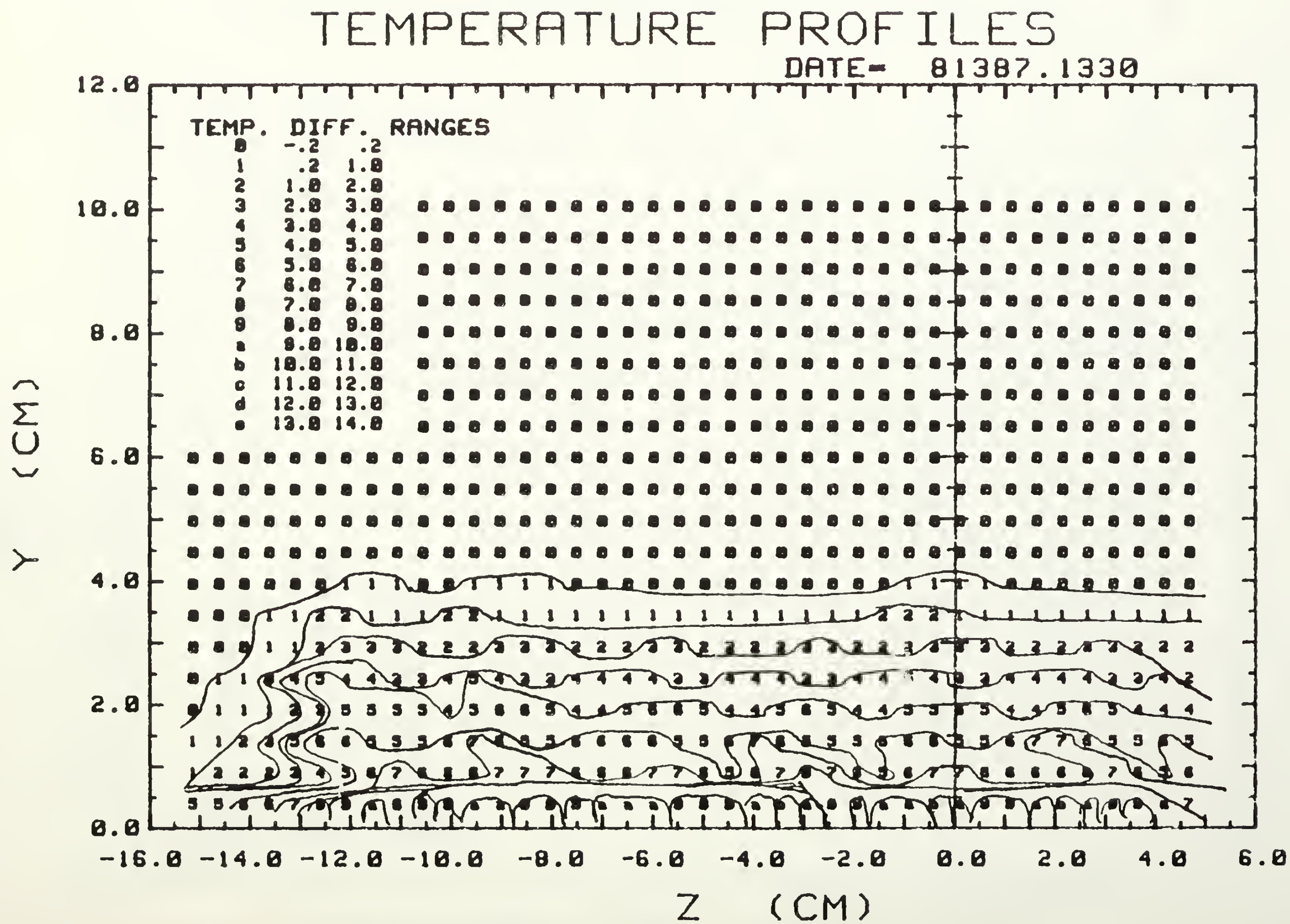

BOUNDARY LAYER, 10 M/S WITH FILM COOLING, M=.98

Fig. 30. X=1.480 M, HEATED PLATE, NO VORTEX

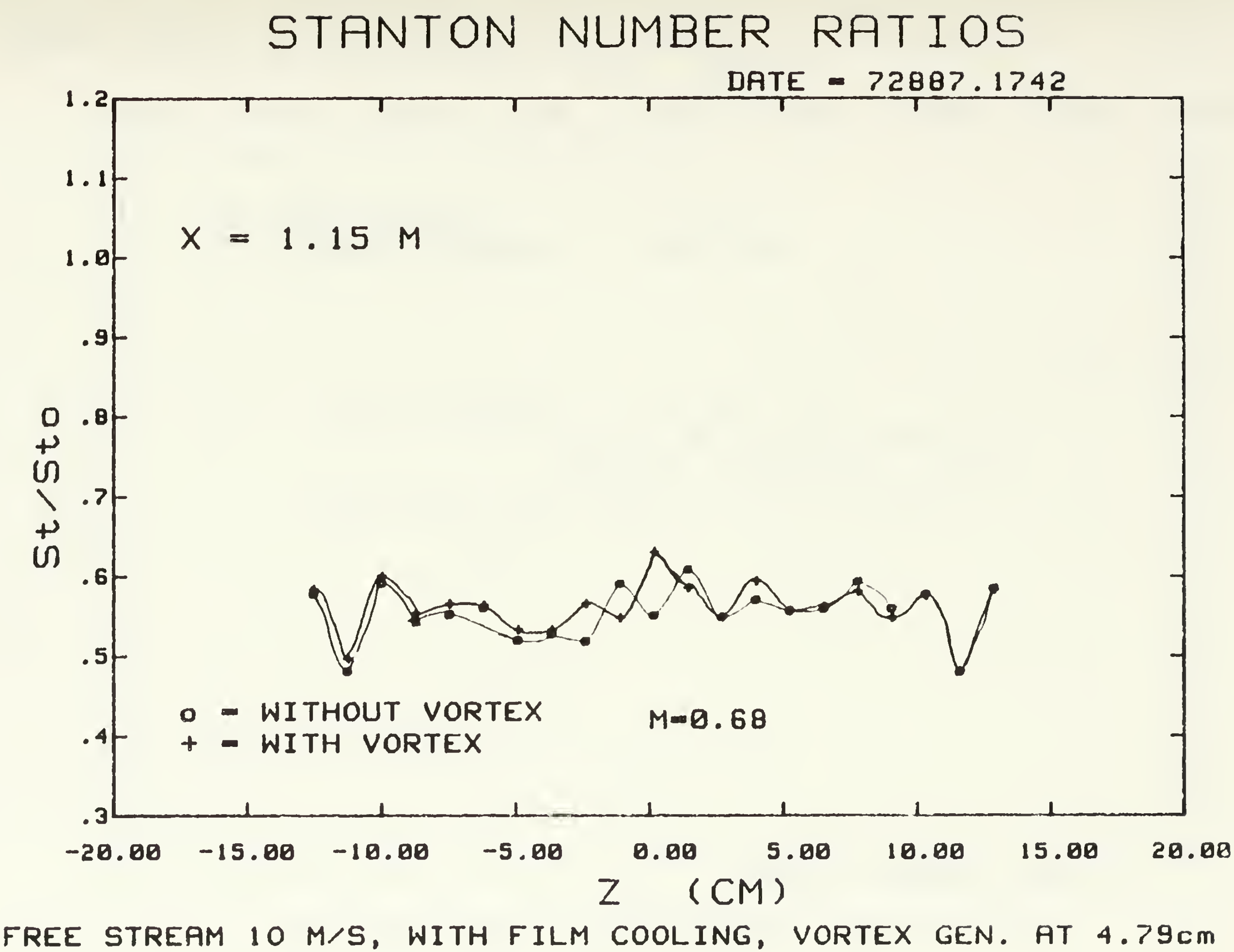

Fig. 31a. Spanwise Variation of Stanton Number Ratios.

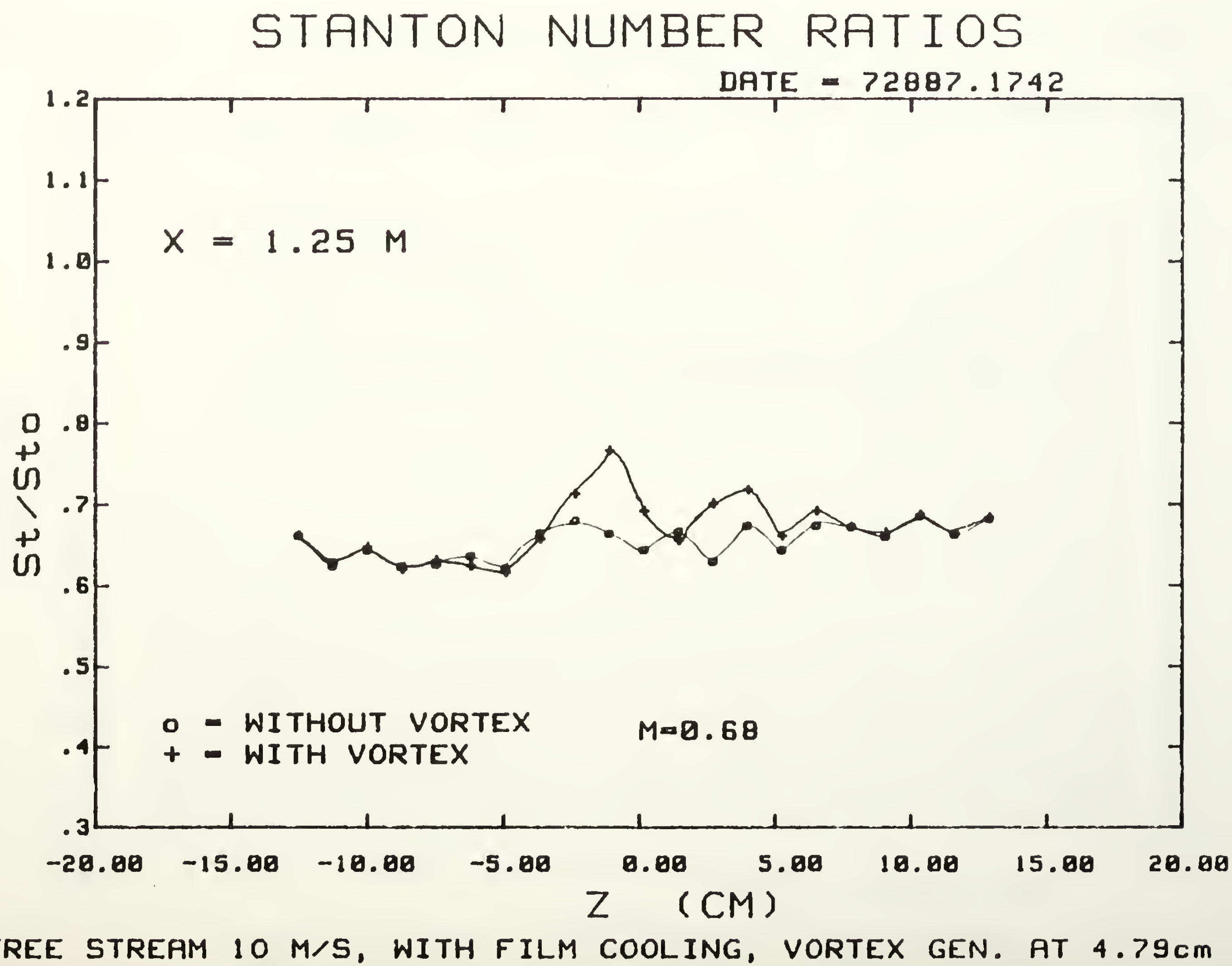

Fig. 31b. Spanwise Variation of Stanton Number Ratios.

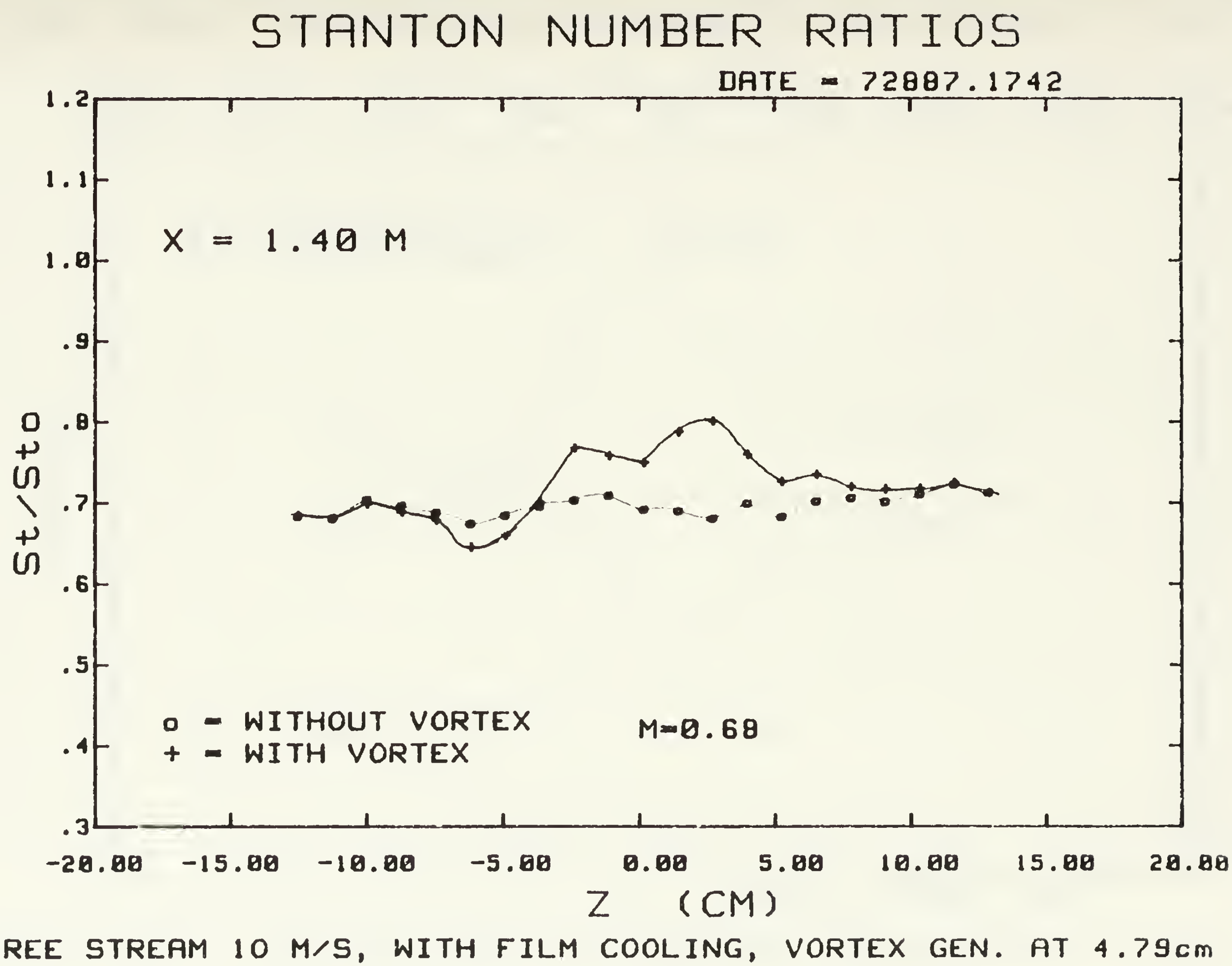

Fig. 31c. Spanwise Variation of Stanton Number Ratios.

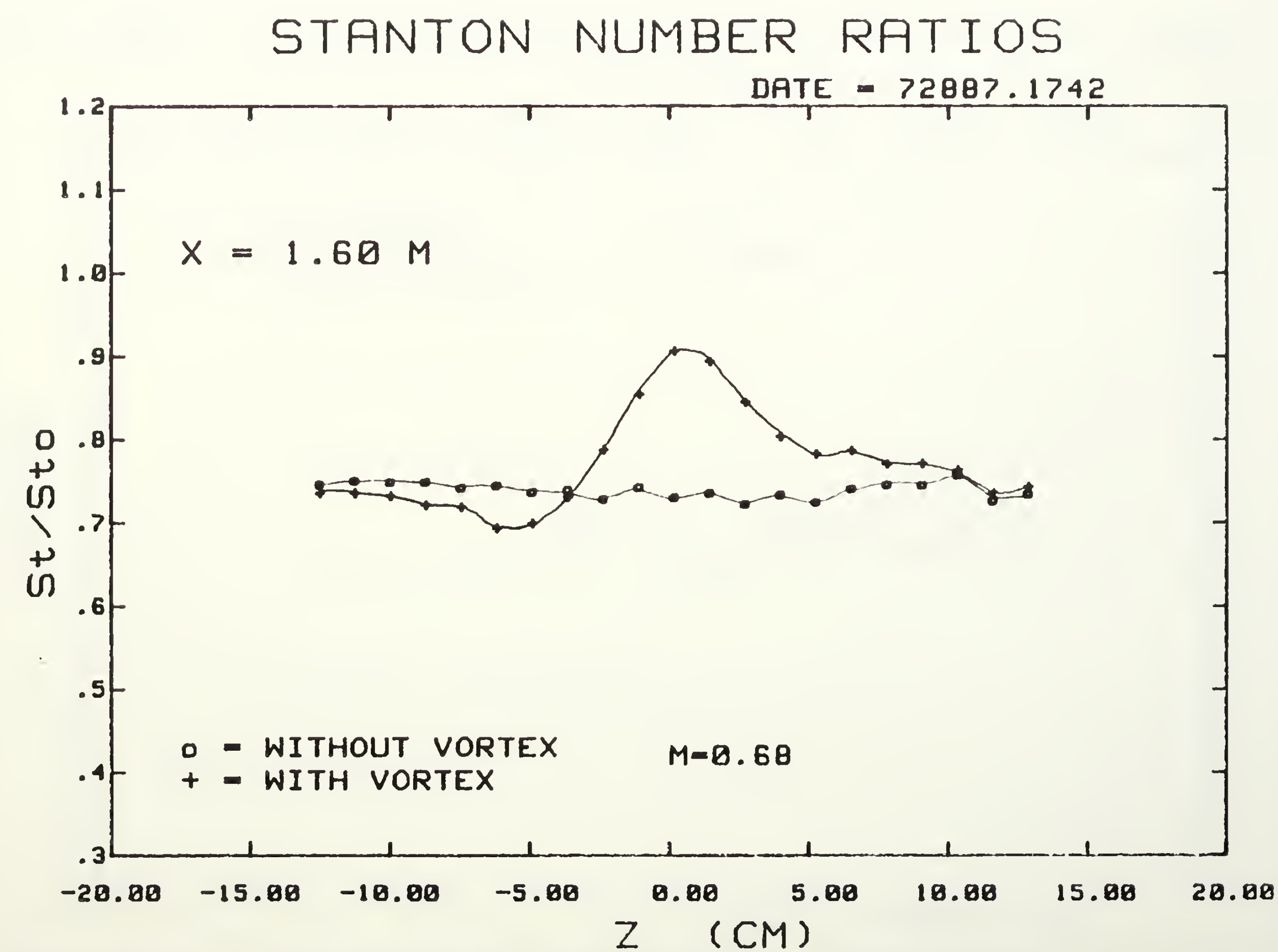

FREE STREAM 10 M/S, WITH FILM COOLING, VORTEX GEN. AT 4.79cm

Fig. 31d. Spanwise Variation of Stanton Number Ratios.

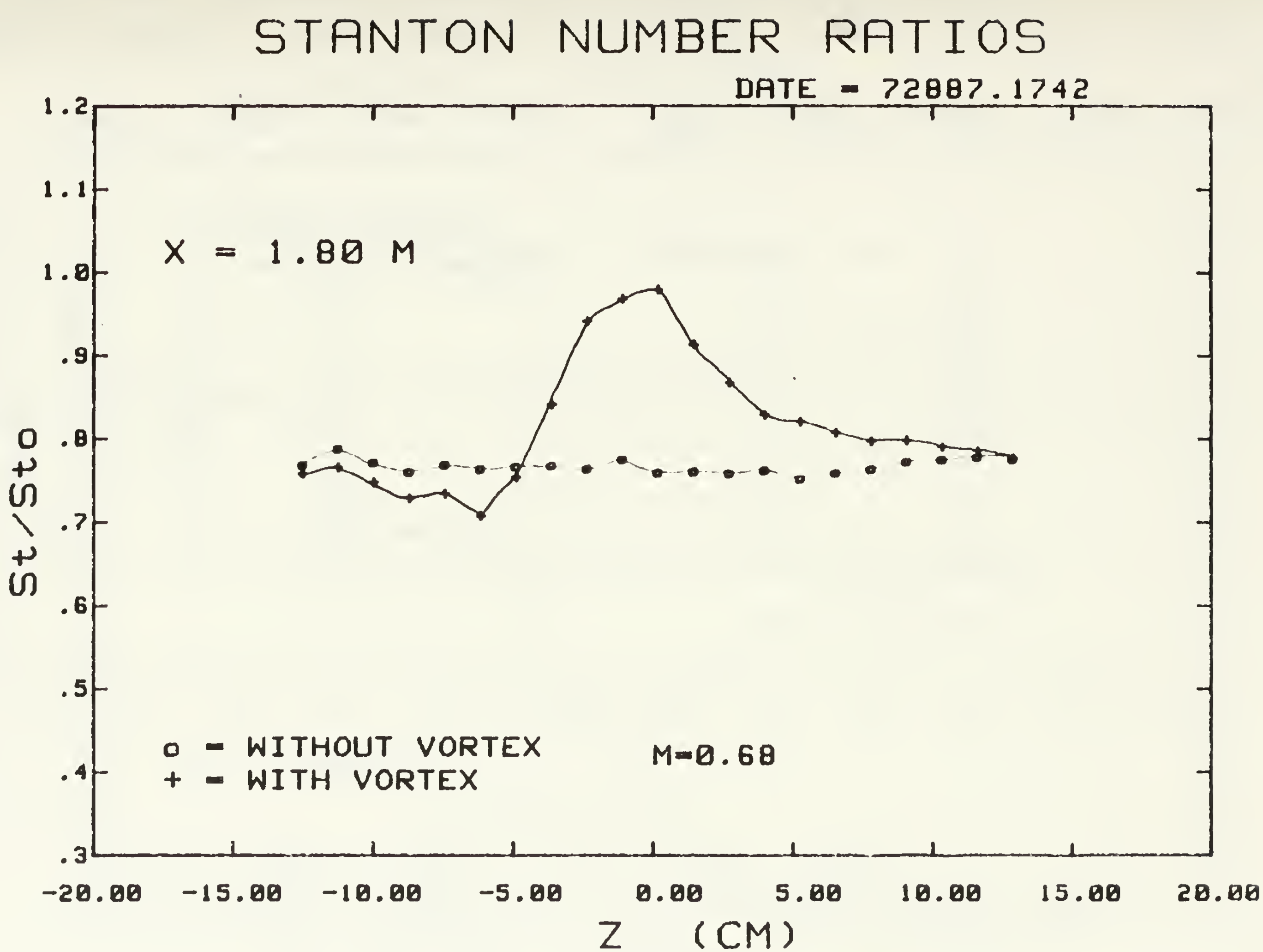

FREE STREAM 10 M/S, WITH FILM COOLING, VORTEX GEN. AT 4.79cm

Fig. 31e. Spanwise Variation of Stanton Number Ratios.

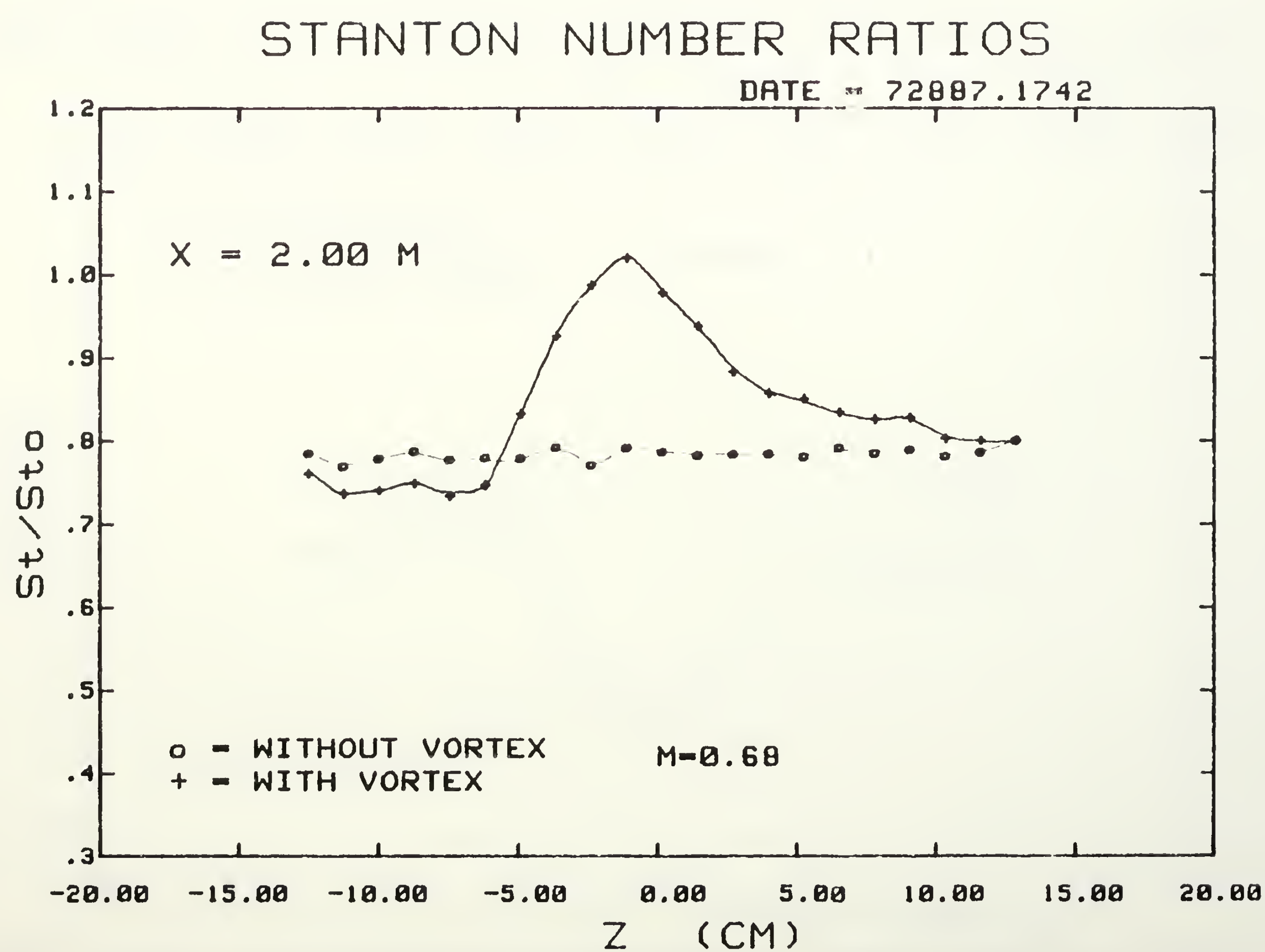

FREE STREAM 10 M/S, WITH FILM COOLING, VORTEX GEN. AT 4.79cm

Fig. 31f. Spanwise Variation of Stanton Number Ratios.

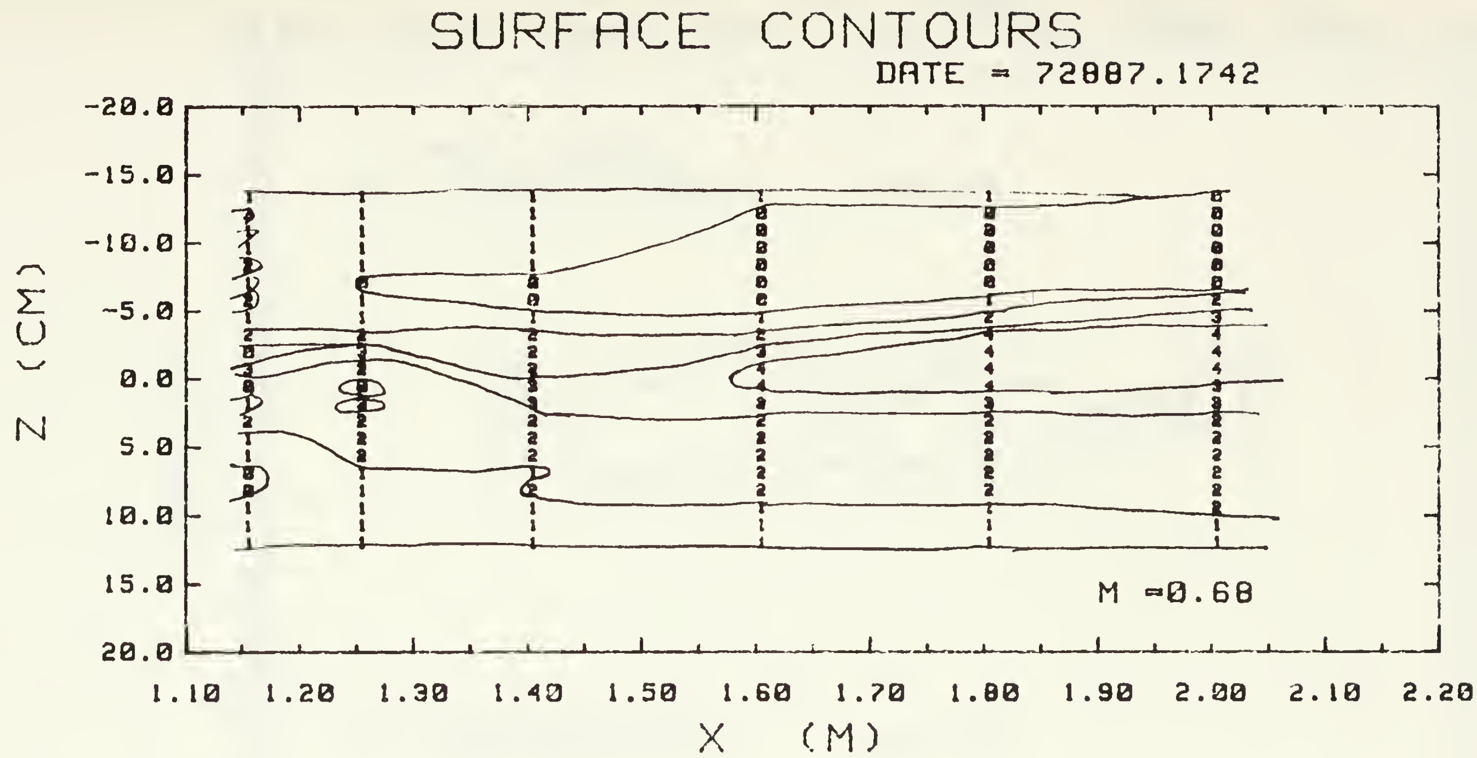

St/Stf RANGES

0	.900	.980		3	1.100	1.200
1	.980	1.020		4	1.200	1.300
2	1.020	1.100				

FREE STREAM 10 M/S, WITH FILM COOLING, VORTEX GEN. #2 AT 4.79 cm

Fig. 32. Surface Contours.

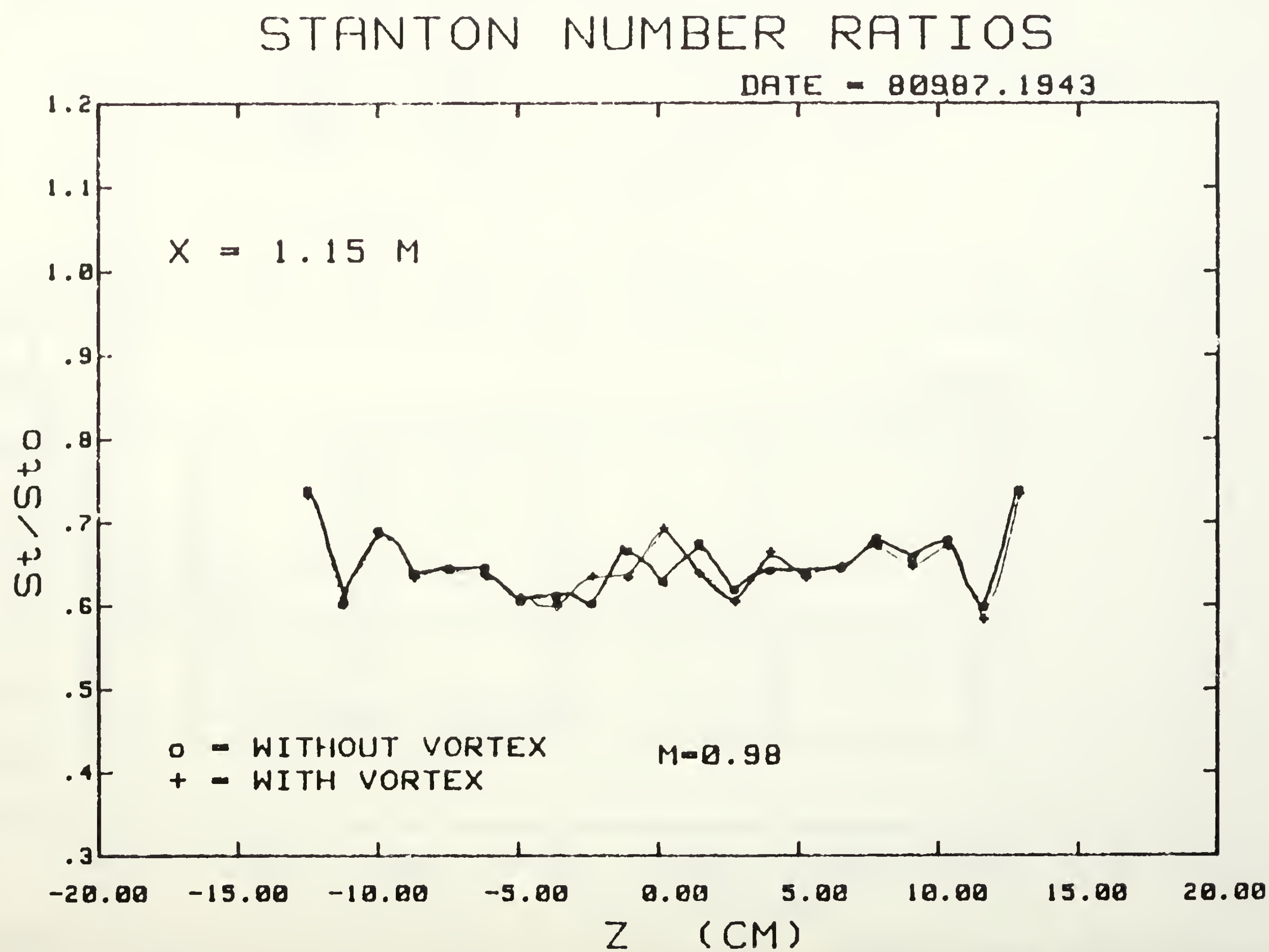

FREE STREAM 10 M/S, WITH FILM COOLING, VORTEX GEN.#2 AT 4.79 cm

Fig. 33a. Spanwise Variation of Stanton Number Ratios.

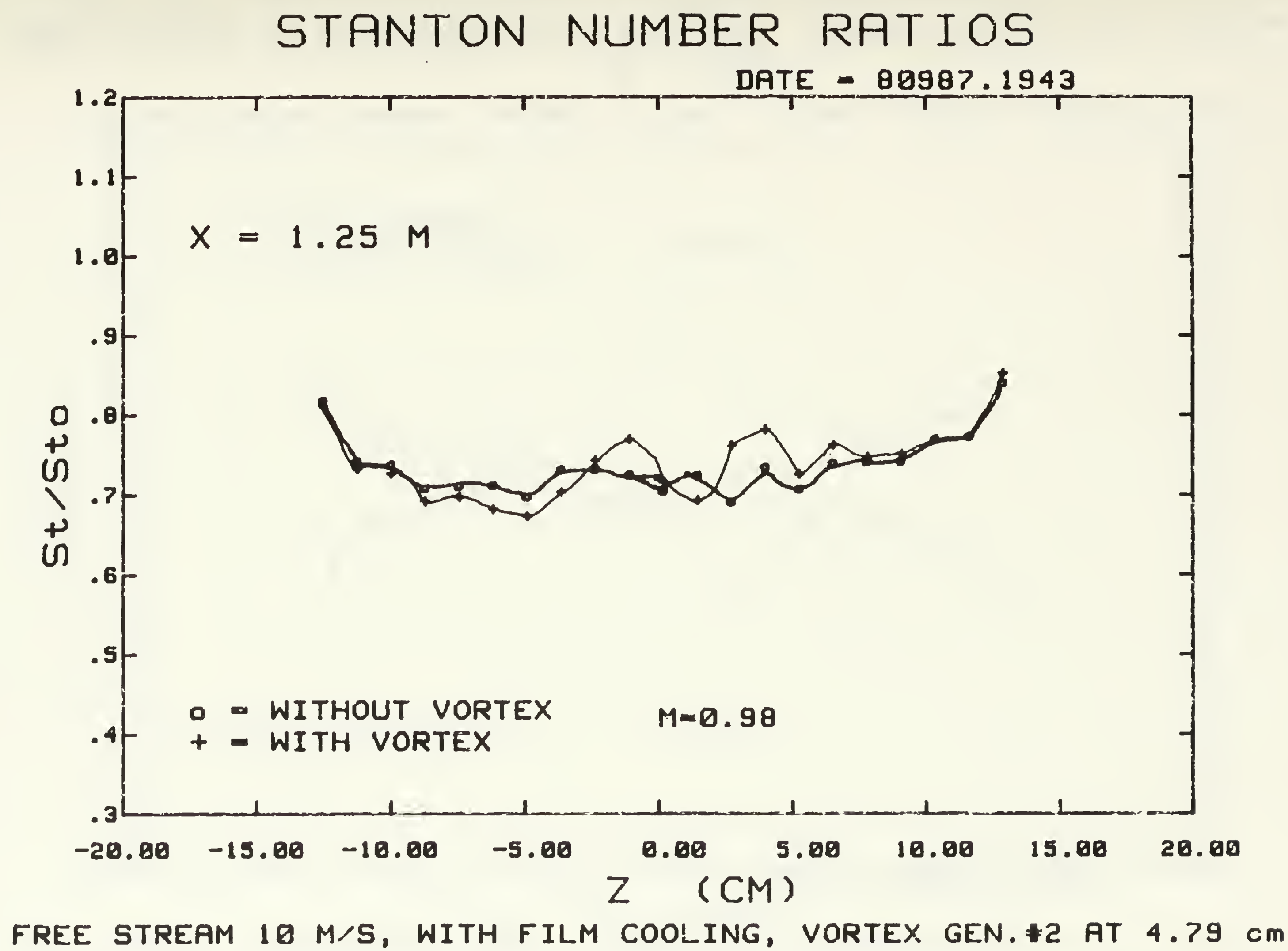

Fig. 33b. Spanwise Variations of Stanton Number Ratios.

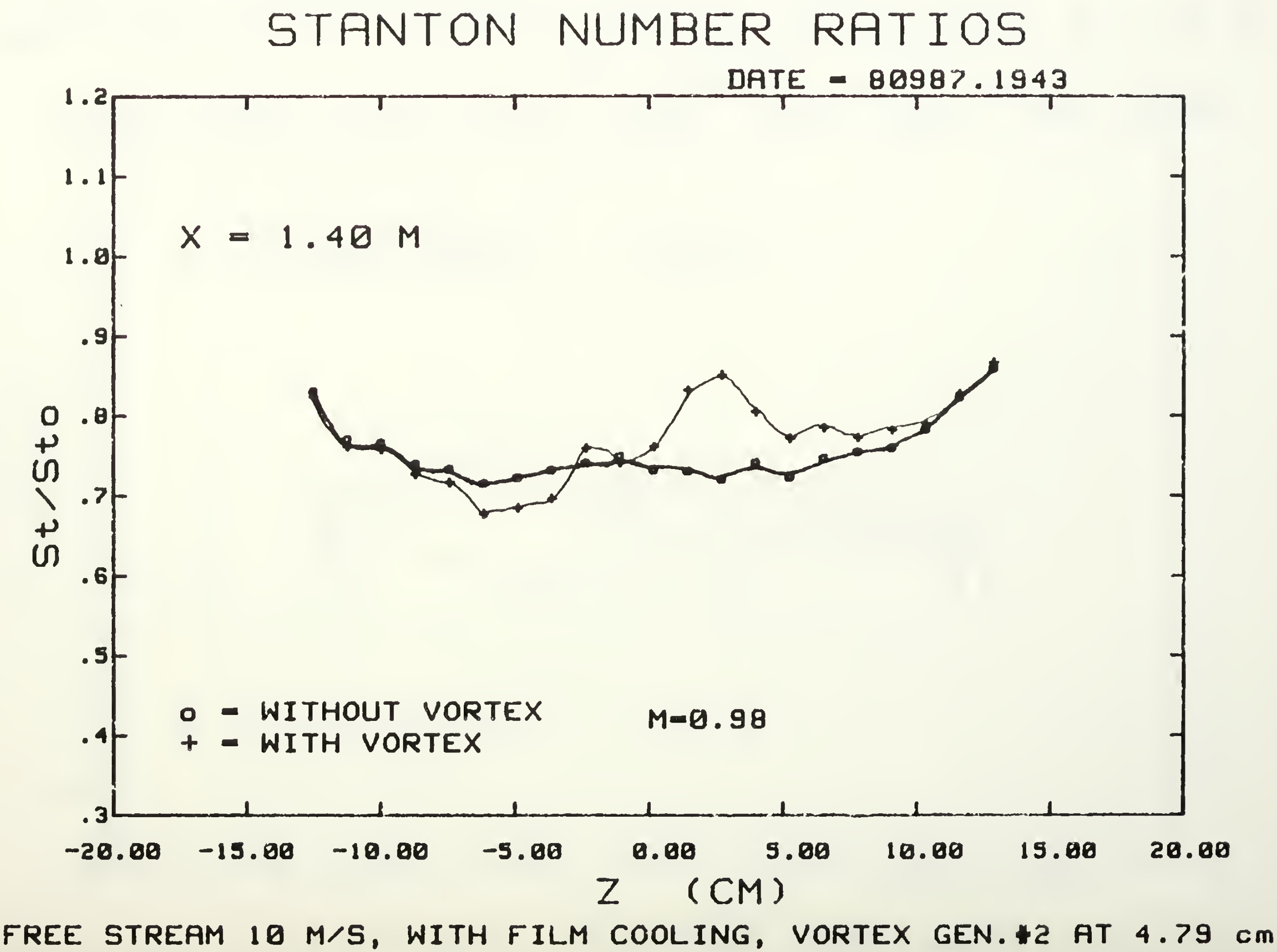

Fig. 30c. Spanwise Variations of Stanton Number Ratios.

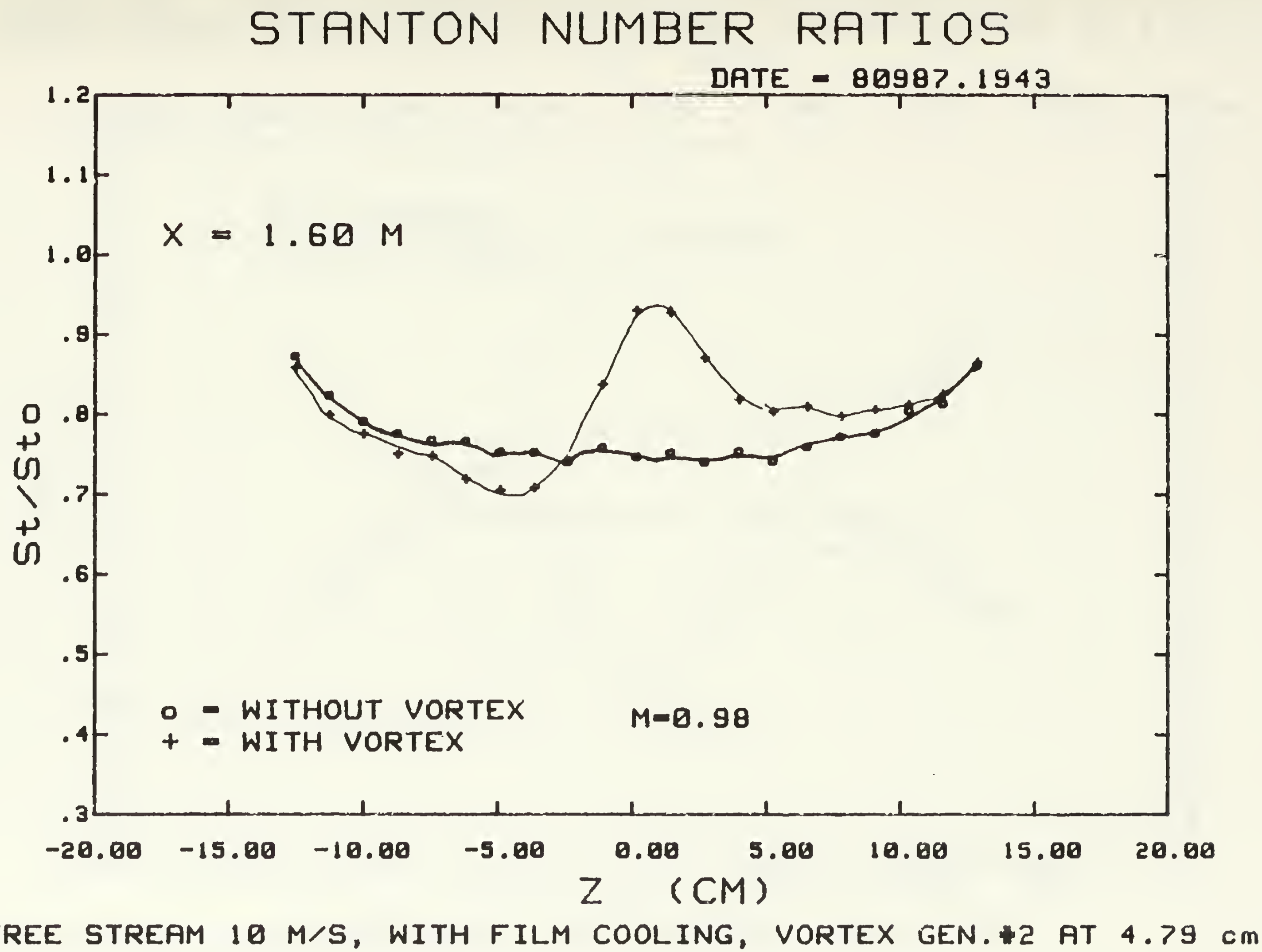

Fig. 33d. Spanwise Variations of Stanton Number Ratios.

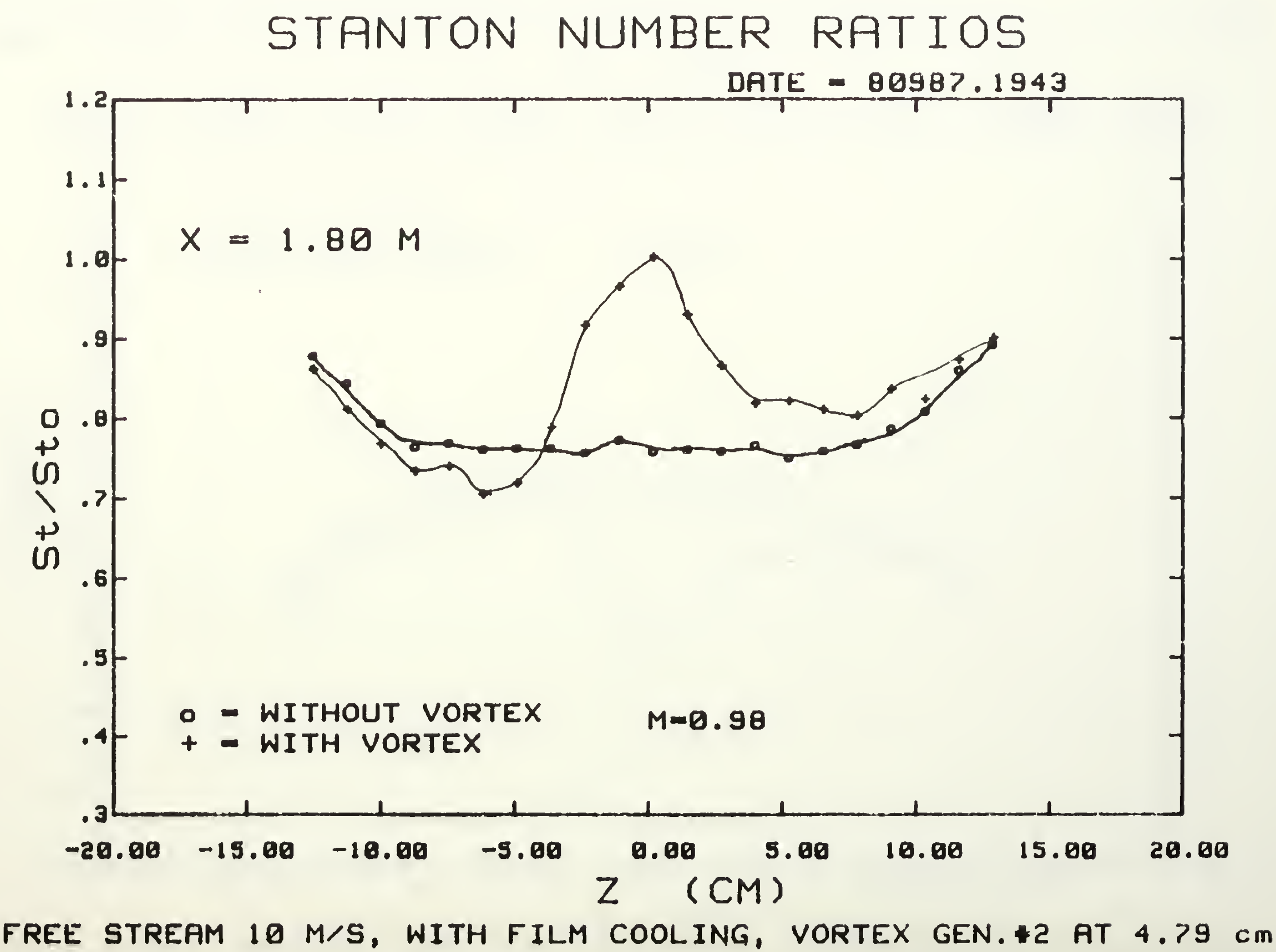

Fig. 33e. Spanwise Variations of Stanton Number Ratios.

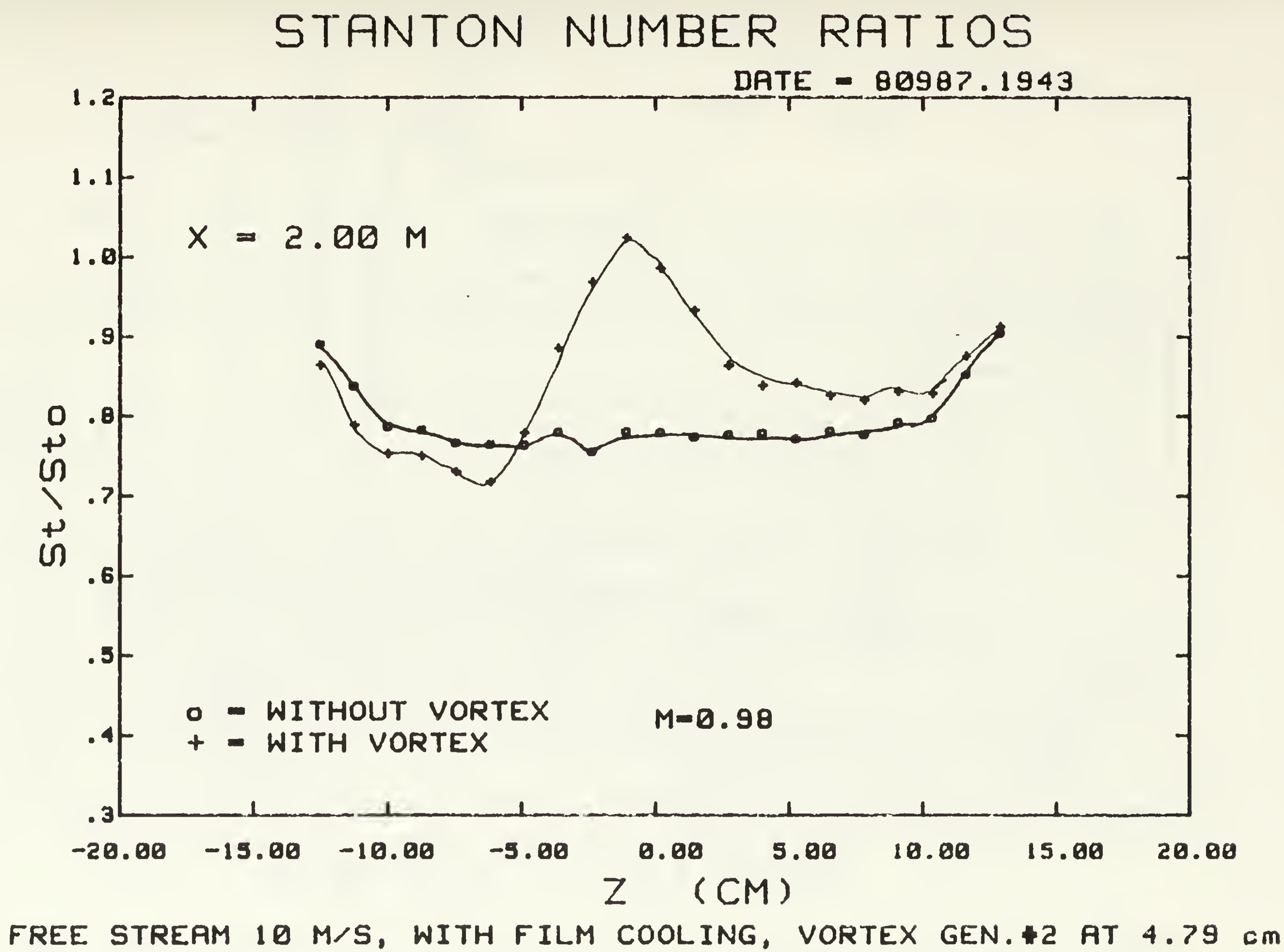

Fig. 33f. Spanwise Variations of Stanton Number Ratios.

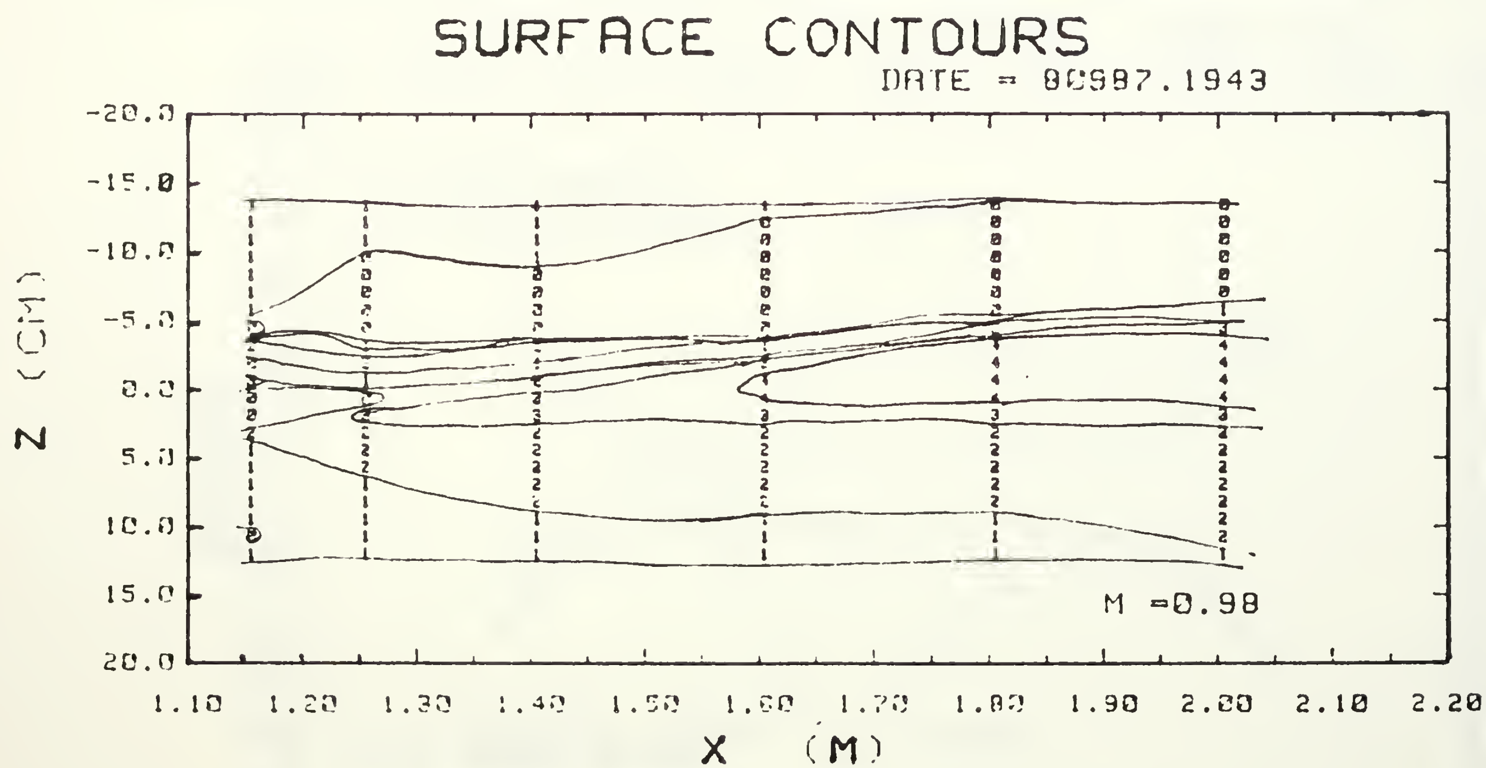

St/Stf RANGES

0	.900	.980	3	1.100	1.200
1	.980	1.020	4	1.200	1.300
2	1.020	1.100			

FREE STREAM 10 M/S, WITH FILM COOLING, VORTEX GEN. #2 AT 4.79 cm

Fig. 34. Surface Contours.

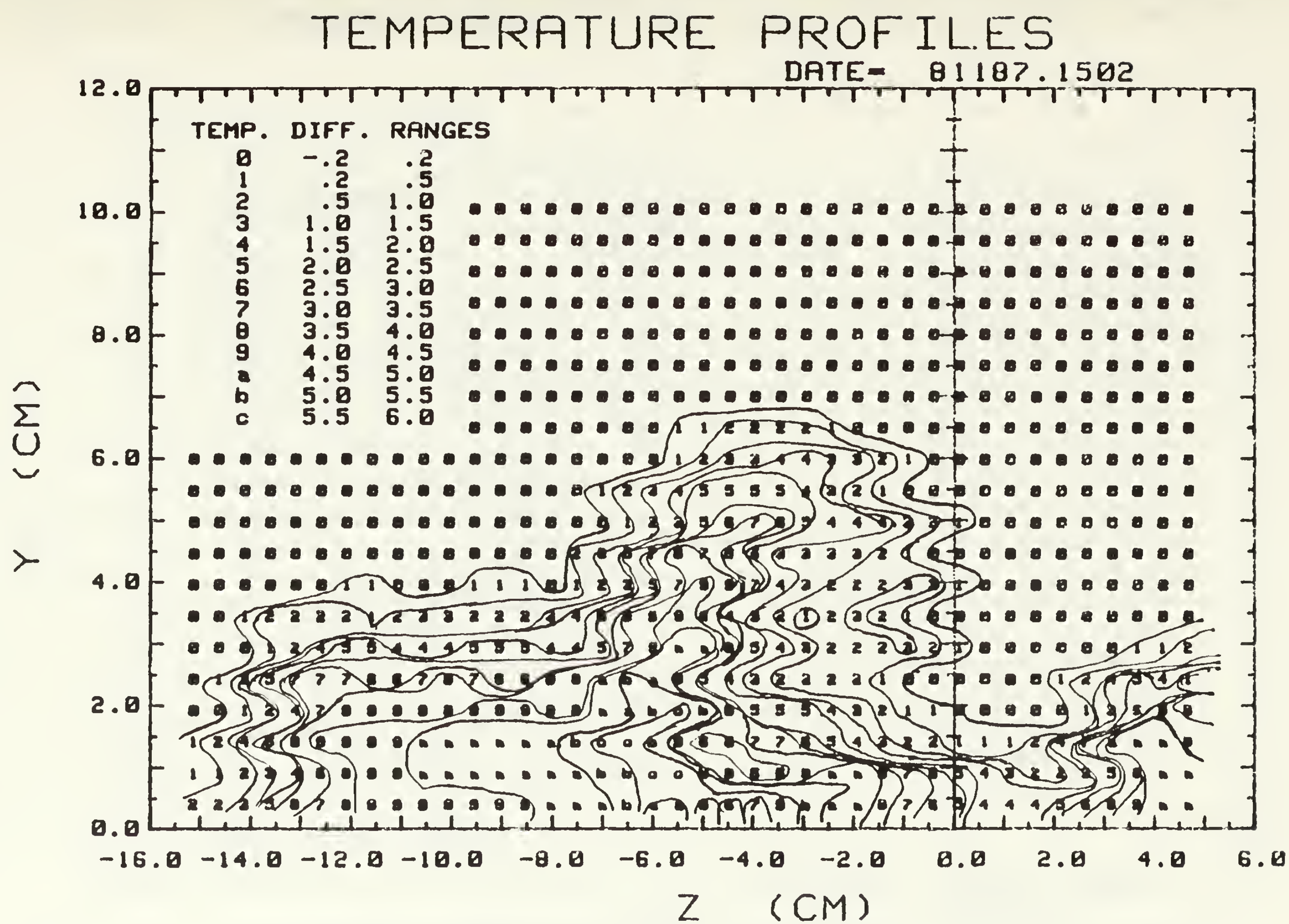

Fig. 35a. EMBEDDED VORTEX 10 M/S WITH FILM COOLING, M=0.98
X=1.480 M, UNHEATED PLATE, VORTEX GEN. AT 4.79 cm

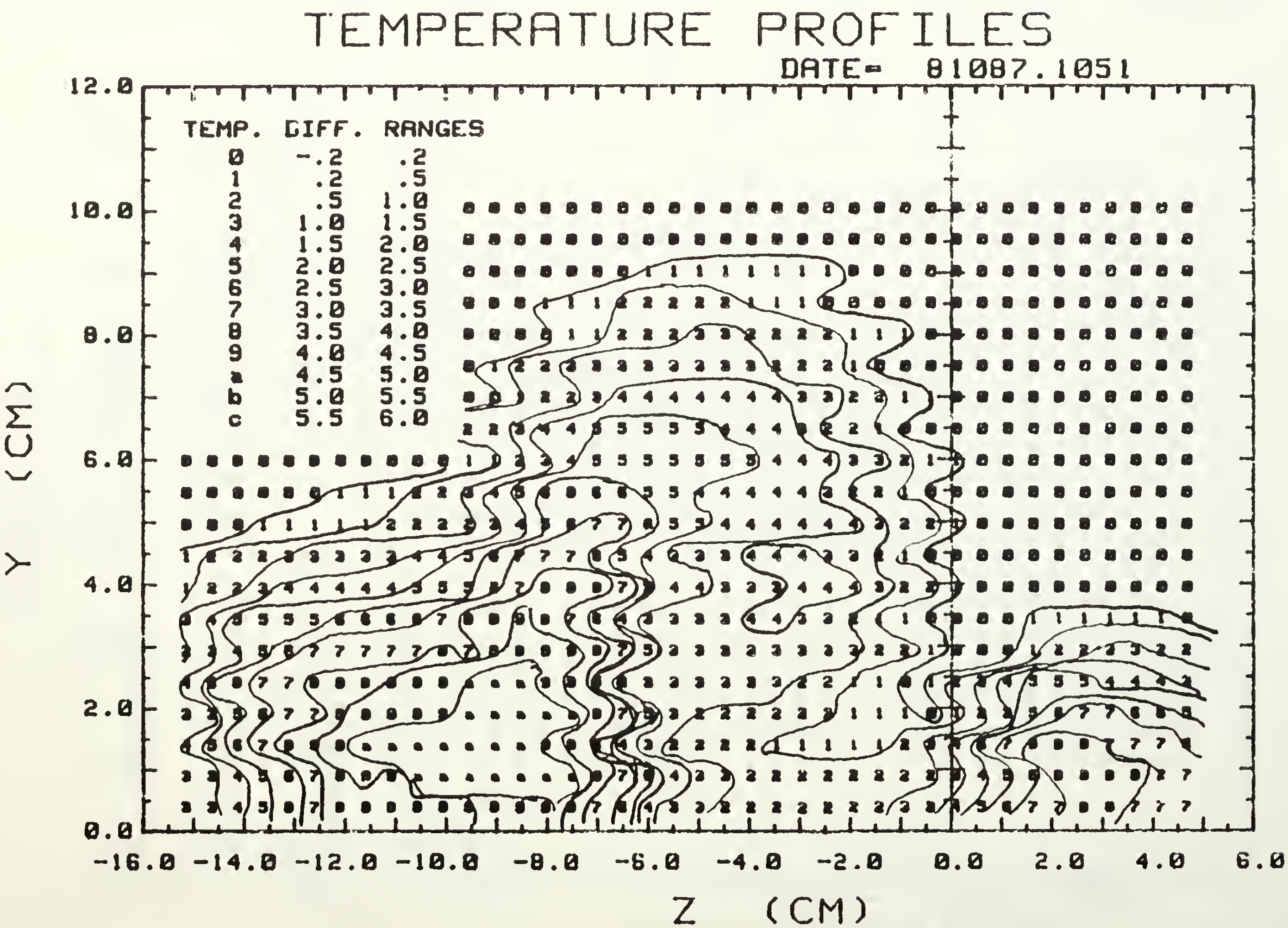

Fig. 35b. EMBEDDED VORTEX 10 M/S WITH FILM COOLING, M=0.98
X=1.867 M, UNHEATED PLATE, VORTEX GEN. AT 4.79 cm

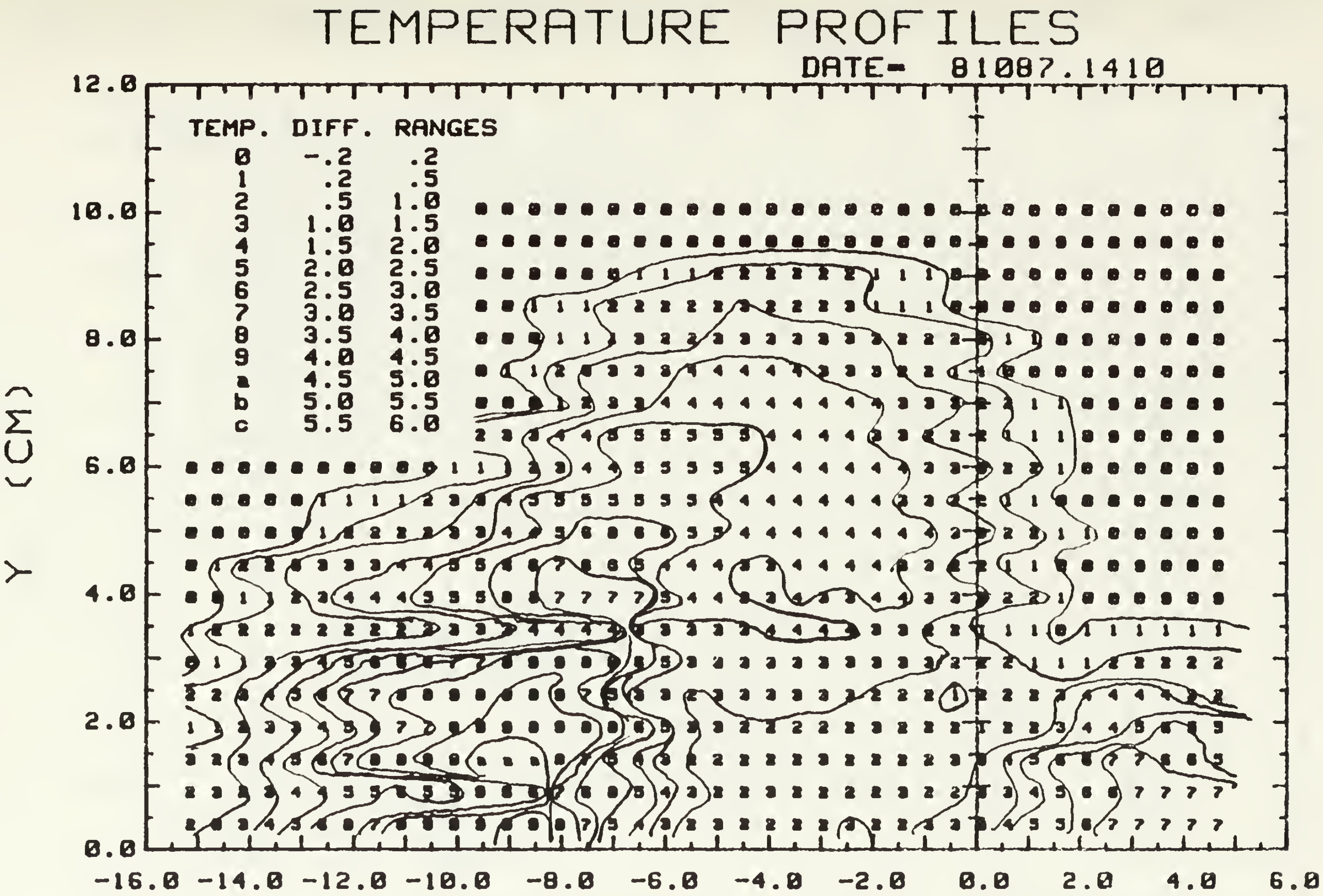

Fig. 35c. EMBEDDED VORTEX 10 M/S WITH FILM COOLING, M=0.98
X=2.172 M, UNHEATED PLATE, VORTEX GEN. AT 4.79 cm

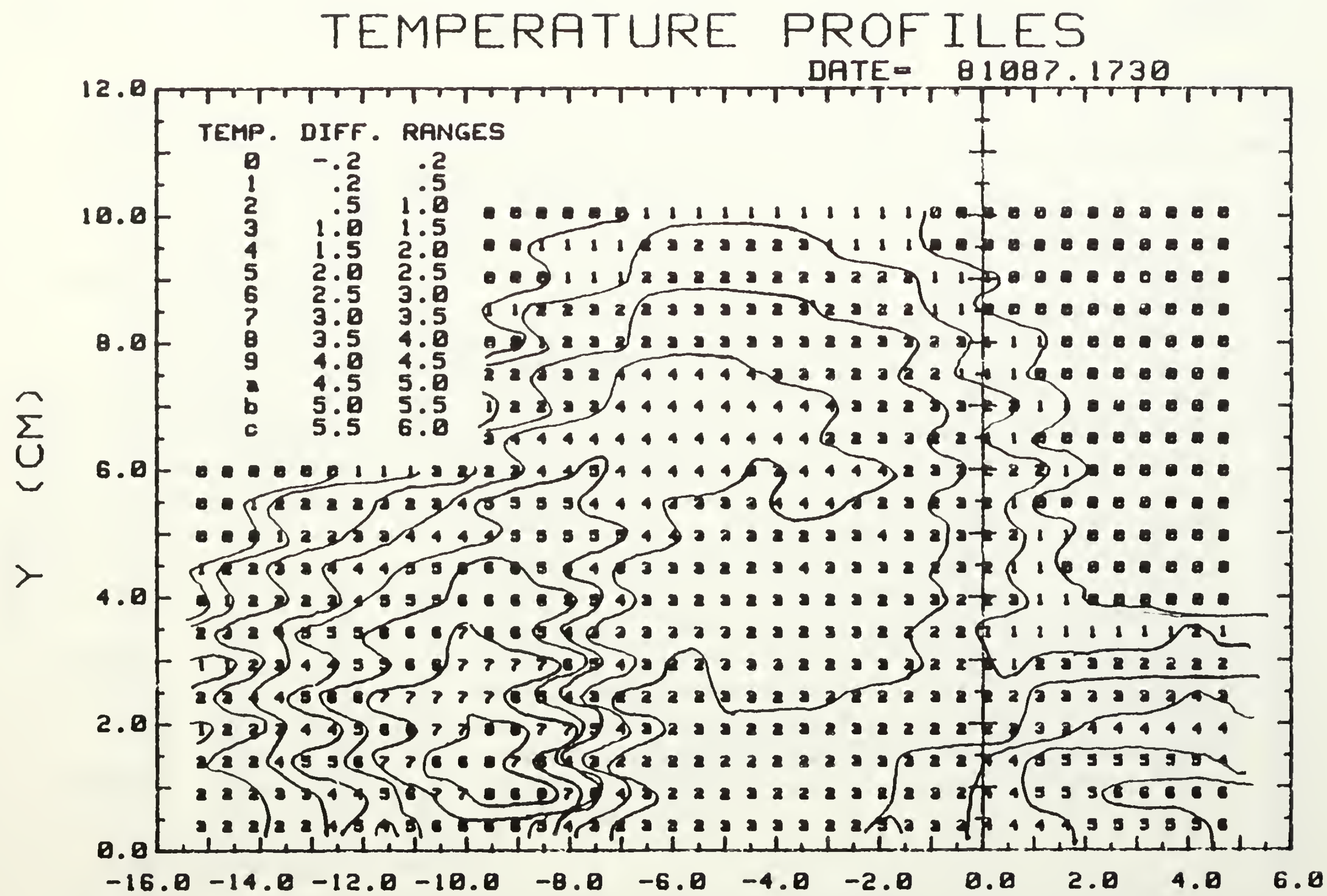

Fig. 35d. EMBEDDED VORTEX 10 M/S WITH FILM COOLING, M=0.98
X=2.480 M, UNHEATED PLATE, VORTEX GEN. AT 4.79 cm

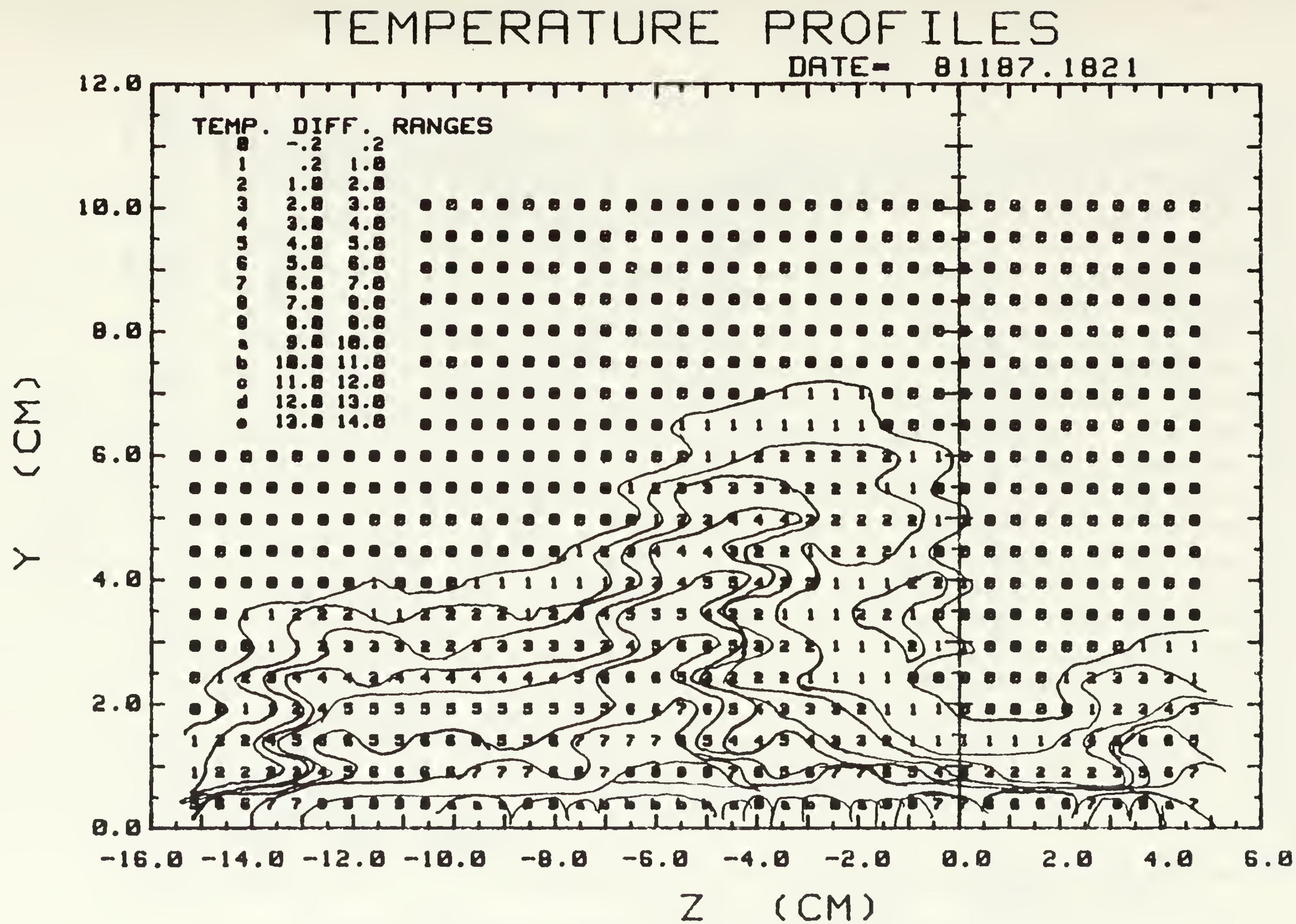

Fig. 36a. EMBEDED VORTEX, 10 M/S WITH FILM COOLING, M=.98
X=1.480 M, HEATED PLATE, VORTEX GEN AT 4.79 cm

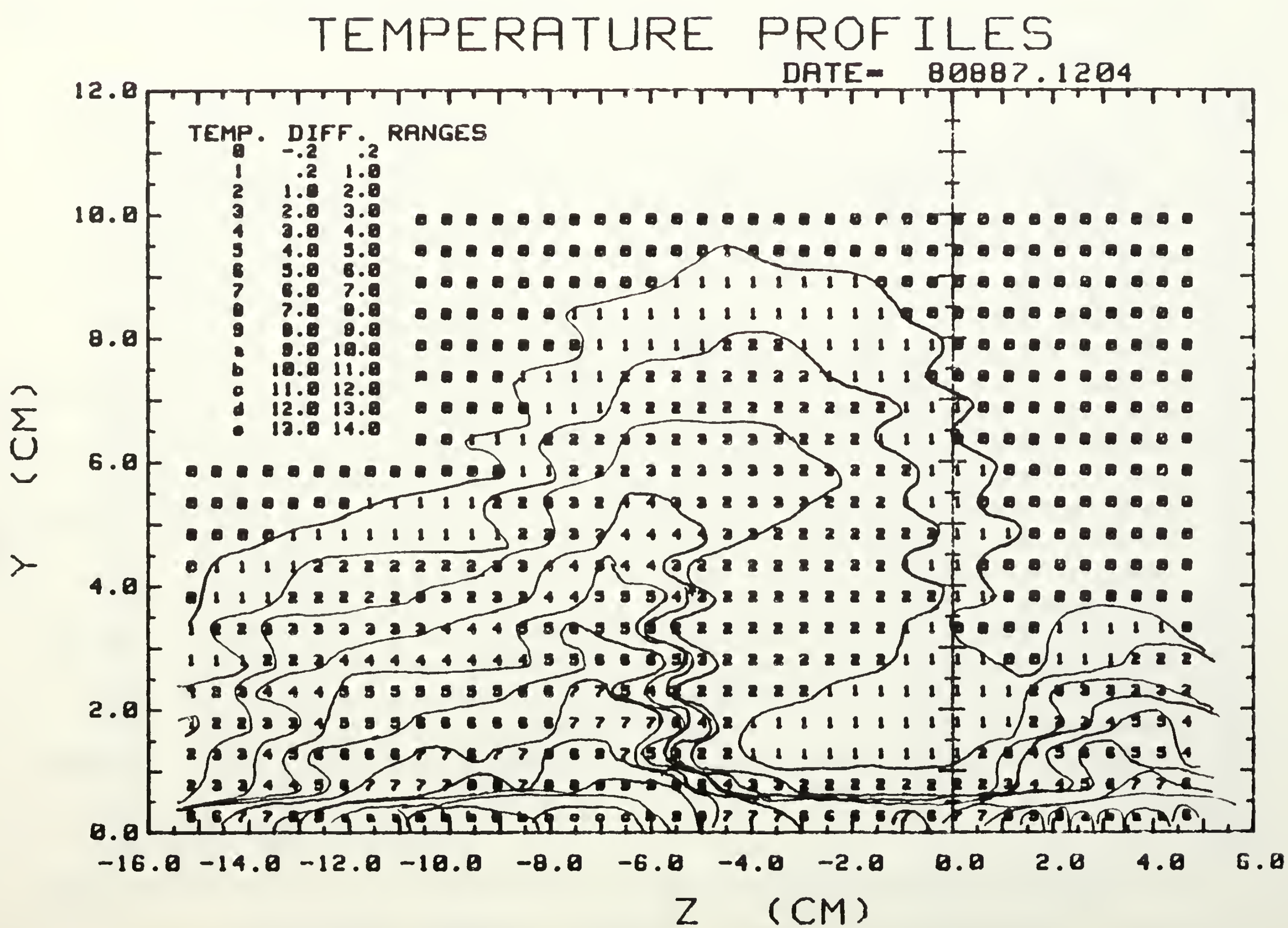

Fig. 36b. EMBEDED VORTEX, 10 M/S WITH FILM COOLING, M=.98
X=1.867 M, HEATED PLATE, VORTEX GEN AT 4.79 cm

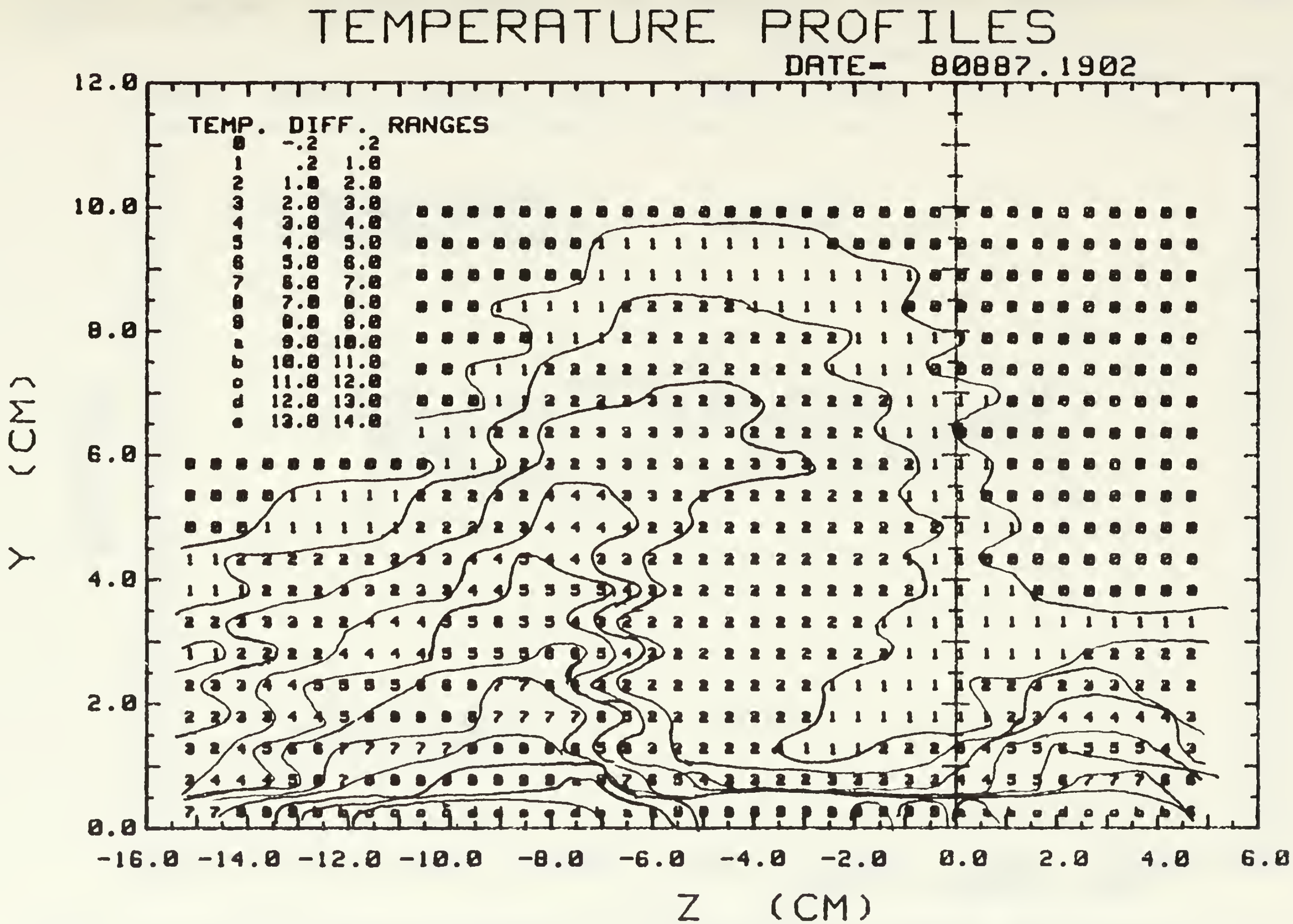

Fig. 36c. EMBEDED VORTEX, 10 M/S WITH FILM COOLING, M=.98
X=2.172 M, HEATED PLATE,VORTEX GEN AT 4.79 cm

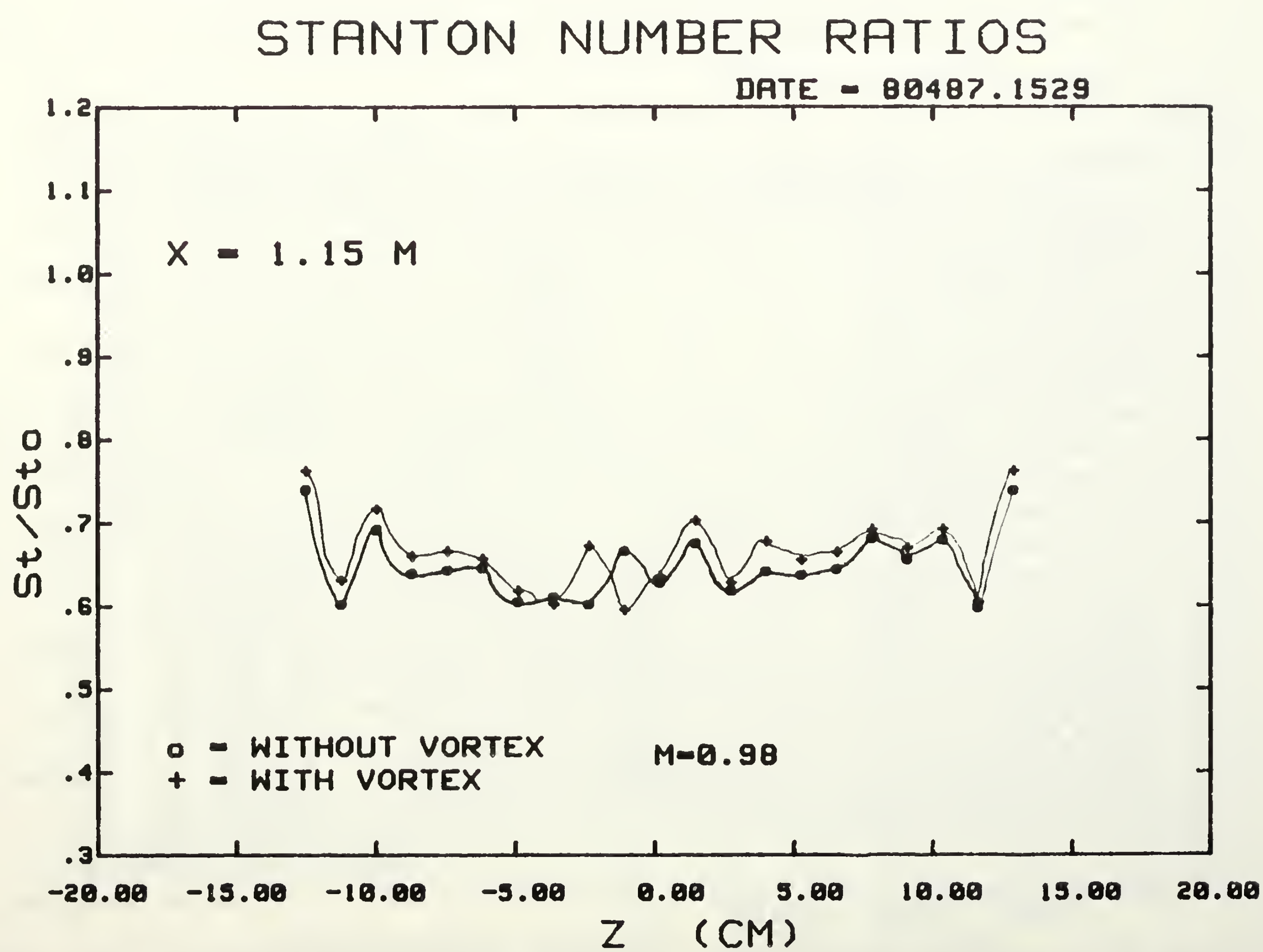

FREE STREAM 10 M/S, WITH FILM COOLING, VORTEX GEN.#2 AT 3.52 cm

Fig. 37a. Spanwise Variations of Stanton Number Ratios.

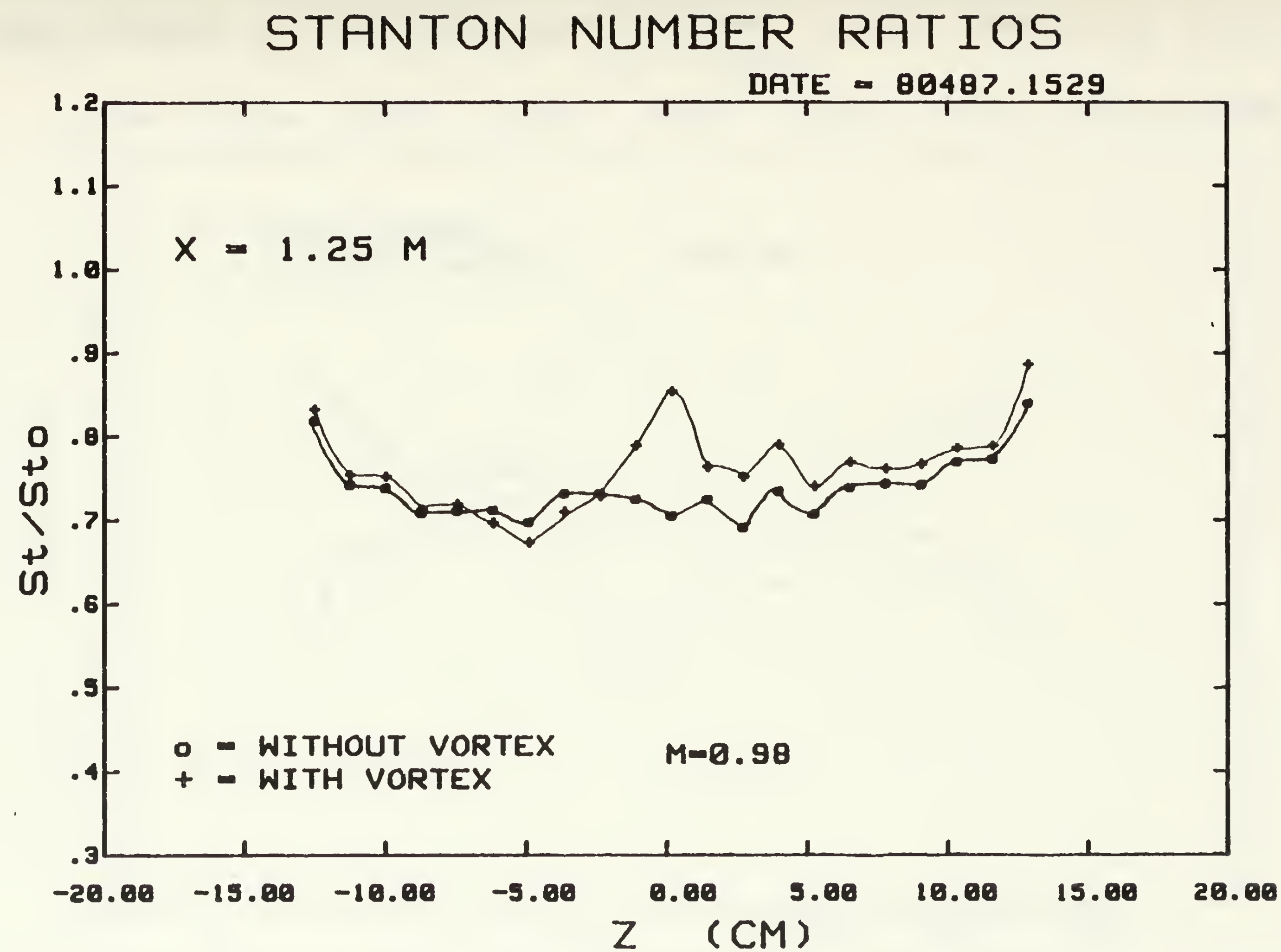

FREE STREAM 10 M/S, WITH FILM COOLING, VORTEX GEN.#2 AT 3.52 cm

Fig. 37b. Spanwise Variations of Stanton Number Ratios.

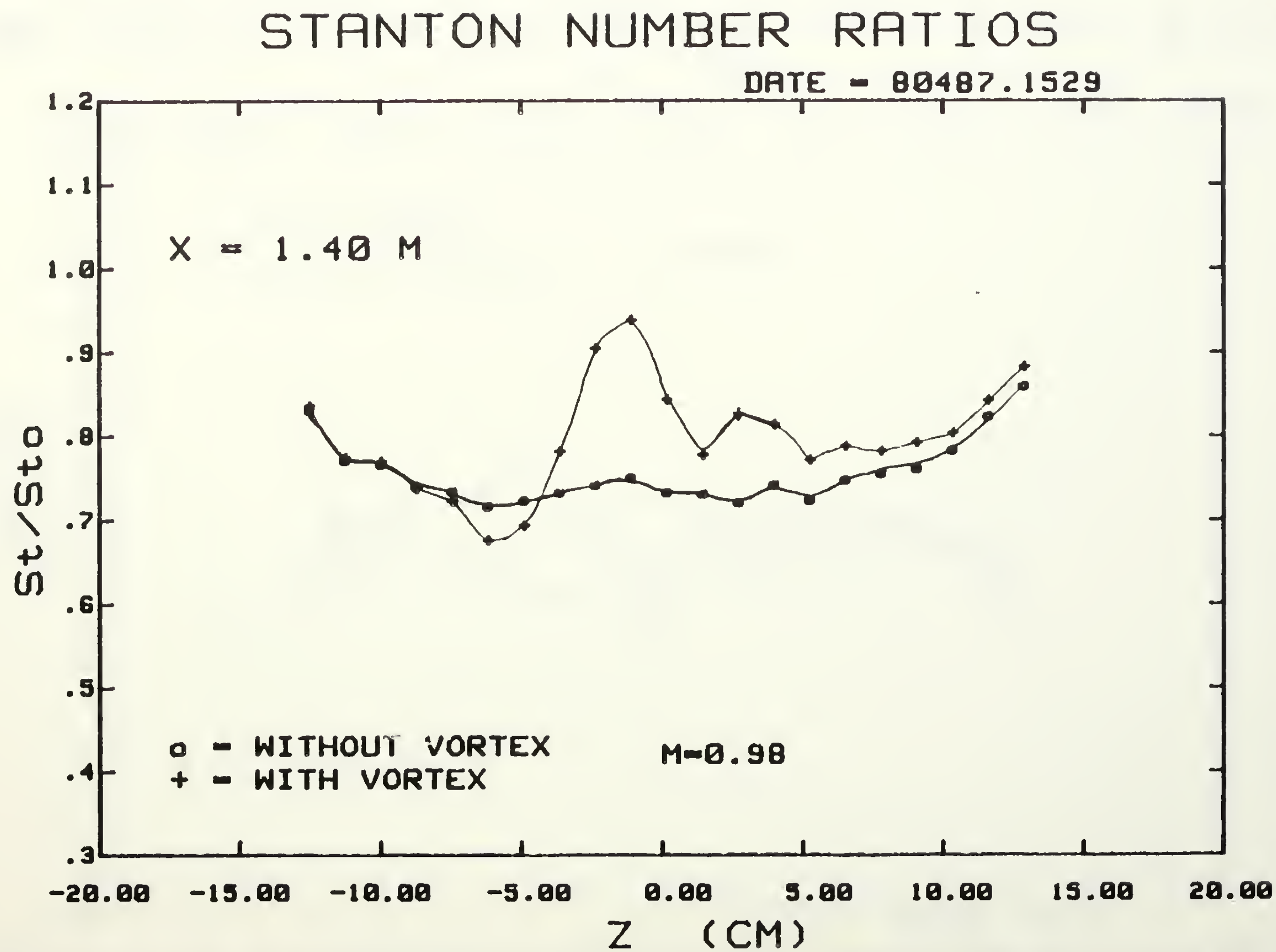

FREE STREAM 10 M/S, WITH FILM COOLING, VORTEX GEN.#2 AT 3.52 cm

Fig. 37c. Spanwise Variations of Stanton Number Ratios.

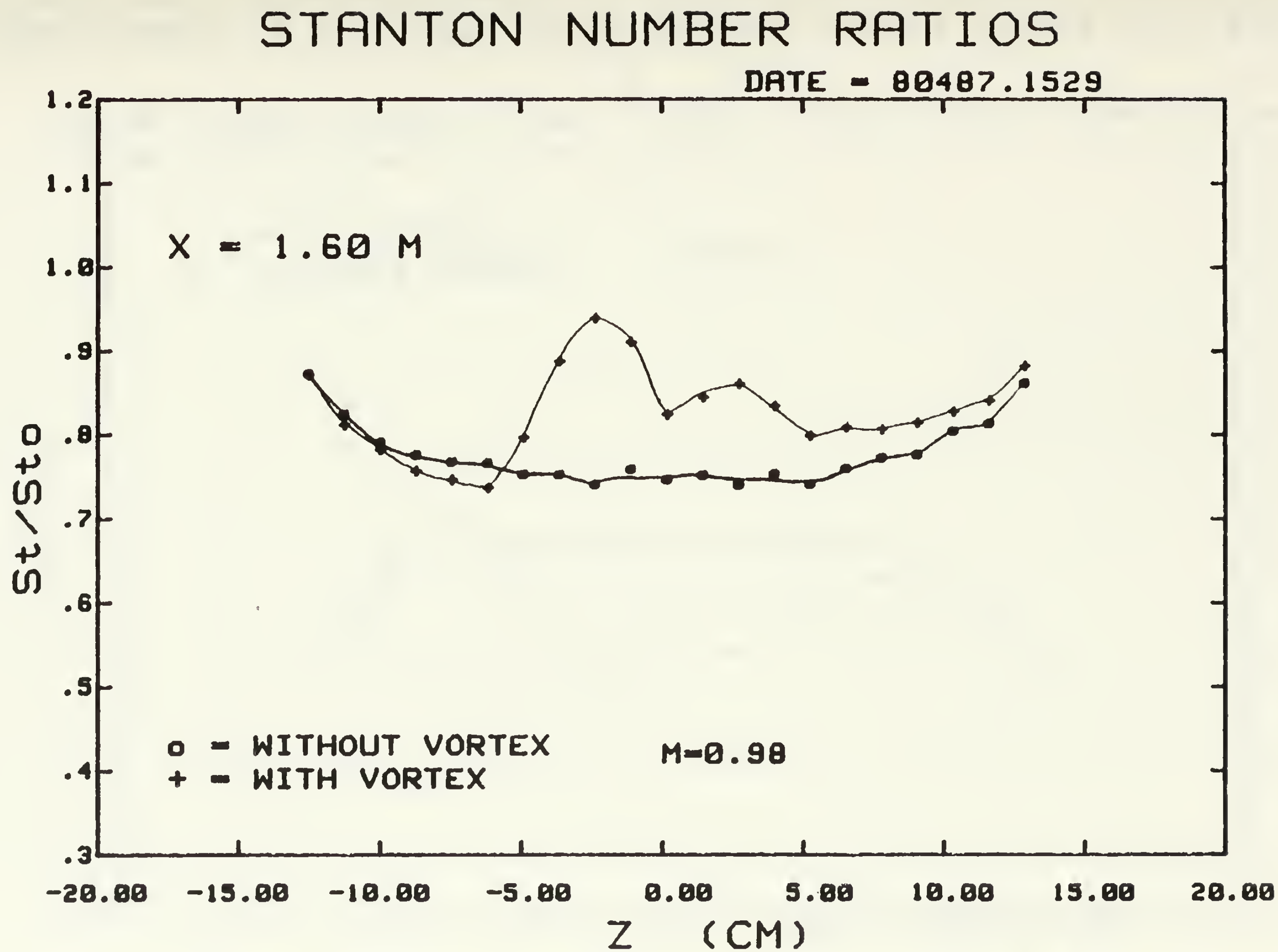

FREE STREAM 10 M/S, WITH FILM COOLING, VORTEX GEN.#2 AT 3.52 cm

Fig. 37d. Spanwise Variations of Stanton Number Ratios.

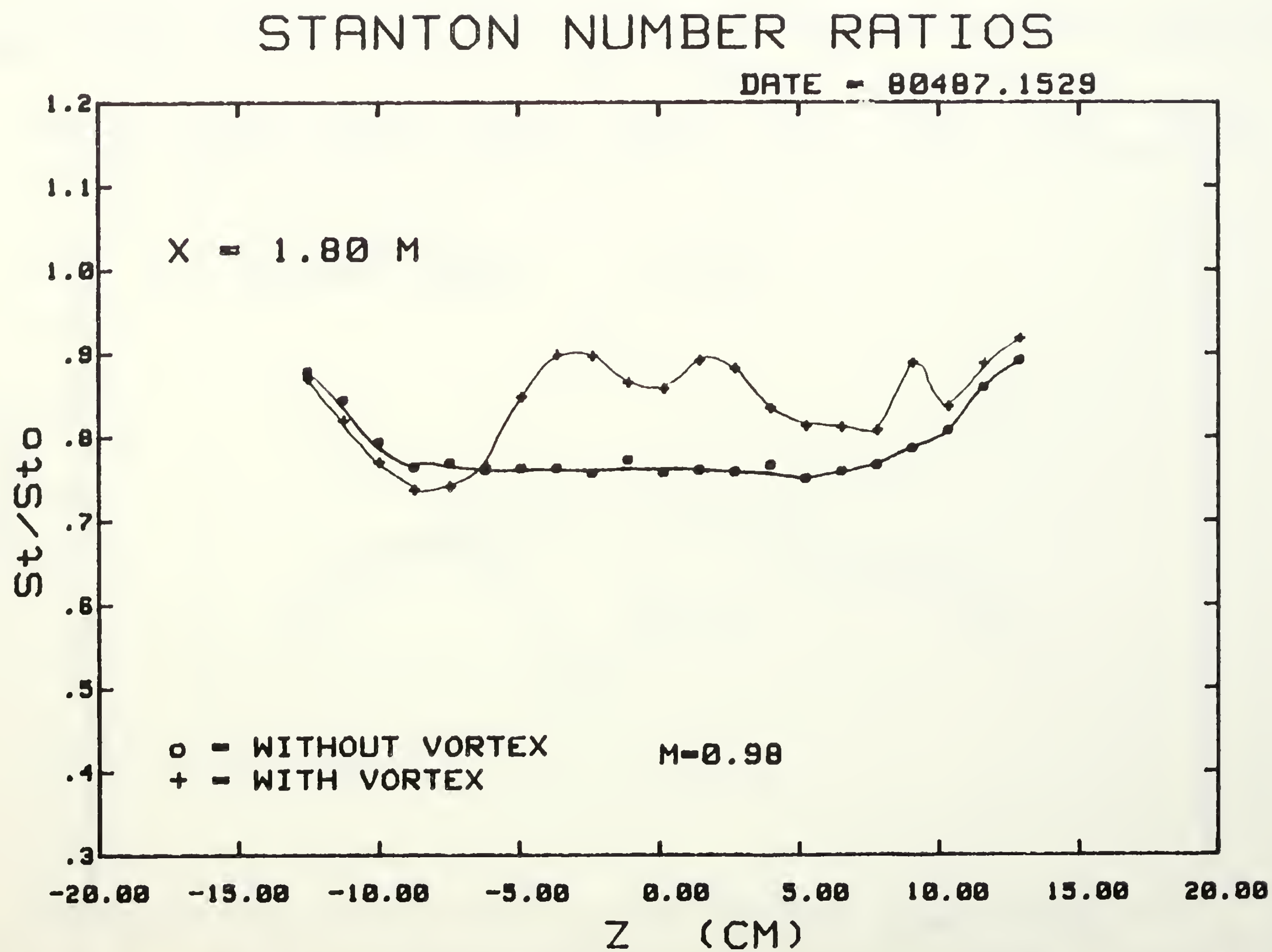

FREE STREAM 10 M/S, WITH FILM COOLING, VORTEX GEN.#2 AT 3.52 cm

Fig. 37e. Spanwise Variations of Stanton Number Ratios.

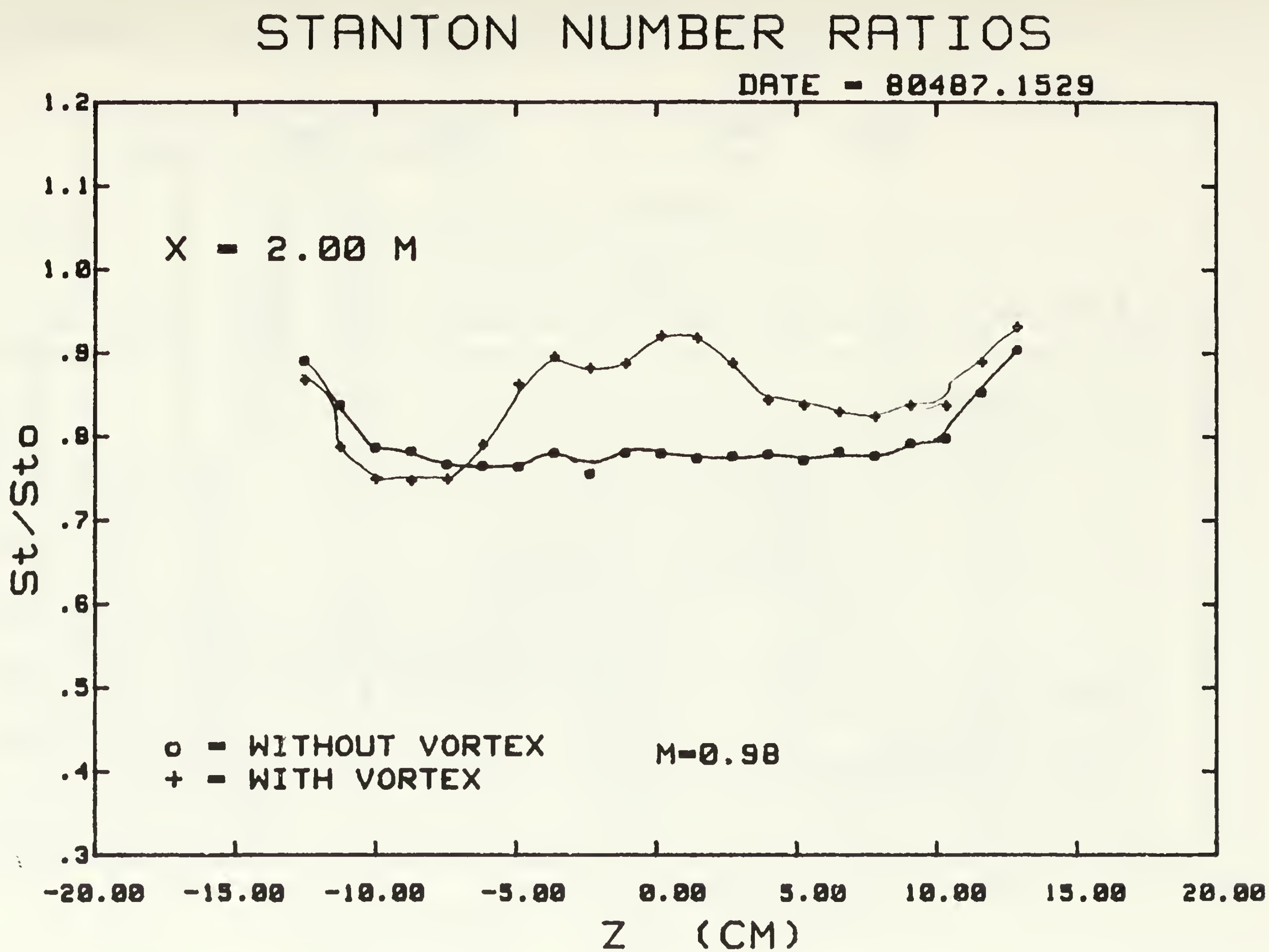

FREE STREAM 10 M/S, WITH FILM COOLING, VORTEX GEN.#2 AT 3.52 cm

Fig.37f. Spanwise Variations of Stanton Number Ratios.

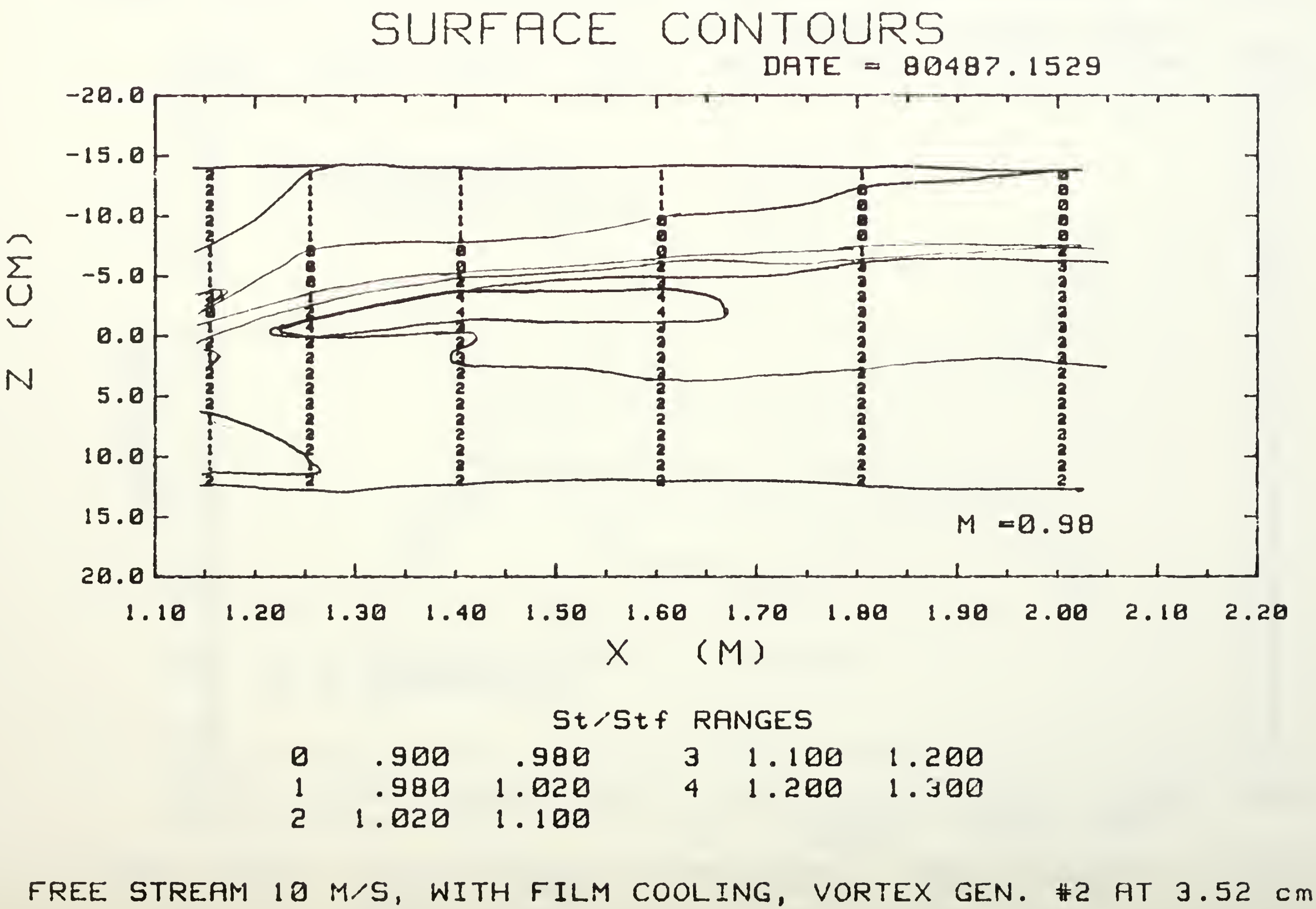

Fig. 38. Surface Contour.

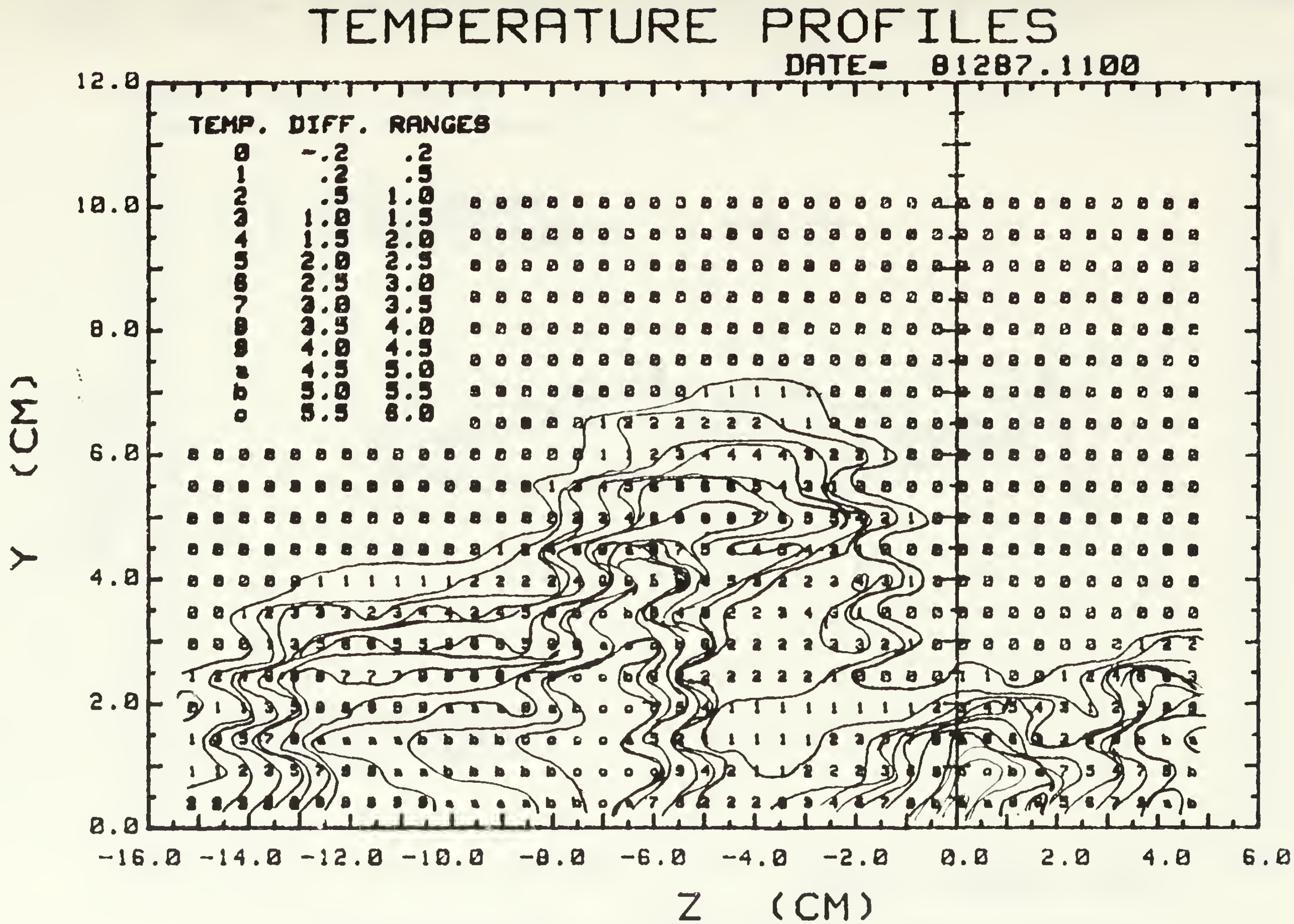

Fig. 39. EMBEDDED VORTEX 10 M/S WITH FILM COOLING, M=0.98
X=1.480 M, UNHEATED PLATE, VORTEX GEN. AT 3.52 cm

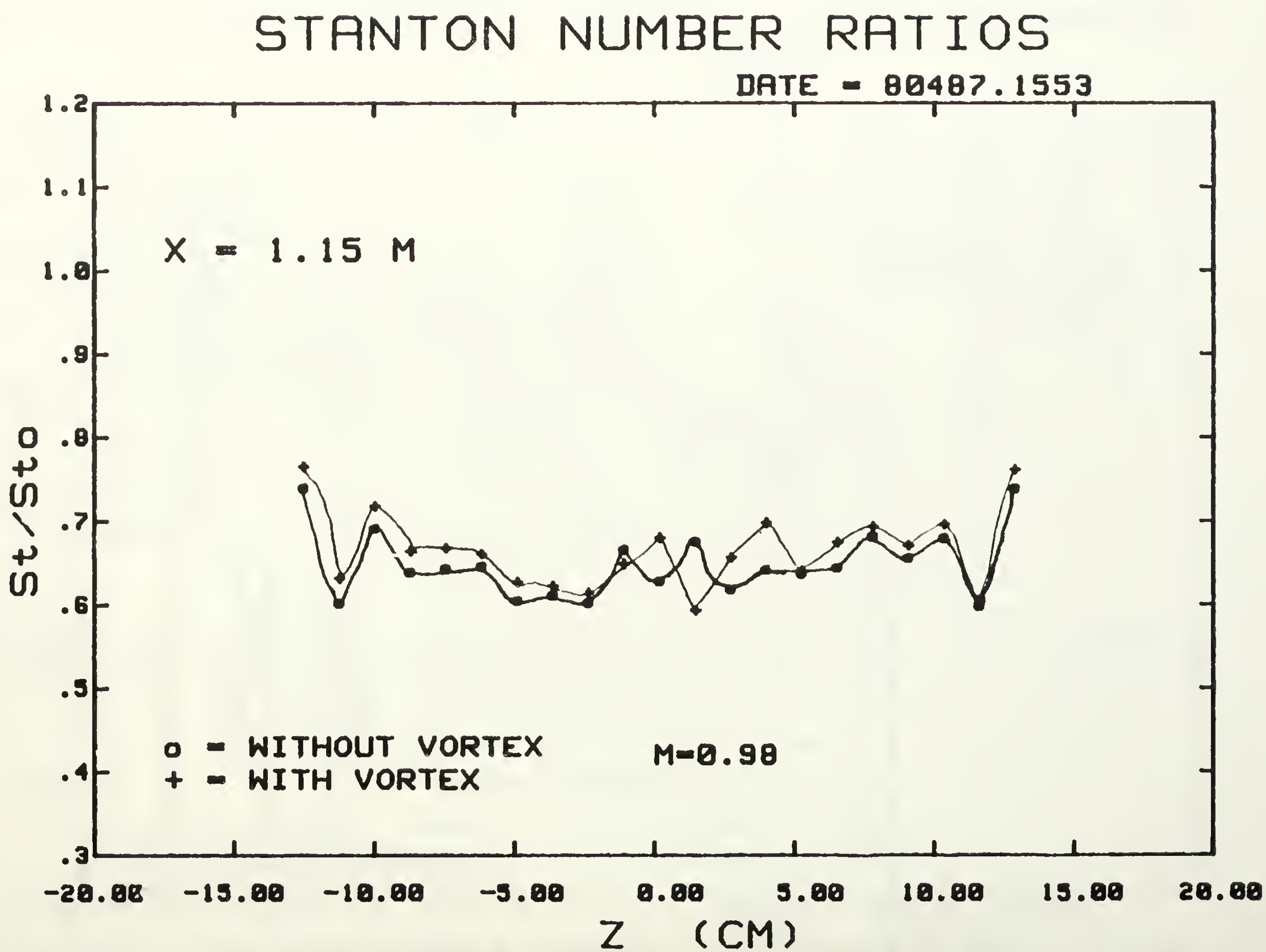

FREE STREAM 10 M/S, WITH FILM COOLING, VORTEX GEN.#2 AT 6.06 cm

Fig. 40a. Spanwise Variations of Stanton Number Ratios.

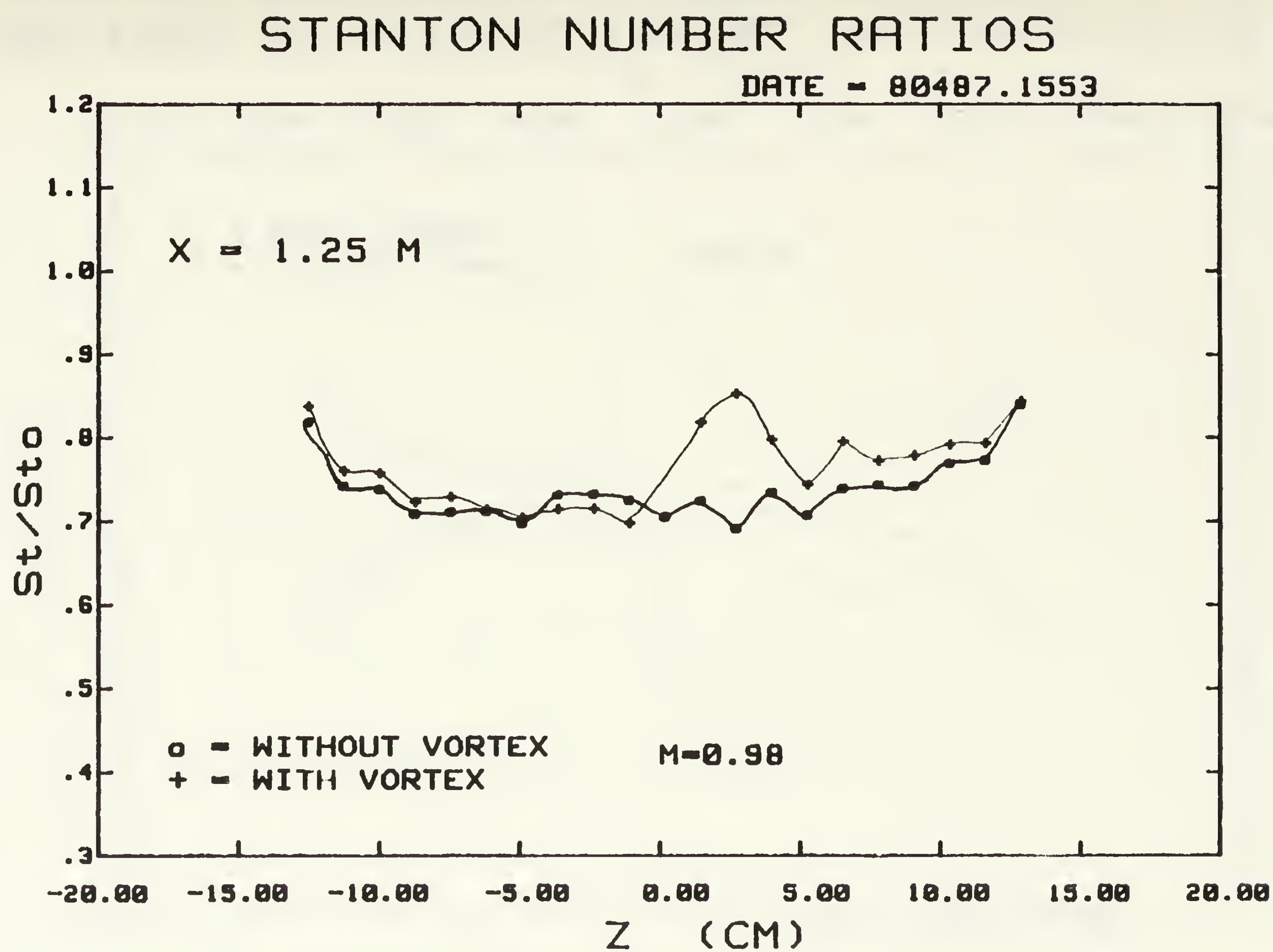

FREE STREAM 10 M/S, WITH FILM COOLING, VORTEX GEN.#2 AT 6.06 cm

Fig. 40b. Spanwise Variations of Stanton Number Ratios.

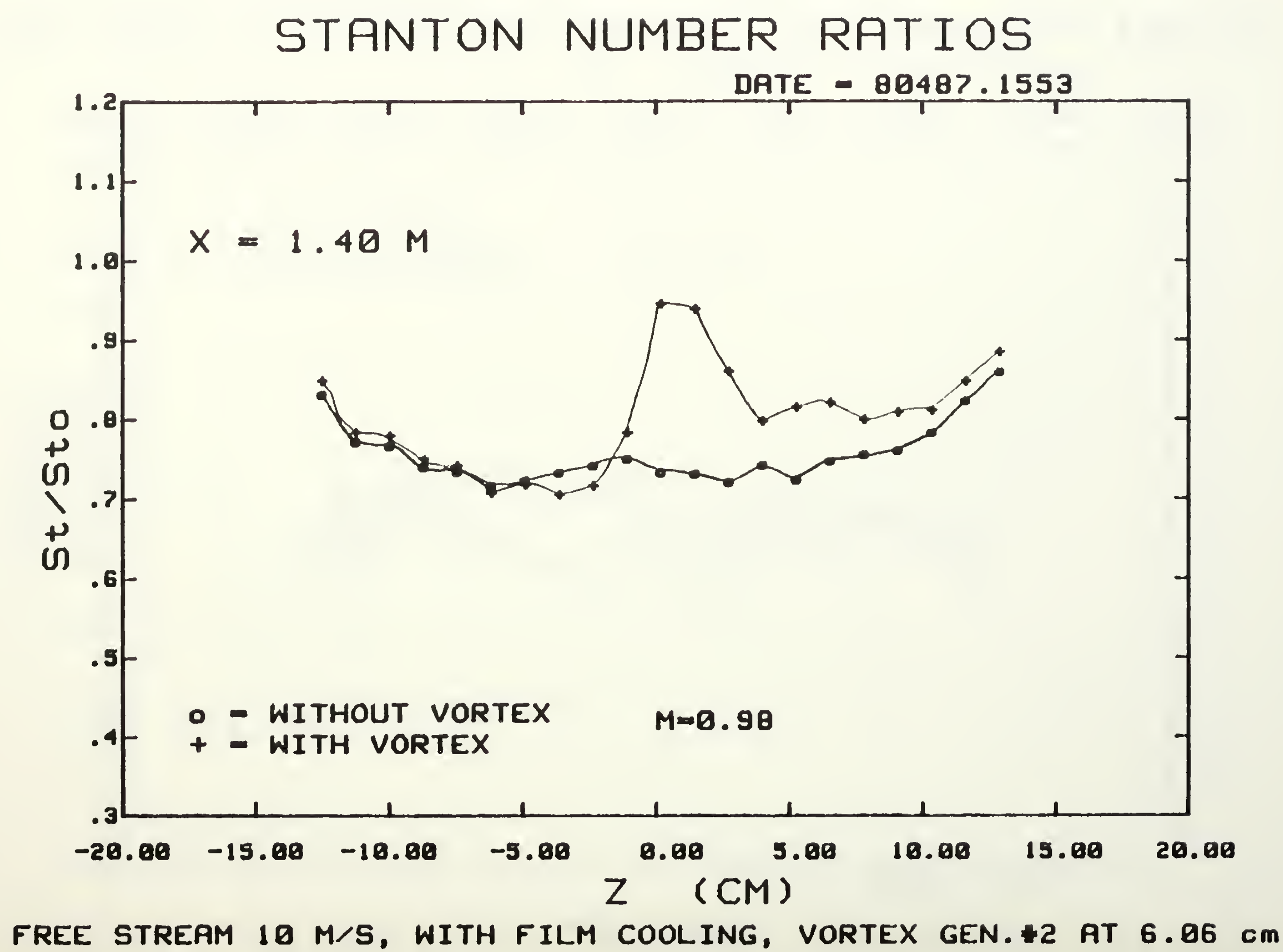

Fig. 40c. Spanwise Variations of Stanton Number Ratios.

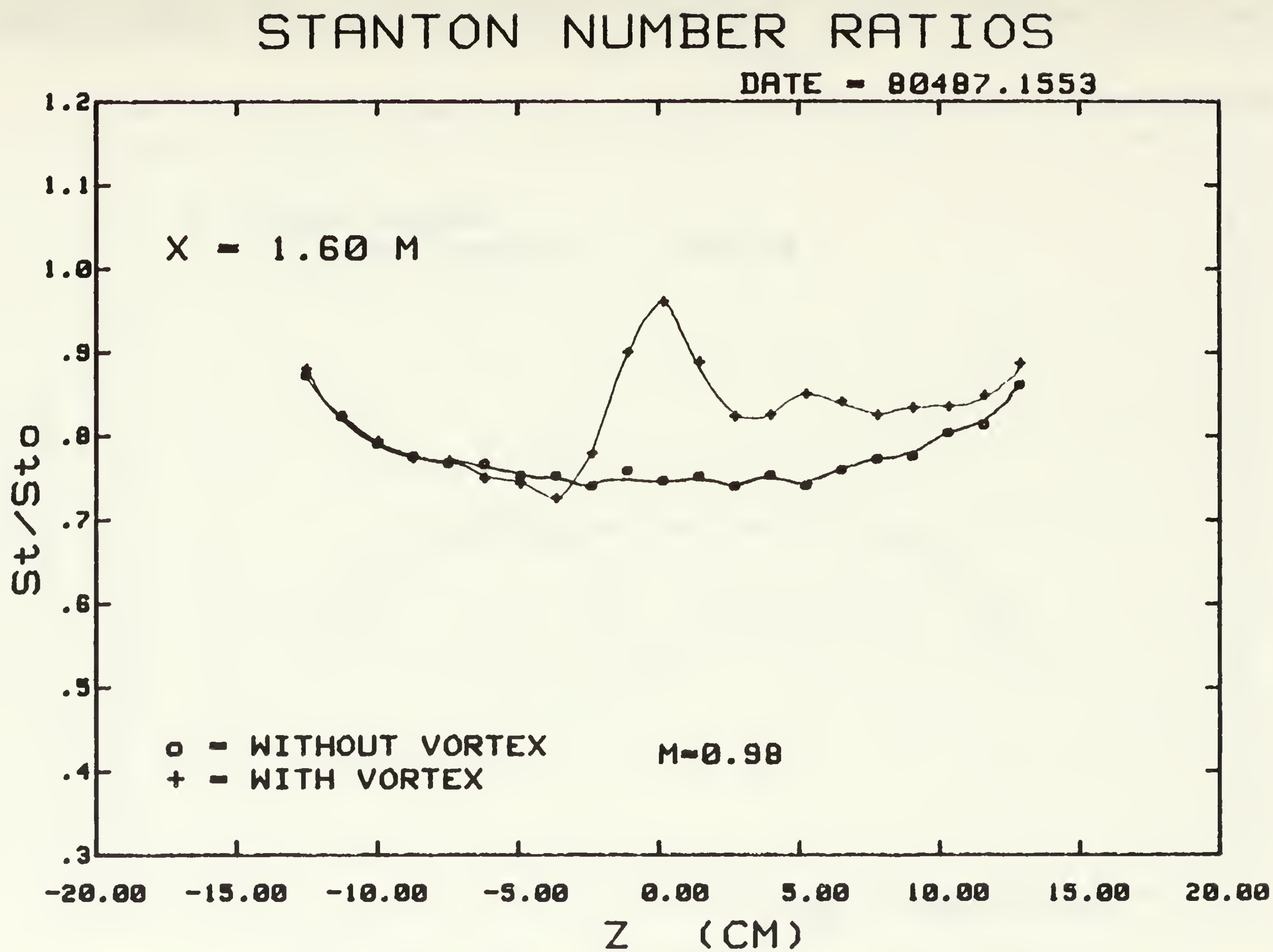

FREE STREAM 10 M/S, WITH FILM COOLING, VORTEX GEN.#2 AT 6.06 cm

Fig. 40d. Spanwise Variations of Stanton Number Ratios.

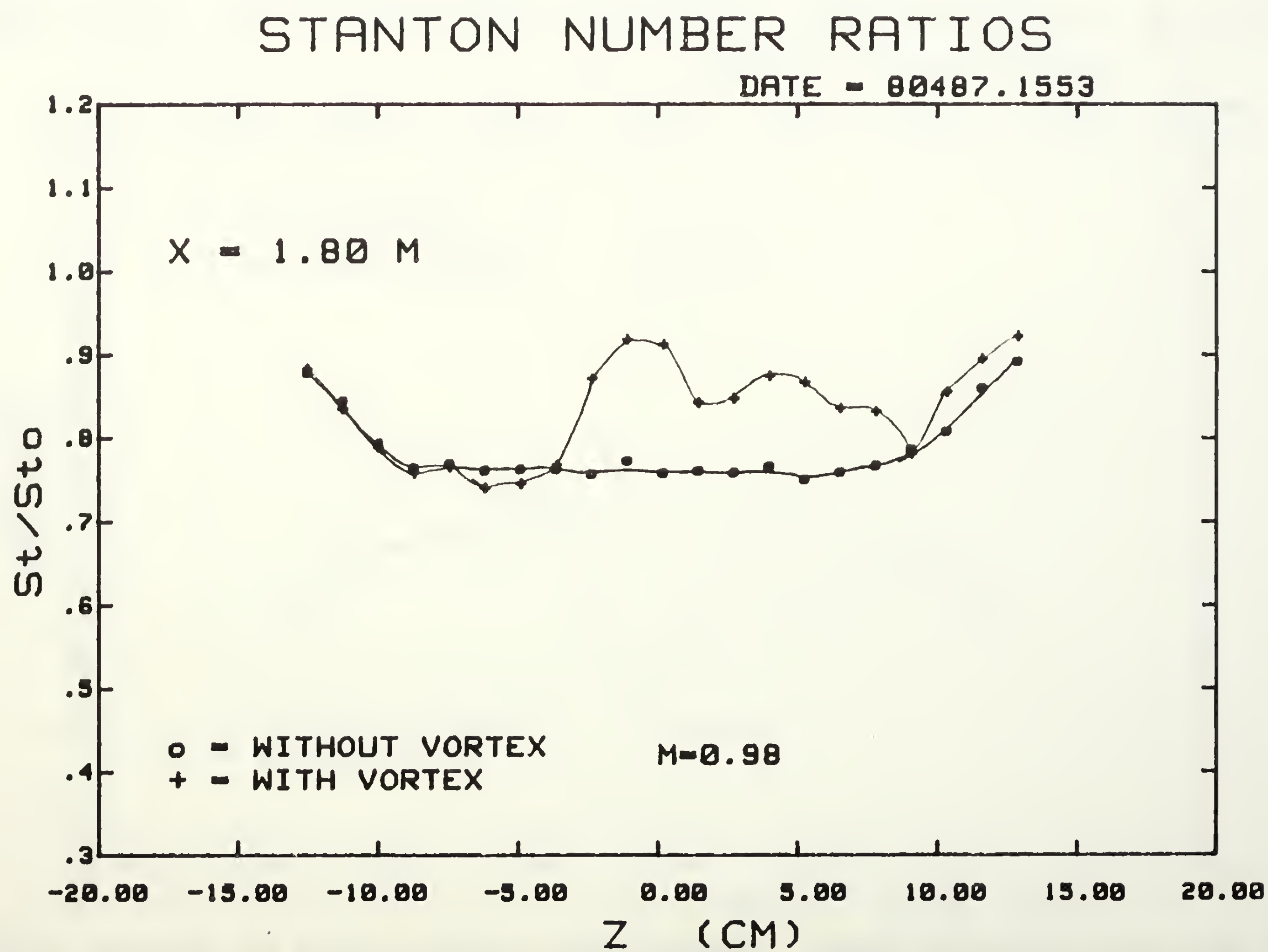

FREE STREAM 10 M/S, WITH FILM COOLING, VORTEX GEN.#2 AT 6.06 cm

Fig. 40e. Spanwise Variations of Stanton Number Ratios.

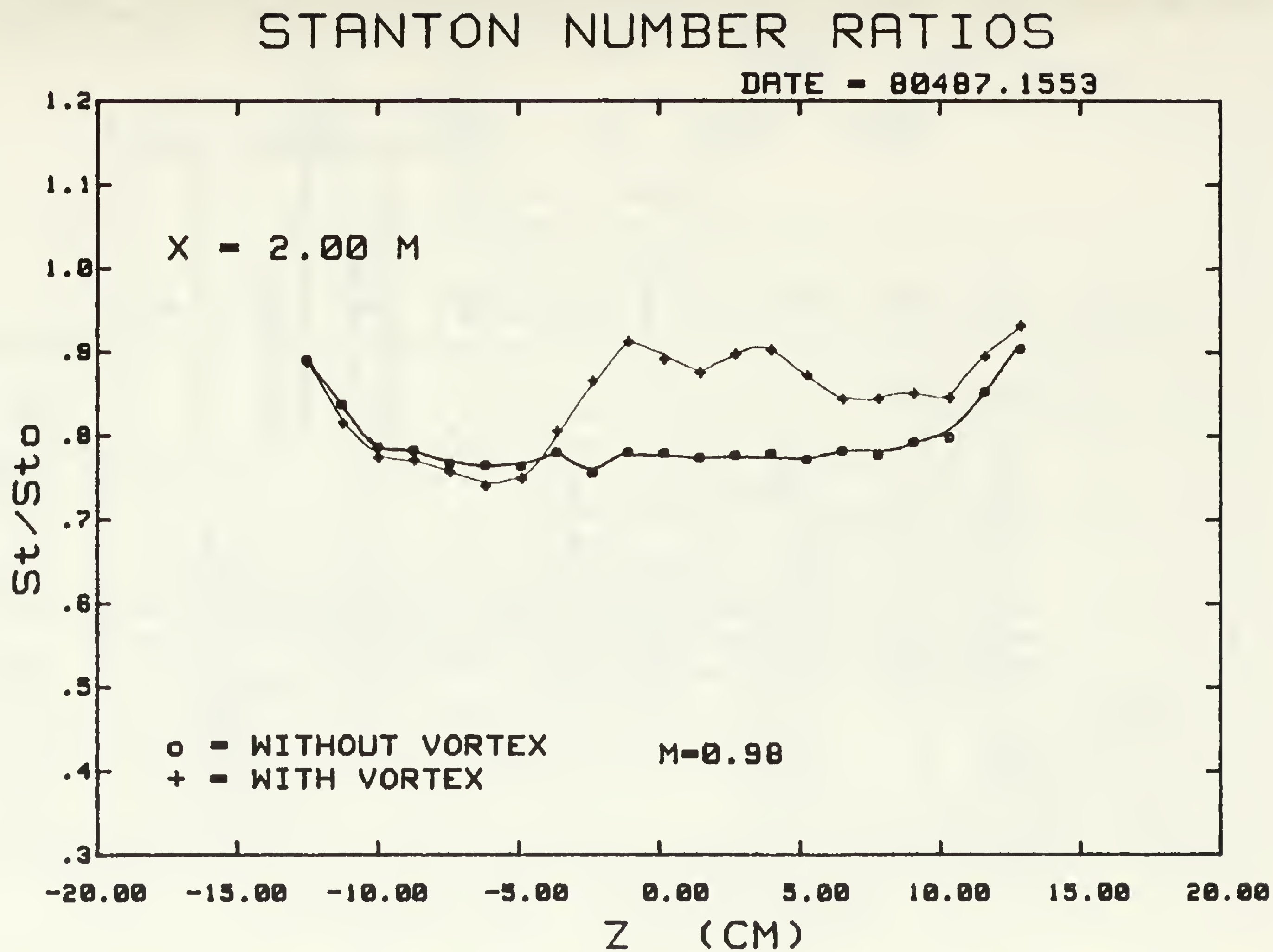

FREE STREAM 10 M/S, WITH FILM COOLING, VORTEX GEN.#2 AT 6.06 cm

Fig. 40f. Spanwise Variations of Stanton Number Ratios.

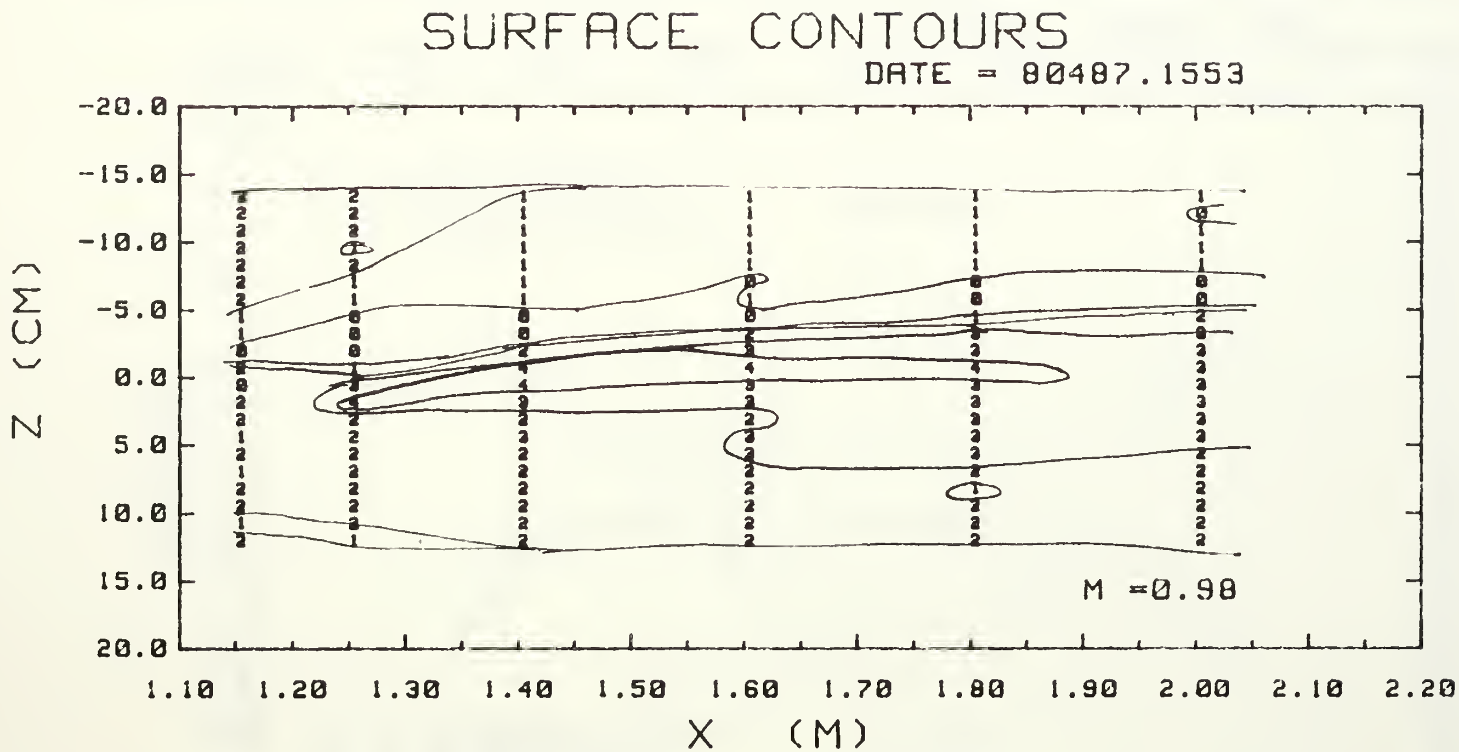

St/Stf RANGES

0	.900	.980	3	1.100	1.200
1	.980	1.020	4	1.200	1.300
2	1.020	1.100			

FREE STREAM 10 M/S, WITH FILM COOLING, VORTEX GEN. #2 AT 6.06 cm

Fig. 41. Surface Contour.

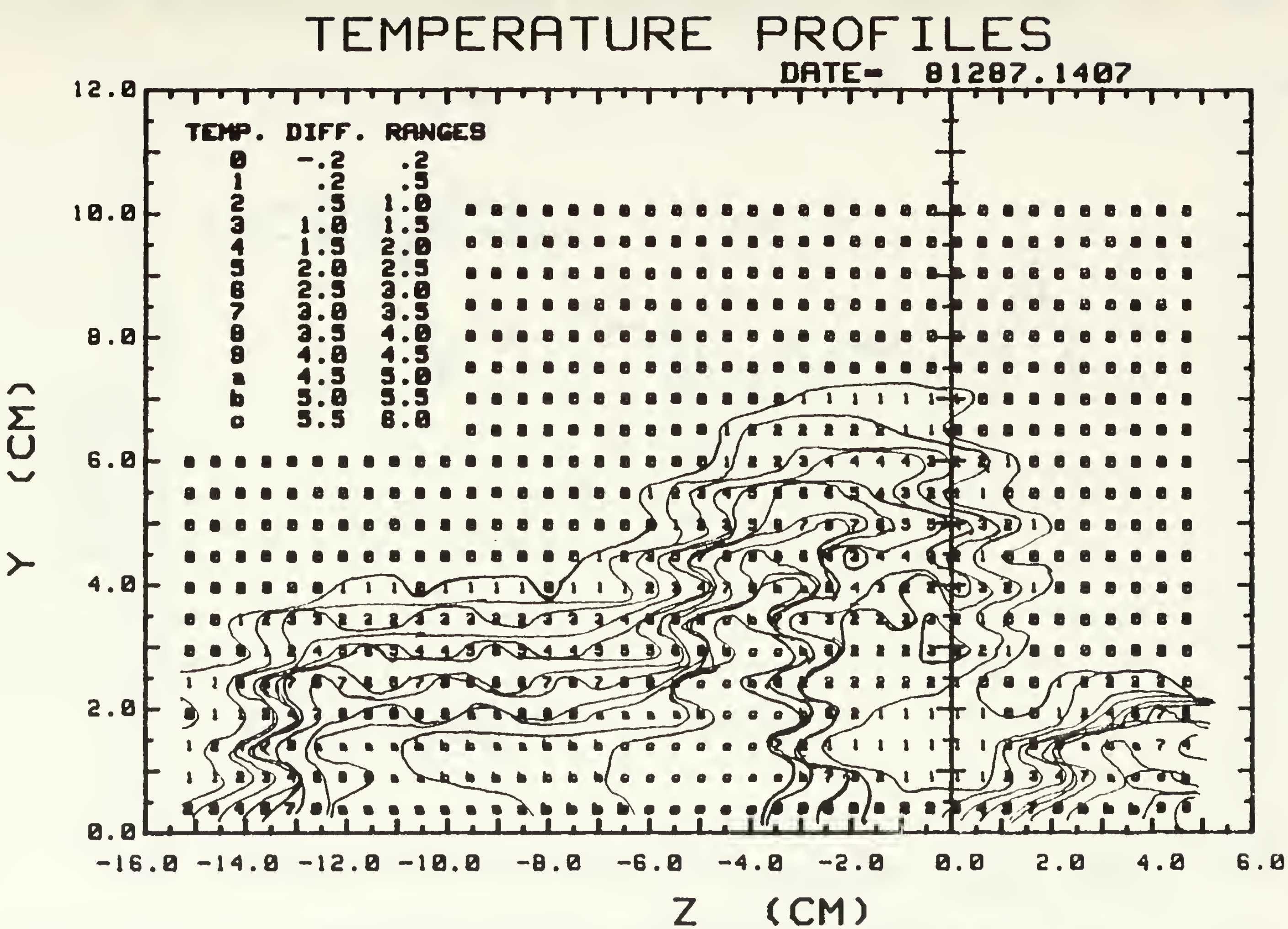

Fig. 42. EMBEDDED VORTEX 10 M/S WITH FILM COOLING
X=1.480 M, UNHEATED PLATE, VOTEX GEN. AT 6.06 cm

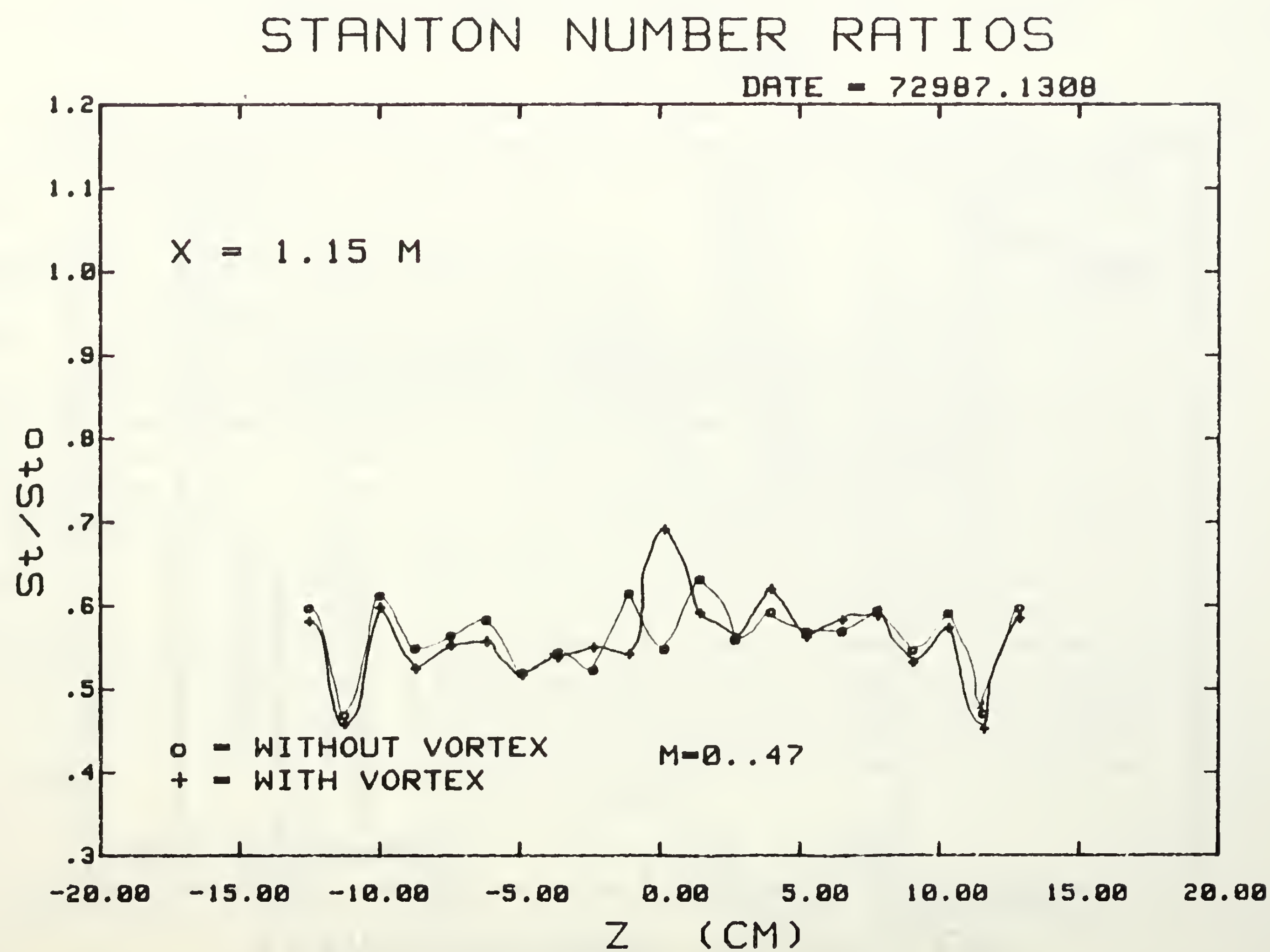

FREE STREAM 15 M/S, WITH FILM COOLING, VORTEX GEN. AT 4.79cm

Fig. 43a. Spanwise Variations of Stanton Number Ratios.

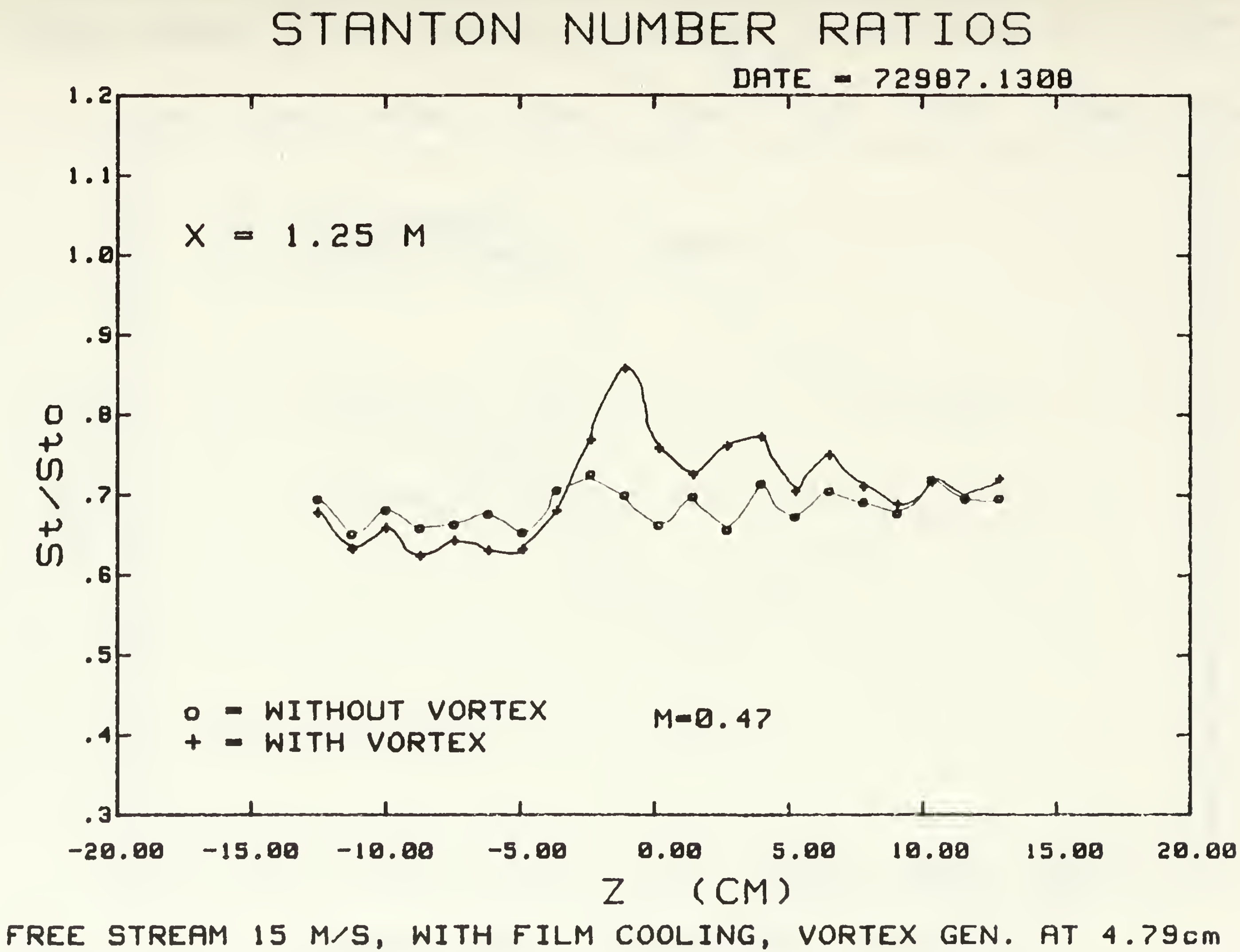

Fig. 43b. Spanwise Variations of Stanton Number Ratios.

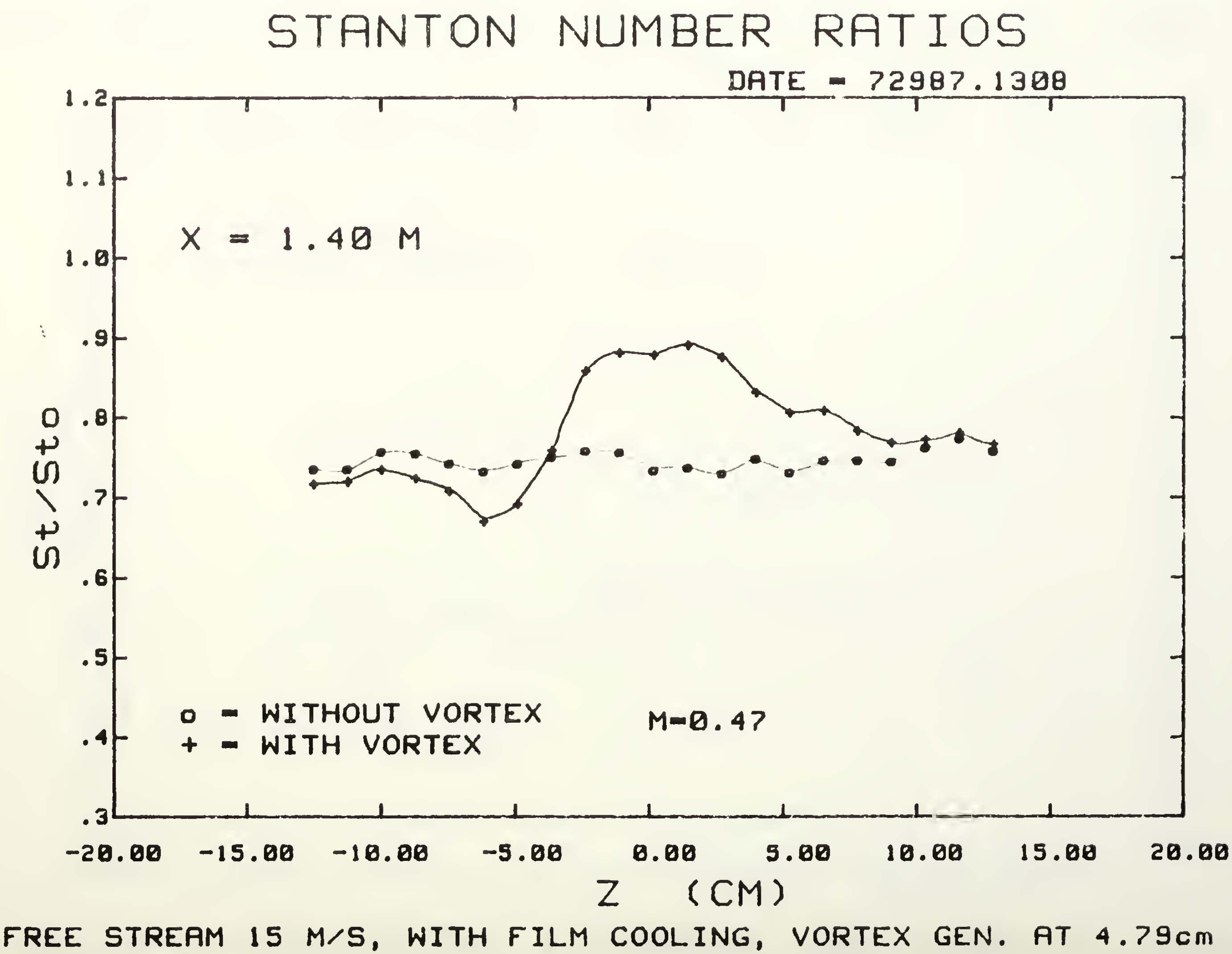

Fig. 43c. Spanwise Variations of Stanton Number Ratios.

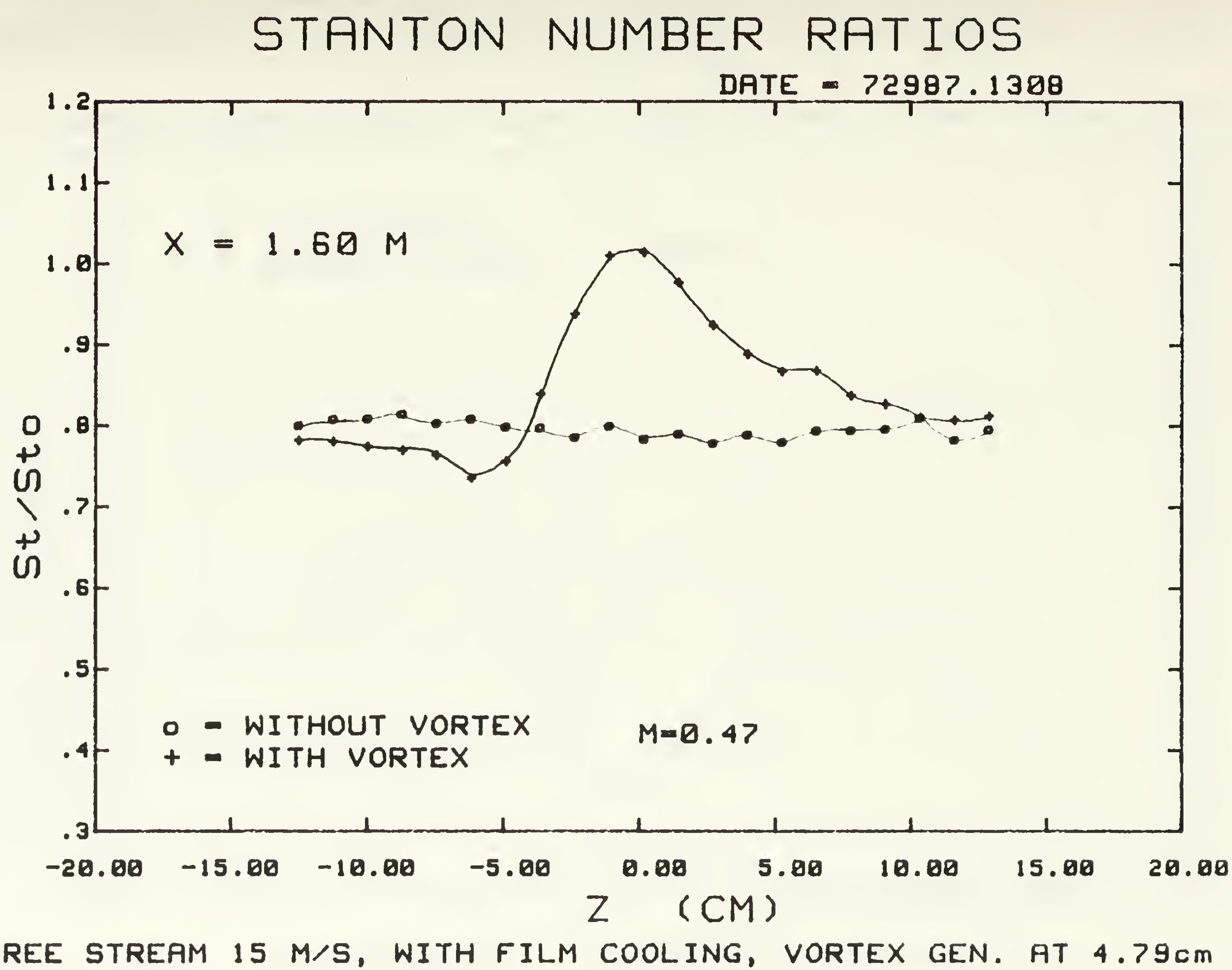

Fig. 43d. Spanwise Variations of Stanton Number Ratios.

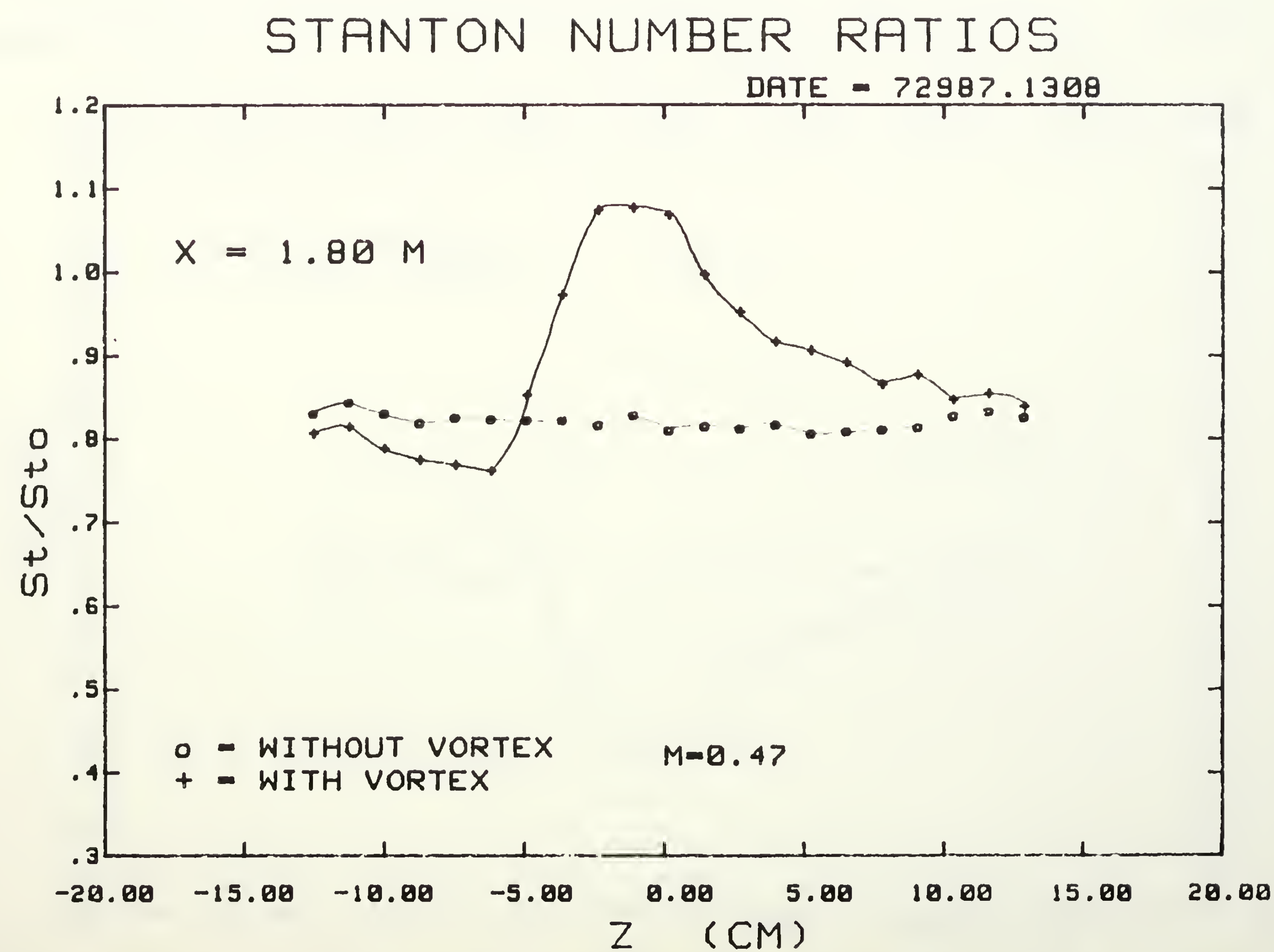

FREE STREAM 15 M/S, WITH FILM COOLING, VORTEX GEN. AT 4.79cm

Fig. 43e. Spanwise Variations of Stanton Number Ratios.

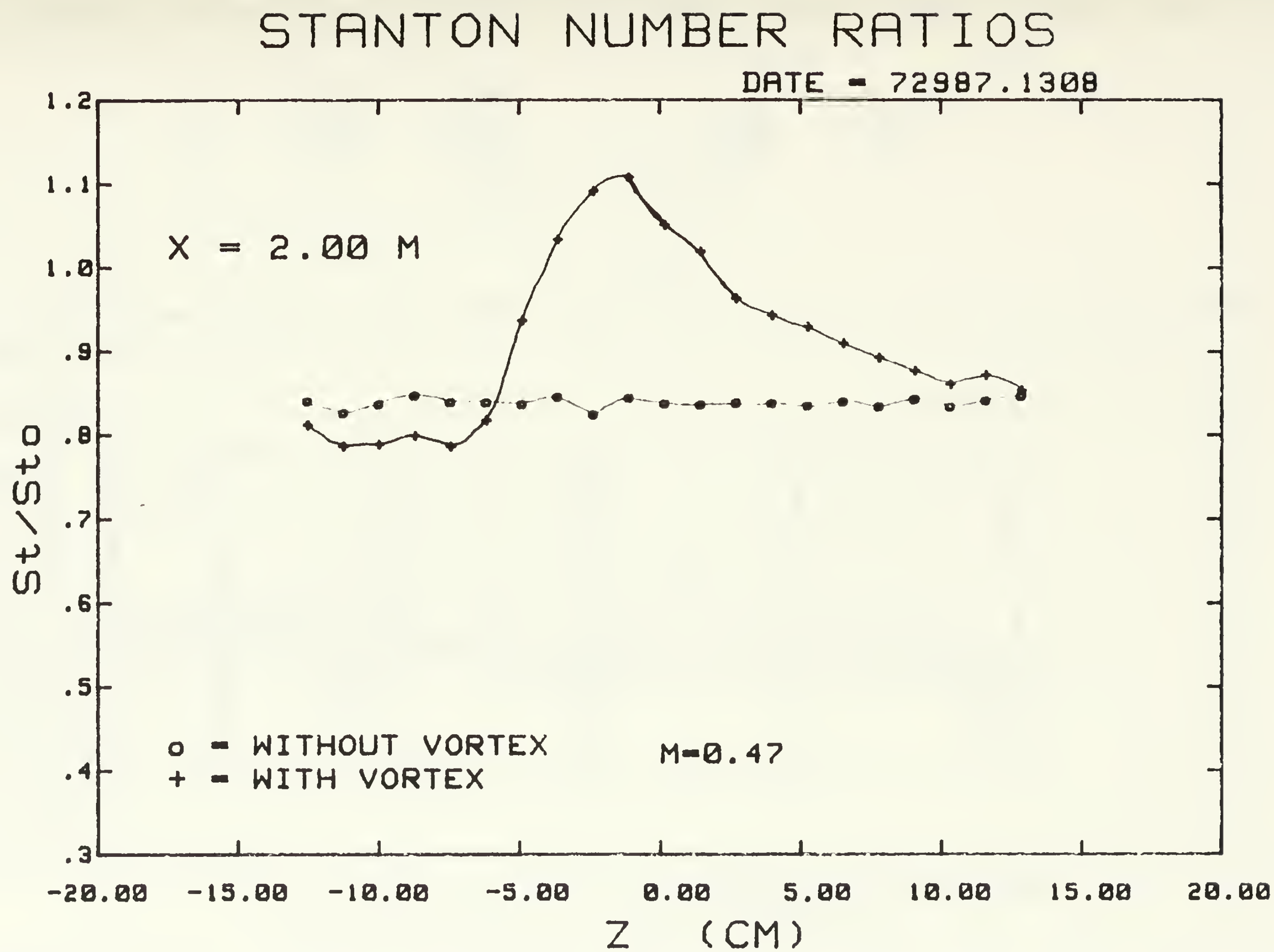

FREE STREAM 15 M/S, WITH FILM COOLING, VORTEX GEN. AT 4.79 cm

Fig. 43f. Spanwise Variations of Stanton Number Ratios.

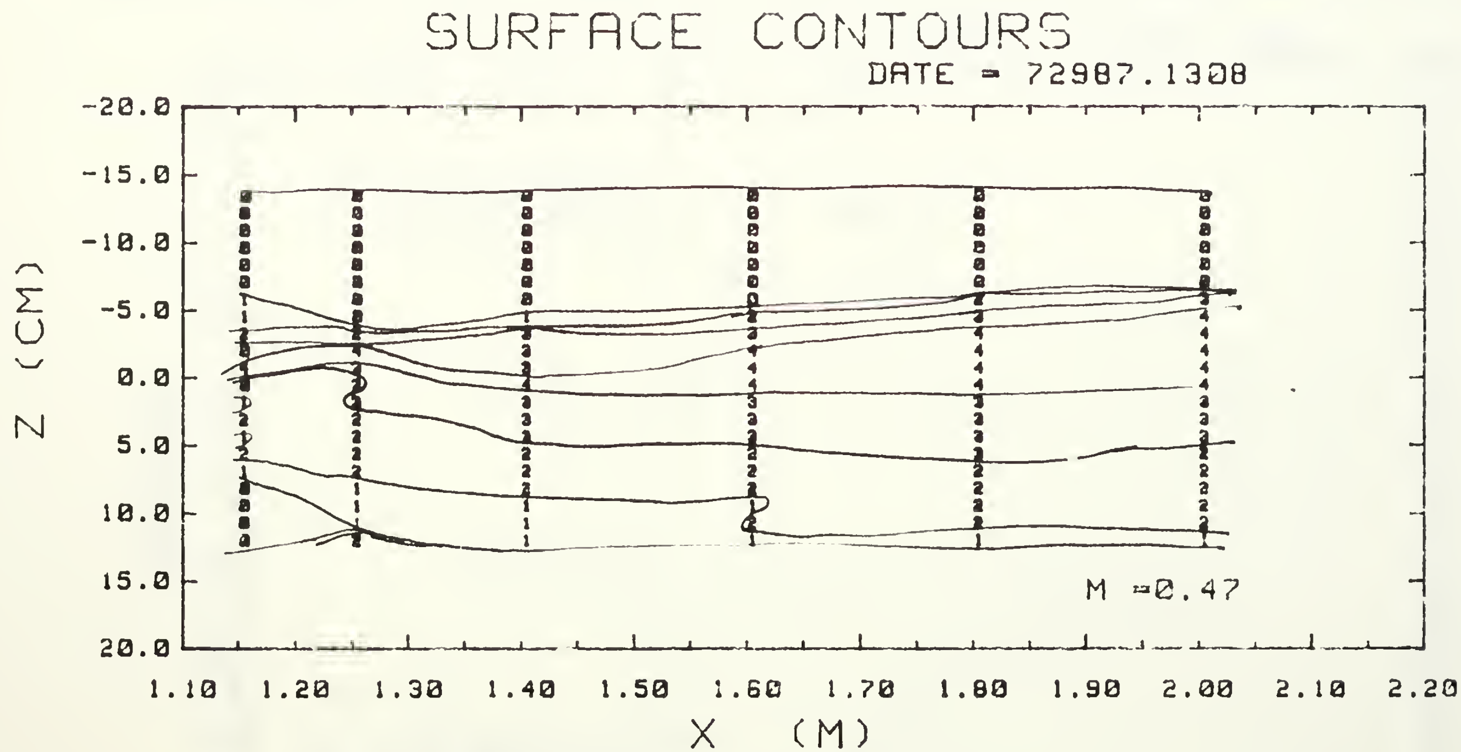

St/Stf RANGES

0	.900	.980	3	1.100	1.200
1	.980	1.020	4	1.200	1.300
2	1.020	1.100			

FREE STREAM 15 M/S, WITH FILM COOLING, VORTEX GEN. #2 AT 4.79 cm

Fig. 44. Surface Contour.

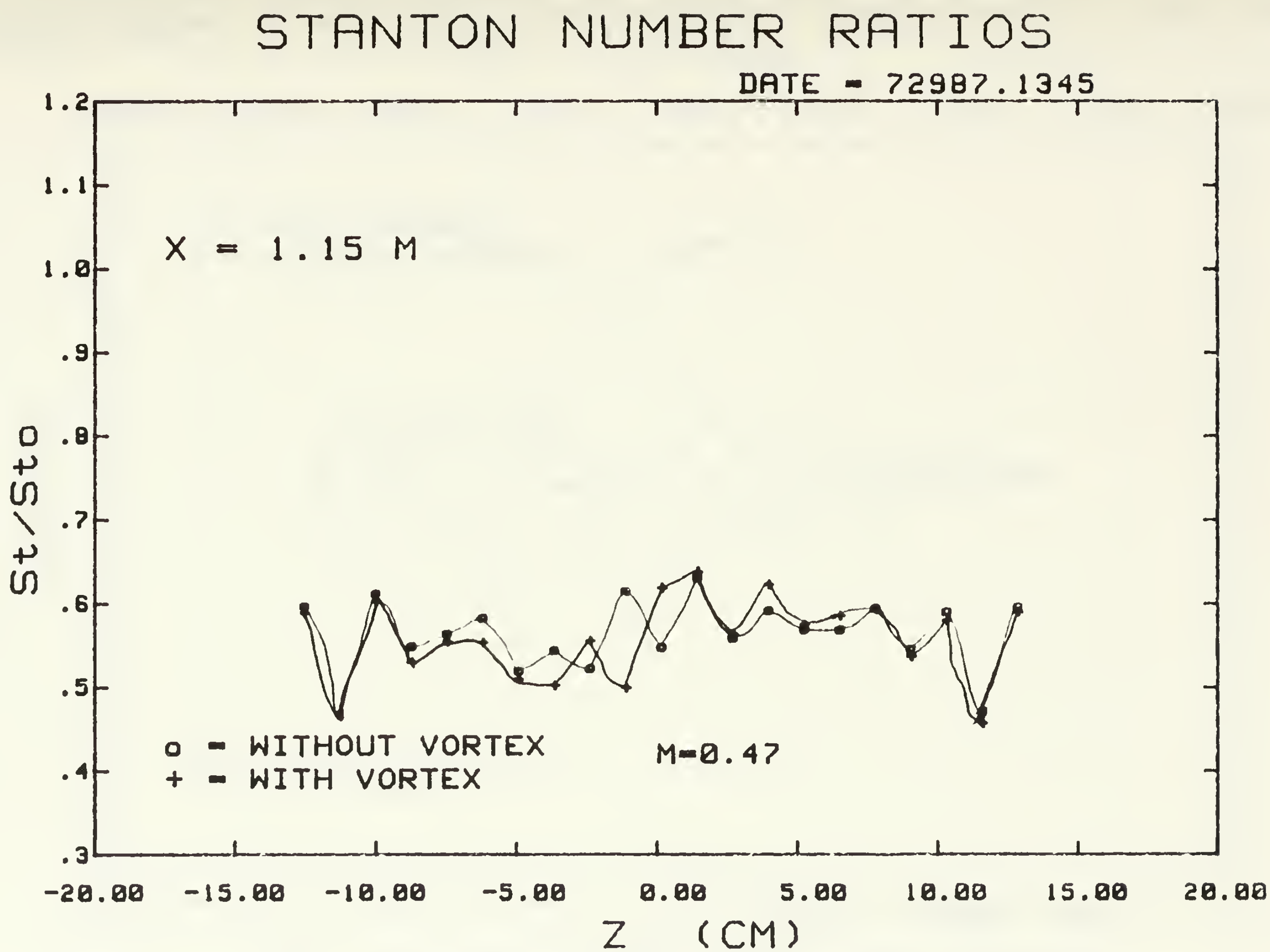

FREE STREAM 15 M/S, WITH FILM COOLING, VORTEX GEN. AT 3.52 cm

Fig. 45a. Spanwise Variations of Stanton Number Ratios.

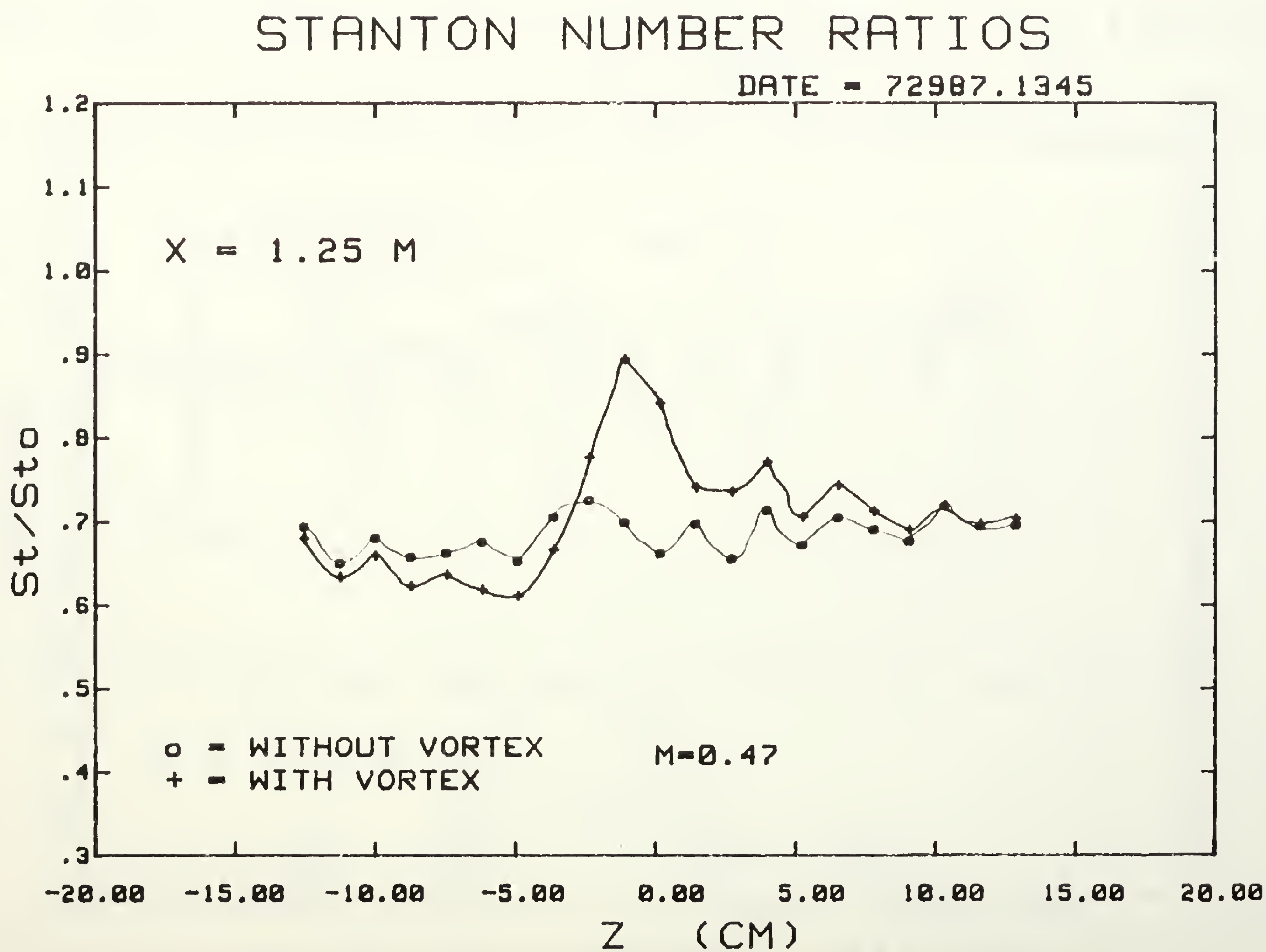

FREE STREAM 15 M/S, WITH FILM COOLING, VORTEX GEN. AT 3.52 cm

Fig. 45b. Spanwise Variations of Stanton Number Ratios.

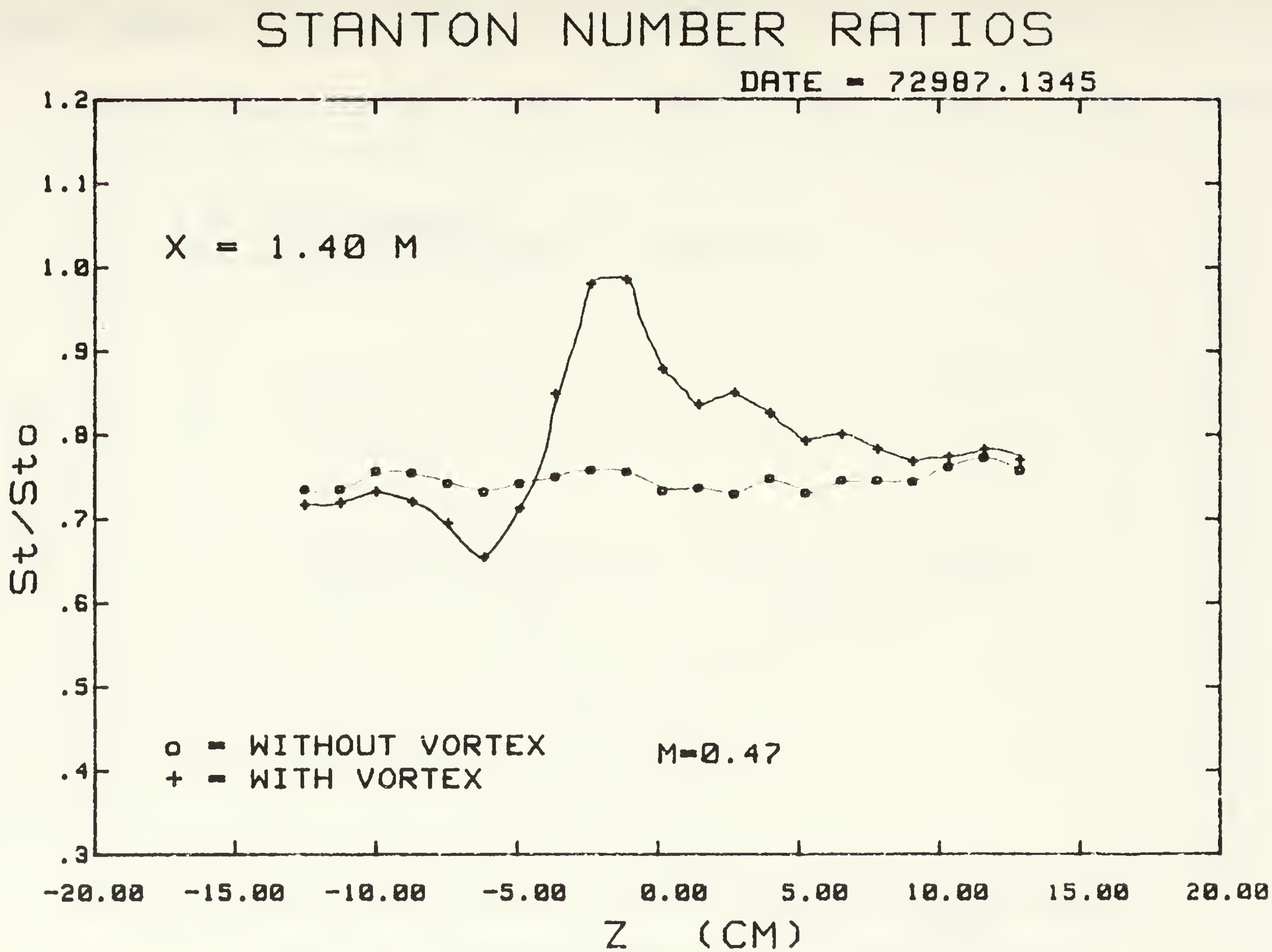

FREE STREAM 15 M/S, WITH FILM COOLING, VORTEX GEN. AT 3.52 cm

Fig. 45c. Sparwise Variations of Stanton Number Ratios.

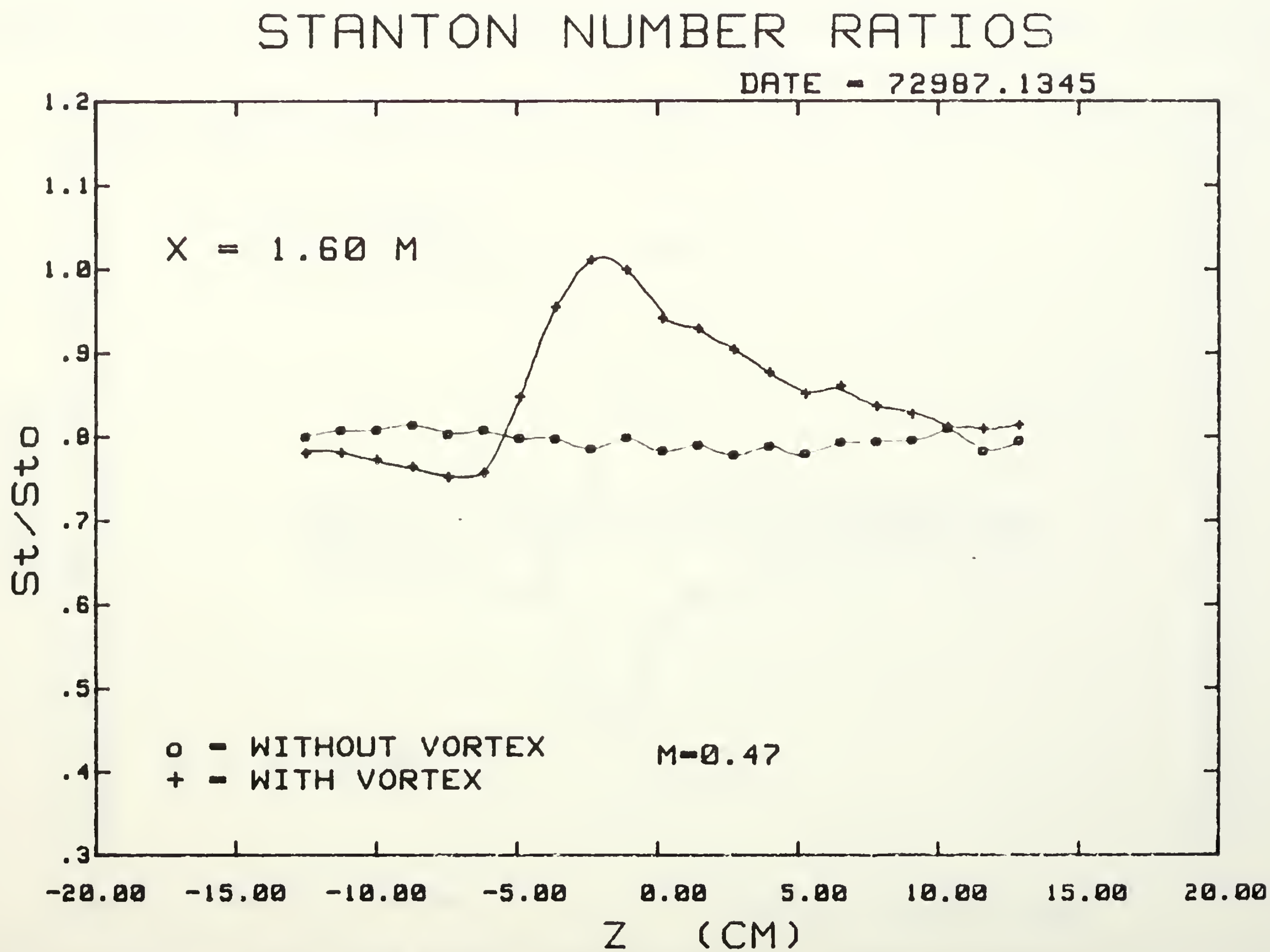

FREE STREAM 15 M/S, WITH FILM COOLING, VORTEX GEN. AT 3.52 cm

Fig. 45d. Spanwise Variations of Stanton Number Ratios.

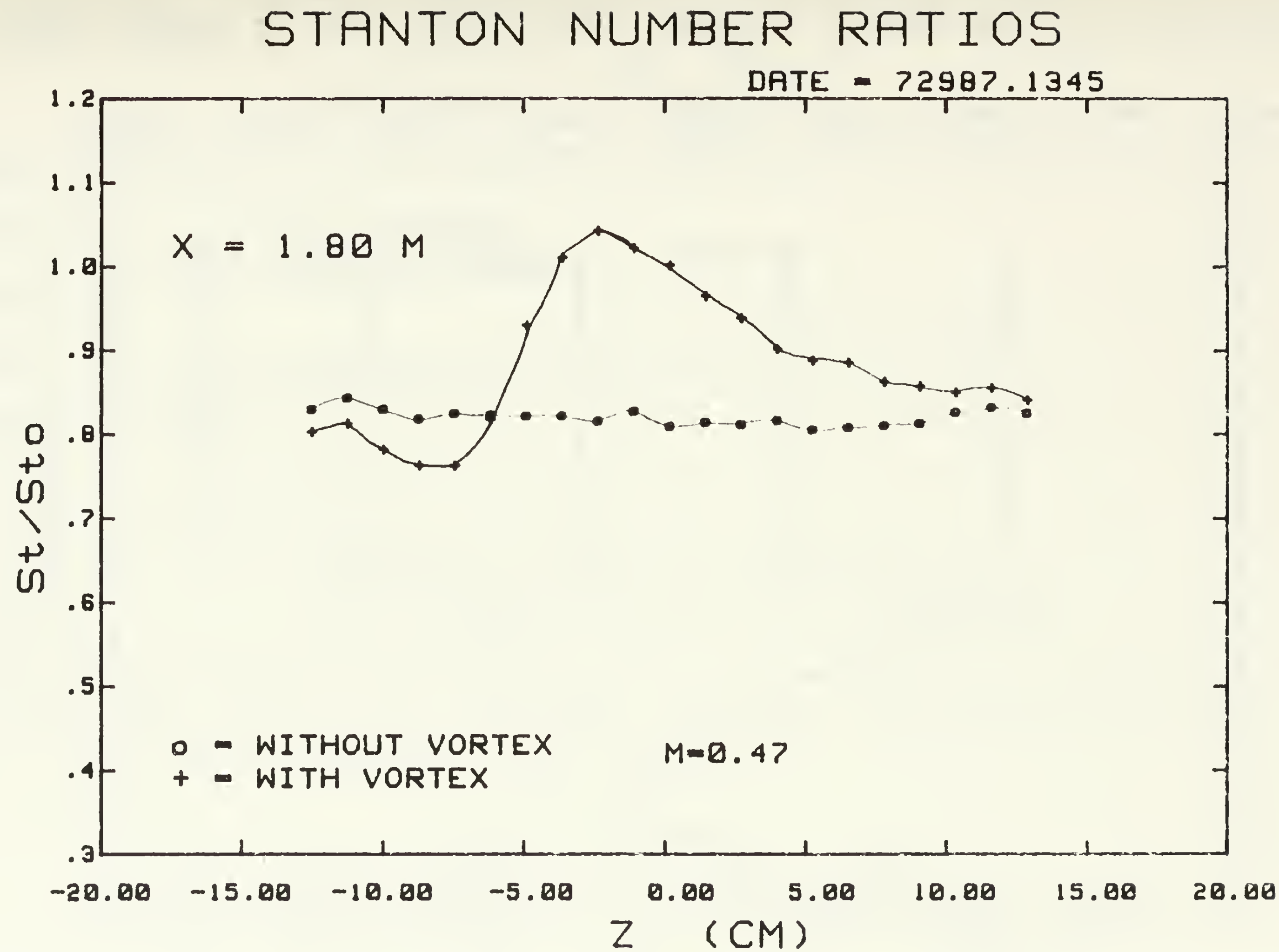

FREE STREAM 15 M/S, WITH FILM COOLING, VORTEX GEN. AT 3.52 cm

Fig. 45e. Spanwise Variations of Stanton Number Ratios.

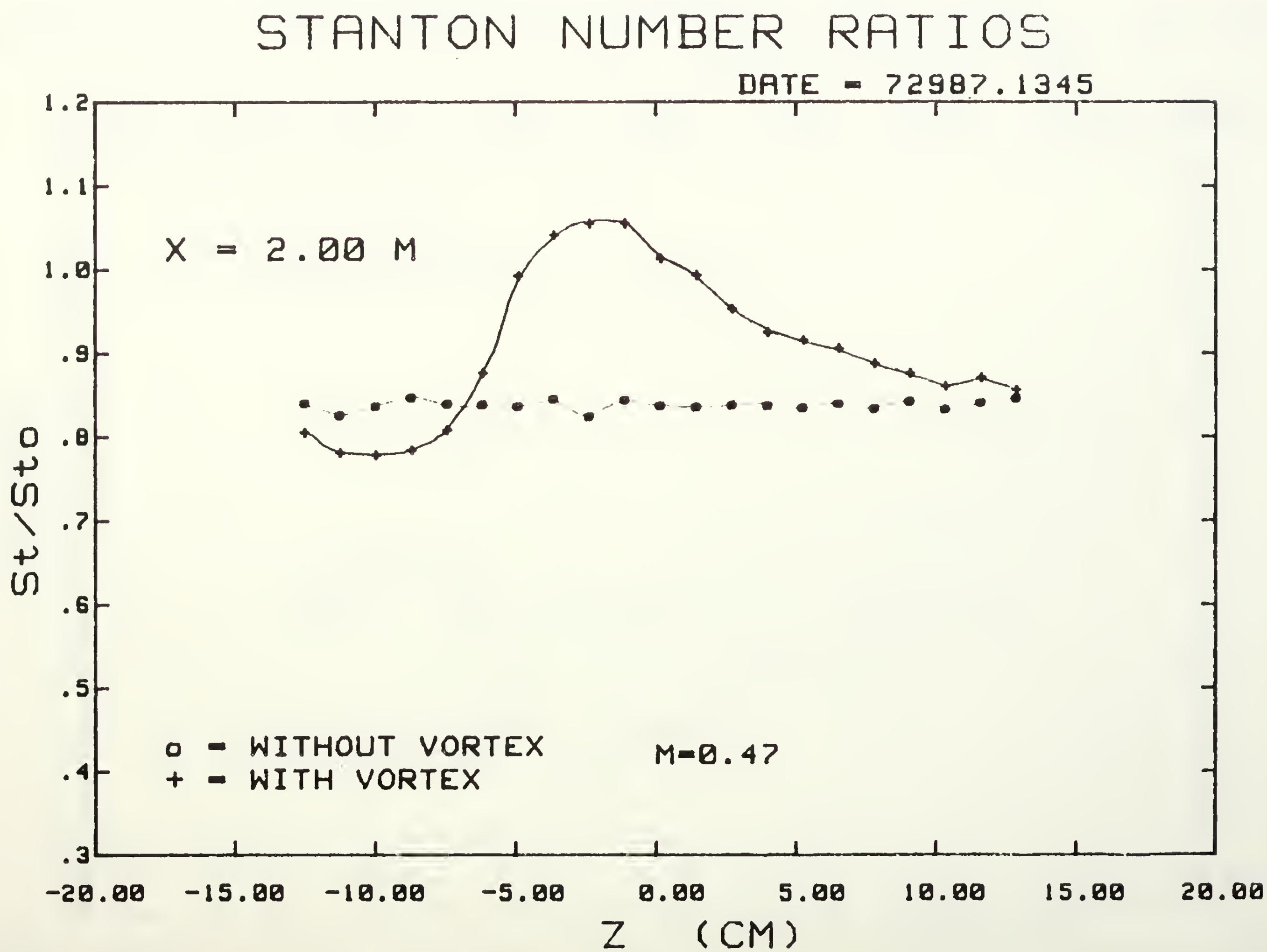

FREE STREAM 15 M/S, WITH FILM COOLING, VORTEX GEN. AT 3.52 cm

Fig. 45f. Spanwise Variations of Stanton Number Ratios.

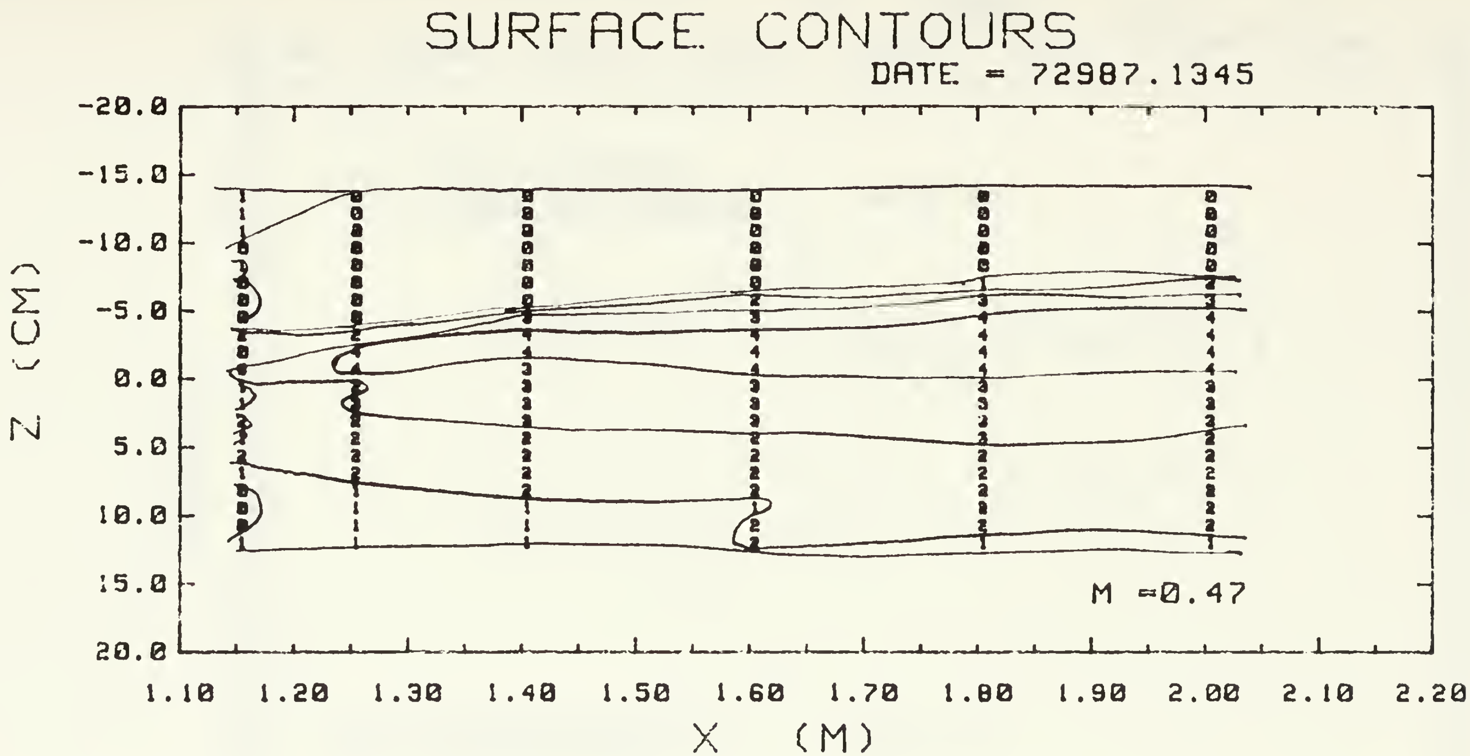

St/Stf RANGES

0	.900	.980	3	1.100	1.200
1	.980	1.020	4	1.200	1.300
2	1.020	1.100			

FREE STREAM 15 M/S, WITH FILM COOLING, VORTEX GEN. #2 AT 3.52 cm

Fig. 46. Surface Contour.

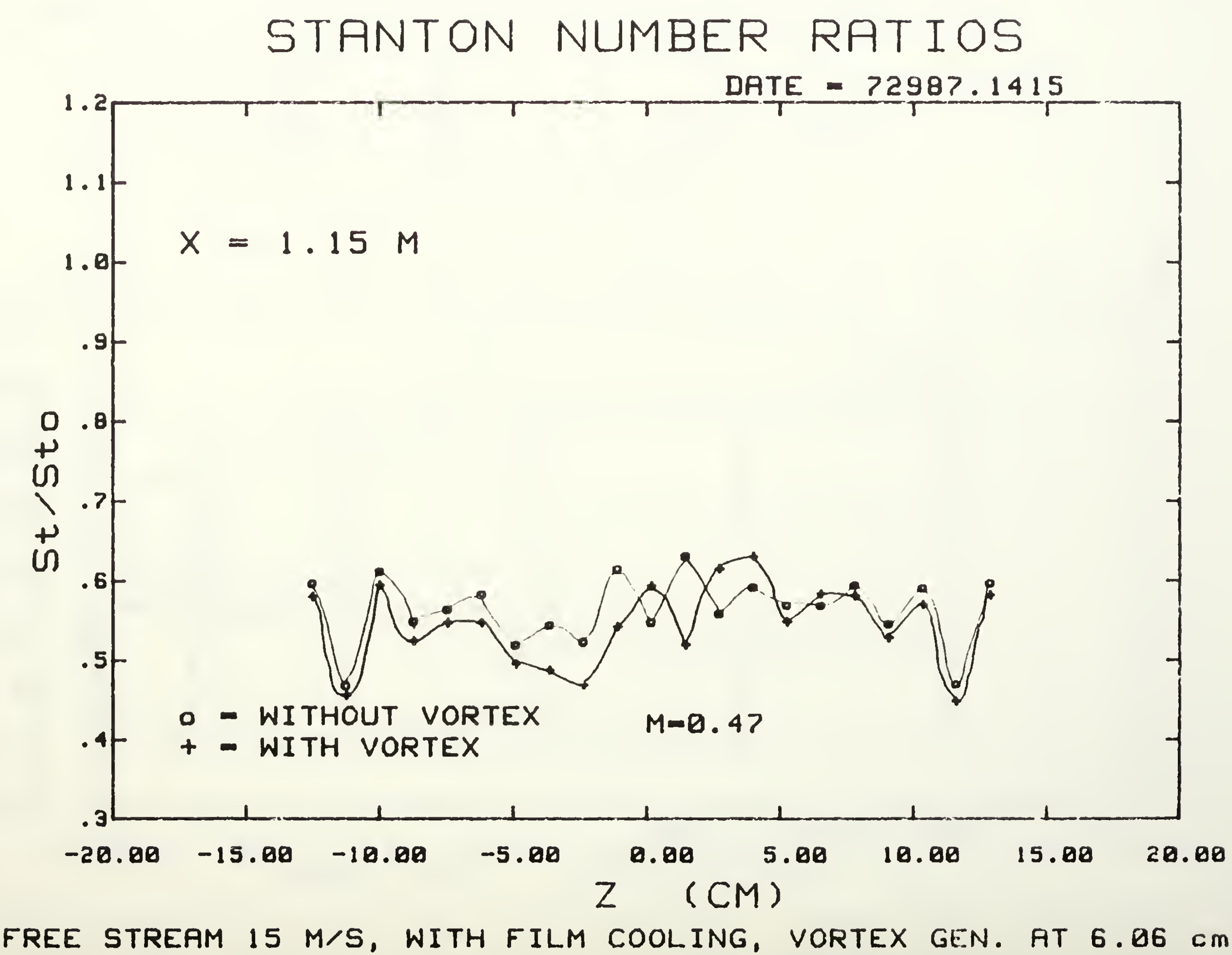

Fig. 47a. Spanwise Variations of Stanton Number ratios.

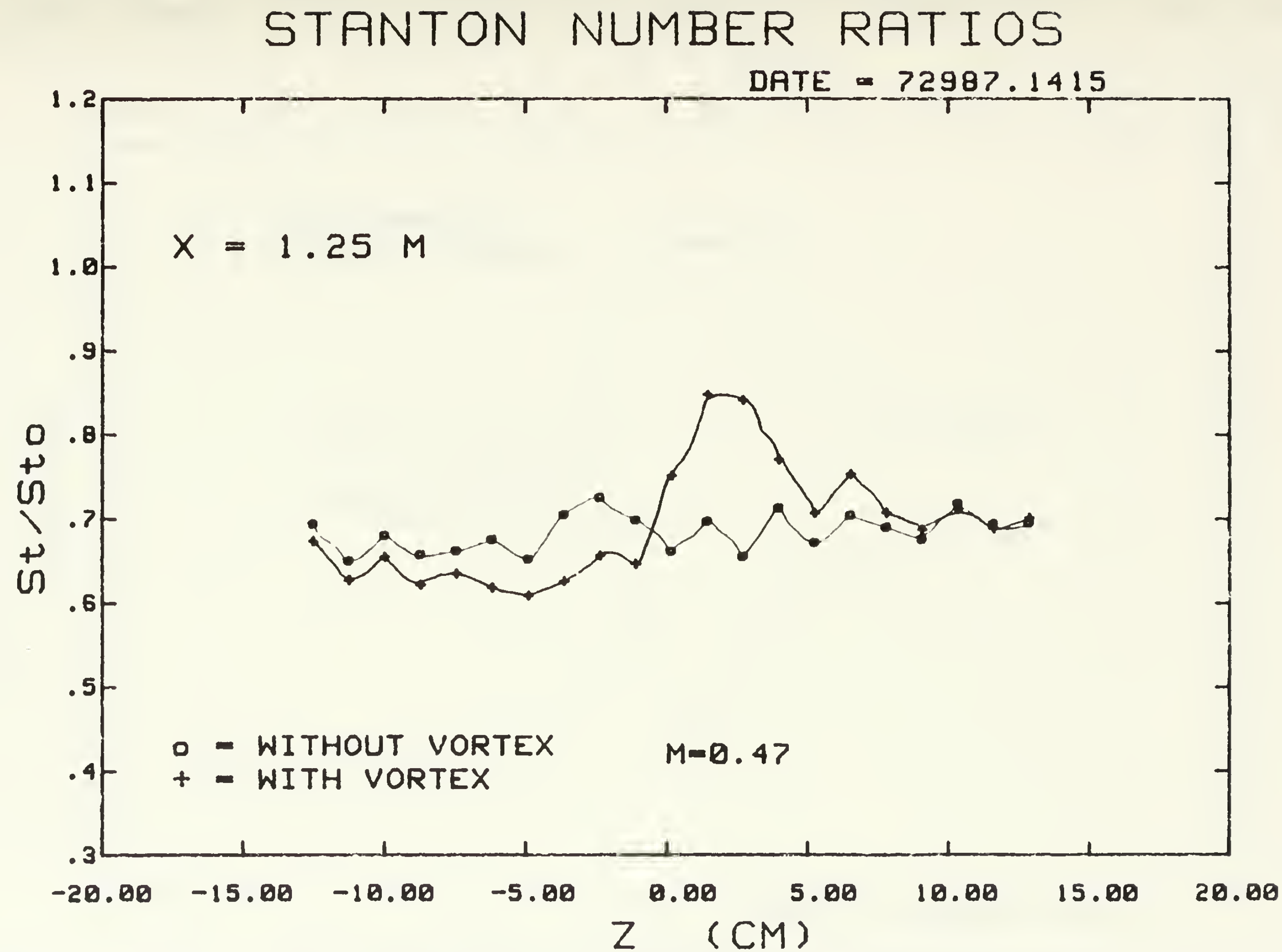

FREE STREAM 15 M/S, WITH FILM COOLING, VORTEX GEN. AT 6.06 cm

Fig. 47b. Spanwise Variations of Stanton Number Ratios.

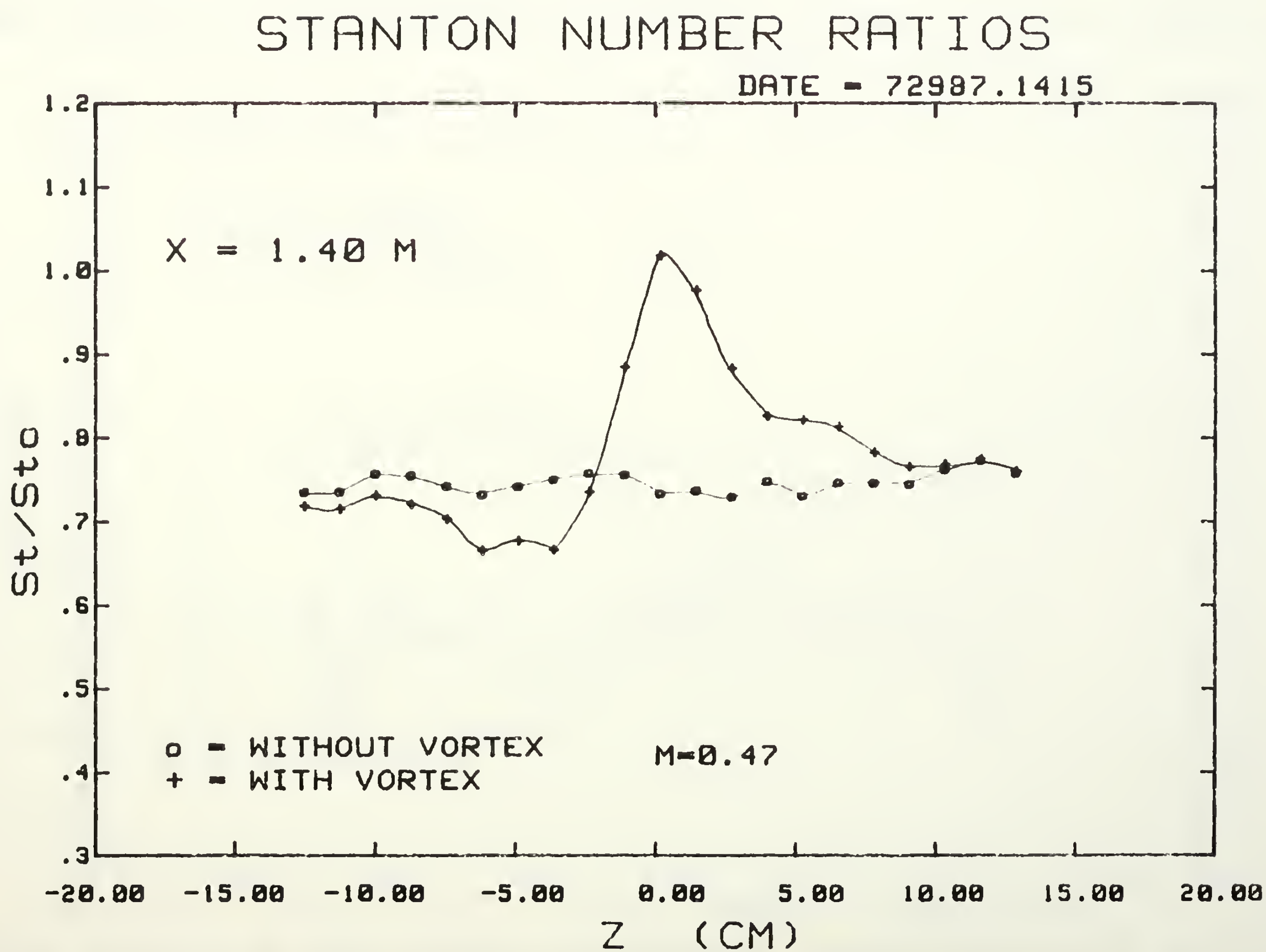

FREE STREAM 15 M/S, WITH FILM COOLING, VORTEX GEN. AT 6.06 cm

Fig. 47c. Spanwise Variations of Stanton Number Ratios.

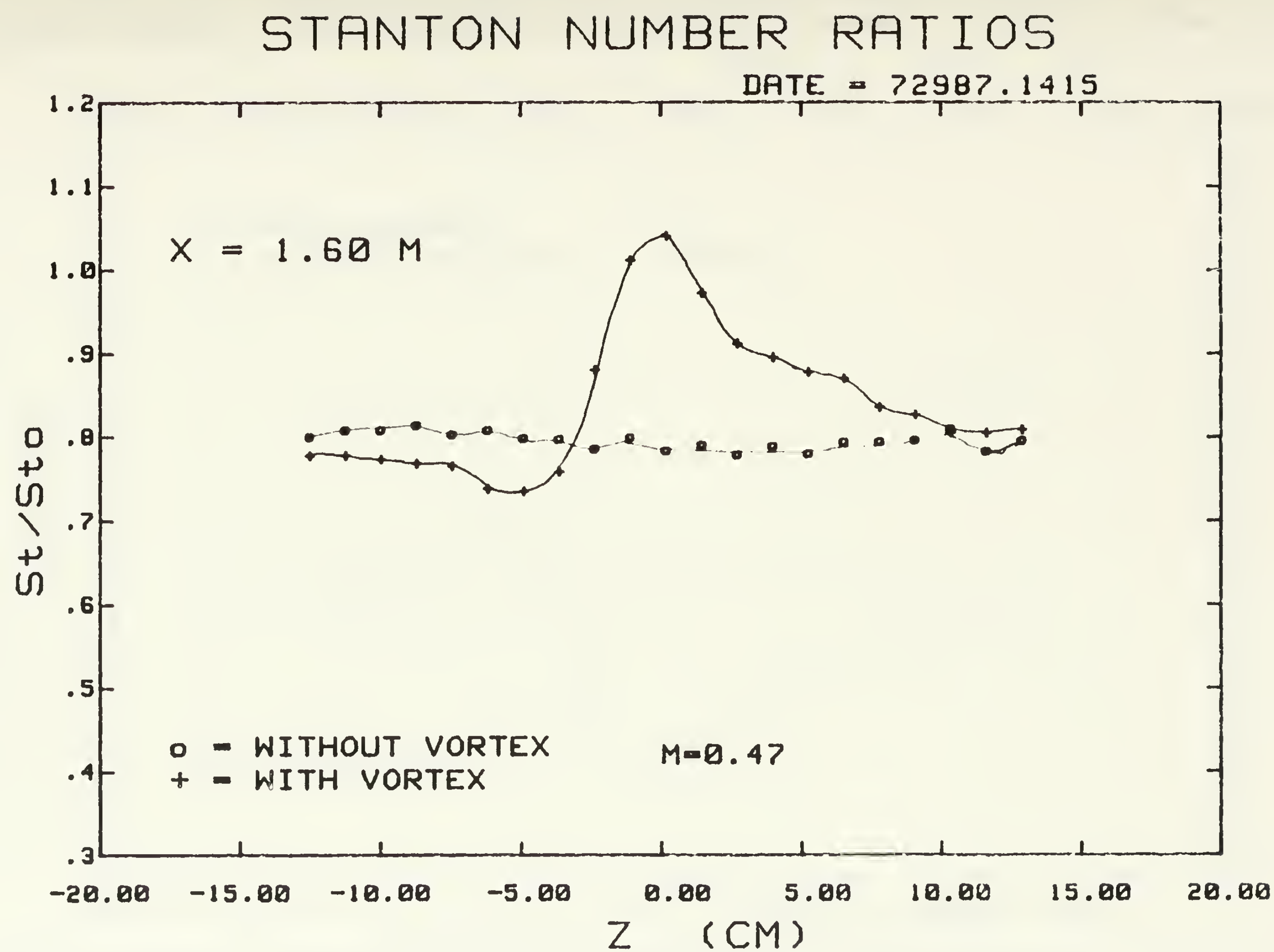

FREE STREAM 15 M/S, WITH FILM COOLING, VORTEX GEN. AT 6.06 cm

Fig. 47d. Spanwise Variations of Stanton Number Ratios.

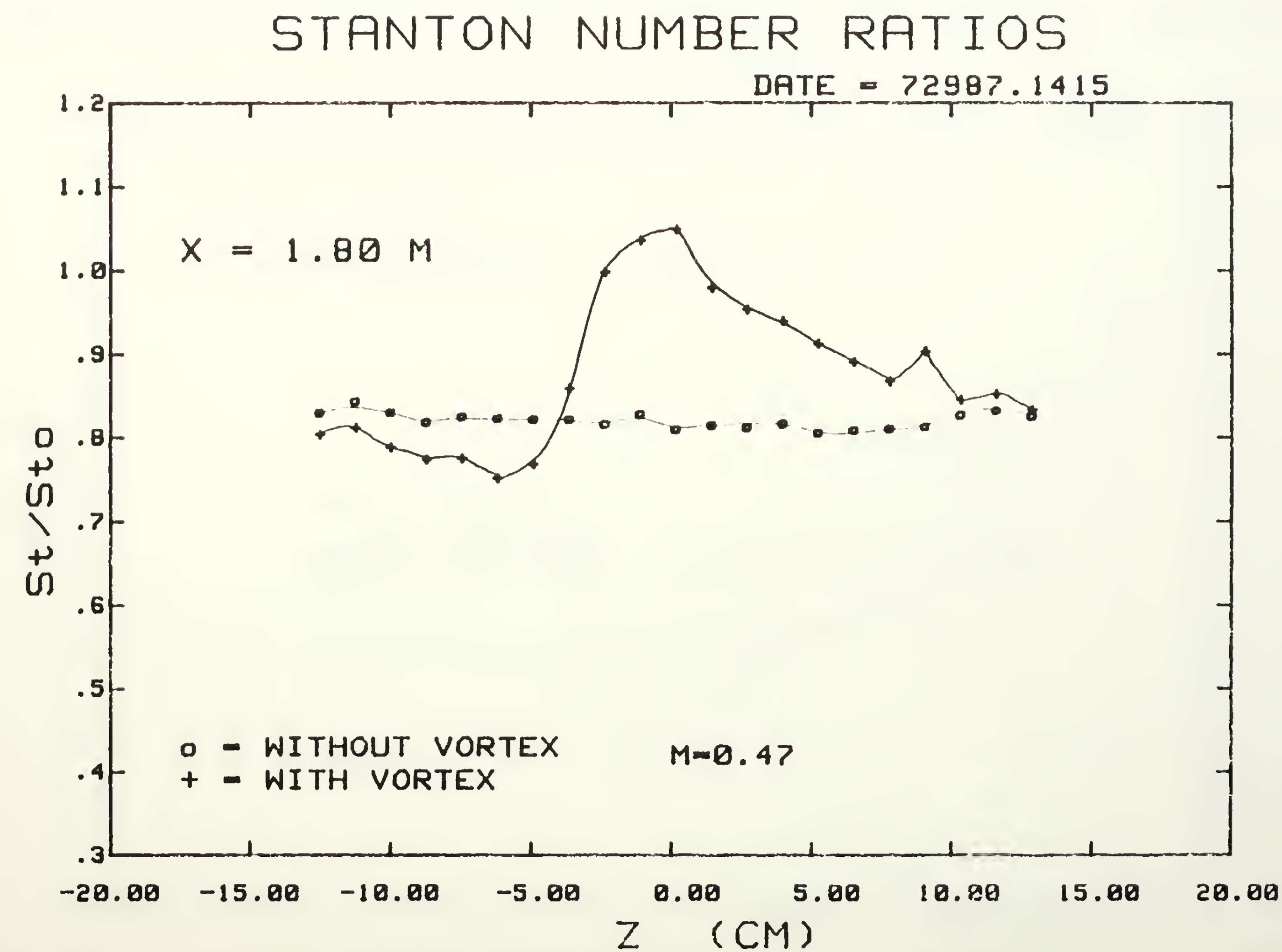

FREE STREAM 15 M/S, WITH FILM COOLING, VORTEX GEN. AT 6.06 cm

Fig. 47d. Spanwise Variations of Stanton Number Ratios.

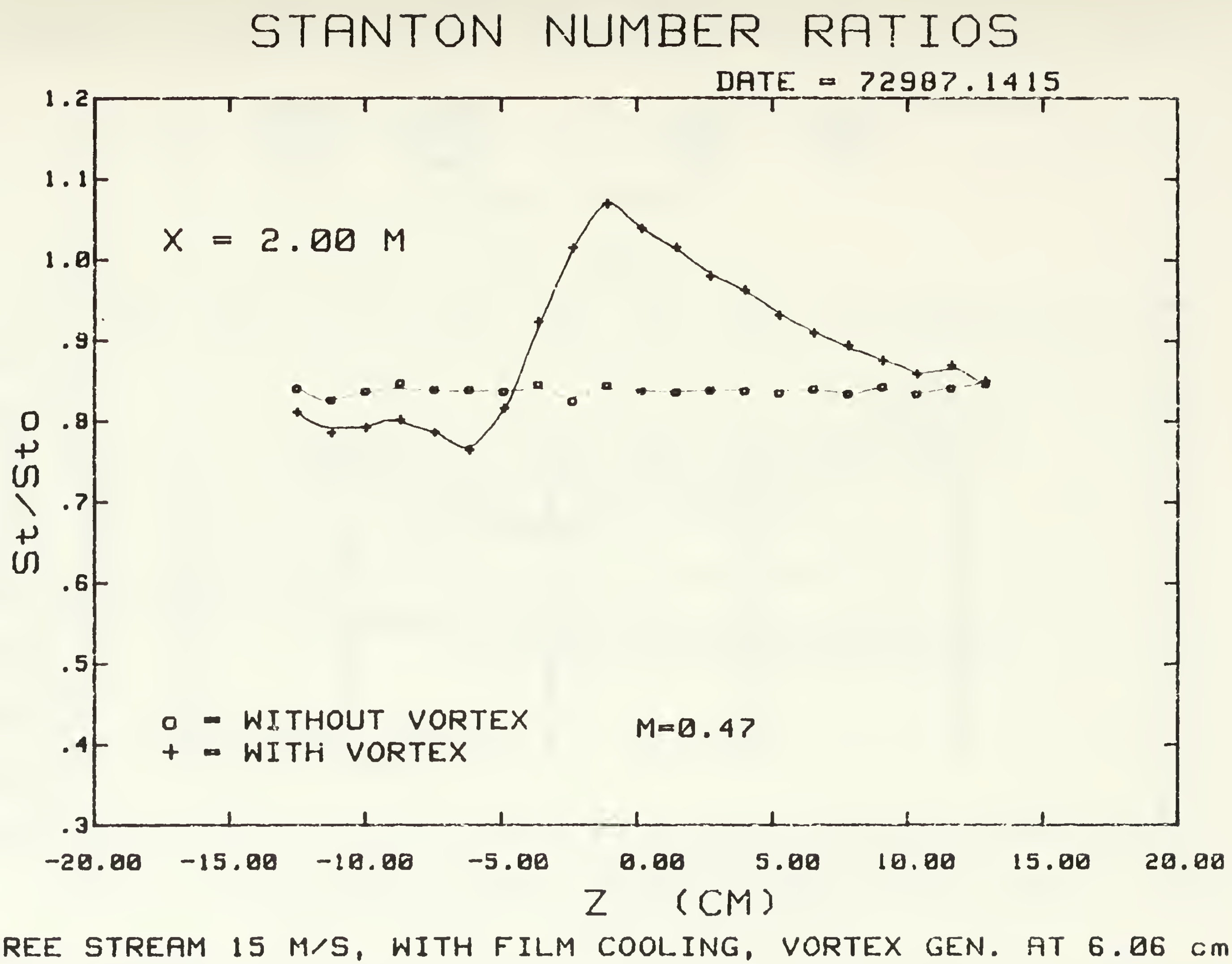

Fig. 47f. Spanwise Variations of Stanton Number Ratios.

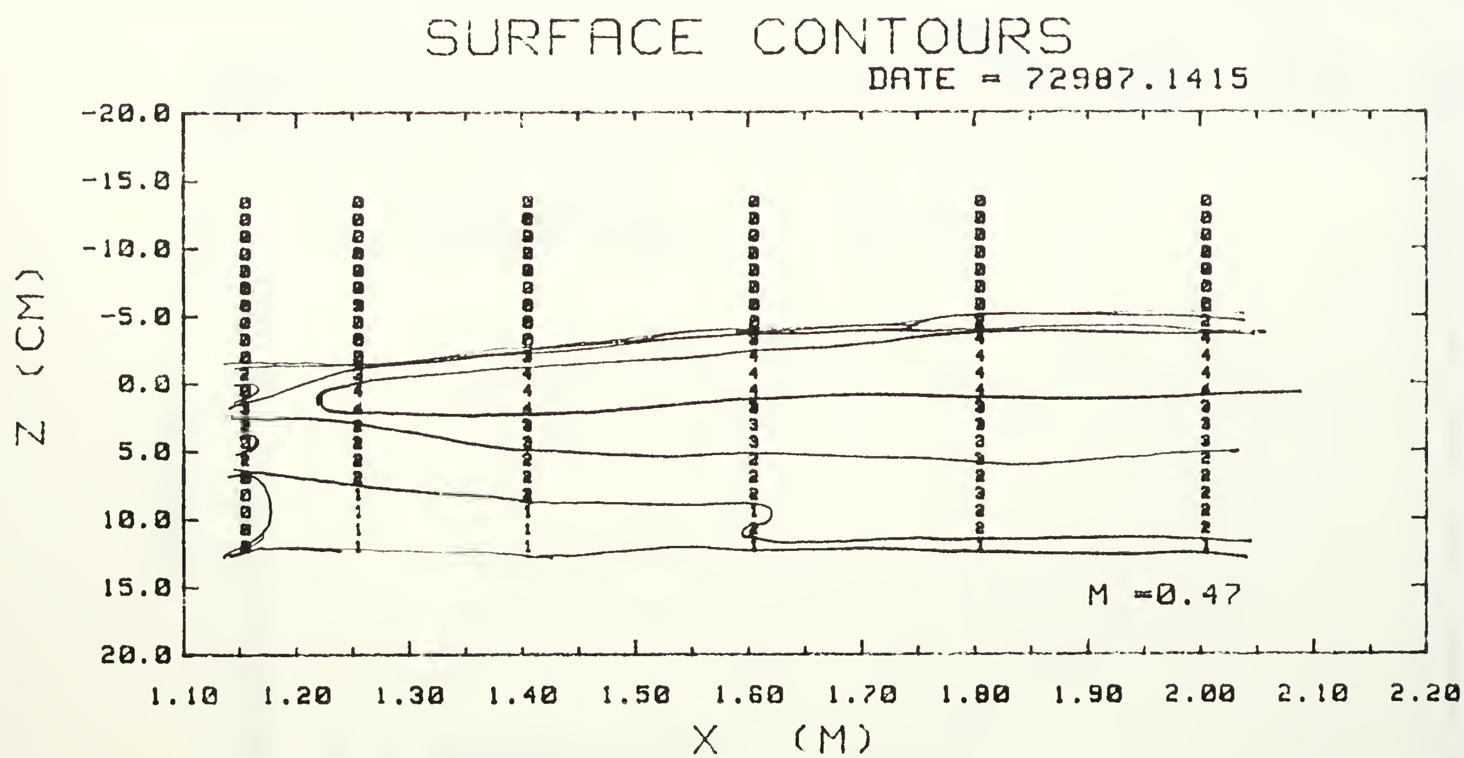

St/Stf RANGES

0	.900	.980	3	1.100	1.200
1	.980	1.020	4	1.200	1.300
2	1.020	1.100			

FREE STREAM 15 M/S, WITH FILM COOLING, VORTEX GEN. #2 AT 6.06 cm

Fig. 48. Surface Contours

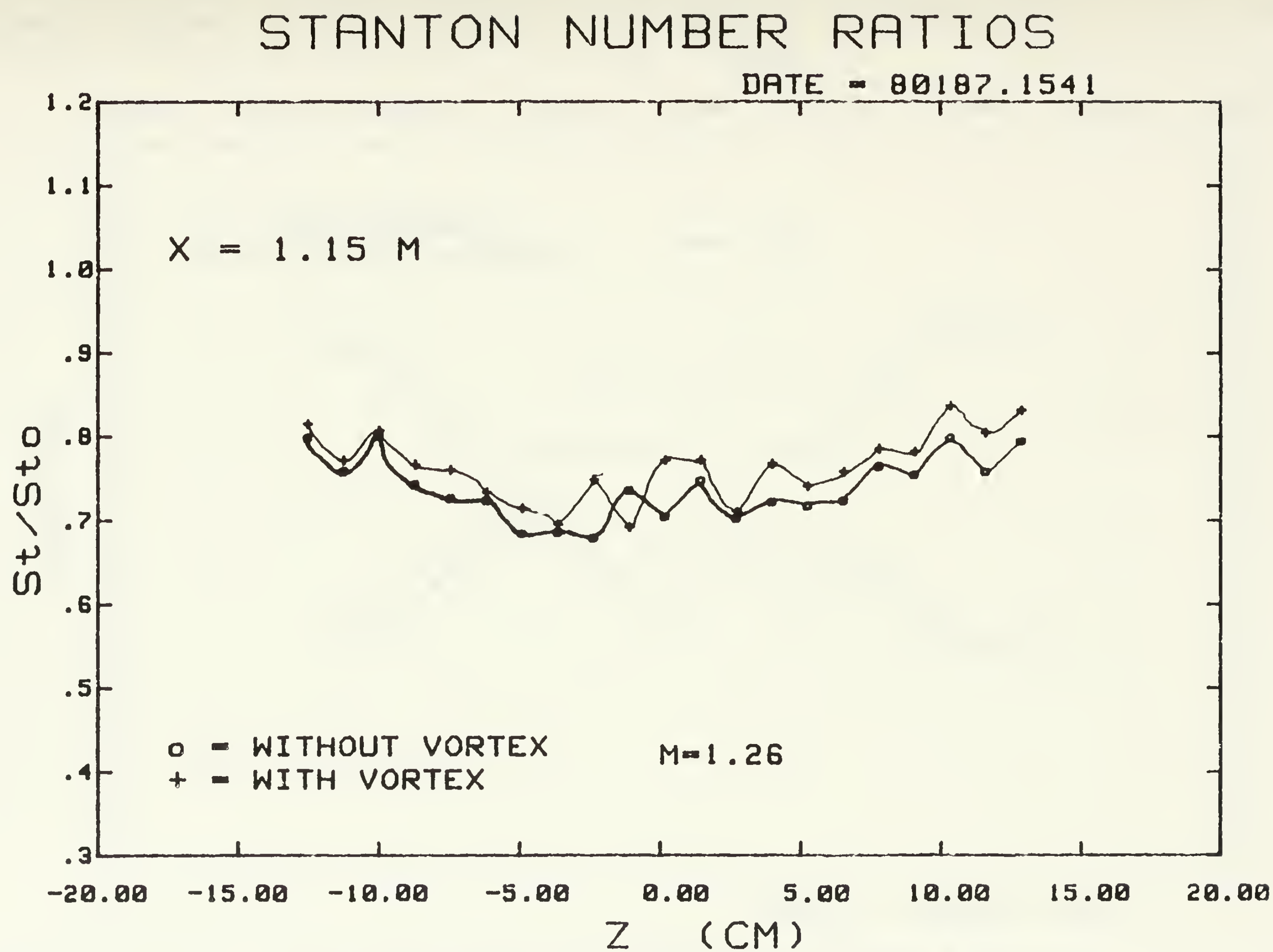

FREE STREAM 10 M/S, WITH FILM COOLING, VORTEX GEN. AT 4.79 cm

Fig. 49a. Spanwise Variations of Stanton Number Ratios.

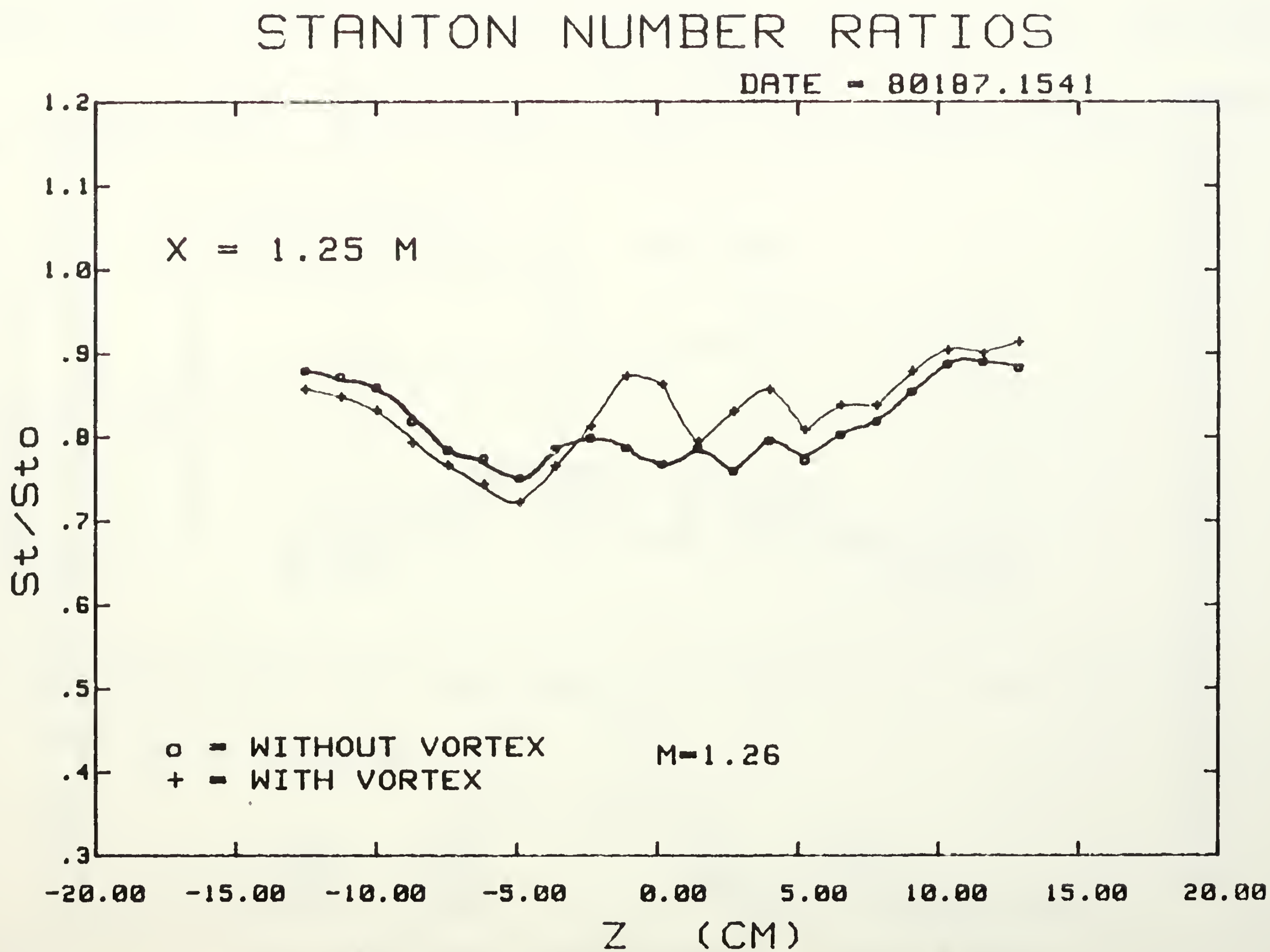

FREE STREAM 10 M/S, WITH FILM COOLING, VORTEX GEN. AT 4.79 cm

Fig. 49b. Spanwise Variations of Stanton Number Ratios.

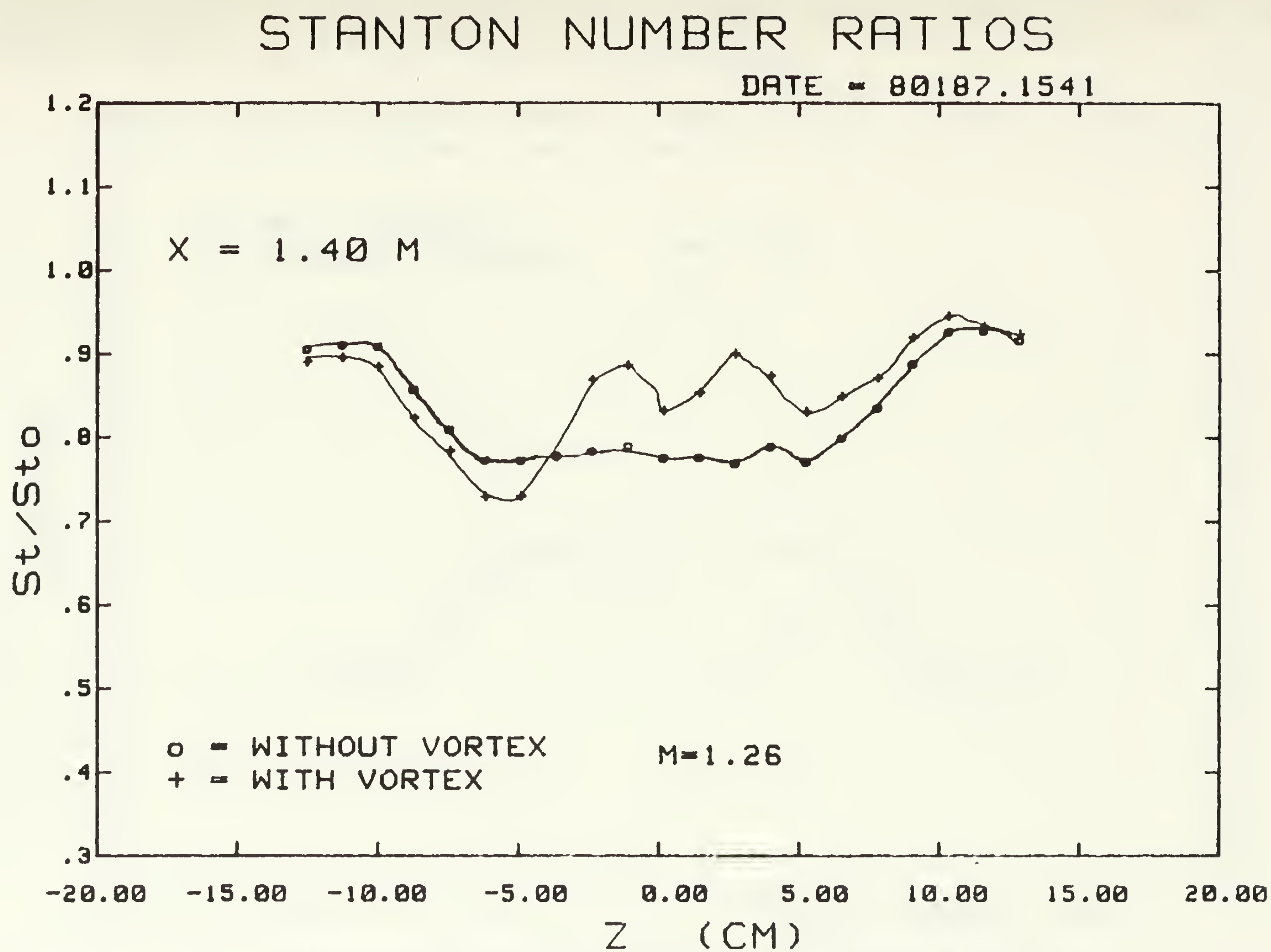

FREE STREAM 10 M/S, WITH FILM COOLING, VORTEX GEN. AT 4.79 cm

Fig. 49c. Spanwise Variations of Stanton Number Ratios.

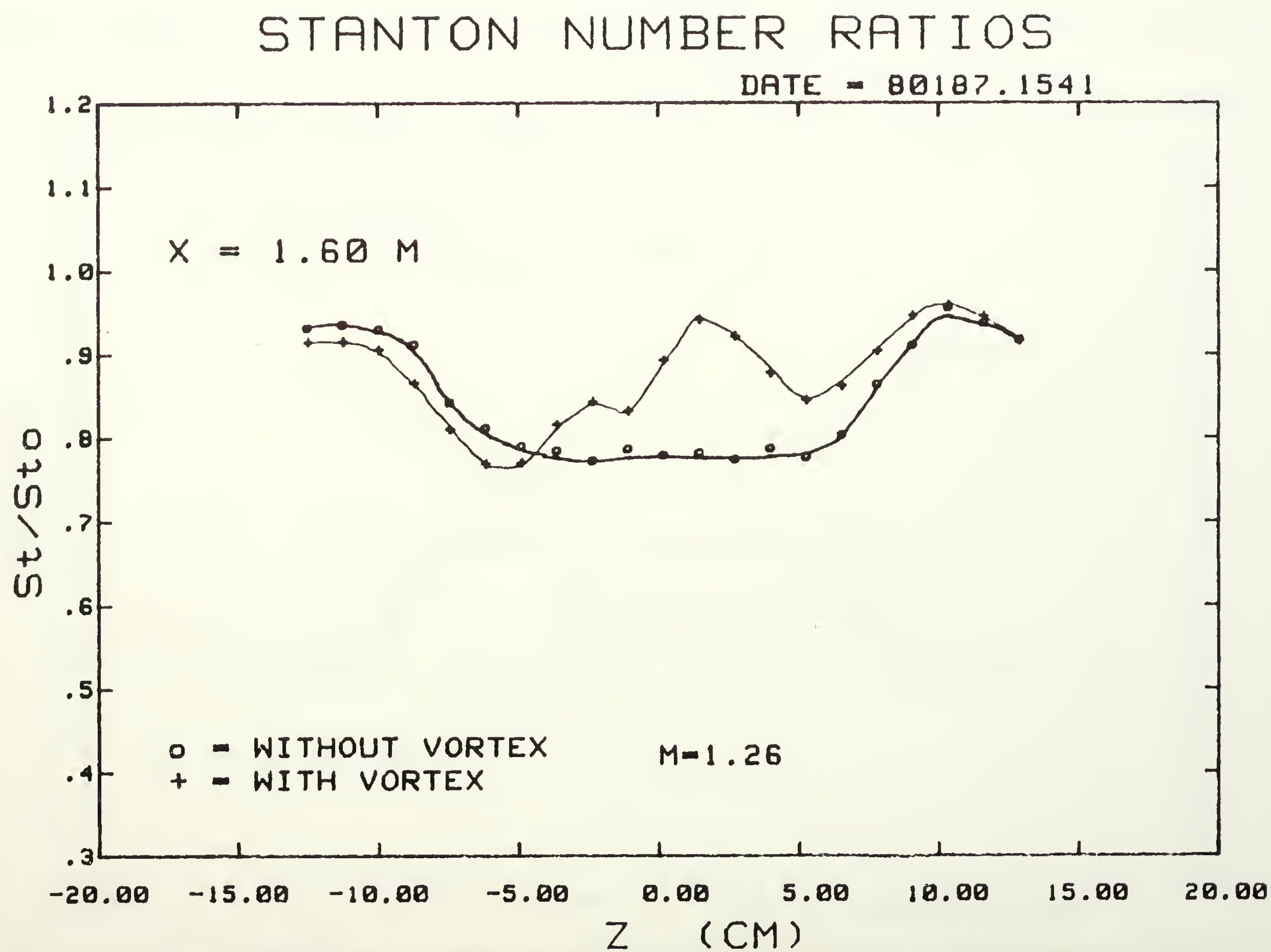

FREE STREAM 10 M/S, WITH FILM COOLING, VORTEX GEN. AT 4.79 cm

Fig. 49d. Spanwise Variations of Stanton Number Ratios.

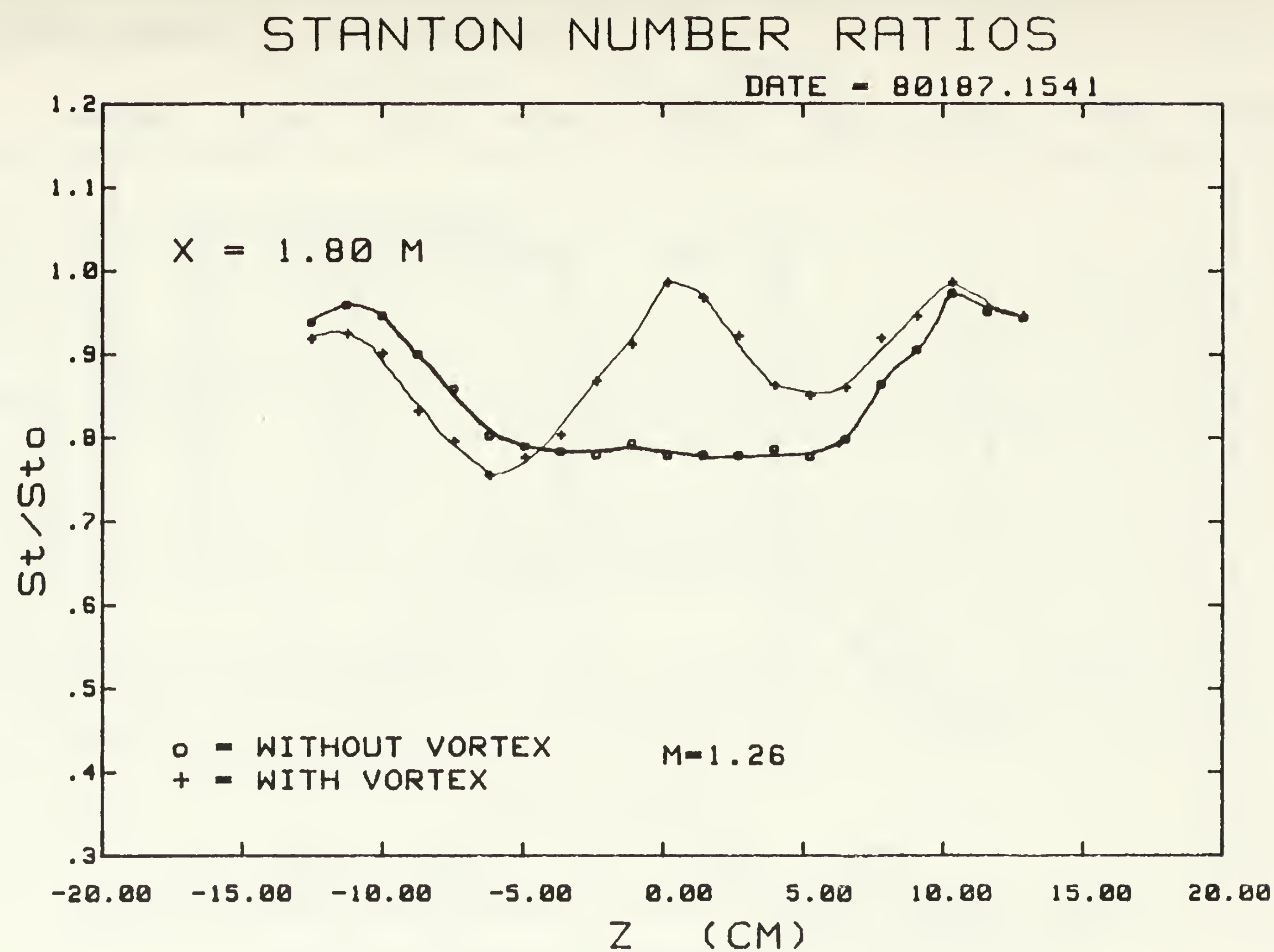

FREE STREAM 10 M/S, WITH FILM COOLING, VORTEX GEN. AT 4.79 cm

Fig. 49e. Spanwise Variations of Stanton Number Ratios.

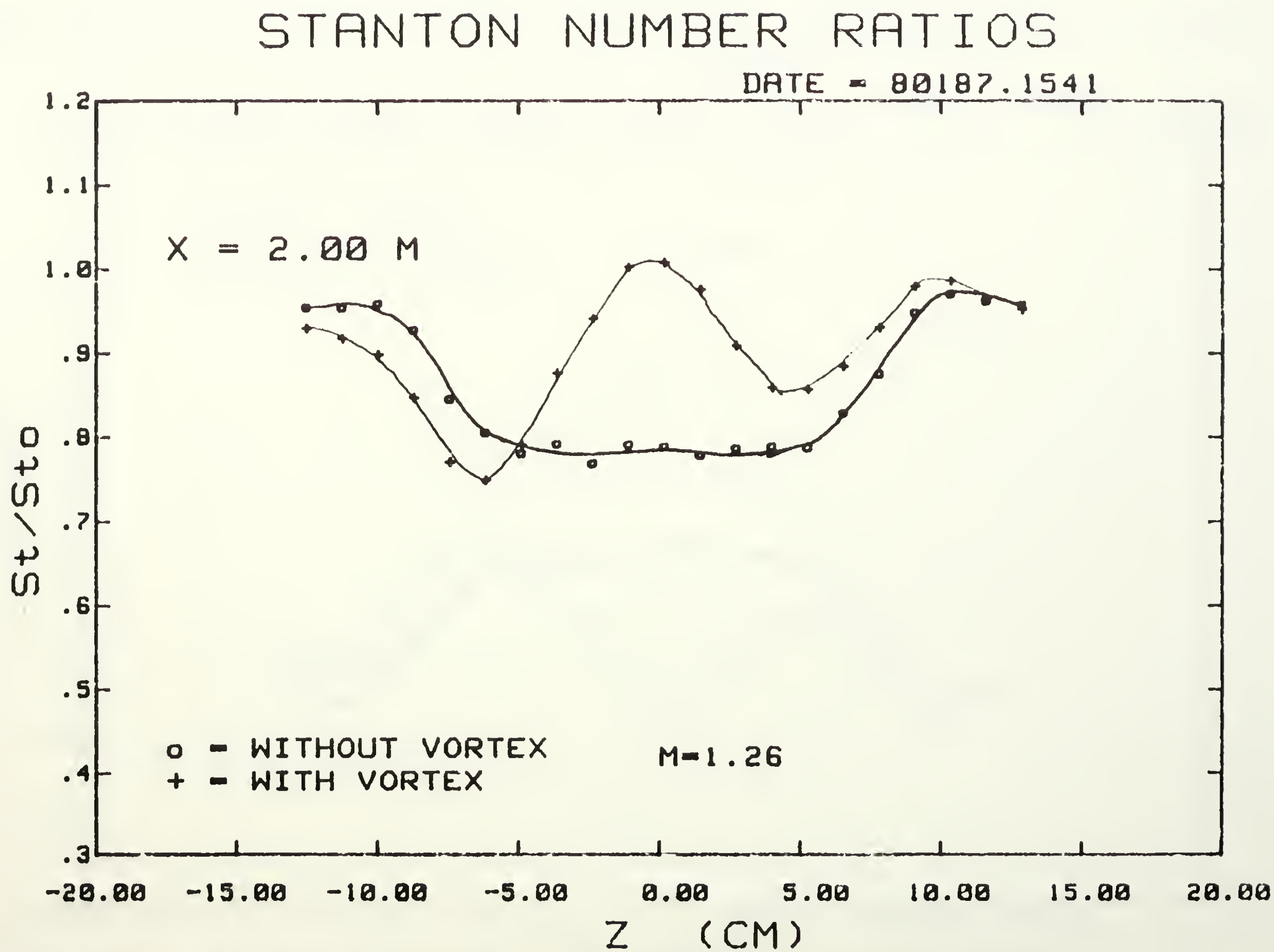

FREE STREAM 10 M/S, WITH FILM COOLING, VORTEX GEN. AT 4.79 cm

Fig. 49f. Spanwise Variations of Stanton Number Ratios.

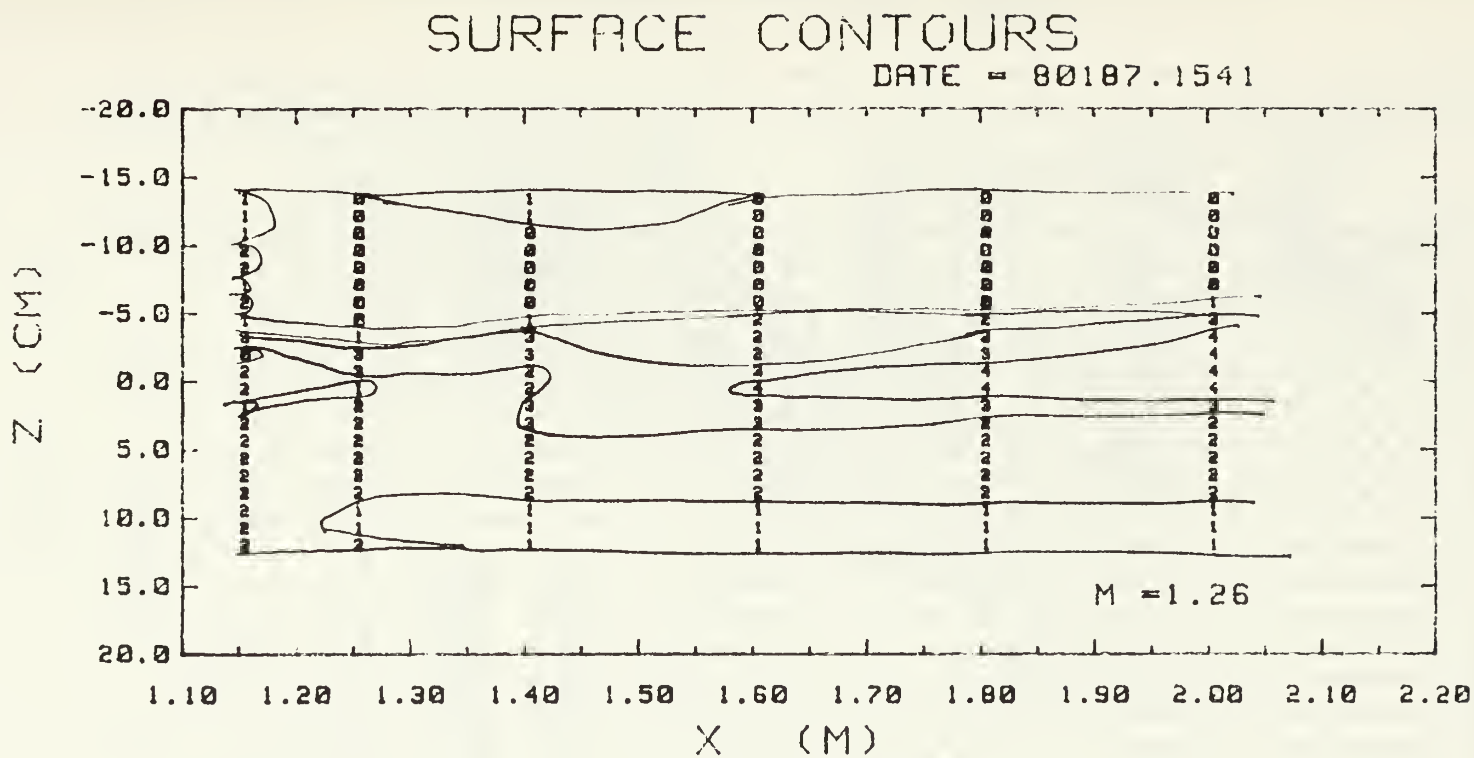

St/Stf RANGES

0	.900	.980	3	1.100	1.200
1	.980	1.020	4	1.200	1.300
2	1.020	1.100			

FREE STREAM 10 M/S, WITH FILM COOLING, VORTEX GEN. #2 AT 4.79 cm

Fig. 50. Surface Contours.

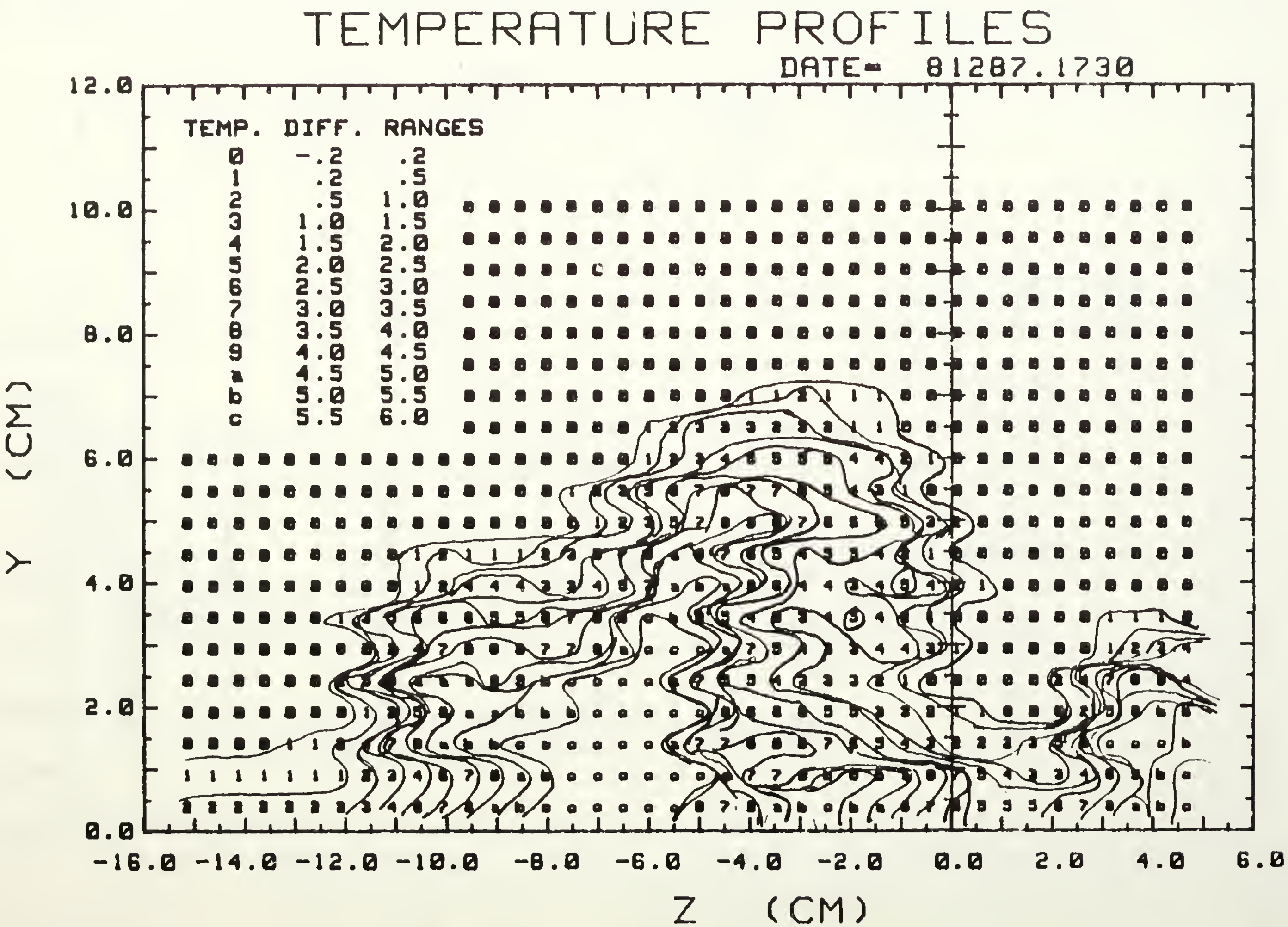

Fig. 51. EMBEDDED VORTEX 10 M/S WITH FILM COOLING, M=1.26
X=1.480 M, UNHEATED PLATE, VORTEX GEN. AT 4.79 cm

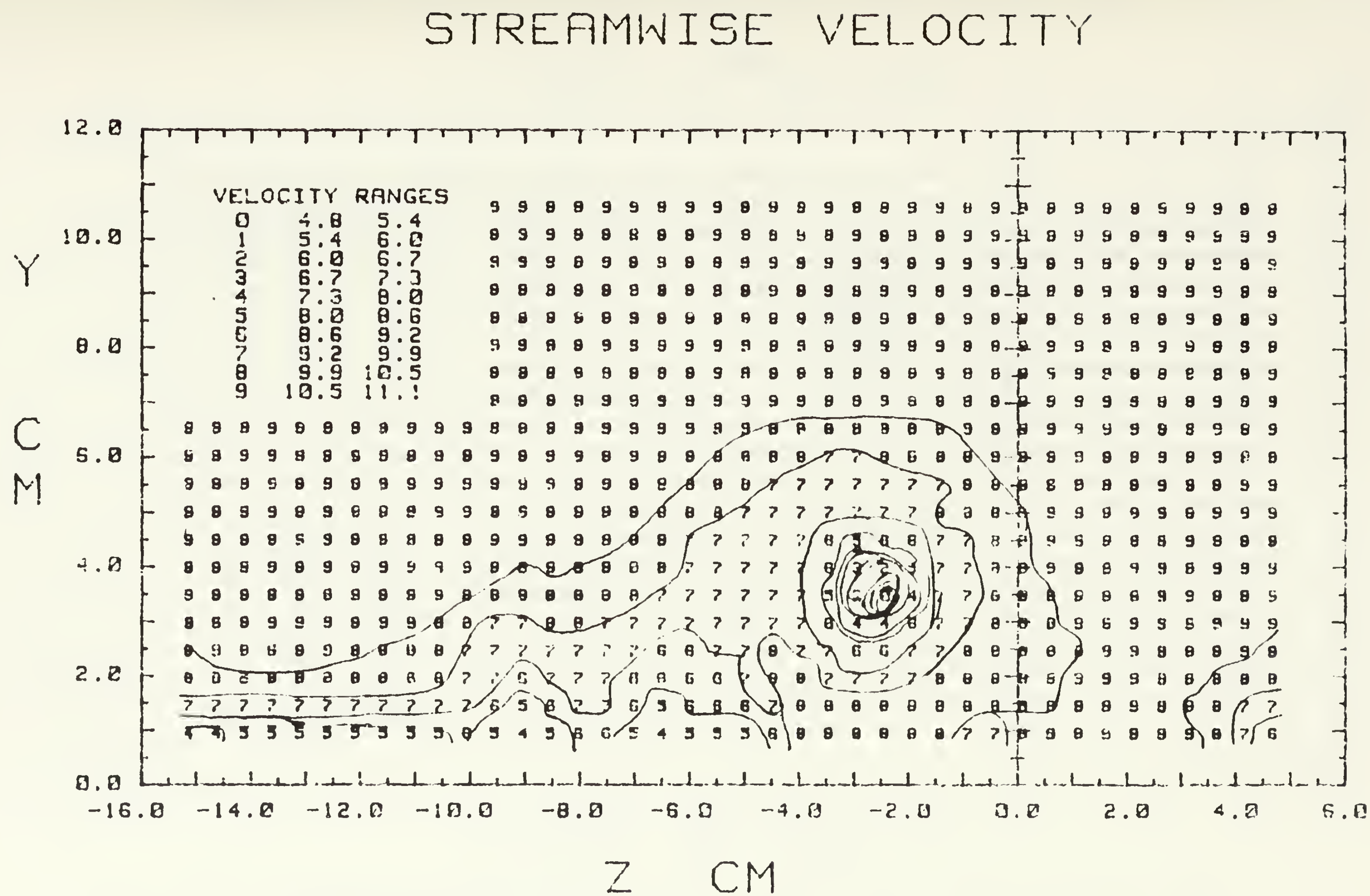

EMBEDDED VORTEX 10 M/S WITH FILM COOLING, M=1.26, VORTEX GEN AT 4.79 cm

Fig. 52a. Streamwise Velocity Contour

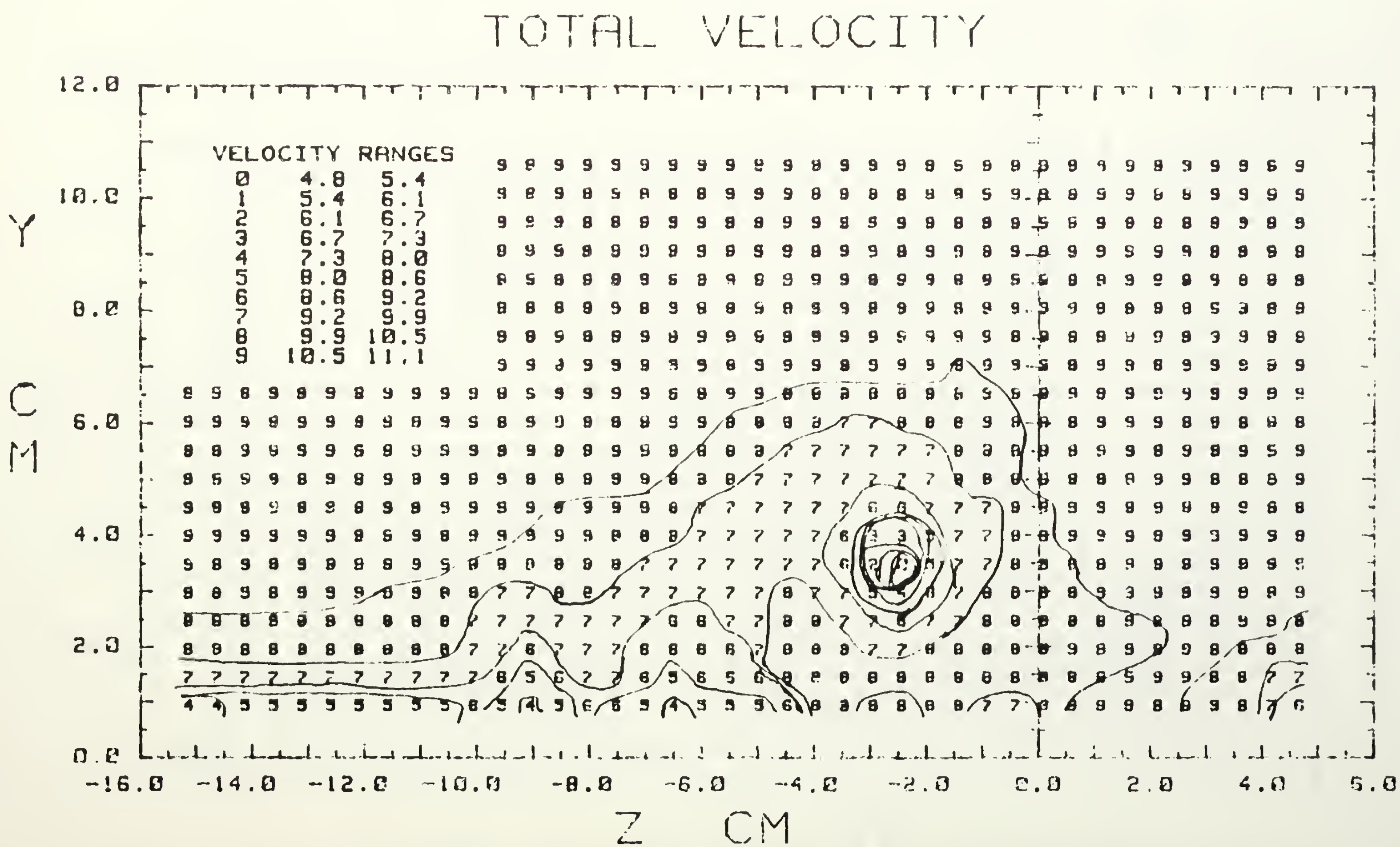

EMBEDDED VORTEX 10 M/S WITH FILM COOLING, M=1.25
VORTEX GEN. AT 4.79 cm

Fig. 52b. Total Velocity Contour.

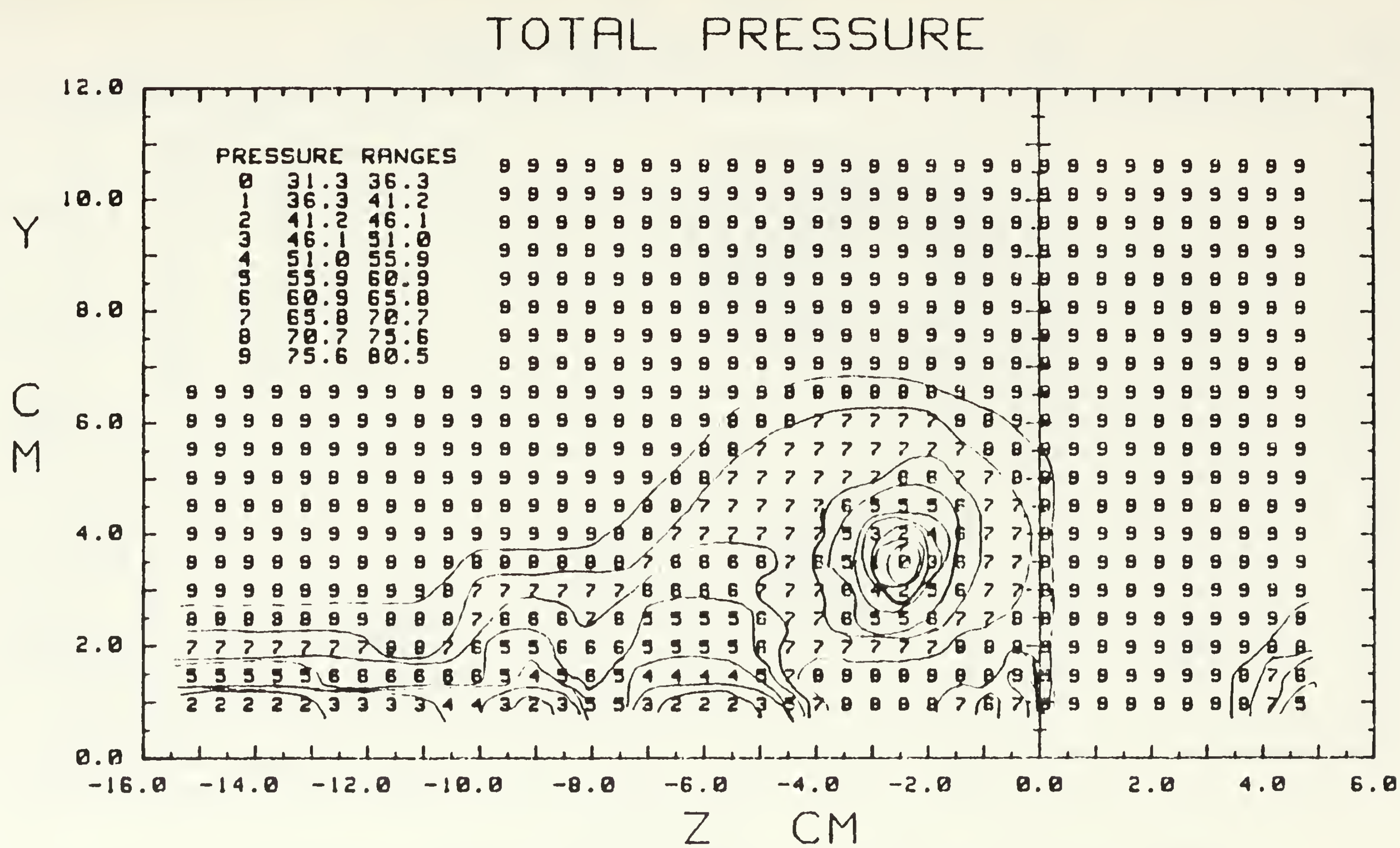

Fig. 52c. EMBEDDED VORTEX 10 M/S WITH FILM COOLING, M=1.26
VORTEX GEN. AT 4.79 cm

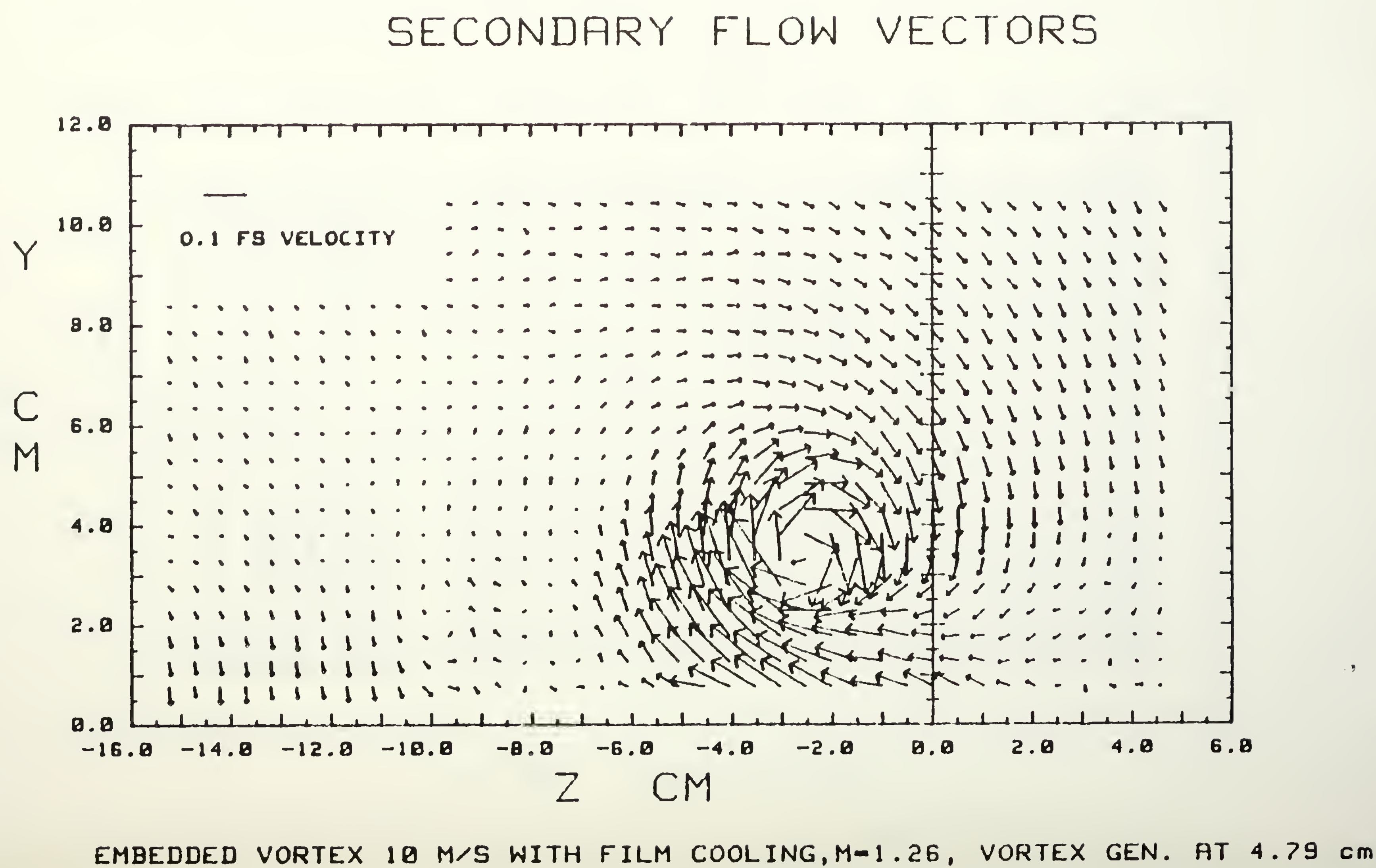

Fig. 52d. Secondary Flow Vectors.

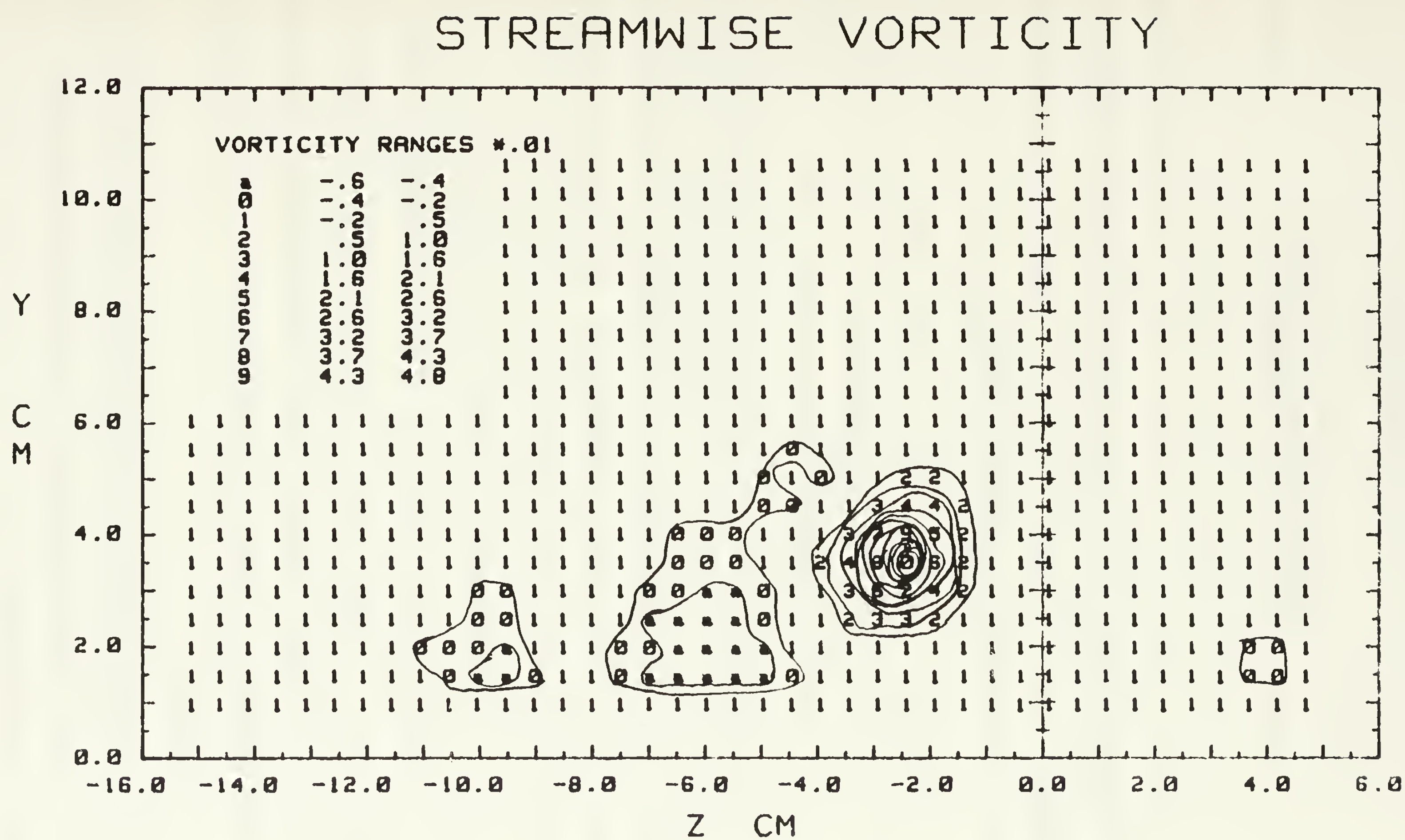

Fig. 52e. EMBEDDED VORTEX 10 M/S, VORTEX GEN. AT 4.79 cm
FILM COOLING, M=1.26

APPENDIX B

UNCERTAINTY ANALYSIS

Uncertainty analysis was performed using the method proposed by Kline and McClintock [Ref. 19]. This is the root sum square method, where the uncertainty, δ_F, of some function F, is a function of the independent variables X_n, according to the following expression:

$$\delta_F = \left(\sum_{i=1}^{n} \left(\frac{\partial F}{\partial X_i} \delta_i \right)^2 \right)^{1/2} \qquad \text{(eqn. C.1)}$$

All uncertainties are based on 95% confidence levels. To calculate the uncertainty of the Stanton number, it is necessary to calculate first the uncertainty in the heat transfer coefficient, h. The following independent variable uncertainties were determined : $\delta_q = \pm 16$ W/m^2, $\delta_{T_w} = \pm 0.5$ ºC, $\delta_{T_\infty} = \pm 0.1$ ºC. Here, the uncertainty of heat loss by convection was based on a 5% error in radiation losses and 2.5% error in conduction losses. The uncertainty of T_w is higher than T_∞ due to higher uncertainty in the calculation of the contact resistance. From these parameters the uncertainty of h was determined to be 4.8% or approximately ± 1.7 W/m^2 ºC, based on an h value of 35 W/m^2 ºC.

To calculate the uncertainty of the Stanton number, besides the uncertainty of the heat transfer coefficient, the following independent variable uncertainties were determine : $\delta_{\rho\infty} = \pm 0.01$ Kg/m^3, $\delta_{U\infty} = \pm 0.5$ m/s and C_p =

$\pm$ 10 J/Kg °K. The uncertainty of C_p was based on the assumption of constant properties. From these parameters the uncertainty of the Stanton number was calculated to be $\pm$ 6.04%, or approximately 1.87×10^{-4} based on a typical Stanton number of 0.0035. The uncertainty of St/Sto is derived from the parameters already mentioned and was estimated to be $\pm$ 7.2% or $\pm$ 0.05 based on a St/Sto of 0.75.

To calculate the uncertainty of the blowing ratio, M, along the uncertainty values determined for U_∞ and ρ_∞, the following independent variable uncertainties were: $\delta_{U_{inj}} = \pm$ 1.0 m/s, and $\delta_{\rho_{inj}} = \pm$ .02 Kg/m³. The uncertainty of U_{inj} is higher than U_∞ due to higher uncertainty of the rotometer and the area of the injection holes, and the uncertainty of ρ_{inj} is also higher than ρ_∞ due to higher uncertainty in the estimation of T_{inj} from T_p. From these parameters the uncertainty of M was calculated to be $\pm$ 8.9% or about $\pm$ 0.0876 for a M value of 0.98.

APPENDIX C

SOFTWARE

The following programs are listed :

ENERB : energy balance estimation for conduction losses

STANFC1 : heat transfer program to acquire thermocouple readings from DAS., and store information in data files in floppy disk

STANFC2 : heat transfer program to calculate Stanton numbers for all flow conditions

ACQTPRO : heat transfer program to acquire temperatures from automatic traversing device for temperature surveys

PLOTRUN : program to read a data file to plot temperature contours

PTSTAV : programs read a data file to plot spanwise averaged Stanton numbers vs. Reynolds number

PTSTLC : reads a data file to plot spanwise local heat transfer coefficients

PLSTRTIO : plots spanwise St/Sto for film cooling only.

PLSTRVOR: plots spanwise variations of St/Sto for embedded vortex data only

PLSTRVV. plots spanwise variations of St/Sto for film cooling only and St/Sto for film cooling and embedded vortex by rows.

SURFCONT: plots surface contours of St/St_f

PLSTRFC : plots spanwise variations of local St/St_o for film cooling data only.

Name of variables used are intended to be self explanatory

```
10    ! PROGRAM ENERGB
20    !
30    !THIS PROGRAM ACQUIRES MULTIPLE CHANEL THERMOCOUPLE DATA
40    !AND PERFORMS ENERGY BALANCE TO ESTIMATE CONDUCTION LOSSES
50    !LIGRANI/ORTIZ VERSION, JUNE 1986
60    !
70    DIM E(200),T(200)
80    !
90    !CHANNELS 0-79,100-146
100   !COPPER CONSTANTAN THERMOCOUPLES
110   !
120   PRINTER IS 701
130   PRINT
140   PRINT "ENERGY BALANCE RESULTS"
150   PRINT "++++++++++++++++++++++++"
160   ! ENTER POWER IN (WATTS)
161   DISP "(HIT(CONTINUE))"
162   PAUSE
170   DISP "ENTER SUPPLY CURRENT IN AMPS, AND VOLTAGE IN VOLTS"
180   INPUT Amps,Volts
190   PRINT
200   PRINT "CURRENT =";Amps," VOLTS = ";Volts
210   PRINT
220   PRINT "TEMPERATURE RESULTS"
230   PRINT
240   Tave=0.
250   PRINT
260   FOR I=1 TO 19
270   OUTPUT 709;"AI";I;"VT1"
280   ENTER 709;X
290   E(I)=X*1000000.
300   T(I)=.018205+.025846*E(I)-.000000581*E(I)*E(I)
310   Tave=Tave+T(I)
320   PRINT USING 330;I,E(I),T(I)
330   IMAGE DDD,3X,DDDDD.D,3X,DDDD.DD
340   NEXT I
350   PRINT "++++++++++++++++++++++++++++++++++++++++"
360   PRINT
370   PRINT
380   FOR I=40 TO 66
390   OUTPUT 709;"AI";I;"VT1"
400   ENTER 709;X
410   E(I)=X*1000000.
420   T(I)=.018205+.025846*E(I)-.000000581*E(I)*E(I)
430   Tave=Tave+T(I)
440   PRINT USING 450;I,E(I),T(I)
450   IMAGE DDD,3X,DDDDD.D,3X,DDDD.DD
460   NEXT I
470   PRINT "++++++++++++++++++++++++++++++++++++++++++++++++++++"
480   PRINT
490   Tave=Tave/46.
500   PRINT "AVERAGE PLATE TEMP. MEASURED (DEG C) =";Tave
```

```
540   PRINT
550   !GET T AMBIENT
560   OUTPUT 709;"AI";0;"VT1"
570   ENTER 709;X
580   E(0)=X*1000
590   T(0)=26.573*E(0)-1.936879*E(0)*E(0)+.99785*E(0)*E(0)*E(0)-.251277*E(0)*E(0
)*E(0)*E(0)
610   Tamb=T(0)
620   PRINT "AMBIENT TEMP. =";Tamb
630   PRINT
640   Tdiff=Tave-Tamb
650   PRINT "TPLATE-TAMB =";Tdiff
660   PRINT
670   !GET AVERAGE TEMP IN INSULATION
680   Tins1=0.
690   FOR I=147 TO 149
700   OUTPUT 709;"AI";I;"VT1"
710   ENTER 709;X
720   E(I)=X*1000.
730   T(I)=26.573*E(I)-1.936879*E(I)*E(I)-.99785*E(I)*E(I)*E(I)-.261277*E(I)*E(I
)*E(I)*E(I)
750   Tins1=Tins1+T(I)
760   !PRINT USING 460;I,E(I),T(I)
770   NEXT I
780   Tins1=Tins1/3.
790   Tins2=0.
800   FOR I=150 TO 152
810   OUTPUT 709;"AI";I;"VT1"
820   ENTER 709;X
830   E(I)=X*1000.
840   T(I)=26.573*E(I)-1.936879*E(I)*E(I)-.99785*E(I)*E(I)*E(I)-.261277*E(I)*E(I
)*E(I)*E(I)
850   !PRINT USING 460;I,E(I),T(I)
870   Tins2=Tins2+T(I)
880   NEXT I
890   Tins2=Tins2/3.
900   PRINT
910   PRINT "TINS1 =";Tins1," TINS2 =";Tins2
920   PRINT
930   !ENTER VALUES OF THERMALCONDUCT., AREA, AND THICKNESS OF INSULATION
940   K=.04     !W/M DEG C
950   Dx=.0254      !M
960   A=.4397       !M^2
970   !CALCULATE HEAT FLUX THROUGH INSULATION
980   Qins=K*A*(Tins1-Tins2)/Dx
990   !GET Q IN (WATTS)
1000  Qin=Volts*Amps
1010  Qcond=Qin-Qins
1020  PRINT "Q IN =";Qin," QINSULATION =";Qins," QCONDUCTION =";Qcond
1030  PRINT "**********************************************"
1040  STOP
1050  END
```

```
10    ! PROGRAM STANFC1
20    !
30    !THIS PROGRAM ACQUIRES MULTIPLE CHANEL THERMOCOUPLE DATA
40    !CREATES AND CREATES A FILE TO BE READ BY OTHER PROGRAM.
50    !UPDATED BY ORTIZ, JULY 1987.
60    !
70    !
80    MASS STORAGE IS ":INTERNAL,4,1"
90    CREATE BDAT "TDAFC26",252,8   !OPEN FILE TO RETRIEVE BASELINE TEMPERATURES
100   ASSIGN @Path_1 TO "TDAFC26"
110   CREATE BDAT "IDAFC26",11,8
120   ASSIGN @Path_2 TO "IDAFC26"    !OPEN FILE TO RETRIEVE INPUT DATA
130   DIM E(200),T(200)
140   PRINTER IS 1
150   !
160   PRINT "ARE YOU WORKING WITH(1), OR WITHOUT(2) FILMCOOLING?"
170   INPUT Ans
180   IF Ans=1 THEN GOTO 1060      !SUBROUTINE FOR FILMCOOLING DATA
190   !
200   !CHANELS 0-79, 100-150
210   !COPPER CONSTANTAN THERMOCOUPLES
220   !
230   PRINT "ENTER RUN # (MONTH,DAY,YEAR,HOUR,MINUTES=MMDDYY.HHMM)"
240   INPUT Runno
250   PRINT "RUN # (MONTH,DAY,YEAR.HOUR,MINUTES) =";Runno
260   PRINT
270   !
280   !ENTER AMPS AND VOLTS FROM VARIAC
290   PRINT "ENTER CURRENT(AMPS.)"
300   INPUT Amps
310   PRINT "ENTER VOLTAGE(VOLTS)"
320   INPUT Volts
330   PRINT "AMPS =";Amps,"VOLTS =";Volts
340   PRINT
350   !ENTER AMBIENT CONDITIONS
360   PRINT "ENTER AMBIENT PRESSURE(IN HG)"
370   INPUT Pamb
380   PRINT "ENTER AMBIENT TEMPERATURE(DEG C)"
390   INPUT Tamb
400   PRINT "ENTER PRESSURE DIFFERENCE(IN H2O)"
410   INPUT Deltap
420   PRINT "PAMB(IN HG)=";Pamb,"DELTAP(IN H2O)=";Deltap,"TAMB(DEG C)=";Tamb
430   PRINT
440   !
450   DISP "(HIT<CONTINUE>)"
460   PAUSE
470   PRINTER IS 1
480   PRINT "TEMPERATURES DEG C"
490   PRINT "************************"
500   PRINT
510   PRINT "RUN # (MONTH,DAY,YEAR.HOUR,MIN)=";Runno
520   PRINT
```

```
530   PRINT "No    T DEG C"
540   ! ACQUIRE THERMOCOUPLE READINGS
550   PRINT
560   FOR I=1 TO 79
570   OUTPUT 709;"AI";I;"VT1"
580   ENTER 709;X
590   E(I)=X*1000000
600   T(I)=.018205+.025846*E(I)-.000000581*E(I)*E(I)
610   PRINT USING 620;I,T(I)
620   IMAGE DDD,4X,DD.DD
630   OUTPUT @Path_1;T(I)
640   NEXT I
650   !
660   FOR I=100 TO 146
670   OUTPUT 709;"AI";I;"VT1"
680   ENTER 709;X
690   E(I)=X*1000000
700   T(I)=.01825+.025846*E(I)-.000000581*E(I)*E(I)
710   I1=I-20
720   PRINT USING 620;I1,T(I)
730   OUTPUT @Path_1;T(I)
740   NEXT I
750   !GET AMBIENT TEMPERATURE
760   OUTPUT 709;"AI";0;"VT1"
770   ENTER 709;X
780   E(0)=X*1000.
790   T(0)=25.573*E(0)-1.936879*E(0)*E(0)+.99783*E(0)*E(0)*E(0)-.261277*E(0)^4
800   Tchamb=T(0)
810   PRINT "THERMOCOUPLE AMBIENT TEMP.(DEG C) =";Tchamb
820   PRINT
830   !GET THE REST OF THERMOCOUPLES
840   FOR I=147 TO 150
850   OUTPUT 709;"AI";I;"VT1"
860   ENTER 709;X
870   E(I)=X*1000.
880   T(I)=25.573*E(I)-1.936879*E(I)*E(I)+.997875*E(I)*E(I)*E(I)-.261277*E(I)^4
890   PRINT USING 620;I,T(I)
900   OUTPUT @Path_1;T(I)
910   NEXT I
920   ASSIGN @Path_1 TO *
930   !TRANSFORM TO SI UNITS
940   !
950   Pamb=Pamb*3386.82          !PASCALS(N/M^2)
960   Deltap=Deltap*248.7        !PASCALS(N/M^2)
970   Fstemp=T(147)+273.15       !DEG KELVIN
980   Ro=Pamb/(287*Fstemp)       !AIR DENSITY (KG/M3)
990   Uinf=(2*Deltap/Ro)^.5      !FREE STREAM VELOCITY (M/S)
1000  !
1010  PRINT
1020  OUTPUT @Path_2;Runno,Amps,Volts,Pamb,Deltap,Tamb,Tchamb,Uinf,Ro,Fstemp,Ans
1030  ASSIGN @Path_2 TO *
1040   !
1050   GOTO 1190
1060  !SUBROUTINE TO CALCULATE FILM COOLING DATA
```

```
1070  PRINTER IS 1
1080  PRINT "ENTER FLOW % FROM ROTOMETER"
1090  INPUT Flw
1100  PRINT "ENTER PLENUM PRESSURE DIFFERENCE (IN H2O)"
1110  INPUT Delpi
1120  Delpi=Delpi*248.7
1130  Flw=Flw*.000033456
1140  CREATE BDAT "FILDT26",2,8
1150  ASSIGN @Path3 TO "FILDT26"      !OPEN FILE TO RETRIEVE FILMCOOLING DATA
1160  OUTPUT @Path3;Flw,Delpi
1170  ASSIGN @Path3 TO *
1180  GOTO 190
1190  MASS STORAGE IS ":INTERNAL,4"
1200  END
```

```
10    ! PROGRAM STANFC2
20    !
30    !10 M/S FREE STREAM VELOCITY, 13 INJECTION HOLES OPEN
40    !THIS PROGRAM ACQUIRES MULTIPLE CHANEL THERMOCOUPLE DATA
50    !CALCULATES HEAT TRANSFER COEFFICIENTS AND STANTON NUMBERS RATIOS
60    !AND FILMCOOLING PARAMETERS.
70    !LIGRANI/ORTIZ/JOSEPH VERSION, NOVEMBER 1986
80    !UPDATED BY ORTIZ, JULY 1987.
90    !
100   !
110   MASS STORAGE IS ":INTERNAL,4,1"
120   CREATE BDAT "STRFCV10",504,8      !OPEN FILE TO RETRIEVE STANTON Nos RATIOS
130   ASSIGN @Path_4 TO "STRFCV10"
140   DIM T(200),H(200),St(200),X1(6),H1(6),St1(6),X2(200),Z(200),Stf(200)
150   DIM Ho(200),Sto(200),X1o(6),X2o(200),Zo(200),Str(200),Stfr(200)
160   !
170   PRINTER IS 1
180   !
190   PRINT "ARE YOU USING VORTEX GENERATOR? (3,Y OR 4,N) "
200   INPUT Y
210   IF Y=3 THEN
220      PRINT "ENTER TYPE OF VORTEX GENERATOR"
230      INPUT Vort
240      PRINT "ENTER LOCATION FROM CENTER LINE IN cm"
250      INPUT Loc
260   ELSE
270   GOTO 290
280   END IF
290   PRINTER IS 701
300   PRINT CHR$(27);CHR$(38);CHR$(108):CHR$(53);CHR$(52);CHR$(70)
310   PRINT CHR$(27);CHR$(38);CHR$(108):CHR$(49);CHR$(76)
320   !
330   ASSIGN @Path1 TO "TDAFC10"
340   FOR I=1 TO 130
350   ENTER @Path1;T(I)
360   NEXT I
370   ASSIGN @Path2 TO "IDAFC10"
380   ENTER @Path2;Runno,Amps,Volts,Pamb,Deltap,Tamb,Tchamb,Uinf,Ro,Fstemp,Ans
390   PRINT
400   !
410   DISP "(HIT<CONTINUE>)"
420   PAUSE
430   IF Ans=1 THEN
440   PRINT "STANTON NUMBER RESULTS WITH FILM COOLING"
450   ELSE
460   PRINT "STANTON NUMBER RESULTS"
470   END IF
480   PRINT "*********************************************************"
490   PRINT
500   PRINT "RUN # (MONTH,DAY,YEAR.HOUR,MIN)=";Runno
510   PRINT
520   IF Y=3 THEN
```

```
530   PRINT "VORTEX GENERATOR IS No =";Vort," LOCATED AT (cm) =";Loc
540   PRINT
550   ELSE
560   GOTO 580
570   END IF
580   IF Ans=1 THEN GOTO 2240
590   !PRINT OUT DATA
600   PRINT "AMPS =";Amps," VOLTS =";Volts
610   PRINT
620   PRINT "AMBIENT PRESSURE (N/M^2) = ";Pamb," DELTA P (N/M^2) =";Deltap
630   PRINT
640   !
650   PRINT "AIR DENSITY (KG/M3) =";Ro," VELOCITY (M/S) =";Uinf
660   PRINT
670   PRINT "FREE STREAM TEMP,(DEG K)=";Fstemp
680   PRINT
690   PRINT "THERMOMETER AMBIENT TEMPERATURE (DEG C) =";Tamb
700   PRINT
710   !CALCULATE THE AVERAGE PLATE TEMPERATURE
720   !
730   Tave=0.
740   FOR I=1 TO 126
750     Tave=Tave+T(I)
760   NEXT I
770   Tave=Tave/126
780   PRINT "AVERAGE PLATE TEMPERATURE, MEASURED (DEG C) =";Tave
790   PRINT
800   !ENERGY BALANCE
810   !
820   Tdiff=Tave-Tchamb
830   Qcond=.683+.954*Tdiff-.016*Tdiff^2
840   Tavabs=Tave+273.15
850   Tchabs=Tchamb+273.15
860   Qrad=.00000002189*(Tavabs^4-Tchabs^4)
870   Qin=Amps*Volts
880   Qconv=Qin-Qcond-Qrad
890   Delt=Tavabs-Fstemp
900   !
910   PRINT "T PLATE - T FSTREAM (DEG C)=";Delt,"POWER IN (WATTS)=";Qin
920   PRINT
930   PRINT "CONDUCTION LOSS (WATTS)=";Qcond,"CONVECTION LOSS (WATTS)=";Qconv
940   PRINT
950   PRINT "RADIATION LOSS (WATTS) =";Qrad
960   PRINT
970   !WALL TEMPERATURES CORRECTIONS
980   !
990   Cp=1005.            !SPECIFIC HEAT FOR AIR
1000  Cr=.014             !CONTACT RESISTANCE CORRECTION FACTOR
1010  Dt=Cr*Qconv          !DELTA TEMP. DUE TO CONTACT RESISTANCE
1020  Q=Qconv/.4897       !CONVECTION LOSS CORRECTION
1030  !
1040  Tcavbs=Tavabs-Dt
1050  Deltc=Tcavbs-Fstemp
1060  Theta=(Tijabs-Fstemp)/Deltc
```

```
1610  Z(M)=Z(1)
1620  X2(M)=X3
1630  FOR I=M+1 TO J*21
1640  X2(I)=X3
1650  Z(I)=Z(I-1)+1.27
1660  NEXT I
1670  X3=X3+.2
1680  NEXT J
1690  FOR I=1 TO 126
1700  OUTPUT @Path_4;Str(I),Stfr(I),X2(I),Z(I)
1710  PRINT USING 1720;I,X2(I),Z(I),H(I),Str(I),Stfr(I)
1720  IMAGE DDD,2X,DD.DD,3X,3D.DD,5X,SD.DDDE,5X,SD.DDDE,5X,D.3DE
1730  NEXT I
1740  ASSIGN @Path_4 TO *      !CLOSE FILE WITH STANTON NUMBERS RATIOS
1750  !
1760  !CALCULATE LOCAL REYNOLDS NUMBER
1770  !
1780  PRINT
1790  !
1800  Nu=.0000156               !CINEMATIC VISCOSITY FOR AIR (M2/S)
1810  Fac=Uinf/Nu
1820  X1(1)=1.15
1830  X1(2)=1.25
1840  X1(3)=1.40
1850  X1(4)=1.60
1860  X1(5)=1.80
1870  X1(6)=2.00
1880  !
1890  FOR I=1 TO 6
1900    Rey(I)=X1(I)*Fac
1910  NEXT I
1920  !
1930  !CALCULATE AVERAGE STANTON NUMBER
1940  FOR I=1 TO 6
1950      H(I)=0.
1960      M=I*21-20
1970      FOR J=M TO I*21
1980          H1(I)=H1(I)+H(J)
1990      NEXT J
2000      H1(I)=H1(I)/21
2010      St1(I)=H1(I)/(Ro*Uinf*Cp)
2020  NEXT I
2030  PRINT
2040  !
2050  ASSIGN @Path7 TO "STAV2"
2060  FOR I=1 TO 6
2070  ENTER @Path7;X1o(I),Reo(I),St1o(I)
2080  Strav(I)=St1(I)/St1o(I)
2090  NEXT I
2100  CREATE BDAT "STAVFCV",18,8
2110  ASSIGN @Path_5 TO "STAVFCV"
2120  !PRINT AVERAGE STANTON NUMBERS
2130  !
2140  PRINT "ROW#   X(M)   REYNOLDS No          St/Sto Ave   "
```

```
1070  !
1080  PRINT "TPLATE - T FREESTREAM CORRECTED (DEG C)=";Deltc
1090  PRINT
1100  PRINT "AVERAGE PLATE TEMP. CORRECTED (DEG C)=";Tave-Dt
1110  PRINT
1120  PRINT "NONDIMESIONAL TEMP. THETA =";Theta
1130  PRINT
1140  PRINT "No    X(M)     Z(CM)     H(W/M^2 C)       St/Sto         St/Stf"
1150  PRINT "*****************************************************************"
1160  PRINT
1170  ASSIGN @Path6 TO "HDAT2"
1180  ASSIGN @Path7 TO "STAFC8"
1190  !
1200  FOR I=1 TO 126
1210  ENTER @Path6;Ho(I),Sto(I),XZo(I),Zo(I)
1220  ENTER @Path7;Stf(I)
1230  NEXT I
1240  !CALCULATE THE HEAT TRANSFER CCEFFICIENTS AND SATANTON NUMBERS
1250  !
1260        FOR I=1 TO 126
1270            T(I)=T(I)-Dt
1280            H(I =Q/(T(I)-T(127))
1290            St(I)=H(I)/(Ro*Uinf*Cp)
1300            Str(I)=St(I)/Sto(I)
1310            Stfr(I)=St(I)/Stf(I)
1320        NEXT I
1330   !GENERATE X AND Z POSITION FOR EACH INDIVIDUAL THERMOCOUPLE
1340   Z(1)=-12.7          ! (CM)
1350   X2(1)=1.15
1360   FOR I=2 TO 21
1370   X2(I)=1.15
1380   Z(I)=Z(I-1)+1.27
1390   NEXT I
1400   Z(22)=Z(1)
1410   X2(22)=1.25
1420   FOR I=23 TO 42
1430   X2(I)=1.25
1440   Z(I)=Z(I-1)+1.27
1450   NEXT I
1460   Z(43)=Z(1)
1470   X2(43)=1.40
1480   FOR I=44 TO 63
1490   X2(I)=1.40
1500   Z(I)=Z(I-1)+1.27
1510   NEXT I
1520   Z(64)=Z(1)
1530   X2(64)=1.6
1540   FOR I=65 TO 84
1550   X2(I)=1.6
1560   Z(I)=Z(I-1)+1.27
1570   NEXT I
1580   X3=1.8
1590   FOR J=5 TO 6
1600   M=J*21-20
```

```
2150   PRINT "*****************************************************"
2160   FOR I=1 TO 6
2170      PRINT USING 2180;I,X1(I),Rey(I),Strav(I)
2180      IMAGE DD,4X,DD.DD,4X,D.4DE,7X,D.4DE
2190      OUTPUT @Path_5;X1(I),Rey(I),Strav(I)
2200   NEXT I
2210   ASSIGN @Path_5 TO *
2220   !
2230   GOTO 2680
2240   !SUBROUTINE TO CALCULATE DISCHARGE COEFFICIENTS
2250   !
2260   ASSIGN @Path3 TO "FILDT10"
2270   ENTER @Path3;Flw,Delpi
2280   !GET AVERAGE PLENUM TEMPERATURE
2290   Tpl=0
2300   FOR I=128 TO 130
2310   Tpl=Tpl+T(I)
2320   NEXT I
2330   Tpl=Tpl/3
2340   !CONVERT PLENUM TEMP. TO INJECTION TEMP.
2350   Tinj=1.45463*Tpl^.868182
2360   Tijabs=Tinj+273.15
2370   Uinj=Flw/.000921458                   !FOR 13 INJ. HOLES
2380   !Uinj=Flw/.000496                     !FOR 7 INJ. HOLES
2390   Tor=Tijabs-(Uinj^2/(2*1005))
2400   Roc=Pamb/(Tor*287)
2410   Imflx=Roc*Uinj             !INJECTION MASS FLUX
2420   Ropl=Pamb/(Tijabs*287)   !TOTAL DENSITY BASED ON To
2430   U3=(Delpi*2/Ropl)^.5
2440   Pmflx=Ropl*U3
2450   Cd=Imflx/Pmflx
2460   Red=Uinj*.009525/.0000156
2470   M=Imflx/(Ro*Uinf)             !BLOWING RATIO
2480   Vrat=Uinj/Uinf              !VELOCITY RATIO
2490   Mfr=Roc*Uinj^2/(Ro*Uinf^2)    !MOMENTUM FLUX RATIO
2500   !
2510   !PRINT RESULTS
2520   PRINT "INJECTION TEMPERATURE ( C)=";Tinj,"PLENUM TEMP (C)=";Tpl
2530   PRINT
2540   !
2550   PRINT "PLENUM PRESSURE DIFF. (N/M^2)=";Delpi
2560   PRINT
2570   PRINT "COOLANT DENSITY KG/M^3) =";Roc," DENSITY RATIO =";Roc/Ro
2580   PRINT
2590   PRINT "INJECTION VELOCITY (M/S)=";Uinj,"MASS FLUX (KG/M^2 S)=";Imflx
2600   PRINT
2610   PRINT "REYNOLDS No (DIA)=";Red,"DISCHARGE COEFF. Cd =";Cd
2620   PRINT
2630   PRINT "BLOWING RATIO =";M,"  VELOCITY RATIO =";Vrat
2640   PRINT
2650   PRINT "MOMENTUM FLUX RATIO = ";Mfr
2660   PRINT
2670   GOTO 590
2680   MASS STORAGE IS ":INTERNAL,4"
2690   END
```

```
10    REM PROGRAM ACQTPRO
20    REM THIS PROGRAM ACQUIRES TEMPERATURES FROM A THERMOCCOUPLE
30    REM MONTED ON A AUTOMATIC TRAVERSE MECHANISIM AND FROM A FREE
40    !   STREAM VELOCITY THERMCOPLE TO PLOT THE TEMPERATURES PROFILES
50    !   USING PROGRAM PLOTDE
60    !
70    !   BY ALFREDO ORTIZ, AUGUST,1987
80    REM
90    REM VARIABLE NAMES
100   REM
110   REM E(I) IS THE VOLTAGE READ FROM THE DATA ACQUISTION SYSTEM
120   REM T(I) IS THE CONVERSION FROM VOLTAGE TO TEMPERATURES
130   REM
140   REM PAMB=AMBIENT PRESSURE
150   REM TFS=FREE STREAM TEMP(KELVIN)
160   REM RO=DENSITY (KG/M^3)
170   REM UINF=VELOCITY OF THE FREESTREAM
180   REM
190   DIM Y(1000),Z(1000),T(1000),T1(1000),D(1000)
200   REM
210   REM
220   INPUT "ENTER DATE,(MMDDYY)",N9
230   INPUT "ENTER TIME,(HHMM)",N8
240   REM
250   INPUT "ENTER DISTANCE FROM THE B.L. TRIP., X(M)",X1
260   INPUT "ENTER POINTS SPANWISE",M3
270   INPUT "ENTER POINTS VERTICAL (MUST BE AN INTEGER)",N3
280   REM N3 MUST BE AN EVEN INTEGER
290   INPUT "ENTER SPANWISE RESOLUTION(IN)",Z4
300   INPUT "ENTER VERTICAL RESOLUTION(IN)",Y4
310   INPUT "INITIAL Z(IN)",Z3
320   INPUT "INITIAL Y(IN)",Y3
330   REM
340   Z(1)=Z3
350   Y(1)=Y3
360   N7=N3/2
370   FOR I7=1 TO N7
380   I6=I7-1
390   J1=2*I6*M3+2
400   J2=2*I6*M3+M3
410   FOR K=J1 TO J2
420   Z(K)=Z(K-1)+Z4
430   Y(K)=Y(K-1)
440   NEXT K
450   J3=2*I6*M3+M3+1
460   Z(J3)=Z(J3-1)
470   Y(J3)=Y(J3-1)+Y4
480   J4=J3+1
490   J5=2*I6*M3+2*M3
500   FOR K=J4 TO J5
510   Z(K)=Z(K-1)-Z4
520   Y(K)=Y(K-1)
530   NEXT K
```

```
540   IF I7=N7 THEN 590
550   J6=J5+1
560   Z(J6)=Z(J6-1)
570   Y(J6)=Y(J6-1)+Y4
580   NEXT I7
590   REM
600   ! ENTER FREE STREAM TEMPERATURE FROM DAS.
610   OUTPUT 709;"AI";151;"VT1"
620   ENTER 709;X
630   E=X*1000000
640   Tfs=-.0783171+.026105454*E-.000000678*E*E
650   Tfs=Tfs+273.15
660   REM ENTER AMBIENT CONDITIONS
670   INPUT "ENTER PAMB (IN.OF HG)",Pamb
680   INPUT "ENTER PRESSURE DIFFERENCE (IN OF H2O)",Deltap
690   REM
700   REM CONVERSION TO SI UNITS
710   Pamb=Pamb*3385.82
720   Ro=Pamb/(287*Tfs)
730   Deltap=Deltap*248.7
740   REM FREESTREAM VELOCITY
750   Uinf=(2*Deltap/Ro)^.5
760   REM
770   REM ENTER THE LOOP FOR ACQUIRING EACH TEMPERATURE COMPUTING COEFFICENTS
780   REM AND COMPUTING TWO TEMPERATURE COEFFICIENTS AND TWO TEMPERATURES
790   PRINTER IS 701
800   PRINT CHR$(27);CHR$(38);CHR$(108);CHR$(53);CHR$(52);CHR$(70)
810   PRINT CHR$(27);CHR$(38);CHR$(108);CHR$(49);CHR$(76)
820   !
830   PRINT "TEMPERATURE PROFILE COMPUTATION "
840   PRINT "=================================="
850   PRINT
860   PRINT "DATE OF RUN IS",N8," TIME =";N9
870   PRINT
880   PRINT "DISTANCE FROM THE BOUNDARY LAYER TRIP, X (M)=";X1
890   PRINT
900   PRINT "DENSITY(KG/M^3)",Ro
910   PRINT
920   PRINT "FREESTREAM VELOCITY (M/S)",Uinf
930   PRINT
940   PRINT "PAMBIENT(N/M^2)",Pamb
950   PRINT
960   PRINT "FREE STREAM TEMPERATURE (DEG C) =";Tfs-273.15
970   PRINT
980   PRINT "POINTS SPANWISE",M3
990   PRINT
1000  PRINT "POINTS VERTICAL",N3
1010  PRINT
1020  PRINT "SPANWISE RESOLUTION (IN)",Z4
1030  PRINT
1040  PRINT "VERTICAL RESOLUTION (IN)",Y4
1050  PRINT
1060  PRINT "INITIAL Z(IN)";Z3
1070  PRINT
```

```
1080  PRINT "INITIAL Y(IN)",Y3
1090  PRINT
1100  PRINT "*******************************************"
1110  PRINT
1120  PRINT "   Y      Z        T      TFS        DT"
1130  PRINT "========================================== "
1140  PRINT
1150  DISP "HIT <<CONTINUE FOR DAS>>"
1160  PAUSE
1170  K9=0
1180  K2=M3*N3
1190  FOR K=1 TO K2
1200  K9=K
1210  REM
1220  WAIT 10
1230  REM  ACQUIRE THE TEMPERATURE FOR EACH POSITION
1240  G1=0
1250  REM
1260  FOR J=1 TO 25     !ENTER THE DAS AND SAMPLE OF TEMPERATURE 25 TIMES
1270  OUTPUT 709;"AI";152;"VT1"
1280  ENTER 709;X
1290  G1=G1+X
1300  NEXT J
1310  REM
1320  X=G1/25           !AVERAGE THE VALUES
1330  E=X*1000000
1340  T(K)=.1836709+.02566713*E-.000000486*E*E   !CONVERSION FROM VOLTAGE TO TEM
PERATURE
1350  REM
1360  ! GET FREE STREAM TEMP 5 TIMES AND AVERAGE IT
1370  G4=0
1380  FOR I=1 TO 5
1390  OUTPUT 709;"AI";151;"VT1"
1400  ENTER 709;X
1410  G4=G4+X
1420  NEXT I
1430  X=G4/5
1440  E=X*1000000
1450  T1(K)=-.0783171+.026105454*E-.000000678*E*E
1460  D(K)=T(K)-T1(K)
1470  PRINT USING 1480;Y(K),Z(K),T(K),T1(K),D(K)
1480  IMAGE MDD.DD,2X,MDD.DD,2X,MDD.DD,3X,MDD.DD,3X,SD.DDE
1490  REM
1500  NEXT K
1510  REM
1520  MASS STORAGE IS ":INTERNAL,4,1"
1530  CREATE BDAT "TPR014",2400,3
1540  ASSIGN @Path2 TO "TPR014"
1550  FOR I=1 TO K9
1560  OUTPUT @Path2;Y(I),Z(I),D(I)
1570  NEXT I
1580  ASSIGN @Path2 TO *
1590  MASS STORAGE IS ":INTERNAL,4"
1600  END
```

```
10    !PROGRAM PLOTPRUN
20    ! THIS PROGRAM READS THE FILE TPRO AND PLOT TEMPERATURES
30    ! PROFILES
40    DIM Y1(800),Z0(800),X$(800)[1],V1(800),Z1(40),Z2(40),C$(13)[1]
50    !  V(I)=D(I)  :TEMPERATURE DIFFERENCE.
60    !
70    INPUT "ENTER RUN NUMBER ",Runno
80    F$="DATE="
90    MASS STORAGE IS ":INTERNAL,4,1"
100   ASSIGN @Path1 TO "TPRO7"
110   FOR I=1 TO 800
120   ENTER @Path1;Y1(I),Z0(I),V1(I)
130   Y1(I)=Y1(I)*2.54
140   Z0(I)=Z0(I)*2.54
150   NEXT I
160   FOR I=1 TO 800
170   IF V1(I)<=.2 THEN X$(I)="0"
180   IF V1(I)<=.5 AND V1(I)>.2 THEN X$(I)="1"
190   IF V1(I)<=1.0 AND V1(I)>.5 THEN X$(I)="2"
200   IF V1(I)<=1.5 AND V1(I)>1.0 THEN X$(I)="3"
210   IF V1(I)<=2.0 AND V1(I)>1.5 THEN X$(I)="4"
220   IF V1(I)<=2.5 AND V1(I)>2.0 THEN X$(I)="5"
230   IF V1(I)<=3.0 AND V1(I)>2.5 THEN X$(I)="6"
240   IF V1(I)<=3.5 AND V1(I)>3.0 THEN X$(I)="7"
250   IF V1(I)<=4.0 AND V1(I)>3.5 THEN X$(I)="8"
260   IF V1(I)<=4.5 AND V1(I)>4.0 THEN X$(I)="9"
270   IF V1(I)<=5.0 AND V1(I)>4.5 THEN X$(I)="a"
280   IF V1(I)<=5.5 AND V1(I)>5.0 THEN X$(I)="b"
290   IF V1(I)>5.5 THEN X$(I)="c"
300   NEXT I
310   GINIT
320   PLOTTER IS 705,"HPGL"
330   !PLOTTER IS CRT,"INTERNAL"
340   GRAPHICS ON
350   CSIZE 2.5,.65
360   MOVE 35,14
370   LABEL "EMBEDDED VORTEX 10 M/S WITH FILM COOLING, M=0.98"
380   MOVE 35,11
390   LABEL "X=1.480 M, UNHEATED PLATE,VORTEX GEN. AT 4.79 cm"
400   MOVE 75,83
410   LABEL USING "6A,#,6D.4D";F$,Runno
420   CSIZE 4.5,.65
430   MOVE 40,85
440   LABEL "TEMPERATURE PROFILES"
450   CSIZE 3.5,.65
460   MOVE 67,17
470   LABEL "Z  (CM) "
480   DEG
490   LDIR 90
500   MOVE 21,45
510   LABEL "Y  (CM) "
520   LDIR 0
```

```
530   VIEWPORT 30,116,25,83
540   WINDOW -16,6,0,12
550   FRAME
560   AXES .5,.5,0,0,2,2
570   AXES .5,.5,-16,12,2,2
580   AXES .5,.5,6,12,2,2
590   CSIZE 2.Ø,.65
600   MOVE -15.2,11.1Ø
610   LABEL "TEMP. DIFF. RANGES"
620   A=10.65
630   FOR K=Ø TO 12
640   B=A-K*.35
650   MOVE -14.3,B
660   IF K<2 THEN
670   Z2(Ø)=-.2
680   Z1(Ø)=.2
690   Z2(1)=.2
700   Z1(1)=.5
710   ELSE
720   Z2(K)=Z1(K-1)
730   Z1(K)=Z2(K)+.5
740   END IF
750   IF K>9 THEN GOTO 780
760   LABEL USING "D,2X,DD.D,X,DD.D";K,Z2(K),Z1(K)
770   GOTO 820
780   C$(10)="a"
790   C$(11)="b"
800   C$(12)="c"
810   LABEL USING "A,2X,DD.D,X,DD.D";C$(K),Z2(K),Z1(K)
820   NEXT K
830   CSIZE 1.3,.72
840   FOR I=1 TO 800
850   MOVE ZØ(I),Y1(I)
860   IF Y1(I)>6.Ø AND ZØ(I)<-1Ø. THEN GOTO 880
870   LABEL USING "A";X$(I)
880   NEXT I
890   CLIP OFF
900   CSIZE 2.Ø,.65
910   FOR I=-.2 TO 11.8 STEP 2
920     MOVE -17.5,I
930     I1=I+.2
940     LABEL USING "#,DD.D";I1
950   NEXT I
960   FOR J=-17.Ø TO 5.Ø STEP 2
970      MOVE J,-.7
980      J1=J+1.Ø
990      LABEL USING "#,MDD.D";J1
1000  NEXT J
1010  MASS STORAGE IS ":INTERNAL,4"
1020  END
```

```
10      !PROGRAM PTSTAV
20      !THIS PROGRAM READS A DATA FILE AND PLOTS AVERAGE STANTON NUMBERS
30      !VERSUS REYNOLDS NUMBERS.
40      !
50      DIM Rey(6),X1(6),St1(6),C$[6],St(6)
60      MASS STORAGE IS ":INTERNAL,4,1"
70      ASSIGN @Path2 TO "STAV1"
80      FOR I=1 TO 6
90      ENTER @Path2;X1(I),Rey(I),St1(I)
100     NEXT I
110     PRINTER IS 1
120     PRINT "ENTER RUN NUMBER TO WHICH THIS DATA CORRESPOND (MMDDYY.HHMM)"
130     INPUT Runno
140     F$="DATE ="
150     GINIT
160     PLOTTER IS 705,"HPGL"
170     !PLOTTER IS CRT,"INTERNAL"
180     GRAPHICS ON
190     CSIZE 2.5,.65
200     MOVE 42,14
210     LABEL "FREESTREAM 15 M/S, NO FILM COOLING"
220     CSIZE 4.5,.65
230     MOVE 40,85
240     LABEL "AVERAGED STANTON NUMBERS"
250     CSIZE 2.5,.65
260     MOVE 75,63
270     LABEL USING "6A,#,6D.4D";F$,Runno
280     CSIZE 3.4,.65
290     MOVE 62,17
300     LABEL "REx * 10^6"
310     DEG
320     LDIR 90
330     MOVE 22,33
340     LABEL "STANTON No *10^-3"
350     LDIR 0
360     VIEWPORT 30,116,25,83
370     WINDOW 0,5,0,6
380     FRAME
390     AXES .5,.5,0,0,2,1
400     AXES .5,.5,5,6,2,1
410     CLIP OFF
420     CSIZE 2.0,.65
430     LORG 2
440     FOR I=0 TO 6 STEP .5
450       MOVE -.32,I
460       LABEL USING "#,D.DD";I
470     NEXT I
480     LORG 4
490     FOR J=0. TO 5.0 STEP .5
500        MOVE J,-.22
510        LABEL USING "#,DD.D";J
520     NEXT J
```

```
530   !ENTER VALUES FOR ANALYTICAL FORMULA
540   Zi=1.1              !METERS
550   Pr=.71              !PRANOTL No FOR AIR
560   FOR I=1 TO 6
570   St(I)=((.030*(Rey(I))^(-.2))*(1.-(Zi/X1(I))^.9)^(-.111))/Pr^.4
580   St(I)=St(I)*1.0E+3
590   Rey(I)=Rey(I)*1.0E-6
600   PLOT Rey(I),St(I)
610   NEXT I
620   CSIZE 1.3,.72
630   FOR I=1 TO 6
640   C$[I]="x"
650   St1(I)=St1(I)*1.0E+3
660   MOVE Rey(I),St1(I)
670   LABEL USING "A";C$[I]
680   PENUP
690   NEXT I
700   MASS STORAGE IS ":INTERNAL,4"
710   END
```

```
10     !PROGRAM PTSTLC
20     !THIS PROGRAM READS A DATA FILE AND PLOTS SPANWISE VARIATIONS
30     !OF HEAT TRANS FER COEFFICIENTS
40     !
50     DIM H(200),St(200),Rey(5),Z(200),X1(6),X2(200),B(126),C$(6)[8]
60     MASS STORAGE IS ":INTERNAL,4,1"
70     ASSIGN @Path1 TO "HDAT2"
80     FOR I=1 TO 126
90     ENTER @Path1;H(I),St(I),X2(I),Z(I)
100    NEXT I
110    F$="DATE ="
120    INPUT "ENTER RUN NUMBER  (MMDDYY.HHMM)",Runno
130    GINIT
140    PLOTTER IS 705,"HPGL"
150    !PLOTTER IS CRT,"INTERNAL"
160    GRAPHICS ON
170    CSIZE 2.5,.65
180    MOVE 42,14
190    LABEL "FREE STREAM 10 M/S, NO FILM COOLING"
200    CSIZE 4.5,.65
210    MOVE 20,85
220    LABEL "SPANWISE HEAT TRANSFER COEFFICIENT"
230    CSIZE 2.5,.55
240    MOVE 75,83
250    LABEL USING "6A,#,6D.4D";F$,Runno
260    CSIZE 3.5,.65
270    MOVE 55,17
280    LABEL "Z  (CM) "
290    MOVE 22,35
300    DEG
310    LDIR 90
320    LABEL "H W/M^2 DEG C"
330    LDIR 0
340    VIEWPORT 30,116,25,83
350    WINDOW -15.24,15.24,0,100
360    FRAME
370    AXES 1.27,10,-15.24,0,2,2
380    AXES 1.27,10,15.24,100,2,2
390    CSIZE 2.0,.65
400    MOVE -13,23
410    LABEL "X (M)"
420    A=22
430    FOR K=1 TO 6
440    D=A-K*3
450    C$(1)="=X=1.15"
460    C$(2)="=X=1.25"
470    C$(3)="=X=1.40"
480    C$(4)="=X=1.60"
490    C$(5)="=X=1.80"
500    C$(6)="=X=2.00"
510    MOVE -14,D
520    LABEL USING "D,8A";K,C$(K)[1;8]
530    PENUP
540    NEXT K
```

```
550   CSIZE 1.3,.72
560   FOR J=1 TO 6
570   M=J*21-20
580   FOR I=M TO J*21
590   B(I)=J
600   MOVE Z(I),H(I)
610   LABEL USING "D";B(I)
620   PENUP
630   NEXT I
640   NEXT J
650   CLIP OFF
660   CSIZE 2.0,.65
670   LORG 2
680   FOR I=0 TO 100 STEP 10
690     MOVE -17.75,I
700     LABEL USING "#,DDD.D";I
710   NEXT I
720   LORG 6
730   FOR J=-15.24 TO 15.24 STEP 5.08
740      MOVE J,-2.0
750      LABEL USING "#,DDD.DD";J
760   NEXT J
770   MASS STORAGE IS ":INTERNAL,4"
780   END
```

```
10    !PROGRAM FLSTRTIO
20    !THIS PROGRAM READS A DATA FILE AND PLOTS THE RATIO OF STANTON NUMBERS
30    !OVER BASE LINE STANTON NUMBERS VERSUS REYNOLDS NUMBERS.
40    !
50    DIM Rey(6),X1(6),St1(6),St2(6),Re1(6),C$(6)[1],P$(6)[1],G$(6)[1]
60    DIM St3(6),Re3(6),St4(6),Re4(6),Str1(6),Str2(6),Str3(6)
70    ASSIGN @Path1 TO "STAV"
80    FOR I=1 TO 6
90    ENTER @Path1;X1(I),Rey(I),St1(I)
100   NEXT I
110   ASSIGN @Path2 TO "STAVFC"
120   FOR I=1 TO 6
130   ENTER @Path2;Re1(I),St2(I)
140   Str1(I)=St2(I)/St1(I)
150   NEXT I
160   ASSIGN @Path3 TO "STAVF1"
170   FOR I=1 TO 6
180   ENTER @Path3;Re3(I),St3(I)
190   Str2(I)=St3(I)/St1(I)
200   NEXT I
210   ASSIGN @Path4 TO "STAVF2"
220   FOR I=1 TO 6
230   ENTER @Path4;Re4(I),St4(I)
240   Str3(I)=St4(I)/St1(I)
250   NEXT I
260   PRINTER IS 1
270   PRINT "ENTER TODAY'S DATE (MMDDYY.HHMM)"
280   INPUT Runno
290   F$="DATE ="
300   PRINT "ENTER IN ORDER CORRESPONDING BLOWING RATIOS, M1,M2, AND M3"
310   FOR I=1 TO 3
320   INPUT M(I)
330   !ECHO PRINT M
340   PRINT "M=";M(I)
350   GINIT
360   !PLOTTER IS 705,"HPGL"
370   PLOTTER IS CRT,"INTERNAL"
380   GRAPHICS ON
390   X_gdu_max=100*MAX(1,RATIO)
400   Y_gdu_max=100*MAX(1,1/RATIO)
410   CSIZE 4.5,.65
420   LORG 6
430   MOVE X_gdu_max/2,.9*Y_gdu_max
440   LABEL "FILM COOLING"
450   DEG
460   LDIR 90
470   CSIZE 3.5
480   MOVE .1*X_gdu_max,Y_gdu_max/2
490   LABEL "St/Sto"
500   LDIR 0
510   LORG 4
520   MOVE X_gdu_max/2,.20*Y_gdu_max
530   LABEL "REYNOLDS No*10^6"
```

```
540   CSIZE 2.5
550   LORG 6
560   MOVE .8*X_gdu_max,.65*Y_gdu_max
570   LABEL USING "6A,#,6D.4D";F$,Runno
580   VIEWPORT .2*X_gdu_max,.9*X_gdu_max,.30*Y_gdu_max,.90*Y_gdu_max
590   FRAME
600   WINDOW .6,1.6,.3,1.0
610   AXES .1,.1,.6,.3,1,1
620   AXES .1,.1,1.6,1.0,1,1
630   CSIZE 2.5
640   MOVE 1.3,.9
650   LABEL "BLOWING RATIOS"
660   A=.55
670   FOR K=1 TO 3
680   D=A-K*.2
690   B$(1)="*=M="
700   B$(2)="o=M="
710   B$(3)="+=M="
720   MOVE 1.28,D
730   LABEL USING "4A,#,D.DD";B$(I),M(I)
740   NEXT K
750   CLIP OFF
760   CSIZE 3.0,.65
770   LORG 2
780   FOR I=.3 TO 1.0 STEP .1
790     MOVE .54,I
800     LABEL USING "#,D.D";I
810   NEXT I
820   LORG 6
830   FOR J=.6 TO 1.7 STEP .1
840      MOVE J,.27
850      LABEL USING "#,D.D";J
860   NEXT J
870   CSIZE 1.3,.72
880   FOR I=1 TO 6
890   C$(I)="*"
900   MOVE Rey(I),Str1(I)
910   LABEL USING "A";C$(I)
920   G$(I)="o"
930   MOVE Rey(I),Str2(I)
940   LABEL USING "A";G$(I)
950   P$(I)="+"
960   MOVE Rey(I),Str3(I)
970   PENUP
980   NEXT I
990   END
```

```
10    !PROGRAM PLSTRVOR
20    !THIS PROGRAM READS A DATA FILE AND PLOTS SPANWISE VARIATIONS
30    !OF STANTON NUMBERS RATIOS BY ROWS
40    !
50    DIM Str(200),Rey(6),Z(200),X1(6),X2(200),C$(6)[8],B(126)
60    MASS STORAGE IS ":INTERNAL,4,1"
70    ASSIGN @Path1 TO "STRDT2"
80    FOR I=1 TO 126
90    ENTER @Path1;Str(I),X2(I),Z(I)
100   NEXT I
110   F$="DATE ="
120   PRINTER IS 1
130   PRINT "ENTER RUN NUMBER TO WHICH THIS PLOT CORRESPOND (MMDDYY.HHMM)"
140   INPUT Runno
150   GINIT
160   PLOTTER IS 705,"HPGL"
170   !PLOTTER IS CRT,"INTERNAL"
180   GRAPHICS ON
190   CSIZE 2.5,.65
200   MOVE 42,14
210   LABEL "FREE STREAM 10 M/S, NO FILM COOLING "
220   CSIZE 4.5,.65
230   MOVE 20,85
240   LABEL "STANTON NUMBER RATIOS, VORTEX GEN #2"
250   CSIZE 2.5,.65
260   MOVE 70,83
270   LABEL USING "6A,#,6D.4D";F$,Runno
280   CSIZE 3.5,.65
290   MOVE 65,17
300   LABEL "Z  (CM) "
310   MOVE 22,45
320   DEG
330   LDIR 90
340   LABEL "St/Sto"
350   LDIR 0
360   VIEWPORT 30,116,25,83
370   WINDOW 20,-20,.4,1.4
380   FRAME
390   AXES 5,.1,20,.40,1,1
400   AXES 5,.1,-20,1.4,1,1
410   CSIZE 2.0,.65
420   MOVE 13.5,.85
430   LABEL "X (M)"
440   A=.80
450   FOR K=1 TO 6
460   D=A-K*.04
470   C$(1)="=X=1.15"
480   C$(2)="=X=1.25"
490   C$(3)="=X=1.40"
500   C$(4)="=X=1.60"
510   C$(5)="=X=1.80"
520   C$(6)="=X=2.00"
530   MOVE 14,D
```

```
540   LABEL USING "D,8A";K,C$(K)
550   PENUP
560   NEXT K
570   CSIZE 1.3,.72
580   FOR J=1 TO 6
590   M=J*21-20
600   FOR I=M TO J*21
610   B(I)=J
620   MOVE Z(I),Str(I)
630   LABEL USING "D";B(I)
640   PENUP
650   NEXT I
660   NEXT J
670   CLIP OFF
680   CSIZE 2.0,.65
690   LORG 2
700   FOR I=.4 TO 1.4 STEP .1
710     MOVE 21.7,I
720     LABEL USING "#,D.D";I
730   NEXT I
740   LORG 6
750   FOR J=-20 TO 20 STEP 5
760      MOVE J,.37
770      LABEL USING "#,DDD.DD";J
780   NEXT J
790   MASS STORAGE IS ":INTERNAL,4"
800   END
```

```
10    !PROGRAM PLSTRVV6
20    !THIS PROGRAM READS A DATA FILE AND PLOTS SPANWISE VARIATIONS
30    !OF STANTON NUMBERS RATIOS BY ROWS FOR FILM COOLING DATA AND
40    !FOR VORTEX DATA
50    !
60    DIM Str1(126),Str2(126),Z(126),X2(126),X3(126),C$(126)[1],B$(126)[1]
70    DIM Stf(126),Z1(126)
80    !
90    MASS STORAGE IS ":INTERNAL,4,1"
100   ASSIGN @Path1 TO "STRFC3"
110   ASSIGN @Path2 TO "STRFCV11"
120   !
130   FOR I=1 TO 126
140   ENTER @Path1;Str1(I),X2(I),Z(I)
150   ENTER @Path2;Str2(I),Stf(I),X3(I),Z1(I)
160   NEXT I
170   F$="DATE ="
180   PRINTER IS 1
190   PRINT "ENTER RUN NUMBER TO WHICH THIS PLOT CORRESPOND (MMDDYY.HHMM)"
200   INPUT Runno
210   GINIT
220   PLOTTER IS 705,"HPGL"
230   !PLOTTER IS CRT,"INTERNAL"
240   GRAPHICS ON
250   CSIZE 2.5,.65
260   MOVE 20,14
270   LABEL "FREE STREAM 15 M/S, WITH FILM COOLING, VORTEX GEN. AT 4.75 cm"
280   CSIZE 4.5,.65
290   MOVE 40,85
300   LABEL "STANTON NUMBER RATIOS"
310   CSIZE 2.5,.65
320   MOVE 75,83
330   LABEL USING "6A,#,6D.4D";F$,Runno
340   CSIZE 3.5,.65
350   MOVE 65,17
360   LABEL "Z  (CM) "
370   MOVE 25,45
380   DEG
390   LDIR 90
400   LABEL "St/Sto"
410   LDIR 0
420   VIEWPORT 30,116,25,63
430   WINDOW -20,20,.3,1.2
440   FRAME
450   AXES 5,.1,-20,.30,1,1
460   AXES 5,.1,20,1.2,1,1
470   CSIZE 3.0,.65
480   MOVE -17.5,1.0
490   LABEL "X = 3.00 M"
500   CSIZE 2.5,.65
510   MOVE 0.,.4
520   LABEL "M=0.47"
530   MOVE -17.5,.41
```

```
540   LABEL "o = WITHOUT VORTEX"
550   MOVE -17.5,.37
560   LABEL "+ = WITH VORTEX"
570   CSIZE 1.3,.72
580   FOR I=106 TO 128
590   B$(I)="o"
600   C$(I)="+"
610   MOVE Z(I),Str1(I)
620   LABEL USING "A";B$(I)
630   MOVE Z1(I),Str2(I)
640   LABEL USING "A";C$(I)
650   PENUP
660   NEXT I
670   CLIP OFF
680   CSIZE 3.0,.65
690   LORG 2
700   FOR I=.3 TO 1.2 STEP .1
710     MOVE -21.9,I
720     LABEL USING "#,D.D";I
730   NEXT I
740   LORG 6
750   FOR J=-20 TO 20 STEP 5
760      MOVE J,.27
770      LABEL USING "#,DDD.DD";J
780   NEXT J
790   MASS STORAGE IS ":INTERNAL,4"
800   END
```

```
10    !PROGRAM SURFCONT!
20    !THIS PROGRAM READS A DATA FILE AND PLOTS SURFACE CONTOURS OF
30    !OF STANTON NUMBERS RATIOS ALONG THE PLATE SPAN.
40    !
50    !ORTIZ VERSION JULY/87
60    DIM Str(126),Strf(126),Z(126),X2(126),B(126),Z1(5),Z2(5)
70    MASS STORAGE IS ":INTERNAL,4,1"
80    ASSIGN @Path1 TO "STRFCV12"
90    PRINTER IS 70!
100   FOR I=1 TO 126
110   ENTER @Path1;Str(I),Strf(I),X2(I),Z(I)
120   NEXT I
130   F$="DATE ="
140   PRINTER IS 1
150   PRINT "ENTER RUN NUMBER TO WHICH THIS PLOT CORRESPOND (MMDDYY.HHMM)"
160   INPUT Runno
170   !
180   Stmin=.90
190   Llim=.98
200   FOR I=1 TO 126
210   IF Strf(I)<Llim THEN B(I)=0
220   IF Strf(I)<=1.02 AND Strf(I)>Llim THEN B(I)=1
410   IF Strf(I)<=1.10 AND Strf(I)>1.02 THEN B(I)=2
411   IF Strf(I)<=1.20 AND Strf(I)>1.10 THEN B(I)=3
412   IF Strf(I)>1.20 THEN B(I)=4
430   NEXT I
440   !
450   GINIT
460   PLOTTER IS 705,"HPGL"
470   !PLOTTER IS CRT,"INTERNAL"
480   GRAPHICS ON
490   CSIZE 2.5,.65
500   MOVE 14,13
510   LABEL "FREE STREAM 10 M/S, WITH FILM COOLING, VORTEX GEN. AT 4.79 cm "
520   CSIZE 4.5,.65
530   MOVE 40,82
540   LABEL "SURFACE CONTOURS"
550   CSIZE 2.5,.65
560   MOVE 70,80
570   LABEL USING "6A,#,6D.4D";F$,Runno
580   CSIZE 3.5,.65
590   MOVE 58,32
600   LABEL "X  (M) "
610   MOVE 16,55
620   DEG
630   LDIR 90
640   LABEL "Z (CM)"
650   LDIR 0
660   CSIZE 2.5,.65
670   MOVE 54,27
680   LABEL "St/Stf RANGES"
```

```
690   A=24
700   FOR K=0 TO 2
710   G=A-K*2.5
720   MOVE 34,G
730   Z2(0)=Stmin+K*Inc
740   Z1(0)=Stmin+(K+1)*Inc
750   Z2(1)=.98
760   Z1(1)=1.02
770   Z2(2)=1.02
780   Z1(2)=1.10
790   LABEL USING 800:K,Z2(K),Z1(K)
800   IMAGE D,2X,D.3D,2X,D.3D
810   NEXT K
820   FOR K=3 TO 4
830   G=A-(K-3)*2.5
840   MOVE 64,G
850   Z2(3)=1.10
860   Z1(3)=1.20
870   Z2(4)=1.20
880   Z1(4)=1.30
890   LABEL USING 800:K,Z2(K),Z1(K)
900   NEXT K
910   VIEWPORT 25,114,40,73
920   WINDOW 1.10,2.20,20.,-20.
930   FRAME
940   AXES .05,5.,1.10,20.,4,1
950   AXES .05,5.,2.20,-20.,4,1
960   MOVE 1.90,17
970   LABEL "M =0.86"
980   CSIZE 1.3,.72
990   FOR I=1 TO 126
1000  MOVE X2(I),Z(I)
1010  LABEL USING "D":B(I)
1020  PENUP
1030  NEXT I
1040  CLIP OFF
1050  CSIZE 2.0,.65
1060  LORG 2
1070  FOR I=-20 TO 20 STEP 5
1080    MOVE 1.01,I
1090    LABEL USING "#,DDD.D";I
1100  NEXT I
1110  LORG 5
1120  FOR J=1.10 TO 2.30 STEP .1
1130     MOVE J,22
1140     LABEL USING "#,D.DD";J
1150  NEXT J
1160  MASS STORAGE IS ":INTERNAL,4"
1170  END
```

```
10    !PROGRAM FLSTRFC
20    !THIS PROGRAM READS A DATA FILE AND PLOTS SPANWISE VARIATIONS
30    !OF STANTON NUMBERS RATIOS BY ROWS FOR FILM COOLING DATA
40    !
50    DIM Str(200),Rey(6),Z(200),X1(6),X2(200),C$(6)[8],B(126)
60    MASS STORAGE IS ":INTERNAL,4,1"
70    ASSIGN @Path1 TO "STRFC"
80    FOR I=1 TO 126
90    ENTER @Path1;Str(I),X2(I),Z(I)
100   NEXT I
110   F$="DATE ="
120   PRINTER IS 1
130   PRINT "ENTER RUN NUMBER TO WHICH THIS PLOT CORRESPOND (MMDDYY.HHMM)"
140   INPUT Runno
150   GINIT
160   PLOTTER IS 705,"HPGL"
170   !PLOTTER IS CRT,"INTERNAL"
180   GRAPHICS ON
190   CSIZE 2.5,.65
200   MOVE 40,14
210   LABEL "FREE STREAM 15 M/S, WITH FILM COOLING "
220   CSIZE 4.5,.65
230   MOVE 40,86
240   LABEL "STANTON NUMBER RATIOS"
250   CSIZE 2.5,.65
260   MOVE 75,83
270   LABEL USING "6A,#,6D.4D";F$,Runno
280   CSIZE 3.5,.65
290   MOVE 65,17
300   LABEL "Z  (CM) "
310   MOVE 25,45
320   DEG
330   LDIR 90
340   LABEL "St/Sto"
350   LDIR 0
360   VIEWPORT 30,115,25,83
370   WINDOW -20,20,.3,1.2
380   FRAME
390   AXES 5,.1,-20,.30,1,1
400   AXES 5,.1,20,1.2,1,1
410   CSIZE 2.0,.65
420   MOVE -17.5,.65
430   LABEL "X (M)"
440   A=.62
450   FOR K=1 TO 6
460   D=A-K*.04
470   C$(1)="=X=1.15"
480   C$(2)="=X=1.25"
490   C$(3)="=X=1.40"
500   C$(4)="=X=1.60"
510   C$(5)="=X=1.80"
520   C$(6)="=X=2.00"
530   MOVE -18.,D
540   LABEL USING "D,8A";K,C$(K)
```

```
550   PENUP
560   NEXT K
570   CSIZE 1.3,.72
580   FOR J=1 TO 6
590   M=J*21-20
600   FOR I=M TO J*21
610   B(I)=J
620   MOVE Z(I),Str(I)
630   LABEL USING "D":B(I)
640   PENUP
650   NEXT I
660   NEXT J
670   CLIP OFF
680   CSIZE 2.0,.65
690   LORG 2
700   FOR I=.2 TO 1.2 STEP .1
710     MOVE -21.9,I
720     LABEL USING "#,D.D":I
730   NEXT I
740   LORG 6
750   FOR J=-20 TO 20 STEP 5
760      MOVE J,.27
770      LABEL USING "#,DDD.DD";J
780   NEXT J
790   MASS STORAGE IS ":INTERNAL,4"
800   END
```

APPENDIX D.

DATA FILES CATALOG

I. HEAT TRANSFER DATA DISK No. 1

No.	File Name	Date	Injec.	Vortex	Description
001	TDAT1	71787.1702	N	N	15 m/s, baseline
002	IDAT1	"	N	N	"
003	STAV1	"	N	N	baseline St_{av}
004	HDAT1	"	N	N	baseline local h
005	TDAT2	72087.1315	N	N	10 m/s base line
006	IDAT2	"	N	N	"
007	STAV2	"	N	N	baseline St_{av}
008	HDAT2	"	N	N	baseline local h
009	STRDT2	72187.1524	N	Y	10 m/s St/Sto
010	STRV2	"	N	Y	10 m/s $(St/Sto)_{av}$
011	TDAT3	"	N	Y	T(I)
012	IDAT3	"	N	Y	input data
013	TDAT4	72187.1748	N	Y	15 m/s T(I)
014	IDAT4	"	N	Y	input data
015	STRDT1	"	N	Y	St/Sto
016	STARV1	"	N	Y	$(St/Sto)_{av}$
017	TDAFC2	72387.1318	Y	N	10 m/s, M = 0.68 T(I)
018	IDAFC2	"	Y	N	input data
019	FILDT2	"	Y	N	film cooling data
020	STRFC2	"	Y	N	St/Sto
021	STAVFC2	"	Y	N	$(St/Sto)_{av}$

022	TDAFC1	72387.1622	Y	N	15 m/s, T(I)
023	IDAFC1	"	Y	N	, input data
024	FILDT1	"	Y	N	,Inj. data
025	STRFC1	"	Y	N	, St/Sto
026	STAVFC1	"	Y	N	, $(St/Sto)_{av}$
027	TDAFC4	72487.1401	Y	N	10 m/s, repeat
028	IDAFC4	"	Y	N	
029	FILDT4	"	Y	N	
030	STRFC4	"	Y	N	
031	STAVFC4	"	Y	N	
032	TDAFC3	72487.1621	Y	N	15 m/s, repeat
033	IDAFC3		Y	N	
034	FILDT3	"	Y	N	
035	STRFC3	"	Y	N	
036	STAVFC3	"	Y	N	
037	TDAFC6	72587.1401	Y	N	10 m/s, M = 1.26
038	IDAFC6	"	Y	N	
039	FILDT6	"	Y	N	
040	STRFC6	"	Y	N	, St/Sto
041	STAVFC6	"	Y	N	, $(St/Sto)_{av}$
042	TDAFC5	72587.1808	Y	N	15 m/s, M = 0.86
043	IDAFC5	"	Y	N	
044	FILDT5	"	Y	N	
045	STRFC5	"	Y	N	,St/Sto
046	STAVFC5	"	Y	N	, $(St/Sto)_{av}$
047	TDAFC7	72887.1206	Y	N	15 m/s, M = 0.86
048	IDAFC7	"	Y	N	, Repeat
049	FILDT7	"	Y	N	
050	STRFC7	"	Y	N	
051	STAVFC7	"	Y	N	
052	TDAFC8	72887.1353	Y	N	10 m/s, M = 0.68
053	IDAFC8	"	Y	N	, Repeat
054	FILDT8	"	Y	N	
055	STRFC8	"	Y	N	, St/Sto
056	STAVFC8	"	Y	N	, $(St/Sto)_{av}$

057	STAFC8	"	Y	N	Stf numbers.
058	TDAFC10	72887.1742	Y	Y	10 m/s, M = 0.68
059	IDAFC10	"	Y	Y	Vortex gen. @ 4.79 cm
060	FILDT10	"	Y	Y	
061	STRFCV10	"	Y	Y	St/Sto
062	STFCV10	"	Y	Y	$(St/Sto)_{av}$
063	TDAFC11	72987.1308	Y	Y	15 m/s, M = 0.47
064	IDAFC11	"	Y	Y	Vortex gen. @ 4.79 cm
065	FILDT11		Y	Y	
066	STRFCV11	"	Y	Y	St/Sto
067	STAFCV11	"	Y	Y	$(St/Sto)_{av}$
068	TDAFC13	72987.1345	Y	Y	15 m/s, M = 0.47
069	IDAFC13	"	Y	Y	Vortex gen. @ 3.52 cm
070	FILDT13	"	Y	Y	"
071	STRFCV13	"	Y	Y	"
072	STAFCV13	"	Y	Y	"
073	TDAFC15	72987.1415	Y	Y	15 m/s, M = 0.47
074	IDAFC15	"	Y	Y	Vortex gen. @ 6.06 cm
075	FILDT15	"	Y	Y	"
076	STRFCV15	"	Y	Y	"
077	STAFCV15	"	Y	Y	"
078	STAFC6	72587.1451	Y	N	10 m/s, M=1.26, Stf No
079	STAFC7	72887.1206	Y	N	15 m/s, M=0.86, Stf No
080	STAFC3	72487.1621	Y	N	15 m/s, M=0.47, Stf No
081	TDAFC21	80187.1354	Y	Y	15 m/s, M = 0.86
082	IDAFC21	"	Y	Y	Vortex @ 6.06 cm
083	FILDT21	"	Y	Y	"
084	STRFCV21	"	Y	Y	St/Sto
085	STFCV21	"	Y	Y	averaged St/Sto
086	TDAFC17	80187.1507	Y	Y	15 m/s, M= 0.86
087	IDAFC17	"	Y	Y	Vortex @ 4.79 cm
088	FILDT17	"	Y	Y	"
089	STRFCV17	"	Y	Y	"
090	STFC17	"	Y	Y	"

091	TDAFC19	80187.1440	Y	Y	15 m/s, M= 0.86
092	IDAFC19	"	Y	Y	Vortex @ 3.52 cm
093	FILDT19	"	Y	Y	"
094	STRFCV19	"	Y	Y	"
095	STFCV19	"	Y	Y	"
096	TDAFC12	80187.1541	Y	Y	10 m/s, M = 1.26
097	IDAFC12	"	Y	Y	Vortex @ 4.79 cm
098	FILDT12	"	Y	Y	"
099	STRFCV12	"	Y	Y	St/Sto
100	STFCV12	"	Y	Y	averaged St/Sto
101	TDAFC14	80487.1321	Y	Y	10 m/s, M=1.26
102	IDAFC14	"	Y	Y	Vortex @ 4.79 cm
103	FILDT14	"	Y	Y	"
104	STRFCV14	"	Y	Y	"
105	STFCV14	"	Y	Y	"

II. HEAT TRANSFER DATA DISK #2

No.	FILE NAME	DATE	INJ.	VORTEX	DESCRIPTION
007	STAV2		N	N	10 m/s, St_{av} baseline
008	HDAT2		N	N	local h baseline.
106	TDAFC16	80487.1412	Y	N	10 m/s, M = 0.98
107	IDAFC16	"	Y	N	no vortex, baseline
108	FILDT16	"	Y	N	for 9 inj. holes F.C.
109	STRFC16	"	Y	N	St/Sto
110	STAFC16	"	Y	N	$St_f(I)$
111	STAVFC16	"	Y	N	averaged St/Sto
112	TDAFC18	80487.1452	Y	Y	10 m/s, M= 0.98
113	IDAFC18	"	Y	Y	Vortex @ 4.79 cm
114	FILDT18	"	Y	Y	"
115	STRFCV18	"	Y	Y	St/Sto
116	STFCV18	"	Y	Y	averaged St/Sto

117	TDAFC20	80487.1529	Y	Y	10 m/s, M=0.98
118	IDAFC20	"	Y	Y	Vortex @3.52 cm
119	FILDT20	"	Y	Y	"
120	STRFC20	"	Y	Y	"
121	STFCV20	"	Y	Y	"
122	TDAFC22	80487.1553	Y	Y	10 m/s, M=0.98
123	IDAFC22	"	Y	Y	Vortex @ 6.06 cm
124	FILDT22	"	Y	Y	"
125	STRFCV22	"	Y	Y	"
126	STFCV22	"	Y	Y	"
127	TDAFC24	80987.1943	Y	Y	10 m/s, M=0.98
128	IDAFC24	"	Y	Y	Vortex @ 4.79 cm
129	FILDT24	"	Y	Y	Run for temp. profiles
130	STRFC24	"	Y	Y	St/Sto

III. TEMPERATURE PROFILES DATA DISK #1

No.	FILE NAME	DESCRIPTION
131	TPRO1	10 m/s, M =0.98, heated plate, X= 1.867 m
132	TPRO2	Vortex @ 4.79 cm , X = 2.172 m
133	TPRO3	" " " , X = 2.48 m
134	TPRO4	10 m/s, M = 0.98, unheated plate, X = 1.867 m
135	TPRO5	Vortex @ 4.79 cm, " , X = 2.172 m
136	TPRO6	" " , " , X = 2.48 m
137	TPRO7	" " , " , X = 1.48 m
138	TPRO8	10 m/s, M=0.98, heated plate, X=1.48 m, Vt. @ 4.79 cm
139	TPRO9	10m/s, M=.98, unheated plate, X=1.48 m, V @ 3.52 cm
140	TPRO10	, V @ 6.06 cm
141	TPRO11	10 m/s, M=1.26, unheated plt., X=1.48 m, V @ 4.79 cm
142	TPRO12	10 m/s, M= 0.98, unheated plate, No vortex, X=1.48 m

IV. TEMPERATURE PROFILES DATA DISK #2

143	TPRO13	10 m/s, boundary layer with film cooling, M= 0.98
144	TPRO14	10 m/s, boundary layer heated plate only.
145	PPROF	10 m/s, M=1.26, V @ 4.79 cm. Pressure probe profile
146	CAL	data, at X= 1.48 m
147	VELPRO	velocity profiles
148	PLOTVOR	vorticity profiles

LIST OF REFERENCES

1. Evans D. L., *Study of Vortices Embeded in Boundary Layers with Film Cooling*, M.S. Thesis, U.S. Naval Postgraduate School, Monterey, Ca., March 1987.

2. Goldstein R.J. and Chen H.P., *Film Cooling on Gas Turbine Blade Near the the End Wall*, Journal of Engineering for Gas Turbines and Power, v 107, p 117- 122, January 1985.

3. Joseph S. L. , *The Effets of an Embeded Vortex on a Film Cooled Turbulent Boundary Layer*, M.E. Thesis, U.S. Naval Postgraduate School, Monterey, Ca., December 1986.

4. Ongören, A., *Heat Transfer on Endwalls of a Turbine Cascade with Film Cooling*, Project Report 1981-19, Von Kárman Institute for Fluid Mechanics, Rhode Saint Genese, Belgium, June 1981.

5. Sieverding, C. H., *Recent Progress in Understanding of Basic Aspects of Secondary Flows in Turbine Blade Passages*, Gas Turbine Division of American Society of Mechanical Engineers, Paper No. 84-GT-78, pp. 1-10, January 1985.

6. Eibeck P. A. and Eaton J.K., *Heat Transfer Effects of a Longitudinal Vortex Embeded in Turbulent B.oundary Layer*, Journal of Heat Transfer, vol. 109, pp. 16–23, February 1987.

7. Golstein, R. J. and Chen, P. H., *Film Cooling of a Turbine Blade with Injection Through Two Rows of holes in the Near Endwall Region* , The American Society of Mechanical Engineers, Paper No. 87-GT-196, pp. 1-7, June 1987.

8. Ligrani P.M. and Camci C., *Adiabatic Film Cooling Effectiveness From Heat Transfer Measurements in Compressible Variable-Property Flow,* Journal of Heat Transfer, v. 107, p 313-320, May 1985.

9. Westphal, R. V., Pualey, W. R. and Eaton J. K., *Interaction Between a Vortex and a Turbulent Boundary Layer, Part I: Mean Flow Evolution and Turbulence Properties,* NASA Technical Memorandum 88361, January 1987.

10. Sato, T., Aoki S., Takeishi, K. and Matsuura, M., *Effect of Three-Dimensional Flow Field on Heat Transfer Problems of a Low Aspect Ratio Turbine Nozzle,* Takasago Research and Development Center, Mitsubishi Heavy Industries, Ltd.

11. Aerolab, *Operating Instructions for Aerolab 8" x 24" Laminar/ Turbulent Shear layer Facility with Variable Height Test Section for U.S. Naval Postgraduate School,* U.S. Naval Postgraduate School, Monterey, Ca., November 1985.

12. Ligrani P. M., *Qualification and Performance of NPS Shear Layer Research Facility,* NPS Report, Department of Mechanical Engineering, U.S. Naval Postgraduate School, Monterey, Ca., in preparation to appear in 1987.

13 Wang, T. *An Investigation of Curvature and Free Stream Turbulence Effects on Heat Transfer and Fluid Mechanics in Transitional Boundary Layer Flows,* Ph.D. Thesis, Mechanical Engineering Department, University of Minnesota, December 1984.

14. Wang, T., Simon, W.T. and Buddhavarapin J.,*Heat Transfer and Fluid Mechanics, Measurements in Transitional Boundary Layers Flows,* Gas Turbine Division of American Society of Mechanical Engineers, paper No. 85-GT-113, pp. 1-9, 1985.

15. Incopera F.P. and DeWitt, *Fundamentals of Heat and Mass Transfer,* 2d edition, pp 624-661, John Wiley and Sons, Inc.,1985.

16 Holman J.P., *Heat Transfer,* 6th. edition, pp 388-389, 400-406, McGraw-Hill, 1986.

17. Kays W.M. and Crawford, M.E., *Convective Heat and MassTransfer*, 2d. edition, pp. 213-217, McGraw-Hill, 1980.

18. Golstein R.J. and Yoshida T., *The Influence of a Laminar Boundary Layer and Laminar Injection on Film Cooling Performance*, Journal of Heat Transfer, vol. 104, pp. 355-362, May 1982.

19. Kline, S. J. and McClintoc, F. A., "Describing Uncertainties in Single-Space Experiments", *in Mechanical Engineering*, pp. 3-8, January 1953.

INITIAL DISTRIBUTION LIST

No. Copies

1. Defense Technical Information Center — 2
   Cameron Station
   Alexandria, VA 22304-6145

2. Library, Code 0142 — 2
   Naval Postgraduate School
   Monterey, CA 93943–5002

3. Professor P. M. Ligrani Code 69Li — 7
   Department of Mechanical Engineering
   Naval Postgraduate School
   Monterey, CA 93943

4. Department Chairman Code 69 — 1
   Department of Mechanical Engineering
   Naval Postgraduate School
   Monterey, CA 93943

5. Dr. Charles MacArthur — 10
   Project Engineer
   Components Branch
   Turbine Engine Division
   Aero Propulsion Laboratory
   Department of the Air Force
   Air Force Wright Aeronautical Laboratories
   Wright-Patterson Air Force Base, OH 45433

6. Señor Vicealmirante — 2
   COMANDANTE ARMADA NACIONAL
   Ministerio de Defensa Nacional
   Comando Armada Nacional
   CAN. Avenida Eldorado
   Bogotá, D.E.
   Colombia, S. A.

7. Señor Contalmirante 2
DIRECTOR ESCUELA NAVAL "ALMIRANTE PADILLA"
Escuela Naval de Cadetes "ALMIRANTE PADILLA"
Cartagena, Bolívar
Colombia, S. A.

8. LT. Stephen L. Joseph, USN 1
15 Brewster Road
Milford, CT 06460

9. LCDR. David L. Evans, USN 1
7103 N. 26th Drive
Phoenix, AZ 85021

10. LT. Alfredo Ortiz C., Col. Navy 2
Calle 7ª No. 4-45 Apto 201
Cartagena, Bolivar
Colombia, S. A.

11. Chief of Naval Operations
OP-01
Navy Department
Washington, D.C. 20350-2000 2

12. Chief of Naval Operations
OP-03
Navy Department
Washington, D.C. 20350-2000 2

13. Chief of Naval Operations
OP-05
Navy Department
Washington, D.C. 20350-2000 2

Thesis
O58933 Ortiz
c.1 The thermal behavior of film cooled turbulent boundary layers as affected by longitudinal vortices.